



The
University
Of
Sheffield.

A geometric morphometric assessment of the foot of *Oreopithecus*

By Kyle Billington

A thesis submitted in partial fulfilment of the requirements for the degree of Doctor of
Philosophy

The University of Sheffield

Department of Archaeology

July 2016

In loving memory of Dave Lloyd

Acknowledgements

There are a great number of people I owe a huge amount of gratitude to and unfortunately this list will not be complete. Omission from this list in no way constitutes a lack of gratitude on my part. Thanks are owed, in the first place, to the people who made this work possible: The University of Sheffield and the Department of Archaeology made the project financially viable and provided a place in which to produce the work; Roberto Portela-Miguez of the Natural History Museum, London, for arranging access to the primate collections there and being extremely accommodating to my needs; Loïc Costeur of the Naturhistorisches Museum, Basel, for granting access to the *Oreopithecus* remains under his care; Marcia Ponce de Léon for arranging permissions for me to access the primate collections and fossil casts at the University of Zürich; Angela Gill for granting access to the primate remains at the Powell-Cotton Museum.

I would like to thank Professor Paul Pettitt for convincing me to continue with this work the first time I considered not completing the project. He showed confidence in me which I didn't have in myself and was a source of great encouragement at a difficult time. Subsequently he offered valuable comments on my work which was outside his area of expertise and beyond his responsibilities. I am also grateful to Doctor Pia Nyström for assuming the role of second supervisor following a change of personnel within the department. A number of students were added to those already under her supervision and she managed to find the time to offer comments and advice when needed despite her incredibly busy schedule. The prompt help and expertise of Paul O'Higgins in making the necessary corrections to the thesis has been invaluable and I am indebted to him for this. Umberto Albarella also provided invaluable comments and Along with Paul made the viva a thoroughly enjoyable experience.

My friends and family have been a constant source of encouragement and inspiration to me and it is to them that I offer the most gratitude. Nichola Austen has been incredibly supportive throughout the project and was instrumental in helping me to arrange my trip to

Switzerland to collect data for the project, huge thanks are owed to her and I wish her all the best with her own PhD. Ed has provided a constant supply of laughs even at times when my mood was low. Other friends; James, Rachael, Ben, Mike, Toby, Rich, Mark, Katie, and many more friends whose inclusion is restricted by space, have provided often needed breaks and distractions to help refocus and remind me that there is a life outside of this project. Very special thanks go to J and Isabelle, two incredible friends and colleagues to whom I often turned to vent frustrations, seek advice, and find unswerving support for the duration of my student career. Noémie is deserving of my deepest and sincerest love and thanks. It is thanks to her that I found the confidence and strength to continue on from the second time I seriously considered not completing this project. She has given me the belief that completing this thesis is a worthwhile undertaking regardless of what follows. Because of her I am confident that whatever the outcome I will ultimately be happy and my future is bright.

None of this would have been possible without the support of my family. My aunts, uncles and cousins, although we're together only rarely, never fail to lift my spirits and make me laugh. My parents and brother have constantly believed in me and offered their love and support at every step of the process and throughout my life to this point; I could never do enough to repay their generosity. My grandparents have been particularly helpful throughout my higher education and always advised me to do what makes me happy. It is with their wise words that I turn to the next chapter of my life confident in the knowledge that I couldn't wish for better friends and family and that whatever the future holds I will always be looked after well.

Abstract

Oreopithecus is an enigmatic primate from the Miocene of Italy. It has been the subject of more than a century of controversial research and debate. Most recently, the claim that *Oreopithecus* exhibited a substantial degree of bipedal behaviour has permeated the literature. Specifically, the pedal anatomy of *Oreopithecus* has been suggested to be unique among the hominoids and this has been advanced as evidence for bipedal adaptations in this taxon. The possibility that *Oreopithecus* was a bipedal ape is examined using geometric morphometric techniques to assess the shape of *Oreopithecus* pedal remains in comparison to other well-known species, and functional interpretations are drawn from these results. This study has examined the medial column of the pedal skeleton of five extant primate taxa, as well as that of *Oreopithecus*, *Homo habilis*, and *Nacholapithecus*. The possible function of the foot is considered in the context of published information regarding the rest of the postcranial skeleton of *Oreopithecus* and the known positional behaviour of the extant species used in the study.

It is found that *Oreopithecus* closely resembles the African ape condition in the shape of its pedal skeleton, though there are subtle differences; however, none of the differences found in the pedal skeleton of *Oreopithecus* offer support to the contention that the foot was especially well-adapted to bipedal behaviour. The morphology of the medial cuneiform suggests that the degree of abduction of the hallux was comparable to that observed in *Pan*. Similarly, the morphology of the navicular, and the lateral and intermediate cuneiforms, indicate that the orientations of the articulations of the midfoot had a configuration that was more or less the same as that observed for extant African apes, particularly *Pan*. It is therefore concluded that *Oreopithecus* was probably not habitually bipedal. But the results presented here do not in and of themselves preclude bipedalism from its locomotory repertoire, as bipedal behaviour is exhibited among the extant apes to which it is similar. However, the finding that the foot of *Oreopithecus* was significantly smaller than it is in any extant ape casts doubt on the likelihood of any significant level of bipedalism and may indicate that *Oreopithecus* was adapted to a forelimb dominated locomotory strategy.

Contents

Acknowledgements	v
Abstract	vii
List of Figures.....	xii
List of Tables.....	xx
1. Introduction.....	1
1.2. Background to the topic	1
1.3. Structure and aims of the thesis.....	4
1.4. <i>Oreopithecus</i>	5
1.5. Overview and evolution of Hominoidea	9
1.5.1. Extant Hominoidea	9
1.5.2. Miocene fossil Hominoidea	13
1.5.3. Plio-Pleistocene Hominoidea	17
1.6. Functional anatomy of the foot.....	21
1.6.1. Functional anatomy of the human foot.....	21
1.6.2. Comparative functional anatomy of the primate foot.....	28
1.7. Positional behaviour of primates in this study.....	31
1.8. Specific hypotheses tested in this study	33
2. Materials and Methods	35
2.1. Materials.....	35
2.2. Methods	39
2.2.1. Choice of geometric morphometrics	39
2.2.2. Structured light scanning.....	41
2.2.3. Collection of data.....	43
2.2.3.1. Procedure for placement of landmarks	43
2.2.3.2. Talus landmarks and semilandmarks	44
2.2.3.3. Navicular landmarks and semilandmarks	48
2.2.3.4. Medial cuneiform landmarks and semilandmarks.....	51
2.2.3.5. Intermediate cuneiform landmarks and semilandmarks	54

2.2.3.6.	Lateral cuneiform landmarks and semilandmarks	58
2.2.3.7.	First metatarsal landmarks and semilandmarks	62
2.2.4.	Analysis of data.....	66
3.	Results	69
3.1.	Talus	70
3.1.1.	Principal components analysis.....	70
3.1.1.1.	Full sample.....	70
3.1.1.2.	Extant species means vs. fossils.....	74
3.1.2.	Statistical tests.....	77
3.1.3.	Visualisation of shape differences	79
3.2.	Navicular.....	89
3.2.1.	Principal components analysis.....	89
3.2.1.1.	Full sample.....	89
3.2.1.2.	Extant species means vs. fossils.....	94
3.2.2.	Statistical tests.....	97
3.2.3.	Visualisation of shape differences	99
3.3.	Medial cuneiform	108
3.3.1.	Principal components analysis.....	108
3.3.1.1.	Full sample.....	108
3.3.1.2.	Extant species means vs. fossils.....	112
3.3.2.	Statistical tests.....	115
3.3.3.	Visualisation of shape differences	118
3.4.	Intermediate cuneiform	130
3.4.1.	Principal components analysis.....	130
3.4.1.1.	Full sample.....	130
3.4.1.2.	Extant species means vs. fossils.....	135
3.4.2.	Statistical tests.....	138
3.4.3.	Visualisation of shape differences	141
3.5.	Lateral cuneiform	153

3.5.1.	Principal components analysis.....	153
3.5.1.1.	Full sample.....	153
3.5.1.2.	Extant species means vs. fossils.....	158
3.5.2.	Statistical tests.....	161
3.5.3.	Visualisation of shape differences	163
3.6.	First metatarsal	172
3.6.1.	Principal components analysis.....	172
3.6.1.1.	Complete first metatarsal: full sample.....	172
3.6.1.2.	Complete first metatarsal: species means.....	174
3.6.1.3.	Proximal first metatarsal: full sample	176
3.6.1.4.	Proximal first metatarsal: species means and Oreopithecus	178
3.6.1.5.	Distal first metatarsal: full sample	180
3.6.1.6.	Distal first metatarsal: species means and Oreopithecus	182
3.6.2.	Statistical tests.....	185
3.6.2.1.	Complete first metatarsal.....	185
3.6.2.2.	Proximal first metatarsal.....	186
3.6.2.3.	Distal first metatarsal.....	188
3.6.3.	Visualisation of shape differences	190
3.6.3.1.	Complete first metatarsal.....	191
3.6.3.2.	Proximal first metatarsal.....	198
3.6.3.3.	Distal first metatarsal.....	200
3.7.	Summary.....	202
4.	Discussion	206
4.1.	Talus	206
4.1.1.	Extant species	206
4.1.2.	Fossil species	210
4.2.	Navicular.....	213
4.2.1.	Extant species	213
4.2.2.	Fossil species	218

4.3.	Medial cuneiform	221
4.3.1.	Extant species	221
4.3.2.	Fossil species	225
4.4.	Intermediate cuneiform	228
4.4.1.	Extant species	228
4.4.2.	Fossil species	232
4.5.	Lateral cuneiform	234
4.5.1.	Extant species	234
4.5.2.	Fossil species	239
4.6.	First metatarsal.....	241
4.6.1.	Extant species	241
4.6.2.	Fossil species	245
5.	Conclusions and future research	247
6.	References.....	255

List of Figures

- 1.1 - Generally accepted taxonomic ranking of the extant hominoid genera - 23
- 1.2 - Possible phylogenetic relationships of Miocene hominoids - 26
- 1.3 - Exploded foot skeleton - 33
- 1.4- Magnetic resonance image of the human foot - 33
- 1.5 - Plantar view of the calcaneocuboid joint - 37
- 1.6 - Congruency and incongruency of the transverse tarsal joint – 37
- 2.1 - Landmarks placed on the lateral trochlea rim - 55
- 2.2 - Landmarks placed on the medial malleolus - 56
- 2.3 - Landmarks placed on the head of the talus - 56
- 2.4 - Semilandmarks placed on the trochlea - 57
- 2.5 - Semilandmarks placed on the medial malleolar facet surface - 58
- 2.6 - Semilandmarks placed on the head of the talus - 58
- 2.7 - Landmarks placed on the proximal navicular - 59
- 2.8 - Landmarks placed on the distal navicular - 60
- 2.9 - Semilandmarks placed on the navicular facet of the navicular - 61
- 2.10 - Semilandmarks placed on the distal navicular - 62
- 2.11 - Landmarks placed on the navicular facet of the medial cuneiform - 63
- 2.12 - Landmarks placed on the facet for the first metatarsal - 63
- 2.13 - Semilandmarks placed on the navicular facet of the medial cuneiform - 64
- 2.14 - Semilandmarks placed on the distal facet of the medial cuneiform - 65
- 2.15 - Landmarks placed on the navicular facet of the intermediate cuneiform - 66
- 2.16 - Landmarks placed on the distal facet of the intermediate cuneiform - 66

- 2.17 - Semilandmarks placed on the surface of the navicular facet of the intermediate cuneiform - 67
- 2.18 - Semilandmarks placed on the distal surface of the intermediate cuneiform - 68
- 2.19 - Landmarks placed on the navicular facet of the lateral cuneiform - 69
- 2.20 - Landmarks placed on the distal facet of the lateral cuneiform - 70
- 2.21 - Semilandmarks placed on surface of the navicular facet of the lateral cuneiform - 71
- 2.22 - Semilandmarks placed on the distal facet of the lateral cuneiform - 72
- 2.23 - Landmarks placed on the medial cuneiform facet of the first metatarsal - 73
- 2.24 - Landmarks placed on the head of the first metatarsal - 74
- 2.25 - Semilandmarks placed on the surface of the medial cuneiform facet of the first metatarsal - 75
- 2.26 - Semilandmarks placed on the head of the first metatarsal – 76
- 3.1.1 - Percentage of the overall variance explained by each principal component for the talus - 82
- 3.1.2 - Principal component 1 vs. principal component 2 of all individuals for the talus – 83
- 3.1.3 - Principal component 1 vs. principal component 3 of all individuals for the talus – 84
- 3.1.4 - Principal component 1 vs. principal component 4 of all individuals for the talus – 85
- 3.1.5 - Percentage of the variance explained by each PC using only species mean shapes – 86
- 3.1.6 - Principal component 1 vs. principal component 2 of species means and fossils for the talus - 87
- 3.1.7 - Principal component 1 vs. principal component 3 of species means and fossils for the talus - 88
- 3.1.8 - Principal component 1 vs. principal component 3 of species means and fossils for the talus - 88
- 3.1.9 - Superior view of the talus displaying terminology used to describe shape differences - 92
- 3.1.10 - Medial view of the talus displaying terminology used to describe shape differences - 92
- 3.1.11 - Warp from the *Gorilla* mean talus to *Oreopithecus* - 94
- 3.1.12 - Warp from the *Homo* mean talus to OH8 - 96
- 3.1.13 - Warp from the *Pan* mean talus to the *Pongo* mean - 97
- 3.1.14 - Warp from the *Pan* mean talus to *Nacholapithecus* - 99

- 3.1.15 - Warp from the *Theropithecus* mean talus to *Nacholapithecus* - 100
- 3.2.1 - Percentage of the overall variance explained by each principal component for the navicular - 101
- 3.2.2 - Principal component 1 vs. principal component 2 of all individuals for the navicular - 102
- 3.2.3 - Principal component 1 vs. principal component 3 of all individuals for the navicular - 103
- 3.2.4 - Principal component 1 vs. principal component 4 of all individuals for the navicular - 104
- 3.2.5 - Principal component 1 vs. principal component 5 of all individuals for the navicular - 105
- 3.2.6 - Principal component 1 vs. principal component 12 of all individuals for the navicular - 105
- 3.2.7 - Percentage of the variance explained by each PC using only species mean shapes - 106
- 3.2.8 - Principal component 1 vs. principal component 2 of species means and fossils for the navicular - 107
- 3.2.9 - Principal component 1 vs. principal component 3 of species means and fossils for the navicular - 108
- 3.2.10 - Principal component 1 vs. principal component 5 of species means and fossils for the navicular - 108
- 3.2.11 - Proximal view of the navicular displaying terminology used to describe shape differences - 111
- 3.2.12 - Distal view of the navicular displaying terminology used to describe shape differences - 112
- 3.2.13 - Warp from the *Pan* mean navicular to the *Gorilla* mean - 113
- 3.2.14 - Warp from the *Homo* mean navicular to the *Theropithecus* mean - 115
- 3.2.15 - Warp from the *Pan* mean navicular to *Oreopithecus* - 118
- 3.2.16 - Warp from the *Pongo* mean navicular to *Oreopithecus* - 119
- 3.3.1 - Percentage of the overall variance explained by each principal component for the medial cuneiform - 120
- 3.3.2 - Principal component 1 vs. principal component 2 of all individuals for the medial cuneiform - 121

- 3.3.3 - Principal component 1 vs. principal component 3 of all individuals for the medial cuneiform - 122
- 3.3.4 - Principal component 1 vs. principal component 4 of all individuals for the medial cuneiform - 123
- 3.3.5 - Principal component 1 vs. principal component 5 of all individuals for the medial cuneiform - 123
- 3.3.6 - Percentage of the variance explained by each PC using only species mean shapes for the medial cuneiform - 124
- 3.3.7 - Principal component 1 vs. principal component 2 of species means and fossils for the medial cuneiform - 125
- 3.3.8 - Principal component 1 vs. principal component 3 of species means and fossils for the medial cuneiform - 126
- 3.3.9 - Principal component 1 vs. principal component 5 of species means and fossils for the medial cuneiform - 126
- 3.3.10 - Proximal view of the medial cuneiform displaying terminology used to describe shape differences - 130
- 3.3.11 - Medial view of the medial cuneiform displaying terminology used to describe shape differences - 131
- 3.3.12 - Warp from the *Pan* mean medial cuneiform to *Oreopithecus* - 132
- 3.3.13 - Warp from the *Gorilla* mean medial cuneiform to *Oreopithecus* - 134
- 3.3.14 - Warp from the *Pongo* mean medial cuneiform to *Oreopithecus* - 136
- 3.3.15 - Warp from the *Theropithecus* mean to *Nacholapithecus* - 138
- 3.3.16 - Warp from the *Pan* mean to *Nacholapithecus* - 139
- 3.3.17 - Warp from the *Homo* mean medial cuneiform to OH8 - 141
- 3.4.1 - Percentage of the overall variance explained by each principal component for the medial cuneiform - 142
- 3.4.2 - Principal component 1 vs. principal component 2 of all individuals for the intermediate cuneiform - 143

- 3.4.3 - Principal component 1 vs. principal component 3 of all individuals for the intermediate cuneiform - 144
- 3.4.4 - Principal component 1 vs. principal component 4 of all individuals for the intermediate cuneiform - 145
- 3.4.5 - Principal component 1 vs. principal component 5 of all individuals for the intermediate cuneiform - 145
- 3.4.6 - Principal component 1 vs. principal component 7 of all individuals for the intermediate cuneiform - 146
- 3.4.7 - Principal component 1 vs. principal component 9 of all individuals for the intermediate cuneiform - 146
- 3.4.8 - Percentage of the variance explained by each PC using only species mean shapes - 147
- 3.4.9 - Principal component 1 vs. principal component 2 of species means and fossils for the intermediate cuneiform - 148
- 3.4.10 - Principal component 1 vs. principal component 3 of species means and fossils for the intermediate cuneiform - 149
- 3.4.11 - Medial view of the Intermediate cuneiform displaying terminology used to describe shape differences - 153
- 3.4.12 - Lateral view of the Intermediate cuneiform displaying terminology used to describe shape differences - 153
- 3.4.13 - Warp from the *Gorilla* mean intermediate cuneiform to *Oreopithecus* - 155
- 3.4.14 - Warp from the *Gorilla* mean intermediate cuneiform to *Oreopithecus* - 156
- 3.4.15 - Warp from the *Pan* mean intermediate cuneiform to *Oreopithecus* - 158
- 3.4.16 - Warp from the *Homo* mean intermediate cuneiform to OH8 - 160
- 3.4.17 - Warp from the *Pan* mean intermediate cuneiform to the *Pongo* mean - 162
- 3.4.18 - Warp from the *Homo* mean intermediate cuneiform to the *Theropithecus* mean - 164
- 3.5.1 - Percentage of the overall variance explained by each principal component for the lateral cuneiform - 165

- 3.5.2 - Principal component 1 vs. principal component 2 of all individuals for the lateral cuneiform - 166
- 3.5.3 - Principal component 1 vs. principal component 3 of all individuals for the lateral cuneiform - 167
- 3.5.4 - Principal component 1 vs. principal component 4 of all individuals for the lateral cuneiform - 168
- 3.5.5 - Principal component 1 vs. principal component 5 of all individuals for the lateral cuneiform - 169
- 3.5.6 - Percentage of the variance explained by each PC using only species mean shapes for the lateral cuneiform - 170
- 3.5.7 - Principal component 1 vs. principal component 2 of species means and fossils for the lateral cuneiform - 171
- 3.5.8 - Principal component 1 vs. principal component 3 of species means and fossils for the lateral cuneiform - 172
- 3.5.9 - Medial view of the lateral cuneiform displaying terminology used to describe shape differences - 175
- 3.5.10 - Lateral view of the lateral cuneiform displaying terminology used to describe shape differences - 176
- 3.5.11 - Warp from the *Gorilla* mean lateral cuneiform to *Oreopithecus* - 177
- 3.5.12 - Warp from the *Pongo* mean lateral cuneiform to *Oreopithecus* - 179
- 3.5.13 - Warp from the *Homo* mean lateral cuneiform to OH8 - 181
- 3.5.14 - Warp from the *Pan* mean lateral cuneiform to the *Theropithecus* mean - 183
- 3.6.1 - Percentage of the overall variance explained by each principal component for the first metatarsal - 184
- 3.6.2 - Principal component 1 vs. principal component 2 of all individuals for the first metatarsal - 185
- 3.6.3 - Percentage of the variance explained by each PC using only species mean shapes for the first metatarsal - 186

- 3.6.4 - Principal component 1 vs. principal component 2 of species means for the first metatarsal - 187
- 3.6.5 - Percentage of the overall variance explained by each principal component for the proximal landmarks of the first metatarsal - 188
- 3.6.6 - Principal component 1 vs. principal component 2 of all individuals for the proximal landmarks of the first metatarsal - 189
- 3.6.7 - Percentage of the variance explained by each PC using only species mean shapes for the proximal landmarks of the first metatarsal - 190
- 3.6.8 - Principal component 1 vs. principal component 2 of species means for the proximal landmarks of the first metatarsal - 191
- 3.6.9 - Percentage of the overall variance explained by each principal component for the distal landmarks of the first metatarsal - 192
- 3.6.10 - Principal component 1 vs. principal component 2 of all individuals for the distal landmarks of the first metatarsal - 193
- 3.6.11 - Percentage of the variance explained by each PC using only species mean shapes for the distal landmarks of the first metatarsal - 194
- 3.6.12 - Principal component 1 vs. principal component 2 of species means for the distal landmarks of the first metatarsal - 195
- 3.6.13 - Principal component 1 vs. principal component 3 of species means for the distal landmarks of the first metatarsal - 196
- 3.6.14 - Medial view of the first metatarsal displaying terminology used to describe shape differences - 202
- 3.6.15 - Inferior view of the first metatarsal displaying terminology used to describe shape differences - 202
- 3.6.16 - Warp from the *Pan* mean first metatarsal to the *Gorilla* mean - 204
- 3.6.17 - Warp from the *Pan* mean first metatarsal to the *Pongo* mean - 206
- 3.6.18 - Warp from the *Homo* mean first metatarsal to the *Gorilla* mean - 207
- 3.6.19 - Warp from the *Pongo* mean first metatarsal to the *Theropithecus* mean - 209

3.6.20 - Warp from the *Gorilla* mean proximal first metatarsal to the *Pongo* mean - 211

3.6.21 - Warp from the *Pongo* mean proximal first metatarsal to *Oreopithecus* - 211

3.6.22 - Warp from the *Pan* mean distal first metatarsal to the *Homo* mean - 213

3.6.23 - Warp from the *Pan* mean distal first metatarsal to *Oreopithecus* - 213

List of Tables

- 1.1 - Summary of some diagnostic features of hominoidea - 22
- 1.2 - Summary of the ligamentous anatomy of the ankle - 35
- 2.1 - Bones included for each species - 57
- 3.1.1 - Procrustes distances amongst species mean shapes and fossils for the talus - 95
- 3.2.1 - Procrustes distances amongst species mean shapes and fossils for the navicular - 115
- 3.3.1 - Average Procrustes distance of individuals from species mean and range of Procrustes distances for the medial cuneiform - 133
- 3.3.2 - Procrustes distances amongst species mean shapes and fossils for the medial cuneiform - 134
- 3.4.1 - Procrustes distances amongst species mean shapes and fossils for the intermediate cuneiform - 156
- 3.5.1 - Procrustes distances amongst species mean shapes and fossils for the lateral cuneiform - 180
- 3.6.1 - Procrustes distances amongst species mean shapes for the complete first metatarsal - 203
- 3.6.2 - Procrustes distances amongst species mean shapes for the proximal first metatarsal - 205
- 3.6.3 - Procrustes distances amongst species mean shapes for the distal first metatarsal - 207

1. Introduction

1.2. Background to the topic

The foot and bipedalism have long been the focus of considerable study in the palaeoanthropological literature, and for good reason. The great specialisation of the human foot and its vast difference to the foot of any other primate has prompted an almost continuous body of study into this morphological peculiarity and the unique bipedal locomotor behaviour it facilitates. There is abundant debate surrounding almost every conceivable facet of the evolution of bipedalism; the possible selective pressures and evolutionary advantages which favoured its adoption (e.g. Marzke, 1988; Wheeler 1992; Wall-Scheffler *et al.* 2007), the morphological condition which was the precursor to the first bipeds (e.g. Gebo 1992; Richmond *et al.* 2001; Thorpe *et al.* 2007), the likelihood of various fossil species having been bipedal (e.g. Oxnard and Lisowski 1980; Köhler and Moyà-Solà 1997; Russo and Shapiro 2013), as well as the temporal and geographical implications for the emergence of bipedalism implicit within all of these debates.

The overwhelming focus of research into the evolution of bipedalism is placed on the hominids of the Pliocene and earliest Pleistocene; this is certainly when the most abundant and convincing evidence for bipedalism appears in the fossil record. Although there has still been considerable debate about the bipedal status of the Australopithecines and *Homo habilis*, there is a general agreement that the available postcranial evidence presents a morphology consistent with habitual bipedalism. However, there are also a number of interesting fossils of Miocene age which warrant attention. *Oreopithecus* has been argued to have been bipedal (Köhler and Moyà-Solà 1997; Rook *et al.* 1999) and even to have had a human-like precision grip of the hand (Moyà-Solà *et al.* 1999, 2005; but see Susman 2004, 2005), as well as having been a cercopithecoid (Delson 1986). The bipedal status of *Sahelanthropus* has been proposed (Brunet *et al.* 2002) and contested (Wolpoff *et al.* 2002), a debate made difficult by the fact that only a single heavily distorted skull represents the entirety of the evidence for bipedalism in this genus. *Orrorin* has been generally agreed to have been bipedal to some extent, but debate remains over its phylogenetic placement (Senut *et al.* 2001; Pickford *et al.* 2002; Richmond and Jungers 2008; Almécija *et al.* 2013). *Ardipithecus* displays features of the hip, pelvis, and foot which seem to indicate that it was adapted to some degree of bipedal behaviour, but certainly retained a significant degree of arboreality (Lovejoy *et al.* 2009a; 2009b). Furthermore, what evidence there is for bipedalism in *Ardipithecus* has been contested (Sarmiento 2010; Sarmiento and Meldrum 2011).

The evidence for well-established habitual bipedal behaviour in *Australopithecus* is abundant. This includes skeletal evidence from the pelvis, leg, and foot (e.g. Day and Wood 1968; Latimer *et al.* 1987; Berge 1994; Ward 2002; Ward *et al.* 2011) and archaeological evidence from the Laetoli foot prints (Leakey and Hay 1979; Raichlen *et al.* 2010) allowing us to conclude with some confidence that the acquisition of bipedalism began a considerable time before the emergence of the australopithecines. Thus, it is of great importance to develop a good understanding of the skeletal morphology and locomotor behaviours of apes in the Miocene and the chronology of these adaptations. One of many proposed mechanisms for the acquisition of bipedalism suggested that the development of the rift valley 8Mya in Africa could have been crucial in human evolution (Coppens 1994). Based on the distribution of human fossil remains and modern apes this model proposes that an ape population, ancestral to humans and chimpanzees, was divided into two subpopulations; the chimpanzee lineage on the west side of the rift in the African forest and the human lineage on the east side forced to adapt to life in the developing savannah. However, evidence suggesting that the open habitats of the Pliocene didn't develop until much later cast doubt on this hypothesis (White *et al.* 2009; Conroy and Ponzler 2012) and evidence that bipedalism may not have originated in the African Savannah casts further doubt (Lovejoy *et al.* 2009a, b, c).

It is vital, then, to determine the timing and appearance of bipedalism in the fossil record. *Oreopithecus* has been proposed as a bipedal Miocene ape from Europe, and if this were in fact the case then there are a number of possible scenarios it might entail. These include that the origins of bipedalism may extend much further back in time and we can expect to find other examples of bipedalism in the Late Miocene, or even earlier; *Oreopithecus* may have independently developed habitual bipedal behaviours, in which case the earliest orthograde crown hominoids would have been likely to have had a morphology from which habitual bipedal behaviour could be expected to evolve relatively easily, but one which did not entail habitual bipedalism; *Oreopithecus* represents a sister group to the crown hominoids leading to hominins and had a unique locomotor behaviour which was not derived from the morphological type which gave rise to *Homo*.

At this stage it is clear that there is no obvious linear pattern to the evolution of bipedalism, or morphological features related to it, in contrast to early work on the topic (Keith 1923a, 1923b). All fossils pertinent to this question have a tendency to exhibit some features which indicate bipedal adaptations while lacking others; in some instances bipedal features may be present in an earlier species while being conspicuously absent in later species. The presence of any supposed bipedal adaptation is often accompanied by a number of "ancestral" traits, and the fossils are often damaged,

distorted, or individual or small numbers of bones found in isolation from the whole skeleton. All of these facts make interpretation of the fossil record difficult, particularly as it relates to the emergence of bipedalism. It is especially difficult when dealing with an apparent mosaic pattern of evolution, which is the case for *Ardipithecus* (Lovejoy *et al.* 2009a; b; c) where evidence for the hindlimb may point to a degree of bipedal behaviour while the forelimb points to climbing adaptations, or features of the foot suggest that the last common ancestor of humans and apes had a cercopithecoid-like foot, and that both ape and human feet are derived from this ancestral morphology. Early *Australopithecus* probably incorporated a considerable arboreal component into its behavioural repertoire (Stern and Susman 1983; Green and Alemseged 2012), while later *Australopithecus* seems to have possessed features of its foot conducive to bipedal behaviour as well as arboreality (Clarke and Tobias 1995). In a similar fashion, the OH8 foot attributed to *Homo habilis* has been argued to possess both arboreal and bipedal adaptations (Day and Wood 1968; Oxnard and Lisowski 1980; Harcourt-Smith 2002; DeSilva *et al.* 2010). It is difficult to understand these apparent mosaic morphologies especially when observing isolated material from extinct animals. However, it is reasonable to assume that any perceived “primitive” traits would have formed part of the organism’s adaptation to its environment (Rose 1991); resolution of these issues is often difficult because of the sparse and fragmentary fossil record and the multiple interpretations of this evidence available in the literature.

This study examines the morphology of the medial column of the pedal skeleton of a number of extant genera (*Pan*, *Gorilla*, *Pongo*, *Homo*, *Theropithecus*) and the fossil species of *Oreopithecus* and *Homo habilis* (represented by OH8). Two tarsals of *Nacholapithecus* were included to provide some small insights into the pedal skeleton from which hominoids may have derived. The status of *Oreopithecus* as a biped has been controversial. Some researchers have argued strongly in favour of this proposal (Rook *et al.* 1999) while others have found evidence for bipedalism lacking (Jungers 1988; Sarmiento and Marcus 2000; Susman 2005). This problem has profound implications for our understanding of bipedalism in the fossil record and needs to be resolved. Primarily, the question of bipedalism in *Oreopithecus* is of interest because, if true, it will offer a number of interesting scenarios to the evolution of bipedalism including the possibility that bipedalism, or adaptations conducive to habitual bipedalism, either have a deep origin, prior to the divergence of the human and African ape clades, or that this highly derived and specialised behaviour has evolved independently on at least two occasions. The pedal skeleton of *Oreopithecus* has previously largely been subjected to qualitative analysis. To address these questions here a geometric morphometric approach is applied to the pedal skeleton in order to objectively quantify the similarities of

Oreopithecus to some extant primates in order that reconstruction of likely function of the foot can be determined.

1.3. Structure and aims of the thesis

The thesis is divided into five sections. The first section introduces the topic and provides relevant background information to frame the question. This begins with a discussion of what hominoids are; what morphology defines Hominoidea. The similarities and differences amongst the extant hominoids are discussed and their relationships to one another are considered. Then, an overview of the evolution of the hominoids is presented. This is not meant to be an exhaustive study of hominoid phylogeny, so only the most well-represented and morphologically derived taxa will be considered. This will give some context to the place of *Nacholapithecus* and *Oreopithecus* in the superfamily. Similarly, a brief overview of Plio-Pleistocene taxa will be presented to give some context to the emergence of obligate bipedalism and the placement of *Homo habilis*. Following this, a functional anatomy of the foot will be presented. This will be split into two sections. The first is a functional anatomy of the human foot and the second is a comparative functional anatomy of the primate foot, which focuses on the differences between great apes and humans primarily, but also considers the Old-World monkey foot. Finally, a brief summary of the positional behaviour of the primates included in the study will be given.

The second section of the thesis presents the materials and methods used to address the question. This begins with a subsection detailing all of the primate material used in the study. Then, the procedures for all of the methods used in the study are outlined. First, an overview of structured light scanning and its application in this study is presented. Second, the procedure for placing landmarks on the specimens is described and then the landmarks and semilandmarks used in the study are shown. Finally, the technique for analysing the landmark data is explained. The third section of the thesis is the results of the analysis, which are presented in subsections relating to each individual bone used in the study. The first subsection presents the results of principal components analyses and the similarities between species. Then the results of statistical tests are considered. Finally the differences in shape explained by the principal components are explored. The fourth section discusses the results. This section is divided into subsections relating to each bone. In each subsection the findings for the extant species are discussed first, and then in the context of this the

results for the fossil species are discussed. The final section summarises all the findings of the thesis and considers the function of the medial column of the foot of *Oreopithecus* and other fossil species.

The thesis aims to objectively describe the morphology of the medial column of the foot in a number of primate species, primarily apes, but also including one monkey species. The similarities and differences between taxa are considered and the species' morphologies are then considered in light of their known positional behaviour. This allows the identification of particular morphological traits which feature in the pedal skeleton of primates known to behave in certain ways. Thus, by considering the shapes of the bones of fossil species, and the ways in which they differ from, or are similar to, extant species it is possible to make reasonable inferences regarding the function of the foot in these extinct species. The three fossil taxa included each provide a different insight to the evolution of the foot. *Nacholapithecus*, as a stem hominoid, allows a consideration of the pedal morphology which preceded the emergence of the "true" hominoids. Comparison with a terrestrial monkey is particularly relevant because it is from a pronograde, quadrupedal primate that hominoids evolved. *Oreopithecus* is of obvious interest due to the controversy it has caused since its discovery. Moreover, the extraordinary claims which have been made about its positional behaviour, particularly as this relates to its foot, have received very little attention in the literature. This is surprising as the pedal skeleton of *Oreopithecus* is one of the best represented for Miocene Hominoidea. The inclusion of OH8 is of interest for two reasons. First, it allows the consideration of the likelihood of bipedal behaviour in this fossil and the pedal morphology which was present at the beginning of obligate bipedalism in the human lineage. Secondly, it has appeared in a similar study which will allow comparisons between the two sets of results, and additionally serve as a yardstick against which to measure the reliability of this study.

1.4. *Oreopithecus*

Oreopithecus is a well-known, well-studied, and controversial primate from Late Miocene lignitic deposits of Italy (Jungers 1987; Rook *et al.* 2011; Matson 2012). *Oreopithecus* was first discovered in 1872 and since its discovery has caused continuous controversy (Delson 1986). There are a number of mines in Tuscany that have yielded *Oreopithecus* material: for example, Monte Bamboli (from which the specific name *O. bambolii* is taken), Serrazano, Ribolla, and Casteani. It is also known from a single site in Sardinia: Fiume Santo (Rook *et al.* 1996; Casanovas-Vilar *et al.* 2011). However, overall the geographical distribution of *Oreopithecus* is limited to southern Tuscany. *Oreopithecus* forms part

of a unique fauna that existed in the Miocene Tusco-Sardinian palaeobioprovince known as the “Maremma Fauna” (Casanovas-Vilar *et al.* 2011), which exhibited unusual morphological affinities, predominantly of the dentition, indicating that the fauna was insular in nature. This region provided a refugium during the Late Miocene offering protection to *Oreopithecus* and other related fauna during a period of mass extinction throughout Europe (Begun 2007). Thus, *Oreopithecus* was the only European hominoid to survive beyond this mass extinction (Matson *et al.* 2012). The known time range of *Oreopithecus* fossils is 8.3 – 6.7 Mya (Rook *et al.* 2011) which makes its latest representatives roughly contemporaneous with *Sahelanthropus tchadensis* (Brunet *et al.* 2002; Zollikofer *et al.* 2005). The dating of the deposits from which *Oreopithecus* derives was done exclusively by biostratigraphic sequencing until the 1970’s at which point a single radiometric date became available with which to apply a fine calibration to the biostratigraphic data (Azzarolli *et al.* 1986). Subsequently, better understanding of the magnetostratigraphy of the area has permitted relatively accurate dating by combining a number of lines of evidence (Rook *et al.* 2011).

Oreopithecus has been known in the palaeoanthropological literature for over a century and agreement on its phylogenetic placement has proven incredibly difficult to achieve. The various proposals for the status of *Oreopithecus* have included pig, cercopithecoid, hominoid, dryopithecine, pongine and hominine. (Harrison 1986; Moyà-Solà and Köhler 1997; Gentili *et al.* 1998; Begun 2007), and it has long been suggested to have possessed bipedal features of its postcranium (de Terra 1956; Straus 1957), but it is generally accepted now that the postcranium represents a general hominoid plan (Harrison 1986; Begun 2002). Indeed, assessment of the body size and limb proportions of the *Oreopithecus* skeleton place it closest in size and proportion to female *Pongo* (Jungers 1987). The thorax of *Oreopithecus* is broad and the clavicle is long and robust; the scapula has a deep glenoid fossa and the humeral head is large (Begun 2002; 2007). These features of the chest and shoulder are strongly indicative of an increased range of movement of the arm above the head, and laterally beyond the parasagittal plane, probably in suspensory postures and vertical climbing on large diameter supports (Harrison 1986; Sarmiento 1987). The distal humerus also resembles that of hominoids in the morphology of the trochlea and capitulum, as well as the olecranon fossa. The well-developed keel of the lateral trochlea border is known to stabilise the elbow throughout a large range of flexion and extension, as well as rotation, and is crucial to the climbing behaviour exhibited by great apes (Harrison 1986). The ulna similarly preserves evidence that the elbow was hominoid-like in its dimensions and form, adapted to resisting large transverse stresses at the elbow joint (Knussman 1967). The trochlea notch has a pronounced keel which aligns *Oreopithecus* closely with *Pongo* and *Pan*, strongly indicating that it was a highly arboreal species (Drapeau 2008).

The hand of *Oreopithecus* provides further support for its hominoid status and adaptation to climbing. The distal radius and ulna preserve evidence of mobility and the styloid process of the ulna was likely extended, which is a hominoid synapomorphy. There is evidence for a pronounced ligamentous attachment on the scaphoid (the radiocarpal ligament) which secures the hand to the forearm, a key adaptation for climbing and suspensory behaviours, and a known hominoid feature (Sarmiento 1987). The os centrale is not fused to the scaphoid, which is a primitive hominoid condition, though one that is shared with *Pongo* (Harrison 1986). This indicates that *Oreopithecus* lacks the derived condition of African apes and *Homo* which secures the wrist in extension, and is thought to be a knuckle-walking adaptation (Richmond and Strait 2000; Richmond *et al.* 2001). The metacarpals are long and slender and are highly curved supporting the arboreal behaviour of *Oreopithecus* (Harrison 1986). It has been suggested that *Oreopithecus* possessed a hand capable of human-like precision grasping based on evidence relating to the proportions of the thumb and index finger (Moyà-Solà *et al.* 1999). Additionally, the presence of a clear attachment site for the flexor pollicis longus muscle was argued to have been evident and to indicate human-like pad-to-pad gripping between the thumb and index finger in *Oreopithecus* (Moyà-Solà *et al.* 2005), and the distal pollical phalanx has been argued to preserve evidence of an increased ability to manually manipulate (Almécija, S. *et al.* 2014). Susman (2004) finds the reconstruction of the hand by Moyà-Solà *et al.* (1999) unconvincing, suggesting that they have mischaracterised bones and made mistakes in measurement to conclude that the thumb is long relative to the index finger. Susman (2005) also criticised their interpretation of skeletal markers on the carpal bones of *Oreopithecus* and their assessment of the insertion sites of thenar musculature. Marzke and Shrewsbury (2006) argue that both Susman and Moyà-Solà *et al.* are mistaken in their identification of skeletal correlates of the insertion of flexor pollicis longus. Their studies found that the insertion site, as determined from dissection of a number of primate species, is highly variable. Thus, they urge caution in reconstructing muscular and ligamentous attachments in fossil species. However, the prevailing view is still that *Oreopithecus* was not in possession of a precision-grasping hand (Begun 2007).

The spinal column of *Oreopithecus* also strongly indicates its hominoid affinities. The acute costal angle of the thoracic vertebrae is indicative of hominoid-like ventral placement of the spine which is typical of orthograde postures (Sarmiento 1987). The reduction in the length of the lumbar spine, and increase in the sacral vertebrae, points to a diagnostic hominoid condition in which the lower back is short and stiff. It has been suggested that the lumbar spine preserves evidence of bipedalism on the basis of increasing distance between postzygapophyseal facets from cranial to caudal

(indicating a human-like increase in size from the first to last lumbar vertebra) and dorsal wedging of the lumbar bodies indicative of lordosis (Köhler and Moyà-Solà 1997). However, the validity of the reconstruction of these metrics from crushed remains has been questioned and alternative, ape-like morphology has been presented (Russo and Shapiro 2013). The pelvis has also been argued to display adaptations to habitual bipedal behaviours in *Oreopithecus*. This argument has been advanced based on external morphology such as a short pubis, and short ischium with large ischial spine, which is interpreted as evidence for a human-like sacrospinous ligament to securely anchor the sacrum (Köhler and Moyà-Solà 1997). The internal architecture of the pelvis has also been used to infer habitual bipedal behaviour in *Oreopithecus*. The orientation and concentration of cancellous bone throughout the pelvis, as revealed in x-ray images, is suggested to be similar to that of humans indicating that high levels of stress are applied through the acetabulum in a manner similar to *Homo* (Rook *et al.* 1999). However, these features have also been argued to be present regularly in highly arboreal primates, including *Pongo* and even non-hominoids (Wunderlich *et al.* 1999).

The lower limb of *Oreopithecus* is also well represented and, unsurprisingly, has been the cause of some controversy. The known femora are unfortunately crushed and difficult to interpret but what remains indicates a hominoid pattern. A globular and distinct femoral head, high angle of the neck which rises above the level of the greater trochanter, and clear fovea capitis (Harrison 1987). These features are all associated with a high degree of mobility at the hip. The distal femur has been proposed to bear evidence of a carrying angle which would be strong evidence for bipedal behaviour (Köhler and Moyà-Solà 1997) but the distortion of the fossil in this location makes it difficult to interpret (Harrison 1987). The foot is well preserved for *Oreopithecus*. Szalay (1975) argued that the subtalar joint of *Oreopithecus* was cercopithecoid-like. However, later Szalay and Langdon (1986) argued that the foot of *Oreopithecus* most resembled that of *Pan*, but found certain features of the foot to imply that the similarities were not shared derived features, but a result of convergence due to similar demands. More recently, Köhler and Moyà-Solà (1997) have argued that the foot of *Oreopithecus* was highly derived and resembles *Gorilla* and *Homo* in terms of foot proportions, but differs from *Gorilla*, in which the increased ratio of power arm to load arm is due to its massive size. They cite the small cuboid, large articulations of the intermediate and lateral cuneiforms and wedging of the base of the second metatarsal between the medial and lateral cuneiforms as evidence that force transmission is increased on the medial side of the foot. The general pattern they propose is of reduced mobility and grasping ability of the foot in *Oreopithecus*. Some support for this view can be found in the pattern of robusticity of the metatarsals. *Oreopithecus* most resembles *Homo* and *Gorilla* with respect to metatarsal robusticity which could indicate that *Oreopithecus* was adapted to a highly terrestrial habitat (Riesenfeld 1975). To date, no objective

quantitative assessment of the shape and morphological similarities of the foot bones of *Oreopithecus* has been conducted and this clearly bears great significance on interpretations of foot function and locomotion.

1.5. Overview and evolution of Hominoidea

Given that *Oreopithecus* is the main focus of this study, and that the status of *Oreopithecus* as a hominoid has been disputed by a number of researchers (Szalay and Delson 1979; Rosenberger and Delson 1985; Delson 1986), it is useful to have an understanding of extant hominoids as well as the evolutionary history of the superfamily Hominoidea. Therefore, this section will briefly summarise the characteristics and phylogenetic relationships of the extant hominoids before summarising the evolutionary relationships and key features of some of the most relevant fossil hominoids beginning with the split of the superfamily from the cercopithecoidea, and then discussing the most well-known and relevant fossils and the key morphological changes over time, as well as key controversies. This will culminate in a section discussing *Oreopithecus* more specifically; discussing the age, geological and palaeobiological context, functional and evolutionary relationships, and controversies surrounding the phylogeny and morphology of *Oreopithecus* to provide some background and context to its inclusion in this study. To conclude the section a brief overview of the Plio-Pleistocene hominins is provided to give some evolutionary context to *Homo habilis* and the emergence of modern humans.

1.5.1. Extant Hominoidea

The superfamily Hominoidea is currently recognised to have two extant families within it, Hylobatidae (containing gibbons and siamangs) and Hominidae (containing *Pan*, *Gorilla*, *Pongo*, and *Homo*), which split from Cercopithecoidea 23-28 Mya (Ruvolo *et al.* 1994; Wood and Richmond 2000; Groves 2001; Crompton *et al.* 2008; Raaum 2015). The previous classification had used Hominidae exclusively for humans and Plio-Pleistocene fossil species deemed more closely related to humans than other species, while grouping *Pan*, *Gorilla*, and *Pongo* together under Pongidae (Livingstone 1962; Radinsky 1973; Kramer 1986). The more recent classification has been adopted to take into account the apparent closer relatedness of African apes and *Homo* to the exclusion of *Pongo*, requiring them to be placed into their own subfamily the Homininae. And the closer relatedness of humans and chimpanzees places them in their own tribe Hominini to the exclusion of gorillas

(Hayasaka *et al.* 1988; Conroy 1990; Pilbeam 1996; Lewin 2005) (but see Grehan and Schwartz 2009 for an alternate view which places *Homo* and *Pongo* in their own clade distinct from the African apes, or Tuttle (2006) for a view which reserves Hominidae for humans and their closest relatives to the exclusion of all great apes.) There are also a number of fossil families which are included in Hominoidea as part of a classificatory scheme to take into account morphological traits which align them clearly with Hominoidea while simultaneously respecting differences which exclude them from extant families and subfamilies (Begun 2002). Considerations such as these clearly bear some relevance to this study given that the phylogenetic position of *Oreopithecus* has been the cause of some controversy historically; its placement in Hominoidea has been disputed as well as its relative placement within the superfamily (Delson 1986).

Hominoids are separated from other primates on the basis of a series of derived characteristics related to both the cranium and postcranium. However, the hominoids are more easily defined on the basis of postcranial characters. As Harrison (1987) points out, Hylobatidae retain a more primitive craniodental anatomy which bears a good likeness to the hypothetical morphotype from which all subsequent cercopithecoid and hominoid clades have derived, and the fact that dental characters are more prone to homoplasy than postcranial characters (Finarelli and Clyde 2004) makes postcranial morphology a better indicator of hominoid membership. Hylobatids share with other hominoids clearly derived features of the postcranium which more readily permit the construction of the superfamily. However, there are still traits of the cranium and dentition of Hylobatidae that are thought to be synapomorphic with other members of Hominoidea (Table 1.1). Hylobatidae are distinguished from the rest of Hominoidea on the basis of characters relating to brachiation. The arms are extremely long and slender compared to the legs and both are elongated relative to the trunk, the hand is long, particularly the metacarpals and digits 2-5, and the wrist is highly mobile with narrowing rather than expansion of the radius and ulna distally, the shoulder joint is highly mobile with a long scapula and humeral head which faces dorsally (Szalay and Delson 1979; Geissman 1995; Chatterjee 2009).

The family Hominidae contains all of the extant great apes, including humans. It is separated from the Hylobatidae on the basis of the unique derived traits of Hylobatidae, some of which are listed above (e.g. long arms with highly mobile shoulder joint), and synapomorphies shared between the extant hominids to the exclusion of Hylobatidae. The shared derived traits of Hominidae include shortening of the ulna styloid process (which is more pronounced in *Gorilla*, *Pan*, and *Homo*), an increased size of the acetabular fossa, a broadening of the humeral trochlea, tibialis posterior does

not insert onto the first digit, supraorbital tori are present with a more strongly developed glabella, robust mandible, deep mandibular symphysis and molars with thick enamel (Andrews and Martin 1987; Shoshani *et al.* 1996; Finarelli and Clyde 2004). Within Hominidae *Gorilla*, *Pan*, and *Homo* (Homininae) form a monophyletic group which excludes *Pongo* and its closest relatives (Ponginae) (Andrews 1992).

Craniodental characters	Tubular tympanic
	Broad nasal aperture
	Broad palate
	Broad interorbital width
	Prominent brow ridges and glabella
	Deep mandible
	Simple molars with Y-5 pattern
Postcranial characters	Long clavicle
	Broad sternum
	Long forelimb relative to hindlimb
	Short, inflexible trunk
	Dorsally placed scapula; long vertebral border
	Cranially oriented glenoid
	High humeral torsion
	Spool shaped distal humerus
	Short olecranon process of the ulna
	Sacralisation of caudal lumbar vertebrae
	No tail
	Highly mobile hip
	Broad femoral condyles
	Short, broad talar neck
	Robust, divergent and mobile hallux

Table 1.1. Summary of some diagnostic features of Hominoidea. (Sources: Andrews and Martin 1987; Harrison 1987; Shoshani *et al.* 1996; Fleagle 1999; Finarelli and Clyde 2004; Lewin 2005; Nystrom and Ashmore 2008)

The systematics of Hominoidea have caused a great deal of controversy (Cela-Conde 1998) and numerous classificatory schemes have been proposed to accurately describe the evolutionary relationships within the superfamily (Szalay and Delson 1979; Goodman *et al.* 1994; Ruvolo *et al.* 1994; Cameron 1997; Strait and Grine 2004; Bjarnason *et al.* 2011). The problem is difficult to resolve to the satisfaction of all researchers due to the conflicting results often found when different criteria are used to construct these phylogenies. The evidence from molecular data is not obviously concordant with morphological data (but Shoshani *et al.* (1996) have attempted to address this problem) and the craniodental evidence is often at odds with postcranial evidence (Finarelli and Clyde 2004). Therefore, to properly construct phylogenies using morphological data it is prudent to use very large numbers of both craniodental and postcranial characters, as well as soft tissue data (e.g. Andrews and Martin 1987; Finarelli and Clyde 2004). This study follows the current most popular system, outlined in Figure 1.1 for the phylogeny of the extant hominoids.

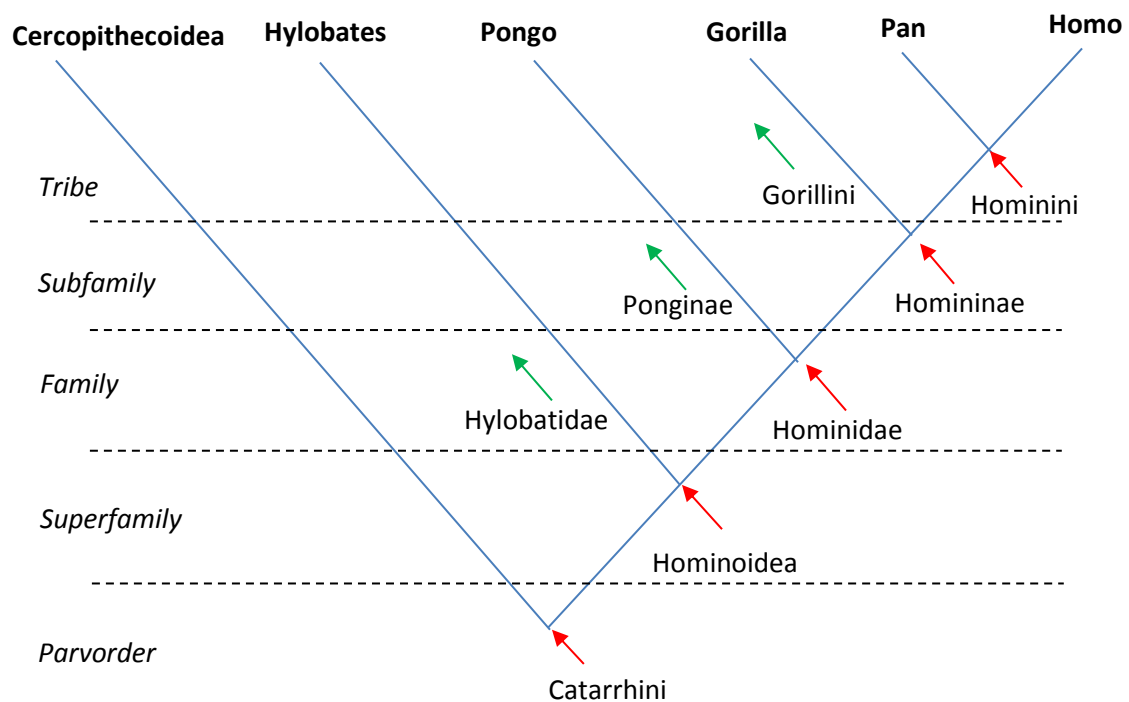


Figure 1.1. Generally accepted taxonomic ranking of the extant hominoid genera. Red arrows indicate assignments which apply to the nodes of the cladogram and thus affect each genus derived from it. Green arrows indicate rank assignments which apply only to the genera associated with that particular branch.

1.5.2. Miocene fossil Hominoidea

There is a hiatus in the African hominoid fossil record after *Kenyapithecus*, *Equatorius*, and *Nacholapithecus* which lasts until the Late Miocene. During this same time period there is a flourishing of hominoid taxa throughout Eurasia. These taxa are the first indisputable hominid (specifically, related to the *Homo*, *Pan*, *Gorilla* clade) fossils, bearing a large number of derived traits with the extant Hominidae in craniodental and postcranial morphology making it easier to differentiate between Homininae and Ponginae. The dryopithecines are known mostly from Western Europe and span the Late Miocene. The relationships of these primates is difficult to understand and subject to the typical splitting vs grouping problem, there are a number of different proposed schemes for classifying the known material and the following is a very general overview of some of the relevant material. *Dryopithecus fontani* is a Middle Miocene representative of the group known from France, and dated to the Middle Miocene based only on biostratigraphy (Begun 2007). There is very little material known for the species but the remains share derived hominid morphology of the dentition such as large incisors and equally sized molars (Moyà-Solà *et al.* 2009) and of the humerus, such as flat and broad olecranon fossa, bicipital groove placement indicative of high torsion, and a broad mediolateral dimension while being flat anteroposteriorly (Begun 1992).

Pierolapithecus is known from Spain and dated to around 13 Mya. There is a well preserved partial skeleton which illustrates that Hominid orthograde posture was well-established in Middle Miocene Eurasia (Moyà-Solà *et al.* 2004). The lumbar spine preserves evidence of a short and stiff lower back, and the ribs indicate that the species had a broad ribcage (Moyà-Solà *et al.* 2004). The carpals and manual phalanges have also been argued to be derived towards the extant hominid state, there is no direct contact between the ulna and triquetrum and the digits may have been adapted to suspensory behaviour (Deane and Begun 2008) although this is contested (Alba *et al.* 2010). There are cranial features such as the high zygomatic root, facial prognathism and large first molar size, which have additionally been used to argue for the hominid status of *Pierolapithecus* (Moyà-Solà *et al.* 2004). However, while the presence of many derived features places *Pierolapithecus* within Hominidae, there are primitive traits of the skeleton which warrant its separation at the generic level from later Miocene dryopithecines such as *Hispanopithecus* (Begun 2007).

Hispanopithecus is a Late Miocene hominoid dated to around 10 Mya from Spain. There are two proposed species, *H. crusafonti* and *H. laietanus*, although *H. crusafonti* is known only from isolated

teeth and fragmentary palatine and mandibular remains. However, the morphology of the remains is sufficient to warrant their placement with the dryopithecines (Begun 1992a). *H. laietanus* provides more material and several postcranial elements (Moyà-Solà and Köhler 1996). *H. laietanus* preserves evidence of well-developed suspensory adaptations such as elongated forelimb with long powerful digits with a short hindlimb and short, stiff lower back (Moyà-Solà and Köhler 1996). *Rudapithecus* was a contemporary dryopithecine from Eastern Europe and possessed many of the same derived adaptations as *H. laietanus* (Kordos and Begun 2001). The high base of the zygomatic, lack of contact between ulna and triquetrum, long curved phalanges with strong muscular attachments, all indicate hominid-like adaptations for suspension (Begun 2007).

The first clear fossil Ponginae are found from Miocene deposits in Eurasia, and referred to the genus *Sivapithecus* (Raza *et al.* 1983). It is dated to around 10-7 Mya and is thought to contain three species, largely separated through time (Begun *et al.* 2012). The craniodental remains are strikingly pongine-like (Pilbeam 1982; Kelley 2002). However, the postcranial remains have caused some controversy because there are a number of primitive characteristics of the postcranium despite the highly derived, and clearly pongine, cranium. The humerus of *Sivapithecus* has been suggested to have been cercopithecoid-like, resembling something close to *Proconsul* (Kelley 2002; Madar *et al.* 2002). The bicipital groove suggests a posterior placement of the head and the distal humerus presents a mosaic of features which may indicate hominoid-like stability but are not clear in their expression (Begun 2005). Features of the wrist also give conflicting evidence, the first metacarpal seems to have been similarly adapted to *Pan* while the hamate seems to represent the morphology of a general anthropoid (Spoor *et al.* 1991). The overall locomotor adaptation of *Sivapithecus* has even been suggested to resemble knuckle-walking based on the similarities of the hamate and capitate to extant apes (Begun and Kivell 2011). *Sivapithecus* presents a difficult problem in the systematics of fossil Hominidae. If it truly represents an early pongine then the postcranial synapomorphies of extant great apes would have to have arisen through parallel evolution. On the other hand, if *Sivapithecus* is primitive and not representative of the pongines then its facial similarities with extant *Pongo* must be explained as parallelisms. Neither scenario is particularly easy to explain (Cameron 1997; Young 2003). Figure 1.2 presents a possible phylogeny of Miocene Hominoidea.

There are numerous other taxa known throughout the Miocene in both Africa and Eurasia. This is not the correct place to give an extensive overview of the Miocene Hominoidea, but a brief overview is useful to give some context to Miocene hominoids included in this study, especially *Oreopithecus* (see below). The last European hominoids are known from deposits dating 9-8 Mya from the

Mediterranean. There is a general west-east disappearance of forest adapted forms throughout Eurasia which is coincident with the appearance of Eurasian forms in Africa. This is part of a period of increasing dryness known as the Vallesian mammal succession which saw a shift from forested and highly wooded environments to open bushy vegetation in Europe (Agustí *et al.* 1997; Merceron *et al.* 2010). During this time all hominoid taxa seem to have migrated south of the tropic of cancer (Begun 2007). Thus it appears that hominoids expanded into Eurasia from Africa during the Middle Miocene and then migrated back into Africa during the Late Miocene when evidence for Hominidea appears again in Africa.

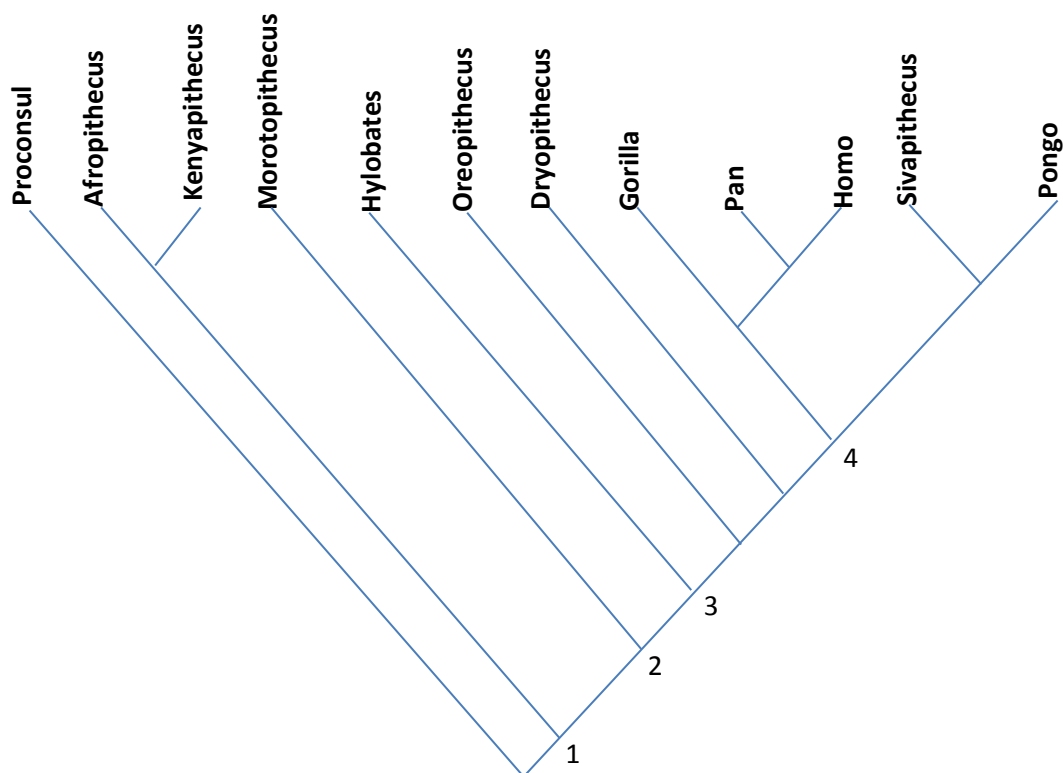


Figure 1.2. Possible phylogenetic relationships of Miocene hominoids (adapted from Finarelli and Clyde 2004). 1 = the stem hominoid node. 2 = crown hominoid node. 3= Split of Hylobatidae and Hominidae. 4 = Split of Homininae and Ponginae.

The earliest hominid to appear in Africa following the hiatus from the Middle Miocene is *Sahelanthropus tchadensis* (Brunet *et al.* 2002). *Sahelanthropus* is known from Late Miocene deposits in Chad. It has been dated biochronologically to between 6-7 Mya (Vignaud *et al.* 2002) and forms part of a fauna associated with forest, savannah, and aquatic environments. It is known only from cranial and dental remains (Brunet *et al.* 2002; 2005). The canines are smaller and seem to lack a

honing complex which separates *Sahelanthropus* from all extant great apes, and there are numerous features which are advanced to distinguish it from each extant and fossil genus on a case by case basis (Brunet *et al.* 2002). Most interestingly, evidence for habitual bipedal behaviour is present in the cranium. The anterior placement of the foramen magnum relative to the bicarotid chord, unlike the much more posterior placement in extant apes, is argued to be evidence for bipedalism (Brunet *et al.* 2002) but this has been disputed, as has the interpretation of dental characters as being derived (Wolpoff *et al.* 2002). A virtual reconstruction of the cranium also revealed that the plane of the foramen magnum was approximately perpendicular to the orbital plane (Zollikofer *et al.* 2005), a feature which is symptomatic of bipedalism in humans, and also known from other early hominins.

Shortly after *Sahelanthropus* comes the appearance of *Orrorin* in the fossil record. *Orrorin* was discovered in Kenya (Senut *et al.* 2001) and has been dated to 6-5.7 Mya using radiometric and magnetostratigraphic methods (Sawada *et al.* 2002). Several fossils were recovered including partial mandibulae and dentition, three partial femora and a partial humerus (Senut *et al.* 2001). The dental and mandibular remains are argued to have been hominin in form (Senut *et al.* 2001) and the femora are argued to have displayed bipedal adaptations, and could reveal that *Orrorin* was a short and light-weight primate (Nakatsukasa *et al.* 2007). It has been argued that the femora of *Orrorin* are most similar in form and function to *Homo* and *Australopithecus* in displaying such features as a groove for obturator externus, lengthened and anteroposteriorly compressed neck of the femur, and a greater proportion of cortex deposited inferiorly in the neck (Pickford *et al.* 2002; Galik *et al.* 2004; Bleuze 2012). However, while other researchers generally agree that the femora display signs of bipedalism, they question whether *Orrorin* represents the beginnings of the human lineage and whether it is as derived as *Australopithecus* (Ohman *et al.* 2005; Richmond and Jungers 2008; Almécija *et al.* 2013).

Finally, at the very end of the Late Miocene *Ardipithecus* is present in the fossil record of Ethiopia. The genus was originally erected for Pliocene aged remains (White *et al.* 1994) but earlier material has since been recovered and deemed sufficiently similar to also be designated as *Ardipithecus* (Haile-Selassie 2001). A fairly complete partial skeleton of *Ardipithecus* was recently discovered which vastly increased our understanding of this genus. The partial skeleton has been dated to 4.4 Mya based on radiometric dating and biostratigraphy, and the environment has been suggested to have been relatively cool and wooded (WoldeGabriel *et al.* 2009). The cranium of *Ardipithecus* has been reconstructed from highly fragmentary remains, but is suggested to be unlike extant chimpanzees even though it is more primitive in morphology to *Australopithecus*. The shorter

basicranium, shorter face with less pronounced prognathism, and weakly developed supraorbital tori are features which are derived towards the *Australopithecus* condition (Suwa *et al.* 2009). The more laterally facing ilia and presence of an anterior inferior iliac spine provide evidence that the musculature of the hip was derived to reduce side to side movement of the centre of gravity during terrestrial bipedal walking (Lovejoy *et al.* 2009b). And the foot preserves evidence of adaptations to increase the rigidity of the foot which are ancestral traits found in old world monkeys, for example the os peroneum is present and the fibularis longus tendon runs oblique to the tarsometatarsal joints (Lovejoy *et al.* 2009a). The overall anatomy of the skeleton of *Ardipithecus* has prompted the discoverers to conclude that it represents the first incontrovertible evidence for the human lineage, but also that preconceptions that humans are derived while apes are primitive are no longer tenable. The apes have evolved many unique skeletal characters which were once thought primitive (Lovejoy 2009). There are, of course, the customary dissensions from these interpretations which find features such as the short lower limb and long toes of *Ardipithecus* incompatible with habitual bipedalism (Sarmiento 2010; Sarmiento and Meldrum 2011).

1.5.3. Plio-Pleistocene Hominoidea

The latest Miocene and earliest Pliocene mark a point in human evolution where a greater degree of 'hominisation' is observed. *Sahelanthropus*, *Orrorin* and *Ardipithecus* are the first specimens to show significant departure from the ape-like anatomy towards an anatomy that can be considered more australopithecine like in some regards, though this is the subject of some debate. The first appearance of *Australopithecus* marks an increase in cranial capacity, adaptations to at least habitual bipedalism, if not obligatory, and features of the cranium unlike those of African apes such as reduced prognathism and canine size (White 2002; Crompton *et al.* 2008; Suwa *et al.* 2009). Features such as these are quite reliable indicators of hominin status, particularly increased cranial capacity. The postcranium has been much more ambiguous prompting different reconstructions of positional behaviour in Pliocene forms.

The *Ardipithecus* partial skeleton only very slightly (in geological terms) predates the first known occurrence of *Australopithecus*. The earliest known species of *Australopithecus* (*A. anamensis*) is from Kenya and radiometrically dated to 3.8-4.2 Mya (Leakey *et al.* 1998; C. Ward *et al.* 1999). The morphology of *A. anamensis* is more primitive than later australopithecines in all regards, but more derived than earlier hominids and extant apes. *A. anamensis* is a thick enamelled hominid and this

has been put forward as a derived trait distinguishing this taxa (and later *Australopithecus*) from *Ar. ramidus* and African apes, however, thick enamel was prevalent in the Miocene hominoids also, and so may actually be plesiomorphic (C. Ward et al. 1999). The tibia displays evidence that it was clearly adapted for bipedality, the shaft is vertically oriented relative to the facet for the talus, morphology of the condyles is similar to *A. afarensis* and there is a marked depression for the pes anserinus tendon insertion (C. Ward et al. 2001). *A. anamensis* and *A. afarensis* probably constitute a continuous evolutionary lineage (Kimbel 2015).

A. afarensis occurs 3.7-3 Mya across eastern Africa (Kimbel & Deleuzene 2009) and bears an unusual mosaic of postcranial characters. It is quite evident that *A. afarensis* moved bipedally when on the ground as attested to by various different sources of evidence (Kimbel 2015). Yet the species still preserves evidence of arboreal adaptations also, and much of the discussion has focussed on the extent to which *A. afarensis* was arboreal (Stern and Susman 1983). The species is unique in its cranial morphology, it has a prognathic snout but almost vertical mandibular symphysis. This is in contrast to humans who have a vertical snout and symphysis, and to *A. anamensis* and African apes that have an inclined snout and symphysis (Kimbel & Deleuzene 2009) this is probably an adaptation to heavy chewing when considered alongside extensive attachments for temporalis. Postcranially *A. afarensis* is known to have been bipedal, but has preserved some ape-like features associated with arboreality. For example a short hindlimb as in African apes, a more cranially directed glenoid fossa and ape-like muscle attachment areas (Stern & Susman 1983; Stern 2000; C. Ward 2002).

Some researchers have argued that *A. afarensis* would have walked with a 'bent-hip, bent-knee' gait, in the same manner that chimpanzees walk bipedally (Stern & Susman 1983). However, other authors have argued that *A. afarensis* would have been capable of efficient human-like striding bipedalism (Nagano et al. 2005); or even that the ape morphology of the spine and pelvis does not represent the primitive condition and therefore a bent-hip, bent-knee gait is a synapomorphy of the African apes (Lovejoy & McCollum 2010). There is also direct evidence for fully human-like erect bipedalism in *A. afarensis* from the fossil footprints at Laetoli, Tanzania. Comparing footprints made by humans in sand during both fully erect and bent-hip, bent-knee postures, and chimpanzee prints, it has been demonstrated that the footprints from Laetoli, made by *A. afarensis* most closely resemble human-like fully erect bipedal gait (Raichlen et al. 2010; Crompton et al. 2011). It is generally believed that *A. anamensis* and *A. afarensis* are 'chronospecies', or *A. afarensis* was derived from the anagenesis of *A. anamensis*, or even more simply put, *A. anamensis* and *A. afarensis* are in fact the same species, separated only by time (Haile-Selassie 2010). It is known that the tibia of *A.*

anamensis exhibited features similar to those known for *A. afarensis* such as a vertical orientation of the shaft relative to the talar articular surface. Therefore, there is good reason to believe that there had been at least 0.5Ma of selection for effective, terrestrial bipedal walking, and so we might expect that the early australopiths were actually very well adapted to walking bipedally (Crompton et al. 2008).

All later species of Pliocene hominid are well adapted bipeds, although there is still some disagreement over the extent that arboreal behaviours played. For example, a partial skeleton of *A. africanus* from South Africa has been interpreted both as displaying a significant adaptation to arborealism (Clarke & Tobias 1995) while others have interpreted the remains as belonging to those of a habitual biped (Harcourt-Smith & Aiello 2004). There has even been a suggestion that walking in *A. africanus* would have been more human-like than in *A. afarensis*, based on pelvic morphology (Haeusler 2003). In its cranium, *A. africanus* has been difficult to define phylogenetically because it lacks any unique apomorphies. Instead it shares various primitive characters with *A. afarensis* and various derived characters with robust australopithecines and *Homo* (Lockwood and Tobias 1999). There is also evidence that the morphology of the mandibular ramus of *A. afarensis* closely aligns it with the robust australopithecines, being adapted for heavy chewing (Rak et al. 2007).

The robust australopithecines (or paranthropines) occur a little later than the australopithecines discussed above. They are uniquely derived away from the condition of other australopithecines in their adaptation for heavy chewing. This is evident in the megadontia of the molars, molarisation of the premolars and extensive attachments on the cranium for the chewing musculature (Walker et al. 1986). In fact, megadontia can be said to progress gradually from *Ar. ramidus* to the hyper-robust australopithecines, a trend which is then drastically reversed in *Homo* (McHenry 2002). There are three species recognised within the robust australopithecines these are *A. robustus*, *A. boisei* and *A. aethiopicus* (White 2002) and they occur approximately at the latest Pliocene and extend into the earliest Pleistocene. *A. aethiopicus* is known only from one cranium and is therefore of little use in understanding the evolution of the foot/bipedalism. There are several postcranial remains attributed to the robust australopithecines, but very little in the way of pedal remains. There are, however, some pedal remains which are firmly attributed to the robust australopithecines. They are clearly well adapted for bipedalism, but are unique in their own right. For example, the talus has an increased curvature of the medial trochlear rim suggesting an enhanced ability for abduction of the foot, while a large talar head and short trochlear may have inhibited the ability for dorsiflexion/plantarflexion (Gebo & Schwartz 2006).

Other australopithecines include *A. garhi* although this is also known only from craniodental remains and so can do little to inform on the evolution of bipedalism. However, despite its small cranial capacity and large postcanine size (White 2002) it is ideally placed temporally and geographically to be a reasonable candidate as an ancestral taxa to the *Homo* genus (Asfaw et al. 1999). *A. sediba* is a recently discovered gracile australopithecine occurring at the Plio-Pleistocene boundary. It has been presented as being unusual in its *Homo*-like appearance but occurs later than the first appearance of *Homo* fossils. Features of the pelvis seem to be similar to *Homo erectus* such as the expansion of the ilia, which is not found in earlier forms (Berger et al. 2010). Fortunately, there are a significant amount of postcranial remains, including some pedal remains. The talocrural joint appears to have been essentially human-like, and there is some evidence that there were human-like arches present in the foot. However, the calcaneus is more gracile than expected, and the species may have practiced a unique form of locomotion (Zipfel et al. 2011). *Homo* species in the Pleistocene (i.e. *H. erectus* onwards) appear to have been morphologically and biomechanically adapted to human-like bipedal, striding gait. As such, they are of limited value in studying the evolution of the foot or the emergence of bipedalism.

Homo habilis is known from 2.3 – 1.6 Mya and has a wide geographical range, being known from South Africa to Ethiopia (Dunsworth and Walker 2002). There has been a great deal of controversy surrounding the phylogenetic placement of remains attributed to *H. habilis*. Immediately after its discovery the criteria for placement within the genus *Homo* were altered in order to accommodate its inclusion. The required cranial capacity was relaxed by 100cm³ or more (Wood and Richmond 2000). While it is now generally accepted that cranially, *H. habilis* represents a departure from the *Australopithecus* morphology and bears derived human-like traits such as increased brain size and reduction in masticatory apparatus (McHenry and Coffing 2000) the postcranium has been more difficult to reconcile with this view. The fragmentary nature of the postcranial remains make reconstruction difficult. Reconstruction of limb lengths have suggested that *H. habilis* had a relatively long and robust forelimb relative to its hindlimb (Haeusler and McHenry 2004; Ruff 2009) which would align it more closely with earlier hominids rather than *Homo*. Whatever the phylogenetic placement of *H. habilis* it has been generally found support for the contention that it represents a bipedal early hominid based in its postcranial skeleton but retained a significant amount of arboreal behaviour (Susman and Stern 1982).

1.6. Functional anatomy of the foot

1.6.1. Functional anatomy of the human foot

Bipedalism is one of the most obvious diagnostic features of the human lineage. Humans are very effective and efficient at walking bipedally (Elftman and Manter 1935; Adamczyk *et al.* 2006; Caravaggi *et al.* 2010) and this is contingent upon a number of anatomical adaptations of the human skeleton. For example, the vertebral column, the hip, the knee, the ankle and the foot must all be conducive to effective bipedal walking and standing. Clearly, it is not enough for an effective biped such as a human to have any one of these features alone, they form part of a structural complex and changes to any part of the complex has profound implications for the function of the unit as a whole. That said, the foot alone forms the basis for this study for a number of reasons; 1) of all the features mentioned above which must be well suited for bipedalism, the foot is the platform upon which the entire weight of the body is supported and transferred during walking and this is rare among the primates, 2) while all features of the postcranium of humans and closely related African apes display significant differences, the foot is so wildly different that the evolution of a bipedally adapted foot warrants special attention, as do possible alternative pedal morphologies which may facilitate bipedal posture in primates, 3) the foot is very well understood, differences in morphology can be relatively reliably inferred to have specific functional consequences.

There are 26 bones in the human foot (Figure 1.3) and two sesamoid bones beneath the head of the first metatarsal in the tendons of flexor hallucis brevis (Saraffian 1983). Although each individual articulation between the bones has its own nuances, there have traditionally been three joint complexes that are of significant importance in considerations of human foot function. These are the talocrural joint, the subtalar joint, and the transverse tarsal joint. The talocrural joint is the articulation between the tibia, fibula, and talus. It is through this joint that the forces imposed on the foot during walking are transmitted to the leg thus it is vital that this joint is secure. Movements are largely restricted to the parasagittal plane (Sarrafian 1983; Frankel & Nordin 1989; Palastanga *et al.* 1994). However, there is some degree of deviation in the axis of rotation at the ankle throughout plantarflexion/dorsiflexion. Due to the geometry of the articulation between the talus and tibia, dorsiflexion naturally causes abduction of the foot while plantarflexion, conversely, causes adduction (Isman & Inman 1969; DeSilva 2008). It is important that the foot remains oriented in the parasagittal plane for the effective transfer of force in the direction of travel. The shape of the bones alone provides stability to the talocrural joint, resembling a mortise and tenon joint (Figure 1.4) (Aiello &

Dean 2002). Additional stability is afforded by the ligamentous anatomy of the ankle which is essential to maintain the function of the foot and leg.

Image redacted on copyright grounds.

Image redacted on copyright grounds.

Figure 1.3 Exploded foot skeleton. 1 = Calcaneus, 2 = Talus, 3 = Navicular, 4 = Medial cuneiform, 5 = Intermediate cuneiform, 6 = Lateral cuneiform, 7 = Cuboid, 8 – 12 = Metatarsals 1 - 5 respectively, 13 & 14 = Hallucial Phalanges, 15, 16 & 17 (as well as all unnumbered bones) = Phalanges of lateral digits. (From <http://www.docbowers.com/aboutthefoot.html>)

Figure 1.4 Magnetic resonance image of the human ankle. Note how the tibia and fibula grip the talus as in a mortise and tenon joint. T = tibia, F = fibula, Ta = talus. The arrow indicates the syndesmotic recess. (From Hermans et al. 2010)

The immobility of the tibia and fibula relative to one another is of paramount importance in the stability at the ankle. Widening of the mortise by just 1mm reduces tibiotalar contact by some 42% and would greatly reduce the efficiency of force transfer and function of the lower limb during bipedal walking (Hermans *et al.* 2010). The inferior tibiofibular syndesmosis strongly binds the tibia and fibula together in their grip of the talus and consists of four separate ligaments (Table 1.2). The tibia and fibula are bound to the rest of the foot via the collateral ligaments. The lateral ligament binds the fibula to the talus and calcaneus and consists of three ligaments. The medial ligament (also known as the deltoid ligament) consists of a deep and superficial layer consisting of two and three ligaments respectively (Pankovich & Shivaram 1979; Sarrafian 1983; Gosling *et al.* 2008). Together

the collateral ligaments strongly bind the tibia (via its malleolus) to the talus, navicular and calcaneus, and the fibula (via its malleolus) to the talus and calcaneus.

Clearly, the talocrural joint is a secure structure offering stability through its osteological and ligamentous anatomy. However, because of the pressure imposed on the human ankle as a by-product of bipedalism the ligaments of the ankle are particularly prone to rupture (Pankovich & Shivaram 1979a, b; Rasmussen 1985; Colville *et al.* 1990; Hollis *et al.* 1995; Motley *et al.* 2010). The features of the ankle highlighted here restrict dorsiflexion in the human ankle to roughly 10°-20° (Sarrafiian 1983; Frankel & Nordin 1989; Sammarco 1989; McMinn *et al.* 1996; Hall 1999). During dorsiflexion the ankle is in its close-packed position and is most stable (Sarrafiian 1983) but extremes of dorsiflexion will likely result in serious damage to the collateral ligaments and inferior tibiofibular syndesmosis (DeSilva 2009).

The rigidity of the talocrural joint is imperative for effective bipedal behaviour in humans, and it is vital for the distal bones of the foot to provide a similar stability. In a manner similar to the talocrural joint, the bones of the human foot are afforded a structural rigidity from their osteological and ligamentous anatomy. The talus is the bone that links the foot and leg and is thus of critical importance. Its relationship with the leg has already been discussed, and now the relationship between the talus and the foot will be reviewed. This involves two joint complexes of particular importance: the subtalar joint and the transverse tarsal joint. The subtalar joint is the articulation between the talus and calcaneus and the ligaments that bind the bones together to provide stability. The articulation occurs at two or sometimes three articular surfaces and the ligaments involved in stability at this joint are the calcaneofibular, lateral talocalcaneal, cervical, and interosseous talocalcaneal ligaments, and part of the inferior extensor retinaculum (Renström & Lynch 1998). There is little movement possible at the subtalar joint as with the rest of the foot's articulations, however, it is clearly important in the transmission of forces during walking.

Ligament Complex	Ligament	Origin	Insertion	Action	References
Distal tibiofibular syndesmosis					
	Distal anterior tibiofibular	Anterior tubercle of distal tibia	Anterior tubercle of distal fibula	Binds the anterior tibia and fibula, weakest of the syndesmotomic ligaments	Bartoníček 2003; Hermans et al. 2010
	Distal posterior tibiofibular	Posterior tibial malleolus	Posterior tubercle of distal fibula	Binds the posterior tibia and fibula, strong so excessive stress often results in fracture of the fibular malleolus rather than rupture of the ligament	Bartoníček 2003; Hermans et al. 2010
	Transverse	Fibular malleolar fossa	Dorso-distal rim of tibia/dorsal medial malleolus	Binds the tibia and fibula together during dorsiflexion, less taut during plantarflexion	Bartoníček 2003; Hermans et al. 2010
	Interosseous	Incisura tibialis to the anterior tubercle of the tibia	Just above the talocrural joint	Acts as a spring during loading of the talocrural joint allowing some widening of the mortise, dampens high impact forces such as heel strike	Bartoníček 2003; Hermans et al. 2010
Medial ligament (superficial)					
	Naviculotibial	Anterior tibial colliculus	Dorsomedial navicular, dorsomedial surface of spring ligament	Largest and widest ligament, but weakest part of deltoid ligament. Becomes taut during plantarflexion	Pankovich & Shivaram 1979 a,b; Motley et al 2010
	Calcaneotibial	Middle of medial anterior tibial colliculus	Medial sustentaculum tali	Strongest of the superficial layer ligaments, resists eversion of the calcaneus	Pankovich & Shivaram 1979 a,b; Motley et al 2011
	Superficial talotibial	Posterior part of medial anterior tibial colliculus	Anterior portion of medial tubercle of talus	Resists dorsiflexion at the ankle	Pankovich & Shivaram 1979 a,b
Medial ligament (deep)					
	Deep anterior talotibial	Anterior tibial colliculus and intercollicular groove	Medial surface of the talus near the neck	Resists eversion of the ankle	Pankovich & Shivaram 1979 a,b
	Deep posterior talotibial	Posterior tibial colliculus and intercollicular groove	Medial tubercle to the edge of the posterior third of the trochlear	Resists eversion of the ankle	Pankovich & Shivaram 1979 a,b
Lateral ligament					
	Anterior talofibular	Anterior fibular malleolus, close to the apex	Lateral talar neck	Resists dorsiflexion and external rotation of the foot	Rasmussen 1985; Colville et al. 1990; Hollis et al. 1995
	Posterior talofibular	Fibular malleolar fossa	Anteriorly on the posterior edge of the talus, Posteriorly on the lateral tubercle of the posterior process of the talus	Resists dorsiflexion and external rotation of the foot	Rasmussen 1985; Colville et al. 1990; Hollis et al. 1996
	calcaneofibular	Apex of fibular malleolus	Lateral surface of the calcaneus	Resists dorsiflexion, plantarflexion, adduction and internal rotation	Rasmussen 1985; Colville et al. 1990; Hollis et al. 1997

Table 1.2. Summary of the ligamentous anatomy of the ankle.

The subtalar joint can be said to behave like a screw, combining rotational movements as well as sliding movements between the talus and calcaneus (Leardini *et al.* 2001; Klenerman & Wood 2006). This screwing motion allows the bones to firmly lock together providing stability to the posterior portion of the foot. Perhaps the most significant feature of the human subtalar joint when compared to that of other primates is the anterior elevation of the calcaneus in normal anatomical position leading to the development of the longitudinal arches of the foot which are pivotal to human bipedalism (Aiello & Dean 2002). This elevation has the consequence that the subtalar joint axis is raised to about 40°-45° from horizontal (Leardini *et al.* 2001) in contrast to the flat longitudinal appearance of the ape foot (Berillon 2003). Additionally, the subtalar joint forms a more acute angle with the functional axis of the foot in humans, while in apes the angle is much larger (Aiello and Dean 2002). The consequence of this is that the foot in humans is not brought into a “grasping attitude” when inverted (Lewis 1980b). Furthermore, since the axis is more in line with the functional axis of the foot it supports body weight through its screwing mechanism in the line of travel.

The transverse tarsal joint (TTJ) is comprised of two distinct joints whose movements relative to each other have profound consequences for flexibility in the human midfoot. The joint is comprised of the talocalcaneonavicular joint (TNJ) and the calcaneocuboid joint (CCJ). The CCJ is particularly immobile in humans; this immobility is caused by the morphology of the distal calcaneus and proximal cuboid, and by the strong calcaneocuboid ligaments (Bojsen-Møller 1979; DeSilva 2010). The cuboid has an extensive process proximally which is received by the calcaneus (Figure 1.5). As well as this, the joints are tightly bound by the dorsal and long plantar calcaneocuboid ligaments forming a particularly rigid joint. The TNJ is much more mobile than the CCJ (Greiner and Ball 2014) and the position of the TNJ relative to the CCJ has implications for the mobility of the human foot. During inversion of the foot the talus and navicular move superiorly relative to the CCJ. When this happens the axes of the two joints are incongruent and so resist movements relative to each other (Figure 1.6) (Shetty and Bendall 2011). This allows the foot to act as a rigid lever during the final push off stage of walking, with the midfoot behaving as a rigid unit. Conversely, at the beginning of the walking cycle (heel strike) the foot is everted. This means that the CCJ and TNJ axes are congruent, and allow a greater degree of movement relative to one another. In this way the foot is able to act as a compliant shock absorber (Saraffian 1983; Gomberg 1985; Sammarco 1989; Klenerman & Wood 2006).

As weight passes over the foot the cuboid and navicular are forced to rotate away from each other causing the height of the foot to lower and allowing the foot to behave in a similar way to a spring. This is because rotations of the cuboid and navicular in opposite directions are restricted by the

cuboideonavicular ligament (Gomberg 1985). Also of particular note in maintaining stability in the foot are the calcaneonavicular (spring) ligament and the plantar aponeurosis. The spring ligament arises from the sustentaculum tali and attaches to the medial and inferior aspects of the navicular, supporting the head of the talus also. This prevents the head of the talus moving relative to the calcaneus during plantarflexion and so maintains a high longitudinal arch to the foot (Rule *et al.* 1993; McMinn *et al.* 1996; Aiello & Dean 2002). Failure of the spring ligament can result in the collapse of the medial arch of the foot and improper function (Tryfonidis *et al.* 2008; Postan *et al.* 2011). The plantar aponeurosis is very thick connective tissue spanning from the calcaneal tuberosity to the phalanges. It becomes very taut during extension of the toes making the foot rigid at toe off (Bojsen-Møller & Flagstad 1976; Erdemir *et al.* 2004; Nowak *et al.* 2010). It also prevents the arches of the foot from flattening by resisting movements of the distal foot away from the proximal foot (Bojsen-Møller & Flagstad 1976; McMinn *et al.* 1996; Aiello & Dean 2002; Erdemir *et al.* 2004; Nowak *et al.* 2010), and transmits forces from the calf muscles to the forefoot at push off (Erdemir *et al.* 2004).

Image redacted on copyright grounds.

Image redacted on copyright grounds.

Figure 1.5. Plantar view of the calcaneocuboid joint. Arrow indicates the calcaneal process. From Bojsen-Møller 1979.

Figure 1.6. Congruency in eversion (left) and incongruency in inversion (right) of the transverse tarsal joint. From Shetty and Bendall 2011.

Another feature of the human foot which contributes to the rigidity necessary to human bipedal walking is the Lisfranc joint, which is the articulation of the second metatarsal with the three cuneiforms. The significance of the joint is in the way the base of the second metatarsal is recessed such that it is gripped by the medial and lateral cuneiforms. This joint helps to form the transverse arch of the foot and resists movements of the metatarsals and cuneiforms relative to one another during walking. The Lisfranc ligament firmly anchors the second metatarsal to the medial cuneiform (Johnson et al. 2008). Each of the metatarsals of the human foot are adapted to cope with the unique forces generated during human walking. The human foot can be thought of as a tripod through which the stress of walking is dissipated. This tripod would be represented by the heel, the head of the first metatarsal and the head of the fifth metatarsal (Marchi 2005). This is consistent with the known transfer of weight from the heel, along the lateral side of the foot and then across the metatarsal heads medially for push off (Elftman & Manter 1935; Aiello & Dean 2002). This is attested to by the more robust first, fourth and fifth metatarsals in humans relative to apes (Aiello & Dean 2002; Marchi 2005). As well as facilitating and supporting force transmission through the foot, the metatarsals are also integral in forming the longitudinal arch of the foot. The heads of the metatarsals are medially twisted relative to the bases. This brings the heads of the metatarsals into contact with the ground while the bases form the high transverse arch unlike in apes. In apes the heads and bases of the metatarsals lie effectively in the same plane (Zipfel et al. 2009).

To summarise, the human foot is uniquely adapted for its task in bipedalism in a number of ways. The vital difference in the human foot as compared to all other primate feet is the extremely rigid nature of the structure. Other primates have much more mobility, for example the hallux is divergent and grasping, the midfoot is much less rigid allowing a significant degree movement and there is often a greater range of motion at the talocrural joint. Of course, these are adaptations necessary in quadrupedal primates, particularly arboreal ones. Rigidity in the human foot is not absolute, however. DeSilva and Gill (2013) found evidence for lateral midfoot compliance in humans, challenging the notion that the key adaptation of the human foot is the immobile lateral column (Kidd *et al.* 1996). Furthermore, throughout the course of the human stride the foot has to act initially as a compliant shock absorber at heel strike, and become a rigid lever from which the forward motion of the body can be maintained for push off, all in the course of one step. The movements within the foot that allow this transformation are subtle but have enormous consequences allowing the efficient transference of energy from step to step (Whittle 2007).

1.6.2. Comparative functional anatomy of the primate foot

The foot of the non-human apes is significantly different from that of humans; the main differences permit a greater amount of mobility in the former. The mobility of the ape foot in comparison to the rigidity of the human foot represents a functional adaptation to a significant amount of arboreal behaviour in the apes. It is always tempting to discuss how derived the human foot is in relation to the non-human hominoid foot, or indeed, how derived humans are in general. However, it is critical to always bear in mind that the great apes have been subject to their own set of evolutionary pressures, and their morphology is one that is extremely well adapted to their habitat. If the evolution of the ape foot was under investigation then when comparing it to the human foot it would have to be noted how derived the ape foot was.

The importance of the fundamental difference between the human and ape foot in both morphology and function has long been well established (Humphry 1867; Sutton 1883; Brooks 1887; Hepburn 1892). Keith (1923b) proposed that the human foot had evolved from an ape-like prehensile one and went some way to describing the similarities between the two. He notes the proportions of the foot in primates change in a predictable fashion from the monkeys through the apes, to man. In the monkeys, the phalanges account for a greater proportion of the total foot length while the tarsus is relatively small, and this is because relatively more weight is borne by the phalanges than by the tarsals or metatarsals (Patel 2010), in humans the converse is true. It has been shown that the human tarsal skeleton is especially well adapted to bipedal standing. The power arm to load arm ratio in humans is much higher than in other primates, with the exception of the gorilla (Wang & Crompton 2004). This reduces the amount of force the calf muscles need to exert in order to maintain a standing posture in humans. Of course, such an adaptation is unnecessary in apes as bipedal posture constitutes a small percentage of their overall behavioural repertoire (Gebo 1989; 1996). This ratio is high in *Gorilla* also, but for a different reason. The force applied by a muscle is directly correlated to its cross-sectional area, not its mass. Therefore, in massive animals, increasing the size of a muscle increases the force it applies at a rate lower than it increases the body mass of an organism. A simple way to overcome this problem is by increasing the power arm the muscle acts on, as is the case in *Gorilla* (Köhler and Moyà-Solà 1997). The foot proportions of *Pongo* are also quite unique. The extremely long digits 2-5 and reduced first digit are unparalleled in other hominoids. These features are related to suspensory behaviour and similar morphology can be found in the hand (Gebo 1992; Ankel-Simons 2000), the cortical thickness of the lateral metapodia is

greater in *Pongo* further supporting the increased reliance on these digits in locomotion (Marchi 2005).

The ankle of the apes is not nearly as rigid as the ankle in humans, and nor are the ligaments that bind it together (Lewis 1980). This is because the ankle in apes has to permit a degree of dorsiflexion more than twice that observed in the human ankle (DeSilva 2009). Pronounced dorsiflexion and inversion at the ankle, as well as a highly flexed hindlimb are functional adaptations to climbing in apes (Meldrum 2004; Thorpe *et al.* 2007; DeSilva 2009). Extreme dorsiflexion and inversion of the foot allows more of the sole to be brought into contact with the substrate and allows the foot to be in contact with the substrate for a longer period of time (DeSilva 2009; Nowak *et al.* 2010). The fact that the efficiency of climbing is largely independent of body size throughout primates indicates that this posture is likely to facilitate safe climbing. And, since the weight of an animal and gravity are constant at any given time, reducing the distance of the centre of gravity from the substrate will reduce the moment acting on the animal during climbing (DeSilva 2009).

Similarly, distal to the ankle there is an increased capacity for mobility in the tarsal and tarsometatarsal articulations at the expense of extreme stability such as that found in humans. During walking the transmission of force can be shown to follow a fairly well-defined path in the human foot (Elftman and Manter 1935; Vereecke *et al.* 2003). Following heel strike the lateral side of the foot makes contact with the ground and pressure beneath the foot passes distally to the fifth metatarsal head before moving medially across the metatarsal heads and finally toe off occurs when pressure is greatest beneath the first and second metatarsal heads (Napier 1993). This occurs because of the rigid human foot and the anatomy of the joints described above, in which the bones of the midfoot are prevented from contacting the ground by the longitudinal arch. In contrast, the ape foot exhibits no such regular pattern of force transmission through the foot (Vereecke *et al.* 2003). The navicular, medial cuneiform, and base of the fifth metatarsal all experience loading (DeSilva 2010) because of the laxity of the ape foot longitudinally. This causes the foot to roll from heel-strike to toe-off in contrast to the rigid fulcrum of the human forefoot. Orang-utans are the least terrestrial of the great ape species and they may experience heel strike and contact of the entire lateral border of the foot simultaneously due to their highly inverted ankle position (Thorpe *et al.* 2007).

In contrast to humans, the lateral column of the ape (and monkey) foot is capable of a considerable amount of movement. The ligaments around this complex are much less extensive than in humans and the calcaneal process of the cuboid is not as prominent either (Gomberg 1985). The articulation between the cuboid and the fourth and fifth metatarsal is curved in apes, where it is flat in humans. Taken together, these features allow dorsiflexion at the midfoot in apes, which is impossible for humans. This is known as the midtarsal break (DeSilva 2010) and its presence allows the ape foot to simultaneously act as a grasping organ distally and a propulsive organ proximally during climbing (Meldrum 2004). The midtarsal break has traditionally been thought to occur predominantly at the transverse tarsal joint (Elftman and Manter 1935a). This has been used to emphasise the importance of the human calcaneocuboid joint in maintaining the longitudinal rigidity of the human foot. However, it has been shown that the midtarsal break is actually more pronounced at the cuboideometatarsal articulation (DeSilva 2010), and that the human lateral foot in fact has a substantial laxity, though not as great as in non-human apes (Bates *et al.* 2013).

The widely divergent first digit is one of the most diagnostic differences between the ape and human foot. This morphology in apes, when coupled with the above mentioned adaptations, renders the foot suitable for grasping large and small diameter supports during climbing and suspension. The first metatarsal adducts, flexes, and medially rotates to oppose the lateral side of the foot (Gebo 1993a) and this is facilitated by the helical form of the articulation between the medial cuneiform and first metatarsal (Gebo 1985; Isidro and Gonzalez-Casanova 2002), unlike the flatter, more immobile joint in humans (Proctor 2008). The wide divergence of the hallux is achieved by medial encroachment of the facet for the first metatarsal onto the medial side of the medial cuneiform (McHenry and Jones 2006). In humans the degree of medial encroachment of the facet is always low. Of the apes the degree of medial encroachment is lowest in *Gorilla*. However, this is a feature which develops late in *Gorilla* as a response to its massive size, whereas the low level of medial encroachment occurs earlier in development in *Homo*, indicating that the two features are not linked evolutionarily (McHenry and Jones 2006). The robusticity of the first metatarsal is not as great in apes as it is in humans, but is roughly the same relative length compared to the hallucal phalanges, however (Ankel-Simons 2000; Aiello and Dean 2002).

Cercopithecoids are unlike other primates in having a syndesmotric rather than synovial talocrural joint, indicating that the ankle of cercopithecoids is considerably less mobile, and more secure, than that of the hominoids (Strasser 1988). The trochlea is not as highly wedged in outline as it is in hominoids but is similarly asymmetrical. The talus has a very high lateral trochlear rim facilitating the

pronounced inversion of the foot (Meldrum 1991) and bringing the lateral digits into contact with the substrate. The subtalar joint is adapted to reduce the range of inversion/eversion and maintain the emphasis on the lateral digits (Strasser 1988). Cercopithecoids are semi-plantigrade and digitigrade in their positional behaviour (Gebo 1992; Schmitt and Larson 1995) and thus have a less well developed calcaneus (Strasser 1988) but the posterior calcaneus is long to increase the lever advantage of the calf muscles in heel-raised foot postures (Strasser 1988). The midfoot tarsals are lengthened relative to those in hominoids, reflecting an adaptation to compressive forces (Langdon 1986). Similarly, the lateral metatarsals of cercopithecoids are quite robust and these primates exhibit raised-heel posture which subjects the metatarsals to more compressive rather than shearing stress (Patel 2010). The cercopithecoid foot also has a sesamoid bone in the tendon of peroneus longus which acts to rigidify the foot during locomotion (Lovejoy *et al* 2009a), and has been proposed as the ancestral condition for the pedal anatomy at the time of the African ape-human divergence.

1.7. Positional behaviour of primates in this study

Each species included here is capable of multiple positional and locomotor behaviours. Humans, although generally considered obligate bipeds, are in fact capable of a range of behaviours. For example, many human populations engage in climbing behaviours (Perry and Dominy 2009; Venkataraman *et al.* 2013), and most humans are capable of climbing to a greater or lesser extent. The degree of dorsiflexion of the ankle in some African hunter-gatherers has even been observed to reach the extremes observed in chimpanzees without leaving any obvious skeletal traces of that behaviour (Venkataraman *et al.* 2013). This presents clear difficulties in interpreting fossil pedal remains. That said, it is still necessary to rely on the remaining skeletal anatomy of fossils to make inferences about their locomotor habits. It is simply necessary to bear in mind that the function of the foot is much more than the sum of its skeletal parts.

The African apes share a similar morphology and positional behaviour (Hunt 1991). The two genera both employ knuckle-walking when progressing quadrupedally on the ground (Richmond *et al.* 2001) and quadrupedal activities account for >85% of the locomotor repertoire of both genera (Doran 1996). Differences that exist between *Pan* and *Gorilla* relate primarily to the increased arboreality of *Pan*. This can largely be attributed to the much greater body size of *Gorilla* (Doran 1997). However, throughout development, if positional behaviour in *Gorilla* and *Pan* are compared based on body size rather than age, the two are always remarkably similar. Although, *Gorilla* never exhibits the same

frequency of suspensory behaviour as *Pan* (Doran 1997) and males do not exhibit suspension as frequently as females (Remis 1995), but suspensory behaviour in *Pan* accounts for a very minor proportion of the locomotor repertoire (Gebo 1996). The main behaviours representing African ape locomotion are terrestrial quadrupedalism and vertical climbing on large diameter supports. Positionally, the African apes most frequently sit and lie, with some small degree of standing (Doran 1996).

Pongo is much more arboreal than the African apes are. While in the trees orang-utans almost exclusively employ careful quadrumanous climbing (Millán *et al.* 2015) and debates persist on the degree to which compressive behaviours are used compared to suspensory ones (Thorpe and Crompton 2006). Most studies, however, find that suspensory behaviour is much more prevalent in the positional repertoire of *Pongo* than the African apes (Hunt 1991; Gebo 1996), during which the lateral digits are hooked over the supporting branch and the hallux is not employed. *Pongo* also exhibits a greater frequency of bipedal behaviour than the African apes (Hunt 1991), although this is exhibited arboreally rather than terrestrially, prompting the suggestion that hominin bipedalism may have originated in an arboreal context (Crompton *et al.* 2008; 2010). *Pongo* moves predominantly quadrupedally when on the ground. However, it does not possess the specialised wrist morphology which permits knuckle-walking in the African apes. Instead, *Pongo* fist-walks, during which behaviour the fist is clenched and the entire ulnar side of the hand contacts the substrate simultaneously (Tuttle 1969).

Theropithecus is notable amongst the cercopithecoids for its high terrestriality (Elton 2002). Furthermore, *Theropithecus* is regularly found in archaeological association with Plio-Pleistocene hominins and therefore is thought to present useful insights into the environmental and ecological factors surrounding the emergence of humans (Foley 1993; Jolly 2001). In general, *Theropithecus* is a terrestrial quadruped and bears broad similarities to other cercopithecoids. The limbs move predominantly in the parasagittal plane. During walking the heel is raised and the fulcrum of the foot lies at the head of the third metatarsal (Strasser 1992). The hindlimb bones are approximately equal in length (Krentz 1993) but the crural index is high because the femur is short and the tibia long, which is suggested to be an adaptation to increase the power generated by the calf muscles (Strasser 1992). The size of the femoral articular surfaces compared to shaft lengths are cercopithecoid-like indicating that the hindlimb is not used in a varied number of positions (Ruff 2002). *Theropithecus* is known to use bipedal shuffling also to move between patches of food and this is thought to be

energetically more efficient than moving quadrupedally between feeding patches (Wrangham 1980). Squatting also comprises a significant part of the postural behaviour of *Theropithecus* (Krentz 1993).

1.8. Specific hypotheses tested in this study

To assess the functional affinities of *Oreopithecus* and other fossils in the study a number of hypotheses were tested and considered. All of the hypotheses were tested for each bone included in the study (where the relevant material was available for study). A set of hypotheses concerning the extant taxa were tested to provide a framework of functional relationships in which the morphological similarities of fossil species could be considered. The first set of hypotheses deals with shape similarities and differences, the second set deals with size relationships. The hypotheses are as follows:

1. *Gorilla* and *Pan* are most similar in terms of ecology and behaviour and therefore will be more similar to each other in pedal anatomy than to any other species.
2. *Pongo* and the African apes are more similar to one another in terms of ecology and behaviour (though substantial differences clearly exist) and will therefore be more similar in pedal anatomy to each other than to either *Homo* or *Theropithecus*, which species, in the context of this study, are more “specialised” (*Homo* a committed biped and *Theropithecus* a pronograde, digitigrade, quadruped).
3. *Theropithecus* represents an outgroup as the only non-hominoid, digitigrade, quadruped and will therefore be the most different of all extant species included in the study.
4. *Oreopithecus* is markedly different in shape to *Theropithecus* and therefore the cercopithecoid hypothesis for *Oreopithecus* has justifiably been discarded.
5. *Oreopithecus* is most similar in shape to one of the African apes, reflecting its probable heritage from the Miocene hominoids of Europe. The details of the similarities and differences to African apes will permit an assessment of the likelihood of unique pedal function.
6. OH8 is most similar in shape to *Homo* reflecting its status as an obligate biped.
7. *Nacholapithecus* is most similar in shape to *Theropithecus* reflecting its pronograde, quadrupedal body shape and position as a stem hominoid.

The following hypotheses considering the sizes of extant species and fossils were also tested.

8. *Gorilla/Homo* will be the largest among the extant species due to the large body size of *Gorilla* and the increased level of force transmission in *Homo*.
9. *Theropithecus* will be the smallest among the extant species due to its small body size.
10. *Oreopithecus* is comparable in size to *Pan*, lacking the increased robusticity of the pedal skeleton which would be expected in a habitually bipedal primate, but having a substantially more robust foot than *Theropithecus*.
11. OH8 is smaller than *Homo* reflecting its small body size and occurrence early in the emergence of obligate bipedalism.
12. *Nacholapithecus* is intermediate in size between *Theropithecus* and the smallest hominoid reflecting the increase in body size which is characteristic of the stem hominoids.

2. Materials and Methods

2.1. Materials

To investigate the likelihood of bipedalism inferred from the foot of *Oreopithecus* (with particular reference to the reconstruction of the hallucal orientation and foot function by Köhler and Moyà-Solà (1997)), and its implications for the evolution of the foot in the hominid lineage, the medial column of the foot of a number of extant primate taxa and fossil specimens was studied. The six bones included in this study are the talus, navicular, each of the cuneiforms, and the first metatarsal. Time constraints and other factors unfortunately made investigating the entire foot unfeasible. Therefore only those bones deemed to be most functionally revealing and relevant to the question at hand were included. The omission of the calcaneus and cuboid will deprive the study of a significant amount of information relating to the habitual orientation of the calcaneus relative to the trochlea, the ability of the calcaneus and cuboid to lock together forming a rigid lateral column, details of the cuboid articulation with the lateral metatarsals, as well as other numerous insights. The omission of the lateral metatarsals and phalanges would have provided information on the length and robusticity of the digits and their suitability for various locomotor behaviours and likenesses of fossils with extant species.

The bones that have been included provide information about the upper and lower ankle joints and the position of the foot at the ankle, the rigidity of the midfoot and its ability to dorsiflex, the transverse arch of the foot, general mobility between the tarsals of the medial column and function of the first metatarsal. By testing the hypotheses outlined at the end of the previous chapter the morphological similarities of the *Oreopithecus* foot with extant primates can be explored. By understanding the morphology and locomotor behaviour of the extant primates it will allow inferences to be made about the likely function of the foot in *Oreopithecus*. All bones included in the study were taken from adult specimens showing no signs of pathology. Only individuals for whom all six bones were available were included in the study to emphasise that the medial column of the foot was under investigation as a unit rather than the individual bones that comprise it. In this way the relationships between species were compared for the entire medial column and always using the same individuals.

Five extant and three fossil primates were included in the study; *Pan troglodytes*, *Gorilla gorilla gorilla*, *Pongo pygmaeus*, *Homo sapiens*, and *Theropithecus gelada* represent the extant taxa; *Nacholapithecus kerioi*, *Oreopithecus bambolii*, and *Homo habilis* represent the fossil sample. Representatives of each of the extant apes were included to fully encapsulate the range of variation present in the pedal skeleton of extant hominoids. It is known that significant differences exist in the morphology of the feet of known subspecies of ape when compared directly and exclusively against one another (Tocheri *et al.* 2011; Dunn *et al.* 2014). However, it has also been found that differences between subspecies have been difficult to observe and explain in geometric morphometric studies which included different genera (Harcourt-Smith 2002), owing to their close similarity to one another in comparison to the total variation present. Therefore it was deemed sufficient to compare the genera of the extant apes for the purposes of this study without focusing on subspecies. Where possible an even number of males and females were used for each species as the sex of the fossil sample is unknown. Differences between sexes are unlikely to be highly visible in the entire sample (Harcourt-Smith 2002). However, the range of variation may differ if one sex or another were omitted. Thus the greatest possible range of variation was included to find the closest affinities of the fossil species. Intraspecific variation was not examined as this has already been done for the tarsal skeleton and strong results were not found (Harcourt-Smith 2002).

Theropithecus was included in the study primarily to act as an outgroup against which the “derived” hominoid condition could be compared. *Theropithecus* was selected over any other cercopithecoid because it regularly exhibits bipedal shuffling between food patches (Wrangham 1980) and furthermore because it is the most terrestrial of all cercopithecoids (Krentz 1993) and the robusticity of the metatarsals of *Oreopithecus* have been suggested to demonstrate it was highly terrestrial (Riesenfeld 1975). Thus, *Theropithecus* offers an opportunity to compare hominoid pedal anatomy against that of a cercopithecoid, while simultaneously allowing an assessment of possible bipedal adaptations in the foot of *Theropithecus*. Additionally, the phylogenetic placement of *Oreopithecus* has long been debated with some authors suggesting that *Oreopithecus* is a cercopithecoid (see Delson 1986 for an overview) and therefore comparing *Oreopithecus* with an extant cercopithecoid in this way is novel and provides new insights into the morphological proximity of *Oreopithecus* to either the cercopithecoids or hominoids. Additionally, *Theropithecus* is frequently archaeologically associated with Plio-Pleistocene hominin fossils (Foley 1993). Thus it has been studied extensively as an analogue for human ecological evolution (Jolly 2001; Elton 2002).

Nacholapithecus was included to provide a reference to the protohominoid morphology from which hominoids are thought to have arisen. Additionally, its similarity to modern cercopithecoids can be observed through its comparison with *Theropithecus* and, potentially, *Oreopithecus*. *Homo habilis* was included to provide the study with a hominid which is generally agreed to have been fully bipedal and against which to compare *Oreopithecus* and also to test previous studies into the pedal skeleton of *Homo habilis* and their findings (e.g. Day and Wood 1968; Oxnard and Lisowski 1980; Kidd *et al* 1996; Harcourt-Smith 2002). More information on the sample is given below.

Pan troglodytes

The chimpanzee sample derived from two institutions, which comprise 9 individuals curated at the University of Zurich (4 male and 5 female) and 6 individuals curated at the Natural History Museum, London (3 male and 3 female). Specimen records at the University of Zurich do not provide sufficient information to place the individuals geographically and so they cannot be assigned to the sub-species level. All of the London specimens were assigned to *Pan troglodytes troglodytes* according to museum records.

Gorilla gorilla gorilla

The gorilla sample was curated at the Powell-Cotton museum in Kent. All specimens were wild shot in the geographical area of modern day Cameroon and are attributed to the species *Gorilla gorilla gorilla*. Twenty individuals were used in the study, 10 male and 10 female.

Pongo pygmaeus

12 specimens of *Pongo pygmaeus pygmaeus* were analysed; one (female) from the University of Sheffield; four (3 male, 1 female) from the University of Zurich, and seven (3 female, 4 male) from the Natural History Museum, London.

Homo sapiens

The human sample is taken from the Barbican collection comprising 682 individuals, housed at the University of Sheffield. The remains originate from a number of excavations in York that took place between 1973 and 2008. Most of the remains are from excavations of a medieval church cemetery

with a substantial number derived from a civil war mass grave. An early hypothesis that the mass graves contained victims seems unlikely given the high prevalence of young to middle aged men. This likely indicates that much of the sample from the mass graves represents soldiers who fought in the civil war (Bruce 2003; Bruce and McIntyre 2009). The individuals represent varying degrees of completeness and preservation, however a large portion of the individuals are highly complete and excellently preserved. The remains have been studied intensively and each has its own skeleton report from which approximate age was ascertained and pathology was avoided. Twenty individuals were used in the study, 10 male and 10 female.

Theropithecus gelada

Six *Theropithecus* specimens were sampled from the University of Zurich. Of these 5 were female and only 1 was male. This disparity in sample size could not be avoided because many of the *Theropithecus* feet there were fully articulated ligamentous specimens and it was not possible to disarticulate them.

Nacholapithecus

The *Nacholapithecus* sample was taken from cast material housed at the University of Zurich. These are the cast of the single individual KNM-BG 35250 (Isheda et al. 2004). Unfortunately not much of the pedal skeleton remained, only a talus and medial cuneiform were available for study.

Oreopithecus

Oreopithecus bambolii is the most represented fossil species in this study. A total of fourteen bones were sampled from the Natural History Museum of Basel, Switzerland. The specimens were originally excavated from Miocene sediments in Tuscany, Italy (Köhler & Moyà-Solà 1997; Begun 2002). The sample consists of many individual bones that were not necessarily associated but at least one of each pedal element in this study is present in the *Oreopithecus* sample. The one available lateral cuneiform had a badly damaged facet for the third metatarsal. There was sufficient remaining morphology to attempt to reconstruct the facet but much of the original anatomy was missing. The first metatarsal is broken across its diaphysis, therefore the proximal and distal ends of the bone were studied in isolation.

Homo habilis

A cast of the OH8 foot housed at the University of Zurich was scanned. All six bones used in this study were present but only the proximal end of the first metatarsal of OH8 was preserved, and it was unsuitable for use in this analysis. There is some damage to the talus, on the posterior calcaneal facet and lateral malleolar facet (Day and Wood 1968). However, as noted by Harcourt-Smith (2002) this facet always displays a high amount of symmetry in hominoids and so can be relatively reliably reconstructed.

	Talus	Naviular	Medial cuneiform	Intermediate cuneiform	Lateral cuneiform	First metatarsal
<i>Pan</i>	15	15	15	15	15	15
<i>Gorilla</i>	20	20	20	20	20	20
<i>Pongo</i>	12	12	12	12	12	12
<i>Homo sapiens</i>	20	20	20	20	20	20
<i>Theropithecus</i>	6	6	6	6	6	6
<i>Nacholapithecus</i>	1	x	1	x	x	x
<i>Oreopithecus</i>	1	1	4	1	1	1
<i>Homo habilis</i>	1	1	1	1	1	x

Table 2.1. Bones included in this study for each species.

2.2. Methods

2.2.1. Choice of geometric morphometrics

The use of geometric morphometric techniques was adopted because of a number of advantages it offers over traditional morphometric techniques. Traditional approaches to understanding biological shape have focused on the use of linear and angular measurements (e.g. Kidd *et al.* 1996). These measurements are taken between two points (or an angle), which (in theory) represent homologous structures throughout the sample and are also biologically informative (Oxnard 1984; Bookstein 1986). This approach is generally revealing, for example, in outlining general proportional differences of the bone, approximating sizes of facets and their orientations, etc. It also serves as a rough

approximation for these shape and size differences. However, it suffers from over-generalising complex structures to angles, linear measurements, and their ratios (Adams *et al.* 2004). Comparing the length of a facet to its width, for example, will provide some useful information relating to the overall size of the facet, the direction in which movement predominantly occurs, how robust an articulation is (which could further allow inferences relating to force transmission at the joint), etc. Yet, despite this potentially interesting information, the ability of such measures to accurately describe the shape under study is clearly deficient. Not least because all biological forms are three-dimensional entities and traditional morphometrics seeks to approximate them using two dimensional measurements. It also suffers from problems of allometry (the relationship between size and shape), homology of the landmarks from which measurements are taken, and accuracy and repeatability of those measurements.

Geometric morphometrics offers a fully three dimensional approach to exploring morphological differences between taxa. The use of a large number of landmarks (and semilandmarks) to more accurately capture the complete shape of bones is a vast improvement upon traditional morphometrics (Slice 2007)). Using increased numbers of landmarks as an alternative to linear measurements between two landmarks is clearly still deficient when trying to compare entire shapes. The morphology between landmarks is still absent, and the landmarks suffer from the same problem of homology as the landmarks used in traditional morphometrics (Bookstein 1991; 1996). However, with careful consideration a set of landmarks can be chosen that represent the key features of a bone and are homologous between all specimens included in the study, i.e. each landmark is biologically homologous across all species (Oxnard & O'Higgins 2009). The three-dimensional coordinates of landmarks between specimens are then compared and this is vastly more informative than traditional morphometric measures. While information such as length and width of the bone, or length and width of facets, is still available from these comparisons, it is intrinsically linked to other fundamental shape differences of the entire bone, such as curvature of facet surfaces, relative expansion of certain areas relative to others, etc. This kind of information is not available using traditional morphometrics. Additionally, geometric morphometrics has the enormous advantage that it completely eliminates scale as a possible factor of variation so that only shape is under investigation (Bookstein 1986; Kendall 1989; Rohlf & Slice 1990), but still permits comparisons of size using the centroid sizes of individual shape configurations.

The above features of geometric morphometrics make it ideal for use in this study. The comparison of shapes independent of size is particularly appealing given the huge range in body size of the taxa

under study. Furthermore, the statistical framework for comparison of shapes in this manner is well established (Rohlf and Slice 1990; Bookstein 1991; Klingenberg & Monteiro 2005; Slice 2005). Using Procrustes distances between shapes in shape space gives a direct and easily interpreted numerical value between individuals. Furthermore, it is possible to generate the mean landmark configurations of taxa and to visually observe the changes which occur in converting one shape to the other. The result is highly visually appealing and intuitive, and it allows a better and fuller appreciation of the differences in shape between taxa.

2.2.2. Structured light scanning

The use of structured light in 3D surface measurement is well-established. The technique was developed in the early 1980's and has a wide range of applications. Structured light has been applied in medicine (Glinkowski et al. 2009; Chen 2010), orthotics/prosthetics (Kommean *et al.* 1996), engineering (Zexiao et al. 2005; Park & Chang 2009) and archaeology and anthropology (Pavlidis et al. 2007; McPherron et al. 2009; Niven et al. 2009). Structured light scanning works by using triangulation to calculate the position of a known pixel of light cast from an automated light source. As the irregular shape of an object distorts the relative positions of these pixels the calculation of the relative positions of the pixels allows for a digital reconstruction of the object in question. Structured light scanning provides a relatively low cost, fast, and highly accurate method for generating a 3D surface rendering of objects. The greatest advantage of this approach is that the range in size of objects that can be scanned is considerable. Everything from a small coin to the size of an adult human, and probably beyond, can be scanned using this equipment.

Structured light scanning is one of a number of technologies used in the digitisation of a 3D surface. These techniques vary in a number of ways and can be characterised based on these variations (Rocchini et al. 2001). The scanner used in this study can be categorised as a non-contact technology as opposed to something like a microscribe. The scanner can be further categorised as a reflective technique in contrast to something like computed tomography, which relies on high energy radiation being transmitted through an object of interest. Of the reflective systems structured light uses radiation from the visible light range of the spectrum and so is thus optical, where other technologies employing microwaves, sonar or radar may be considered non-optical. Finally, these optical devices may be either passive or active, and since the projector is used to cast a light pattern across an object which can later be measured, it is an active system. It is also a stereometric system since it involves

the use of two sensors. To calculate surface coordinates of a given surface the surface must be visible to both sensors simultaneously (Posdamer & Altschuler 1982).

Before scanning an object the equipment must be properly and carefully calibrated to ensure that the most accurate digitisation of the surface is possible. The scanning procedure is relatively straightforward in comparison to the calibration process. The object to be scanned is placed on the turntable such that it occupies the centre of the field of view of both cameras; then the number of scans to be undertaken is selected. Objects with a complex surface geometry will require more scans to accurately capture the surface information; this judgment must be made by the user on a case by case basis. Once all of these conditions have been met the scanning of the object begins. The projector casts the structured light pattern across the object, consisting of a series of vertical stripes of light mixed with vertical stripes where no light is present. The flexscan3D software is able to exploit patterns of light and no light as though it were binary code. Each pixel of light cast over the object will effectively become a 1 in binary if it is illuminated and a 0 if it is not. The coordinates of each pixel are then calculated using triangulation to generate the 3D model of the surface (Sato & Inokuchi 1984). To complete a surface scan of the object, the object must be rotated in some way through 90° in the z-plane. Obviously during the 360° turn of the turntable neither the portion of the object that is in contact with the turntable, nor its opposite side, is visible to the cameras. Another 360° scan of the object in its new orientation must be conducted to capture these missing surfaces. Even though some data will be recorded twice it is useful to carry out another 360° scan of the object in its new orientation. This makes merging the two partial scans together to create the complete surface easier. Flexscan3D offers a number of options for the merging process, these are merging by geometry, mesh alignment or markers manually allocated by the user.

There are some limitations of using the structured light technique detailed here. The scanner will only recognise projected pixels that appear in the field of view of both cameras. This means that objects with a complicated surface geometry will not be easily scanned using this technique. Final scans in such instances may have some missing data if it is not possible to capture the feature with both cameras (it is possible to use a single camera scanner to increase coverage of an object but this comes at the cost of reduced accuracy). The scanner will struggle to function in conditions of high light saturation. If ambient light levels are too high then the scanner cannot differentiate between illuminated and non-illuminated pixels. Similarly, if an object has a glossy texture or is highly reflective the scanner will perform poorly and this can have adverse effects on the accuracy of the data or result in large amounts of missing data. Every effort must be taken to minimise the effects of

these limitations but ultimately, the method is not perfect and it is likely that some error will occur. Finally, any part of the surface not captured during the scanning process will have to be estimated following the scan. It is unavoidable that some small holes in the generated mesh will be present, the larger they are the greater the uncertainty of the scan will be. Geomagic Wrap (3D Systems, Inc 2012) was used to estimate any missing data as it provides a high level of user control and uses advanced algorithms to reconstruct missing information using the surrounding topology. Thus, provided the hole in the mesh is small it can be recreated with a high level of confidence.

A custom made structured light scanner was used to generate 3D digital representations of the bones in the study. A custom rectangular frame on which to mount the equipment was constructed by Prof. Andrew Chamberlain at the University of Sheffield, the frame was then mounted upon a Manfrotto tripod. The remaining parts of the scanner were; Optoma EX330e projector, two uEye 1545LE-M cameras, two Fujinon HF12.5SA-1 machine vision lenses, two Manfrotto photography clamps, one calibration board supplied by Mechinnovation and a motorised turntable supplied by Sherline Products. The device was controlled by the flexscan3D software from 3D3 solutions, and the final scan was also produced in this software. The scans were accurate to ~10 microns.

2.2.3. Collection of data

2.2.3.1. Procedure for placement of landmarks

Some semilandmarks were placed on predefined curves while others were placed on facet surfaces. Since the landmarks chosen for this study were placed on or near to the locations of these curves it was necessary to devise a way to ensure that drawing the curve along which these semilandmarks would slide and placing the initial landmarks were not able to interfere with each other. Therefore the curves were drawn for each bone and each individual in order (e.g. chimpanzee 1, chimpanzee 2, chimpanzee 3,...gorilla 1, gorilla 2,... and so on) on one series of days using the Geomagic Wrap curve drawing function (3D Solutions, Inc 2012). Then, when the curves for all individuals were drawn the landmarks for each individual were placed using the EVAN toolbox (EVAN society 2011) prior to importing the curves, and in the same order (i.e. beginning again at chimp 1) on a subsequent series of days. A sufficient amount of time had elapsed between drawing the curves and placing the landmarks for the two processes to have been unlikely to have affected one another. Then after placement of the landmarks the curves were loaded onto the specimens. During the experiment the EVAN toolkit was only capable of partial sliding of the semilandmarks. This is unlikely to seriously

affect the results presented due to the large number of semilandmarks used, however, the use of full sliding would provide a greater homology between semilandmarks and thus increase the accuracy of the findings. The semilandmarks were only applied to one reference individual (a male chimp chosen on the assumption that it represents a good compromise morphology between the extremes represented in the study, and, therefore, provides a good template from which to begin) and from this reference individual warped to all other individuals. The semilandmarks were then slid along the curve/surface to which they were linked, to minimise the bending energy of each semilandmark on a thin plate spline warped to the target from the reference object (Perez *et al.* 2006; Gunz & Mitteroecker 2013) and the average computed. This was repeated for the next specimen, and so on, until an average semilandmark placement for the entire sample was created and the bending energy of each specimen's semilandmarks to the sample mean semilandmark distribution was minimised.

2.2.3.2. Talus landmarks and semilandmarks

12 landmarks and 166 semilandmarks were placed on the talus to capture the shape of the bone and its articular surfaces. Semilandmarks were placed both along curves and on facet surfaces; 96 semilandmarks placed on curves describing facet borders and 70 placed on the facet surfaces.

Landmarks

1. Posterior most point of the lateral rim of the trochlea marking the posterior union of the trochlea and lateral malleolar facet.
2. Apex of curvature of the lateral trochlear rim.
3. Anterior most point of the lateral rim of the trochlea marking the anterior union of the trochlea and lateral malleolar facet.

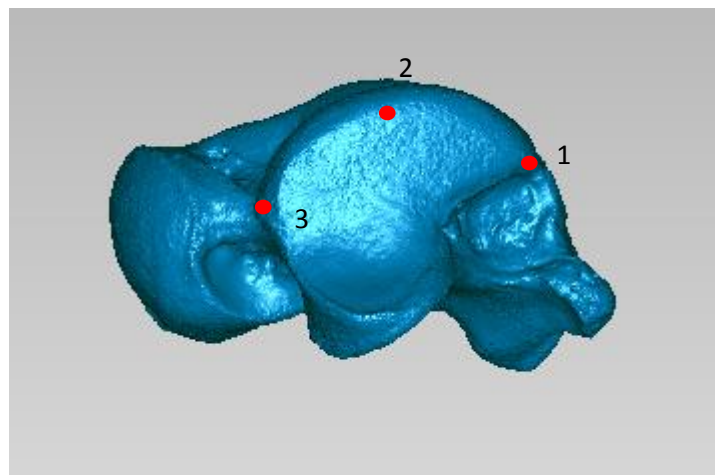


Figure 2.1. Landmarks placed on the lateral trochlea rim.

4. Posterior most point on the medial rim of the trochlea marking the posterior union of the trochlea and medial malleolar facet.
5. Apex of curvature of the medial malleolar rim.
6. Anterior most point of the medial rim of the trochlea prior to its medial divergence.
7. Anterior most point of the medial malleolar facet.
8. Posterior most point of the medial malleolar facet border at which it flares medially.

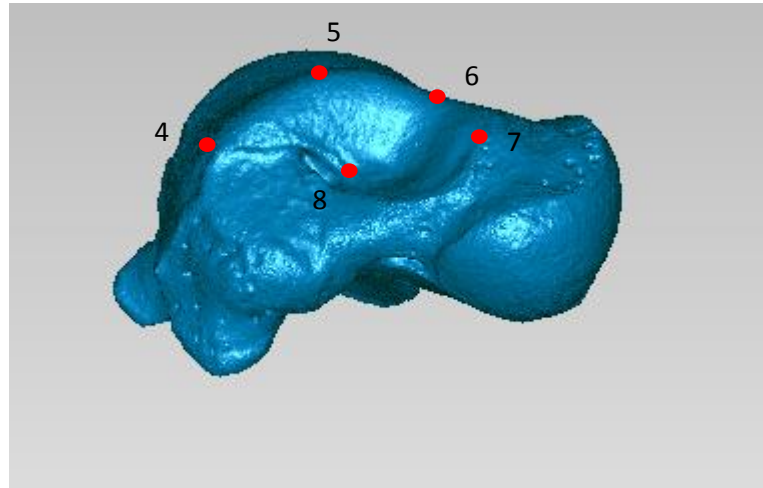


Figure 2.2. Landmarks placed on the medial malleolus

9. Midpoint of the dorsal border of the head.
10. Medial most point of the navicular articular surface.
11. Midpoint of the plantar border of the navicular articular surface.
12. Lateral most point of the navicular articular surface.

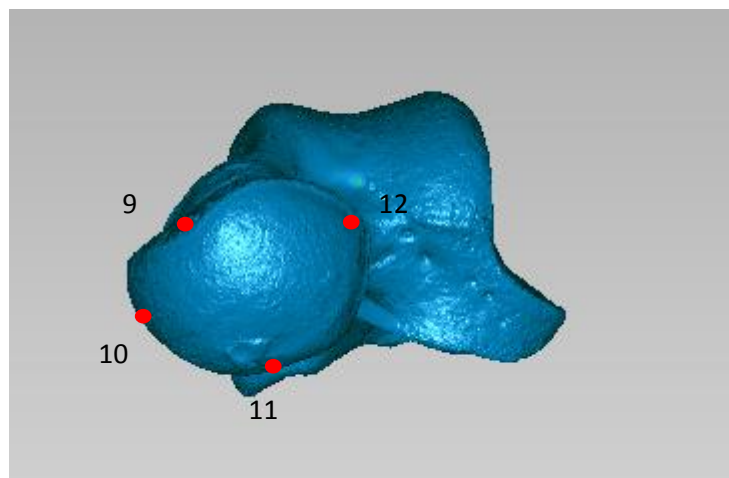


Figure 2.3. Landmarks placed on the head of the talus.

Semilandmarks

TROCHLEA There were 54 semilandmarks placed on the surface of the trochlea. These were arranged in 6 rows of 9 semilandmarks which ran from proximal to distal and began on the lateral side of the bone. The semilandmarks were evenly placed between landmarks 1 and 7 as a baseline horizontally, between landmarks 3 and 10 distally, between landmarks 1 and 3 laterally and between landmarks 7 and 10 medially, taking into account any widening of the trochlea (Fig 2.4). The lateral trochlear rim was outlined using 16 evenly spaced semilandmarks, 8 between landmarks 1 and 2, and 8 between landmarks 2 and 3.

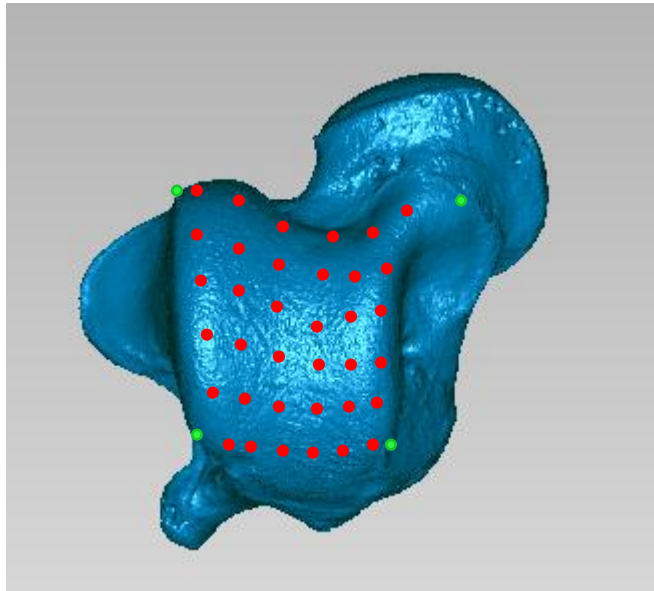


Figure 2.4. Semilandmarks placed on the trochlea. Green markers represent landmarks. Red markers represent semilandmarks.

MEDIAL MALLEOLUS 40 semilandmarks were placed around the border of the facet and 16 on the facet surface. The 40 around the border were approximately evenly spaced around the border using landmark 7 as the approximate start and end point to describe the border in as much detail as possible. The 16 semilandmarks on the facet surface were arranged in 4 rows of 4 running from the inferior border to the superior border beginning on the proximal side of the facet. The semilandmarks were evenly spaced and took into account the contour of the facet.

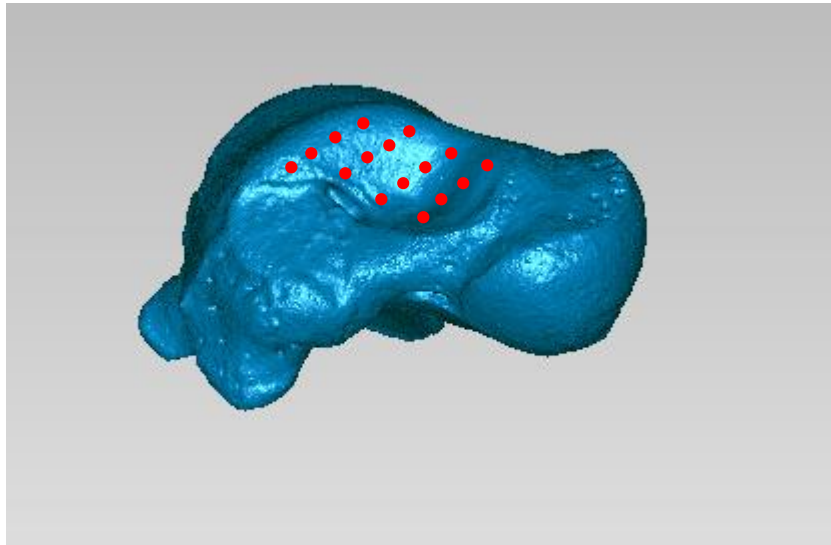


Figure 2.5. Semilandmarks placed on the medial malleolar facet.

HEAD

40 semilandmarks were placed around the border of the head and 16 were placed on the surface. The 40 semilandmarks describing the border of the head were placed around the navicular articular surface and spaced evenly using landmark 12 as the approximate start and end point. The 16 semilandmarks placed on the surface were arranged in 4 rows of 4 which ran vertically from the anteromedial corner to the posterolateral corner (Fig 2.6).

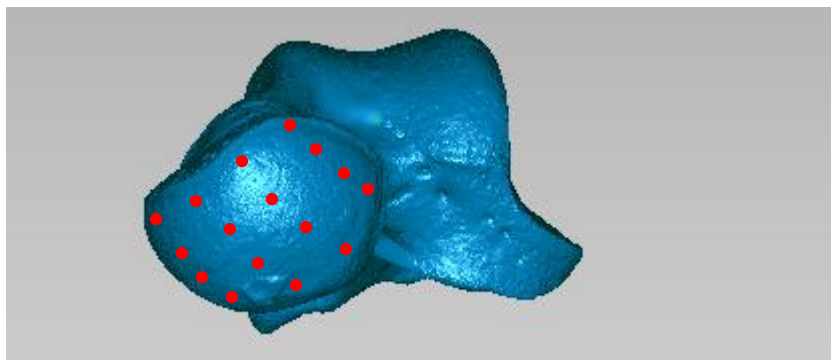


Figure 2.6. Semilandmarks placed on the head of the talus.

2.2.3.3. Navicular landmarks and semilandmarks

10 landmarks and 243 semilandmarks were placed on the navicular to capture the shape of the bone and its articular surfaces. Semilandmarks were placed both along curves and on facet surfaces; 140 semilandmarks placed on curves describing facet borders and 103 placed on the facet surfaces.

Landmarks

1. Lateral most point of the talar facet.
2. Medial most point of the talar facet.
3. Superior most point of the talar facet.

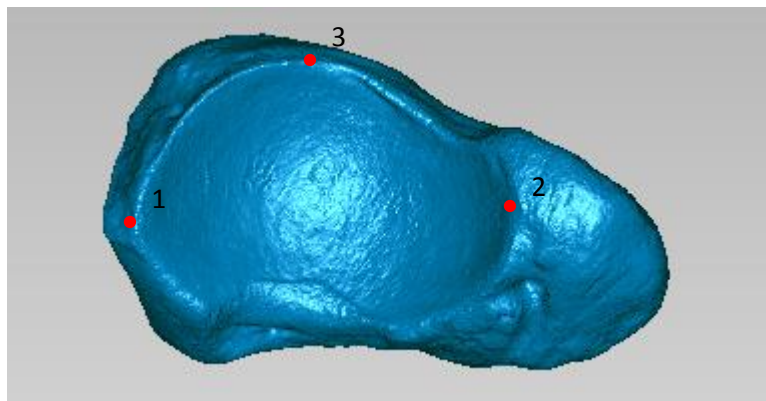


Figure 2.7. Landmarks placed on the proximal navicular.

4. Medial most point of the medial cuneiform facet.
5. Inferior most point of the border between the medial and intermediate cuneiform facets.
6. Inferior most point of the border between the intermediate and lateral cuneiform facets.
7. Inferolateral corner of the lateral cuneiform facet.
8. Superolateral corner of the lateral cuneiform facet.
9. Superior most point of the border between the lateral and intermediate cuneiform facets.
10. Superior most point of the border between the intermediate and medial cuneiform facets.

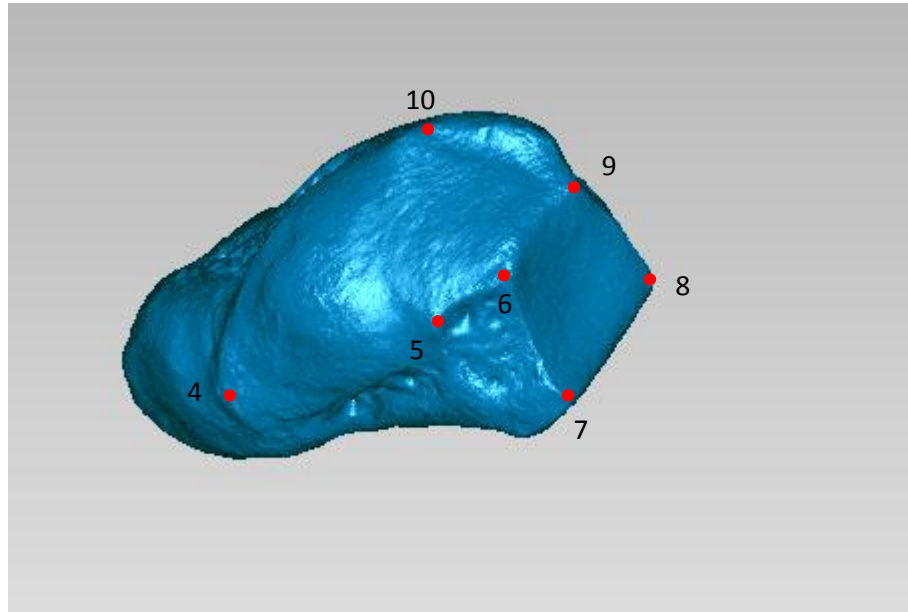


Figure 2.8. Landmarks placed on the distal navicular.

Semilandmarks

TALAR FACET 60 landmarks were placed around the border of the facet and 30 placed on the facet surface. The 60 landmarks placed on the border were evenly spaced using landmark 1 as an approximate start and end point. The 30 semilandmarks on the surface of the facet were placed in concentric ovals. This began with a landmark placed on the lateral side of the facet with an arch describing the superior part of the facet over to the medial side of the facet and an arch back along the inferior border to complete the oval. This was composed of 18 semilandmarks. This was repeated for a smaller oval contained within the one described and constructed in the same way using 11 semilandmarks. Finally, a semilandmark was placed at the centre of the two ovals.

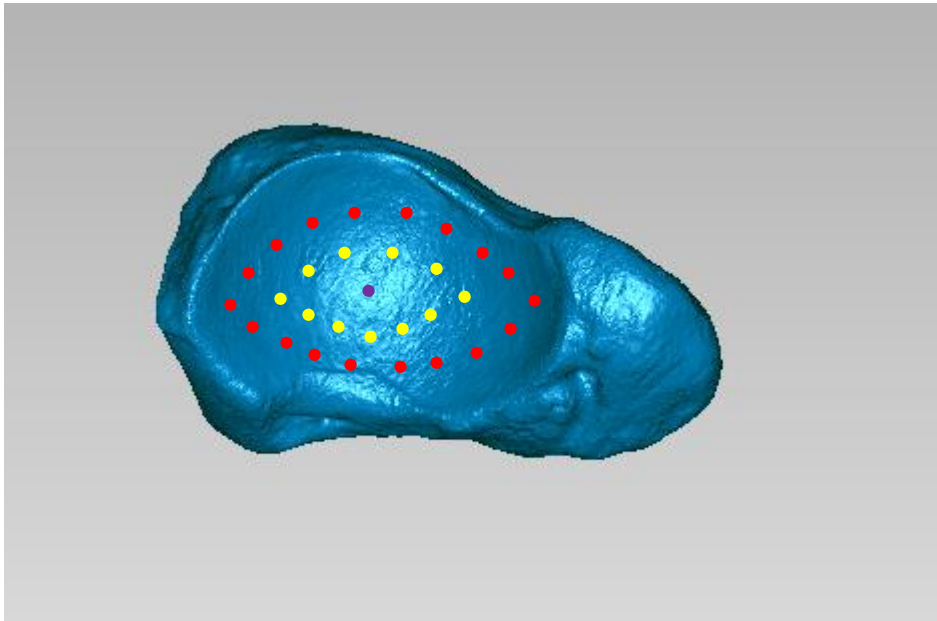


Figure 2.9. Semilandmarks placed on the talar facet. Red semilandmarks are the outer oval. Yellow semilandmarks are the inner oval. Purple semilandmark is the centre of the ovals.

DISTAL FACET 80 semilandmarks were placed around the border of the cuneiform facets and 73 in total in the distal surface. The 80 semilandmarks describing the border of the distal facets were evenly spaced using landmark 4 as the approximate start and end point. The 73 semilandmarks describing the distal surface were shared evenly between the three cuneiform facets.

Medial cuneiform facet – 28 semilandmarks were placed in 5 rows of 5 beginning at the lateral border and running from superior to inferior. As the facet narrows medially an additional row of 3 semilandmarks was added to capture the extreme medial side of the facet.

Intermediate cuneiform facet – 15 semilandmarks were placed in a triangular layout to capture the broad superior border and narrowing inferiorly.

Lateral cuneiform facet – 20 landmarks arranged in 4 evenly spaced rows of 5 semilandmarks running medial to lateral from the superior border to the inferior border.

An additional 5 semilandmarks were added to mark the border between the medial and intermediate cuneiform facets and 5 were added to mark the border between the intermediate and lateral cuneiform facets.

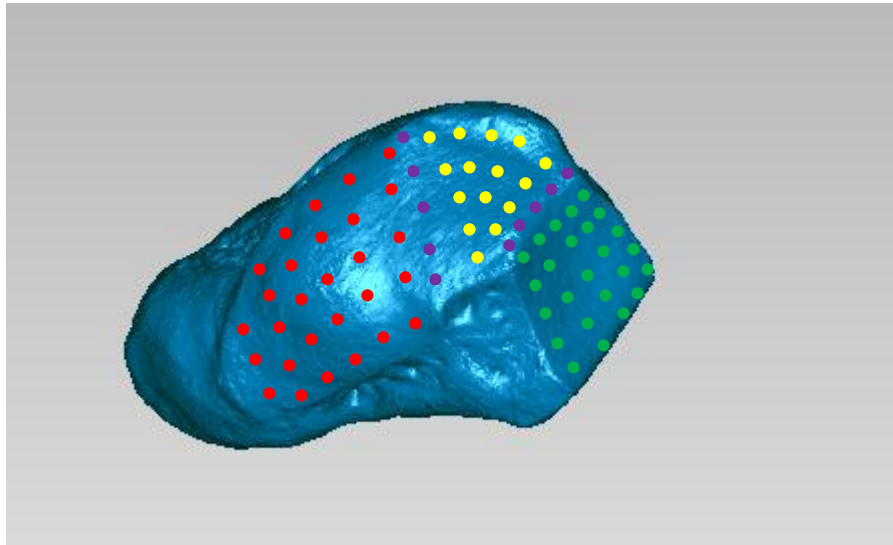


Figure 2.10. Semilandmarks on the distal navicular. Red semilandmarks are those describing the medial cuneiform facet. Yellow semilandmarks are those describing the intermediate cuneiform facet. Green semilandmarks are those describing the lateral cuneiform facet. Purple semilandmarks are those describing the borders between cuneiform facets.

2.2.3.4. Medial cuneiform landmarks and semilandmarks

14 landmarks and 198 semilandmarks were placed on the medial cuneiform. Of the 198 semilandmarks, 150 were placed on the proximal and distal facet borders and 48 were placed on the facet surfaces.

Landmarks

1. Superior most point of navicular facet.
2. Lateral most point of navicular facet.
3. Inferior most point of navicular facet.
4. Medial most point of navicular facet.
5. Anterior most point of the inferior portion of the intermediate cuneiform facet.
6. Inferior point of the distal border of the articulation with the intermediate cuneiform.
7. Superior point of the distal border of the articulation with the intermediate cuneiform.

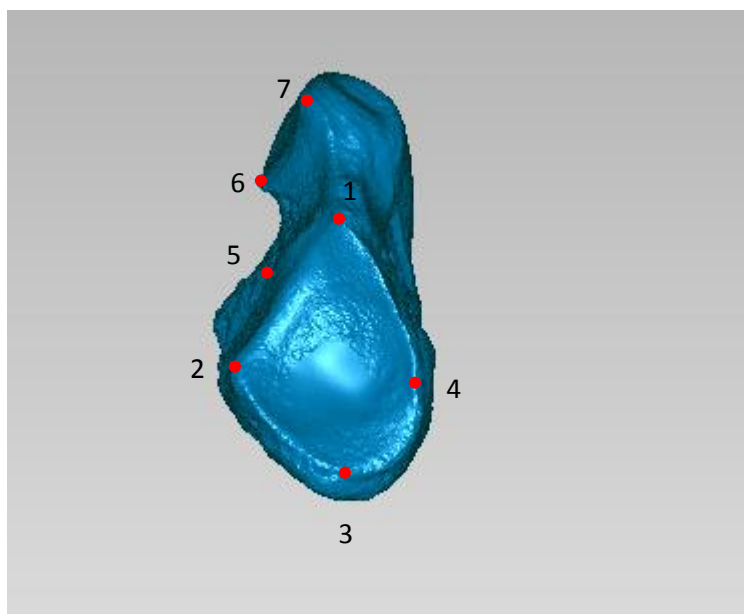


Figure 2.11. Landmarks placed on the navicular facet of the medial cuneiform and the single landmark placed on the lateral surface.

8. Midpoint of the superior border of the facet for the first metatarsal.
9. Superomedial corner of the facet for the first metatarsal.
10. Inferomedial corner of the facet for the first metatarsal.
11. Midpoint of the inferior border of the facet for the first metatarsal.
12. Inferolateral corner of the facet for the first metatarsal.
13. Most medial point of the lateral border of the facet for the first metatarsal.
14. Superolateral corner of the facet for the first metatarsal.

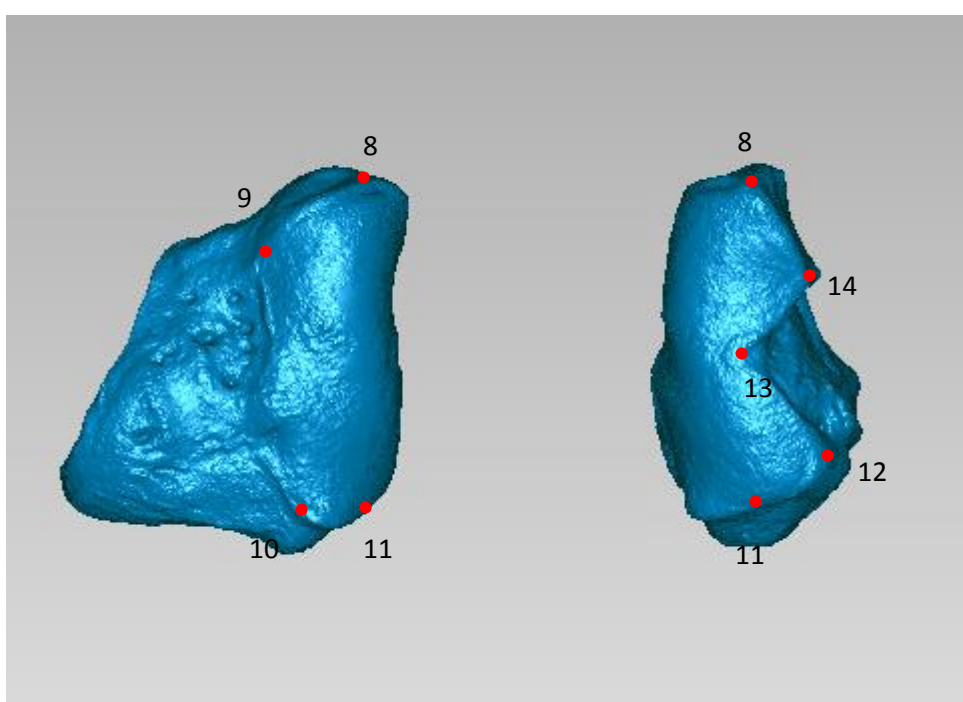


Figure 2.12. Landmarks placed on the facet for the first metatarsal. On the left is a medial view of the medial cuneiform, on the right is a distal view.

Semilandmarks

NAVICULAR FACET 70 semilandmarks were placed around the border of the navicular facet and 20 were placed on the surface. The 70 landmarks describing the border were evenly spaced using landmark 2 as the approximate start and end point. The 20 semilandmarks on the surface were arranged in 5 rows of 4 running from inferolateral to superomedial (Fig 2.13).

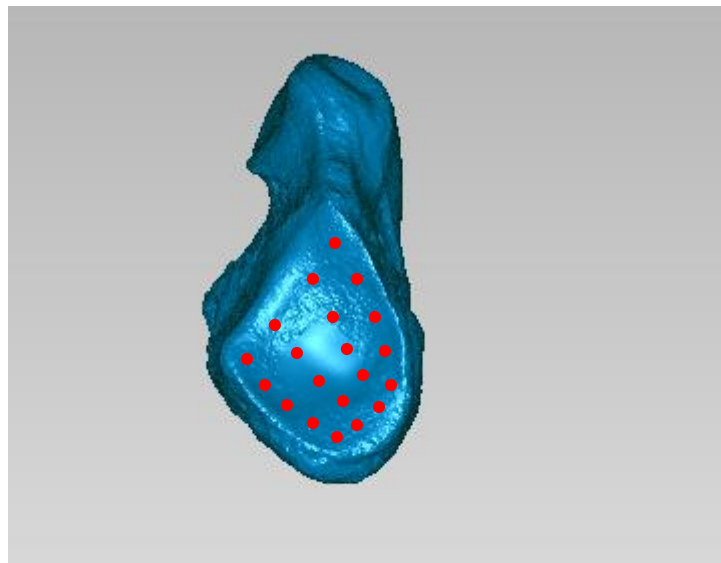


Figure 2.13. Semilandmarks placed on the navicular facet of the medial cuneiform.

DISTAL FACET 80 semilandmarks were placed on the border and 28 were placed on the facet surface. The 80 semilandmarks placed on the border were evenly spaced using landmark 9 as the approximate start and end point. The 28 semilandmarks placed on the surface are placed 7 rows of 4. The third row runs from the medial border to landmark 13 roughly bisecting the facet (Fig 2.14).

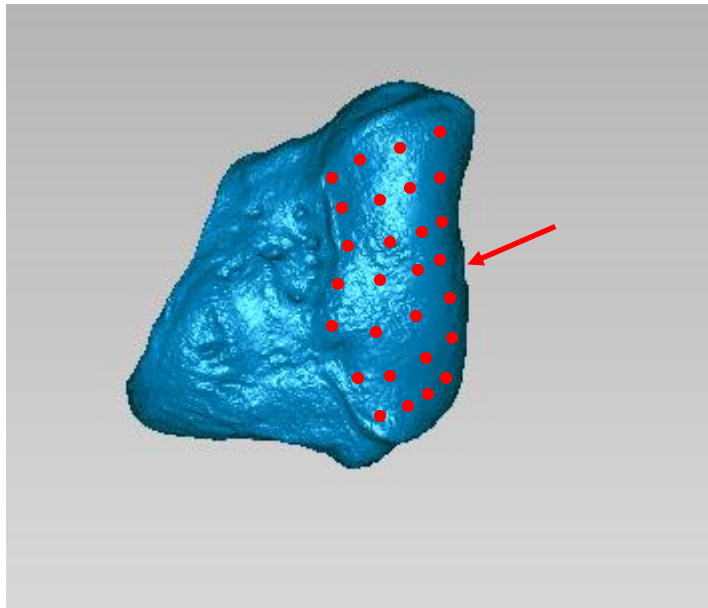


Figure 2.14. Semilandmarks placed on the distal facet of the medial cuneiform. Arrow indicates location of landmark 13.

2.2.3.5. Intermediate cuneiform landmarks and semilandmarks

10 landmarks and 228 semilandmarks were placed on the intermediate cuneiform. Of the 228 semilandmarks 170 were placed on facet borders and 57 were placed on facet surfaces.

Landmarks

1. Superolateral corner of the navicular facet.
2. Inferolateral corner of the navicular facet.
3. Inferomedial corner of the navicular facet.
4. Superomedial corner of the navicular facet.
5. Anterior most point of the inferior portion of the medial cuneiform facet.

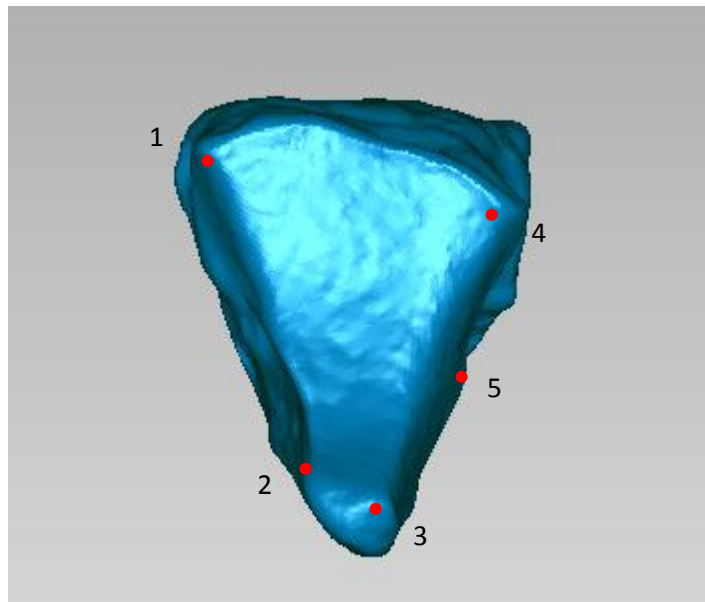


Figure 2.15. Landmarks placed on the navicular facet of the intermediate cuneiform.

- 6. Superomedial corner of distal facet.
- 7. Inferior most point of the medial side of the superior expansion of the distal facet.
- 8. Inferior most point of the distal facet.
- 9. Inferior most point of the lateral side of the superior expansion of the distal facet.
- 10. Superolateral corner of the distal facet.

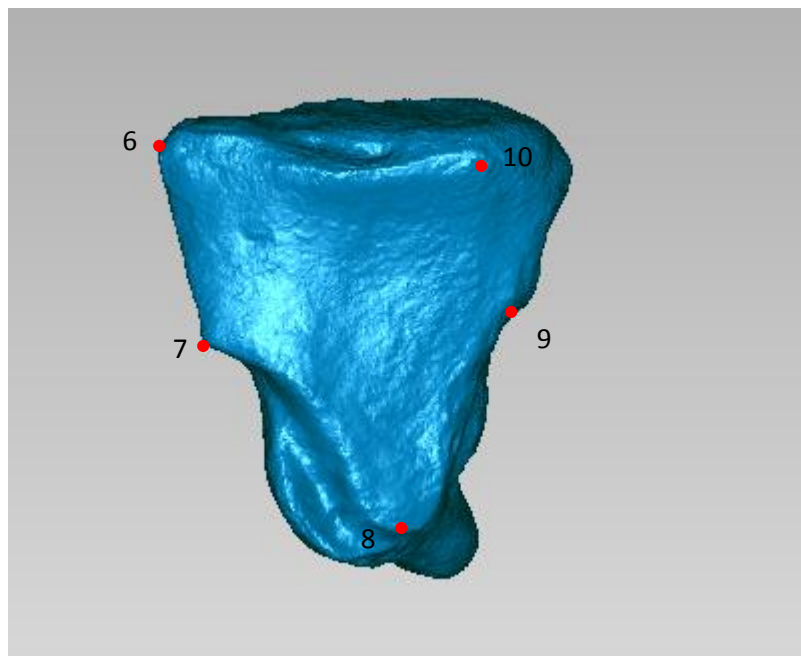


Figure 2.16. Landmarks placed on the distal facet of the intermediate cuneiform.

NAVICULAR FACET 80 semilandmarks were placed around the border of the navicular facet and 28 on the facet surface. The 80 semilandmarks on the border were evenly spaced and used landmark 1 as the approximate start and end point. The 28 semilandmarks on the surface were arranged in a triangle with a base of 7 semilandmarks beginning across the superior part of the facet.

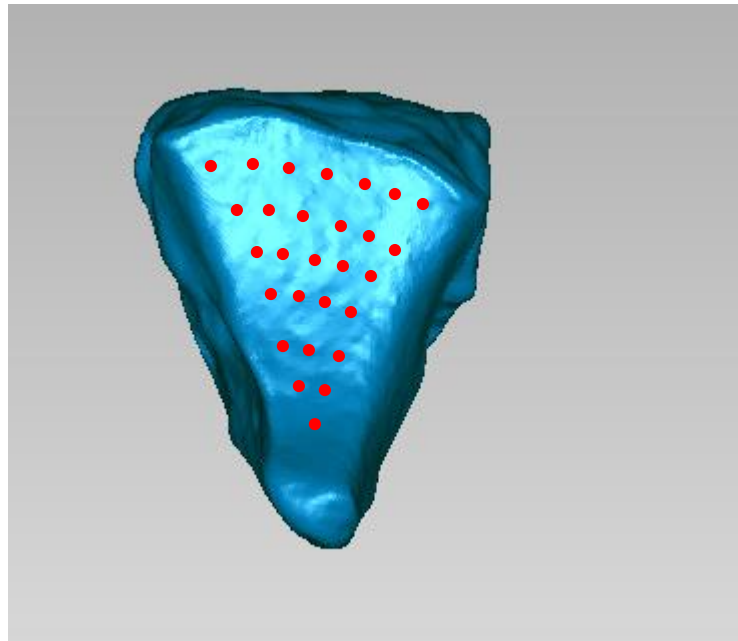


Figure 2.17. Semilandmarks placed on the surface of the navicular facet.

DISTAL FACET 90 semilandmarks were placed around the border of the facet and 29 were placed on the surface of the facet. The 90 semilandmarks placed on the border were evenly spaced and used landmark 6 as the approximate start and end point. The semilandmarks were placed in a triangular fashion similar to that described for the navicular facet. However, the first row (i.e. the superior row) contains 8 rather than 7 semilandmarks because the facet is broader.

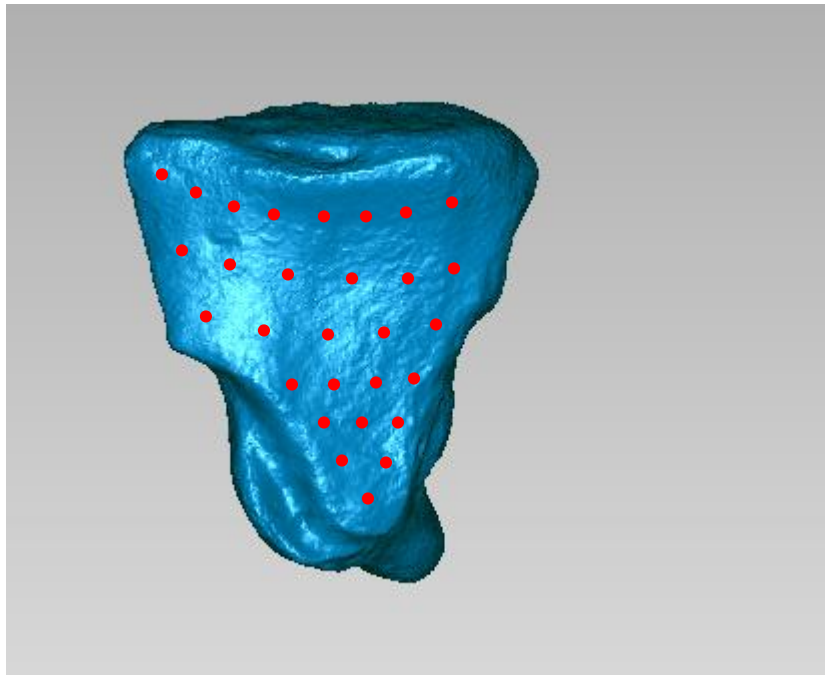


Figure 2.18. Semilandmarks placed on the distal facet of the intermediate cuneiform.

2.2.3.6. Lateral cuneiform landmarks and semilandmarks

15 landmarks and 201 semilandmarks were placed on the lateral cuneiform. Of the 201 semilandmarks 146 were placed around facet borders and 55 were placed on facet surfaces.

Landmarks

1. Superolateral corner of navicular facet.
2. Inferolateral corner of navicular facet.
3. Inferomedial corner of navicular facet.
4. Superomedial corner of navicular facet.

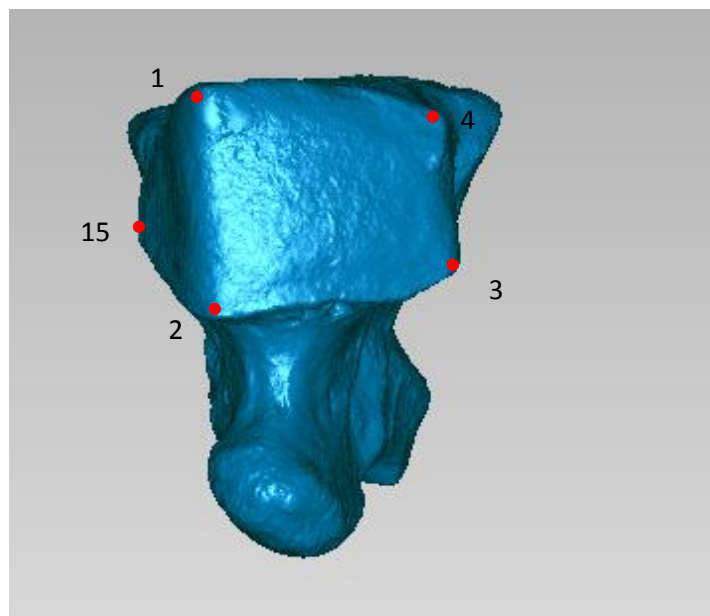


Figure 2.19. Landmarks placed on the navicular facet for the lateral cuneiform.

5. Superomedial corner of distal facet.
6. Inferior most point of medial border prior to constriction of the superior portion.
7. Midpoint of medial border.
8. Medial most point between midpoint of medial border and inferomedial corner of facet.
9. Inferomedial corner of distal facet.
10. Inferolateral corner of distal facet.
11. Midpoint of lateral border.
12. Inferior most point of lateral border prior to constriction of the superior portion.
13. Superolateral corner of distal facet.
14. Midpoint of cuboid articulation.

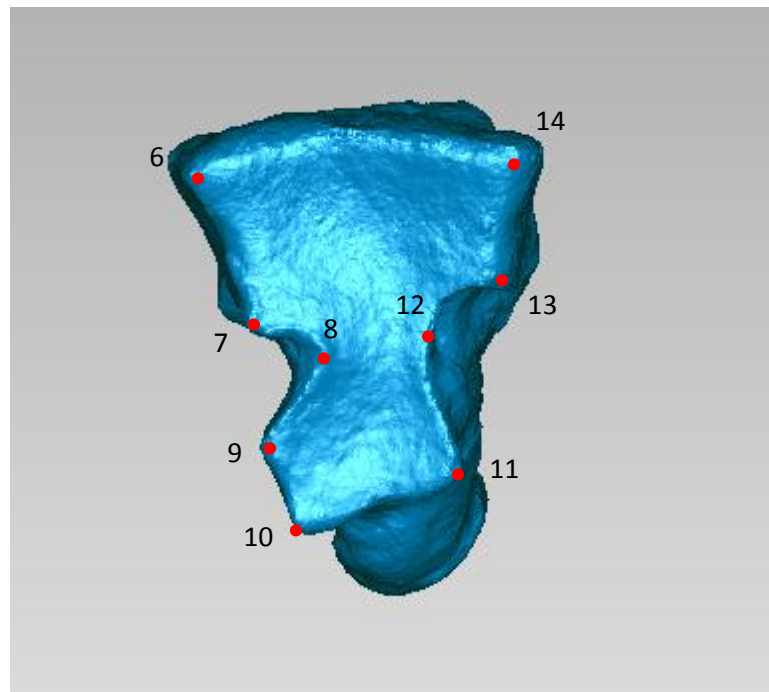


Figure 2.20. Landmarks placed on the distal facet of the lateral cuneiform.

Semilandmarks

NAVICULAR FACET 51 semilandmarks were placed around the facet border and 20 were placed on the surface. The 51 placed on the border were evenly spaced using landmark 1 as the approximate start and end point. The 20 semilandmarks placed on the facet surface were arranged in 4 horizontal rows of 5 beginning in the superolateral corner and ending in the inferomedial corner.

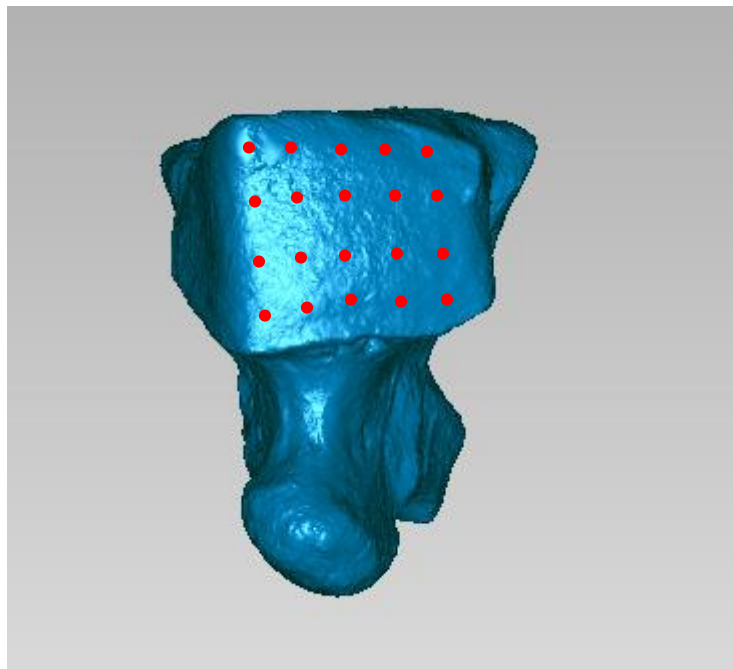


Figure 2.21. Semilandmarks placed on the surface of the navicular facet of the lateral cuneiform.

DISTAL FACET

95 semilandmarks were placed around the border of the facet and 35 on the facet surface. The 95 semilandmarks placed around the border were evenly spaced and used landmark 6 as an approximate start and end point. The 35 surface semilandmarks were placed in 2 horizontal rows of 6 to capture the superior breadth of the facet. Then a row of 5 as the facet narrows. Then 2 rows of 3 to assess constriction at the midpoint of the facet. Then 3 rows of 4 to measure the inferior part of the facet.

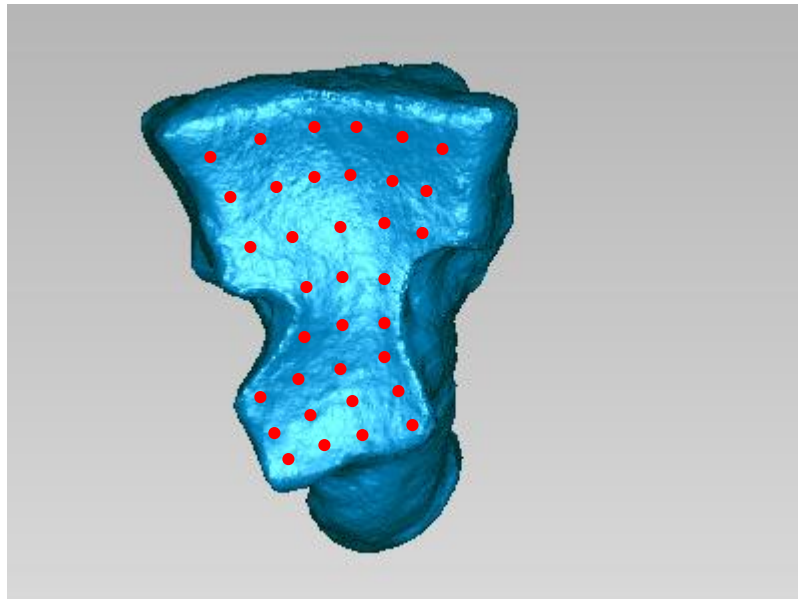


Figure 2.22. Semilandmarks placed on the distal facet of the lateral cuneiform.

2.2.3.7. First metatarsal landmarks and semilandmarks

11 landmarks and 198 semilandmarks were placed on the first metatarsal. Of the 198 semilandmarks 148 were placed around facet borders and 50 were placed on facet surfaces.

Landmarks

1. Midpoint of lateral border of medial cuneiform facet.
2. Inferolateral corner of medial cuneiform facet.
3. Inferomedial corner of medial cuneiform facet.
4. Superomedial corner of medial cuneiform facet.
5. Superolateral corner of medial cuneiform facet.

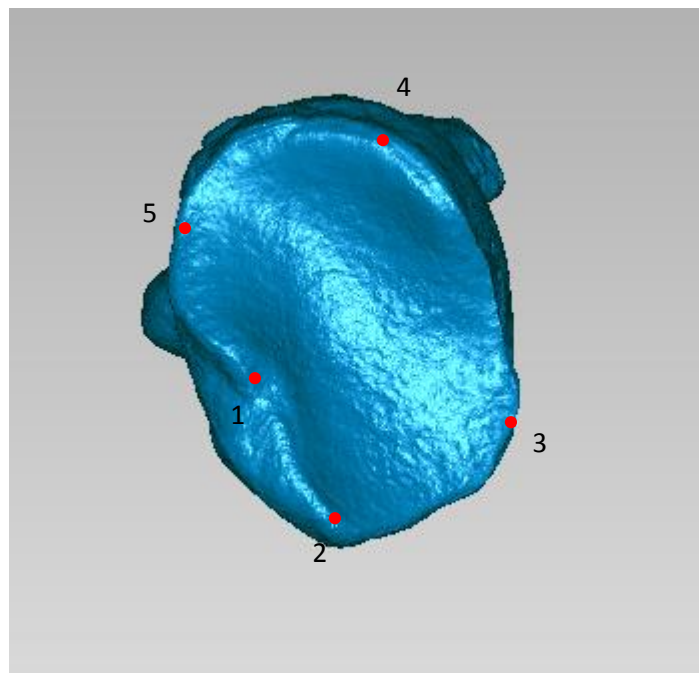


Figure 2.23. Landmarks placed on the medial cuneiform facet of the first metatarsal.

6. Superomedial corner of head.
7. Midpoint of medial border of head.
8. Posterior most point of the medial plantar cornua.
9. Posterior most point of lateral plantar cornua.
10. Midpoint of lateral border of head.
11. Superolateral border of head.

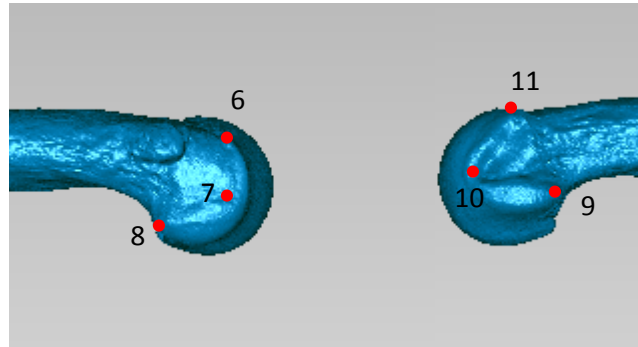


Figure 2.24. Landmarks placed on the head of the first metatarsal.

Semilandmarks

BASE

63 semilandmarks were placed around the border of the proximal facet and 20 were placed on the facet surface. The 63 placed on the border were evenly spaced using landmark 1 as an approximate start and end point. The 20 on the surface were arranged in 5 rows of 4 running medial to lateral, beginning in the superomedial corner.

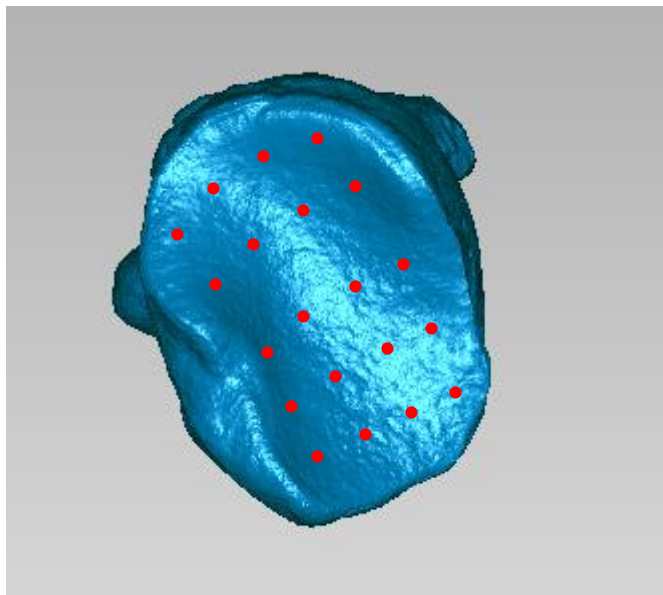


Figure 2.25. Semilandmarks placed on surface of medial cuneiform facet of first metatarsal.

HEAD

85 semilandmarks were placed around the border of the head and 30 were placed on the surface. The 85 that were placed on the border were evenly spaced using landmark 6 as an approximate start and end point. The 30 surface semilandmarks were arranged in 6 rows of 5 running lateral to medial, beginning in the superolateral corner.

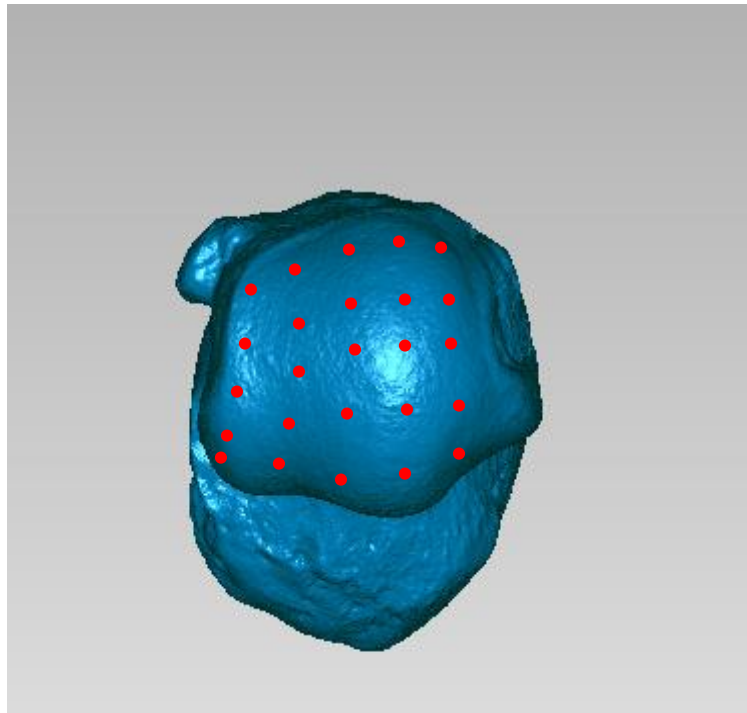


Figure 2.26. Semilandmarks placed on the head of the first metatarsal.

2.2.4. Analysis of data

After collection of all of the landmark and semilandmark data the configurations for each individual were brought into a standardised alignment from which statistical comparisons could be made. This was done using generalised Procrustes analysis in the *EVAN toolkit* (Gower 1975; see O'Higgins *et al.* 2001 for an overview). This procedure is a method of removing information contained within a 3D landmark configuration that is obstructive to analysing shape: size, location, and orientation (Zelditch *et al.* 2004). Location is removed by centring the centroid of each landmark configuration at the origin of the Cartesian coordinate system in which it exists. The centroid is the average landmark location for a given configuration. For a 3D landmark configuration the centroid will have an x-coordinate which is the sum of each landmark x-coordinate divided by the total number of landmarks. The same is true of the y and z-coordinates. Then subtracting the coordinates of the centroid from each landmark and positioning the centroid of each configuration at the origin removes any differences in location from the sample.

Size (or scale) is then removed using centroid size. Centroid size is a measure of the size of an object which relies only on the Cartesian coordinates of the landmarks representing the object and as such does not have a unit. It is defined as the square root of the sum of the squared distances of each landmark from the centroid (Dryden and Mardia 1998). It is therefore a measure of size which uses the cumulative distance of landmarks from their shared average point (the centroid) as a proxy for overall size. To remove the effects of differences in size from the analysis each landmark for each individual is divided by the centroid size for that particular landmark configuration (Rohlf and Slice 1990). Thus, larger individuals (those with a larger centroid size) will be reduced to a relatively greater extent than those with a smaller centroid size, equalising the relative scales of the different specimens.

Finally, rotational effects (orientation), which, like location, are artefacts of the original collection of landmark data and the coordinate system it was conducted in, are removed. This is done by minimising the distance between corresponding landmarks across the entire sample (Baab *et al.* 2012). Of course, this process is mathematically complex and is made more difficult with the addition of more landmarks and specimens. The advantages of geometric morphometrics come at the cost of computing power. The process of finding an optimal alignment of specimens is iterative. First, the optimal alignment is found for all specimens relative to a reference specimen and then the average

shape is calculated. Then all specimens are rotated to find their optimal alignment relative to this average, then a new average is calculated and all specimens aligned to this. This continues until the calculation of the average shape is no longer different than the one that preceded it (Zelditch *et al.* 2004).

These operations have desirable statistical consequences which make the comparison of entire shapes much simpler. Each landmark configuration can be thought of as occupying a single point in a shape space, which describes all possible shape configurations for the particular number of landmarks and dimensions used in the study. The advantage of performing the operations described above is that they allow the construction of a pre-shape space which removes all shapes which differ in centroid size and location (Zelditch *et al.* 2004). Then finding the rotational positions of individual landmark configurations which most closely approximate one another (have the lowest Procrustes distance for all possible rotations of the two configurations) further constricts the possible shapes represented in this higher-dimensional space (Bookstein 1991; 1996). The resulting shape space will contain one point for each individual landmark configuration in the study representing its optimal rotational alignment and allow the calculation of the mean shape of the overall sample. This shape space is known as Kendall's shape space (Kendall 1977; 1989; Rohlf and Slice 1990; Bookstein 1991; 1996; Zelditch *et al.* 2004).

Following the superimposition of the landmarks and calculation of the mean shape a principal components analysis was conducted to extract explanatory factors from the data, also using *EVAN toolkit*. Since each point in shape space represents a unique landmark configuration, and since more similar shapes (i.e. representing members of the same species) will be in much closer proximity in shape space, it will be possible to describe differences between species based on these general similarities of the shape space configurations. Principal components analysis produces components which are entirely orthogonal to one another and the higher numbered components become weaker in terms of their explanatory power. That is to say that the first principal component will explain the greatest amount of the variation in the sample, followed by the second, and so on. The principal components analysis reveals not only a general proximity in shape space and overall similarity, but provides real insights into the precise ways in which landmark configurations differ (Harcourt-Smith 2002; Zelditch *et al.* 2004; Proctor 2008), and this can be visualised using thin plate splines (Bookstein 1989). The principal components graphs were created using PAST (Hammer *et al.* 2001).

While the principal components analysis does provide detailed and valuable information about the proximity of specimens to one another in shape space and the ways in which landmark configurations in the sample vary in shape, it does not give any indication of the level of statistical significance of the observed differences between groups (Proctor 2008). In order to test for significant differences in shape between extant taxa the Procrustes distances between individuals were calculated and examined using permutation tests. This was done using MorphoJ (Klingenberg 2011). Permutation tests are useful because they make no assumptions about normality of the data and they can test for difference between different sample sizes. Permutation tests work by first calculating the mean value of the two original groups under study, and the difference between their means. Then, all data are pooled together and two unique test groups are drawn and their means calculated, and difference calculated. This step is repeated many thousands of times and in this manner a probability distribution of difference of means is created. The difference between the original mean values is then compared to this probability distribution to see if the value lies outside the 95% confidence limit. If it does then it can be concluded that the means are more different than they would be by chance alone, and thus the difference between the means is significant (Hesterberg *et al.* 2003). In the case of fossil specimens permutation tests are not appropriate as they are not valid for use on individual data points. Instead, the Mahalanobis distance of the fossil from extant species mean shapes was calculated, giving a number of standard deviation units from the extant mean shape (z-score) from which the p value of the difference can be calculated.

The relative sizes of the different extant taxa and the comparison of fossil specimens to these taxa is also of interest. The hypotheses relating to size at the end of the previous chapter are tested by examining the centroid sizes of the individuals. In a similar way to the Procrustes distances, permutation tests were used to assess whether or not different extant taxa had statistically significantly different means, and therefore elucidate upon the size relationships of these taxa. The fossil taxa were not prone to exploration using permutation tests, as noted above. To examine the size relationships of the fossils their z-scores were calculated from the species mean values. Z-score calculates the number of standard deviations a single datum is from the mean value of a sample. This is a straightforward calculation in which the difference between the fossil and the mean is divided by the standard deviation of the extant sample thereby expressing how many standard deviations from the mean the fossil is. From the z-score, a p value is then calculated giving the probability that the single datum could have been taken from the sample in question. As per usual with any statistical test, the significance is set to 0.05 for each individual comparison. However, when numerous comparisons are made simultaneously the chance of type 1 error increases. Therefore, Bonferroni

correction is applied in those circumstances. The significance threshold is divided by the number of comparisons being carried out to correct for the probability of type 1 error occurring (Bland 1995).

Finally, the differences in shape between fossils and extant species were visualised using the EVAN toolkit. This was done by generating the hypothetical mean shape of the extant species (as it is from the mean that the Procrustes distances of the fossils are calculated) and warping from this mean shape to the shape of the fossil specimens. This warping is aided by the use of a grid superimposed over the bone being visualised. The grid is not deformed when it is placed over the reference specimen (species mean). However, when the reference is warped to the target the grid deforms revealing how the reference and target differ in shape. More precisely, it reveals the necessary changes that occur to convert the reference shape to the target shape and this allows functional differences to be considered based on these differences in shape.

3. Results

This chapter provides the results of all tests conducted. It is divided into sections for each bone (the proximal and distal first metatarsal was examined in addition to the complete first metatarsal to allow the inclusion of the fragmentary *Oreopithecus* material). Each section is then further divided into three subsections. The first gives the results of the principal components analysis and assesses the proximity of species to one another on each principal component, as well as the proximity of the fossil specimens to species groups. The second assesses the significance of differences between species through examination of the Procrustes distances between species means. The third will visualise the changes in shape represented by each principal component. When describing distributions on the principal components graphs “positive” and “negative” are used to mean right and left, or up and down, respectively, even when the distribution may not have real positive or negative scores.

3.1. Talus

3.1.1. Principal components analysis

3.1.1.1. Full sample

A principal components analysis was conducted on the Procrustes aligned landmark configurations for the trochlea, medial malleolar facet and head of the talus for all specimens in the study. The first three principal components cumulatively explained 53.74% of the variance of the data set, the first five explained 74.06%, and the first 10 explained 86.63%. The remaining 14% of variance was explained by principal components 11-80 (Figure 3.1.1).

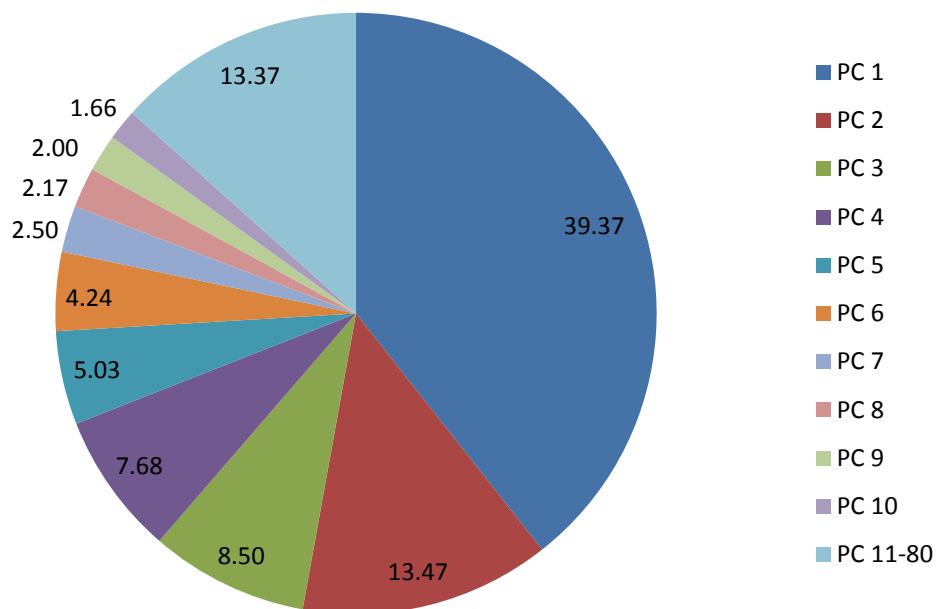


Figure 3.1.1. Percentage of the overall variance explained by each principal component for the talus.

The first three principal components explain just over half of the overall variance of the data set. Higher principal components account for considerably less of the variance and examination of the graphs associated with them reveals that they provide little differentiation between species. However, principal components 1-3 expose patterns in the data which are concordant with previous work (Harcourt-Smith 2002). Figure 3.1.2 displays the distribution of all specimens along PC1 and PC2. With regard to PC1 the biggest difference appears to be between *Homo* and *Pongo*. *Homo* has high positive values for PC1 and its range does not overlap with any other distributions. *Pongo* occupies

the negative end of the axis, but the positive extent of the distribution also coincides slightly with the distribution of *Theropithecus*. The *Pan* and *Gorilla* distributions lie close to the mean value for PC1. The *Gorilla* mean is more positive than *Pan* placing its distribution closer to the *Homo* range. However, there is significant overlap between the two distributions around the mean value for PC1. The *Theropithecus* mean is situated just on the negative periphery of the *Pan* range, overlapping more with this species than with *Pongo*. OH8 lies at the positive edge of the *Gorilla* distribution on PC1. The *Gorilla* and *Homo* ranges do almost overlap on PC1 but OH8 is situated more closely to *Gorilla*. The remaining fossil specimens group together very closely. *Nacholapithecus* lies at roughly the *Pan* mean while *Oreopithecus* lies towards the negative periphery of the *Pan* range. Nonetheless, both of the specimens fall well within the distribution of *Pan*.

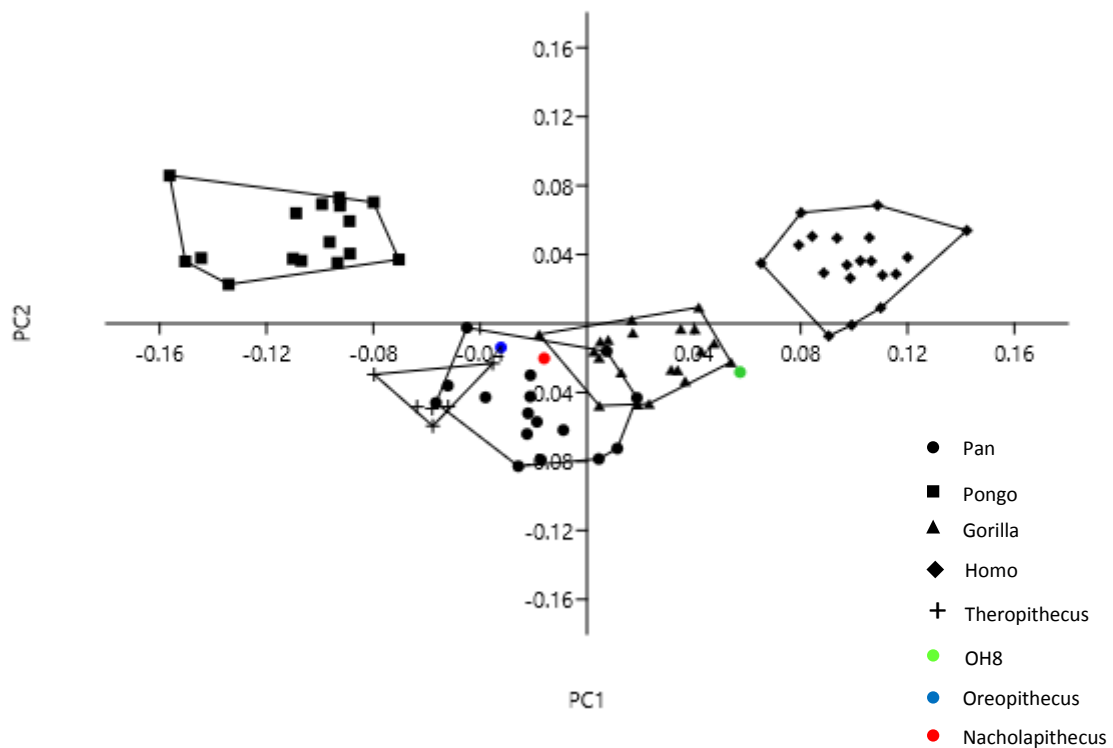


Figure 3.1.2. Principal component 1 vs. principal component 2 of all individuals for the talus.

PC2 is less informative than PC1, as should be expected. However, notable patterns do emerge. *Homo* and *Pongo* are grouped together to the exclusion of African apes and *Theropithecus*, which form a cluster in the negative range. The *Pongo* mean is further from the PC2 mean than the *Homo* mean, but the two species clearly group together in the positive PC2 range. *Pan* and *Gorilla* again cluster closely together, as they do for PC1. *Gorilla* lies slightly closer to the mean PC2 score, closer to

the *Homo/Pongo* group, than does *Pan*. *Theropithecus* lies between the *Pan* and *Gorilla* distributions but its mean is slightly closer to the mean of *Pan*. All fossil specimens score slightly below the average PC2 score lying close to the *Gorilla* mean. *Oreopithecus* and *Nacholapithecus* have approximately the same value as the *Gorilla* mean; OH8 scores slightly more negatively. OH8 is therefore located further from the *Homo* range than other fossil specimens on PC2. Taken together PC1 and PC2 create an African ape group which clusters close to the origin of the plot. The *Homo* and *Pongo* distributions are clearly distinct from the African ape/*Theropithecus* cluster but in opposing directions.

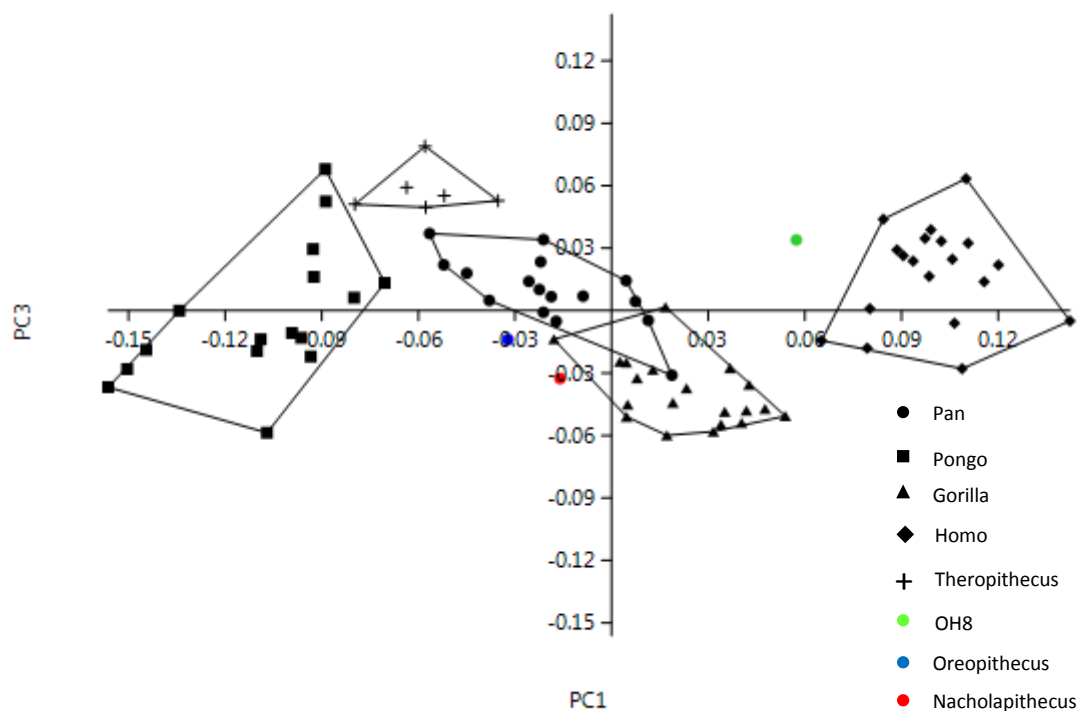


Figure 3.1.3. Principal component 1 vs. principal component 3 of all individuals for the talus.

PC3 accounts for 8.5% of variance (Figure 3.1.1). The mean values for the ape species all lie close to the mean PC3 score (Figure 3.1.3), though there are clearly some differences between the species means and their distributions. *Pongo* has a much greater range across PC3 than any of the other species but its average is roughly 0 (0.0028) on PC3. The distributions of *Pan* and *Gorilla* across PC3 are distinct. *Gorilla* is distributed largely below 0 on the PC3 axis while the *Pan* mean lies just above 0, though the two distributions overlap somewhat. The *Homo* mean is similar to that of *Pan* and their ranges are similar also. The most notable feature of the PC3 axis is the distribution of *Theropithecus*.

The *Theropithecus* mean is higher than any other species, however its range overlaps with *Pongo* and *Homo*. The greatest separation on PC3 is between *Theropithecus* and *Gorilla*. OH8 falls within the *Pan* and *Homo* range, but also that of *Pongo*. *Nacholapithecus* has a negative value on the PC3 axis placing it close to the *Gorilla* mean. *Oreopithecus* has a score similar to the mean of *Pongo*.

PC4 represents a similar distribution to PC3, separating the *Theropithecus* distribution from the apes. However, *Theropithecus* is more clearly defined along PC4 than it is along PC3 (Figure 3.1.4). Additionally, PC4 separates *Nacholapithecus* from the apes and aligns it quite closely with *Theropithecus* (although it lies within the *Homo* range). The higher principal components do not illustrate notable differences between species groups but in some instances separate fossil specimens from other individuals. For example, principal component 8 clearly separates *Nacholapithecus*.

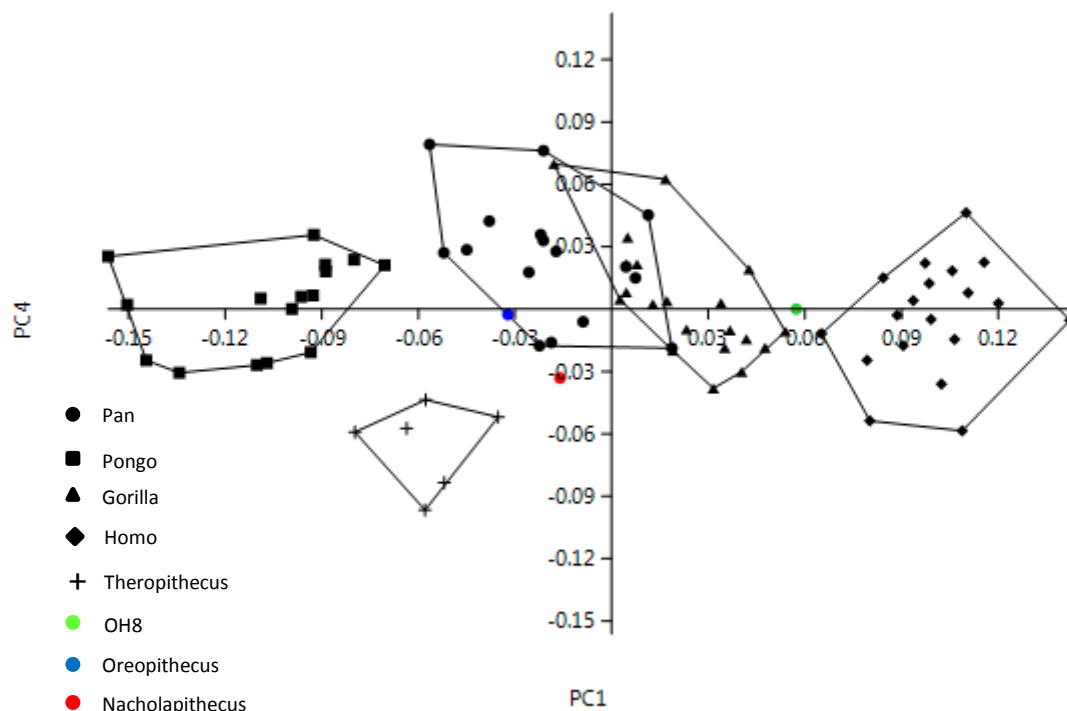


Figure 3.1.4. Principal component 1 vs. principal component 4 of all individuals for the talus.

3.1.1.2. Extant species means vs. fossils

A principal components analysis was conducted on the Procrustes aligned landmarks for the trochlea, medial malleolar facet and head of the talus using the species mean shapes and fossils only. There were eight principal components, of which the first seven explained practically 100% of the variance in the data, while the amount of variance described by the eighth is negligible (Figure 3.1.5). The first three principal components account for 75% of the variance and the first four account for 85%.

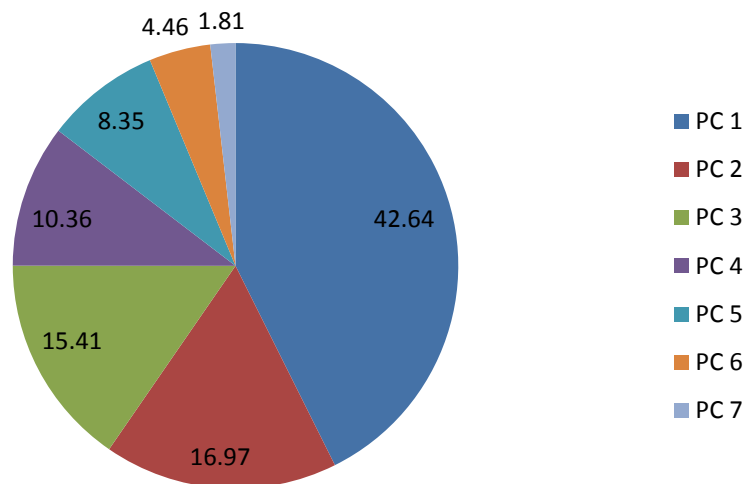


Figure 3.1.5. Percentage of the variance explained by each PC using only species mean shapes.

Principal component 1 provides a data distribution which is broadly concordant with the principal component analysis featuring all individuals as opposed to just the species means. *Homo* and *Pongo* occupy the extreme negative and positive ends of the axis, respectively (Figure 3.1.6). Meanwhile, the African apes cluster around the average PC1 value. Unlike the analysis featuring all individuals, *Theropithecus* is distanced from the African apes along the first principal component, falling between the African apes and *Pongo*. The fossil species also present a similar pattern when compared against the species mean shapes. Both *Oreopithecus* and *Nacholapithecus* lie close to the African apes, notably closest to *Pan*. OH8 again falls between *Homo* and *Gorilla* along the first principal component but in this instance is much closer to *Homo*. On the second principal component *Nacholapithecus* has the most negative value by quite a margin while *Theropithecus* is separated from all other species on the positive end of the axis. *Homo* and *Pongo* lie approximately on the axis while *Gorilla* and *Oreopithecus* have more or less the same value, slightly in the negative range, but still clearly distinct

from *Nacholapithecus*. OH8 has a strong positive value for PC2, distinguishing it from *Homo* and placing it between *Pan* and *Theropithecus*.

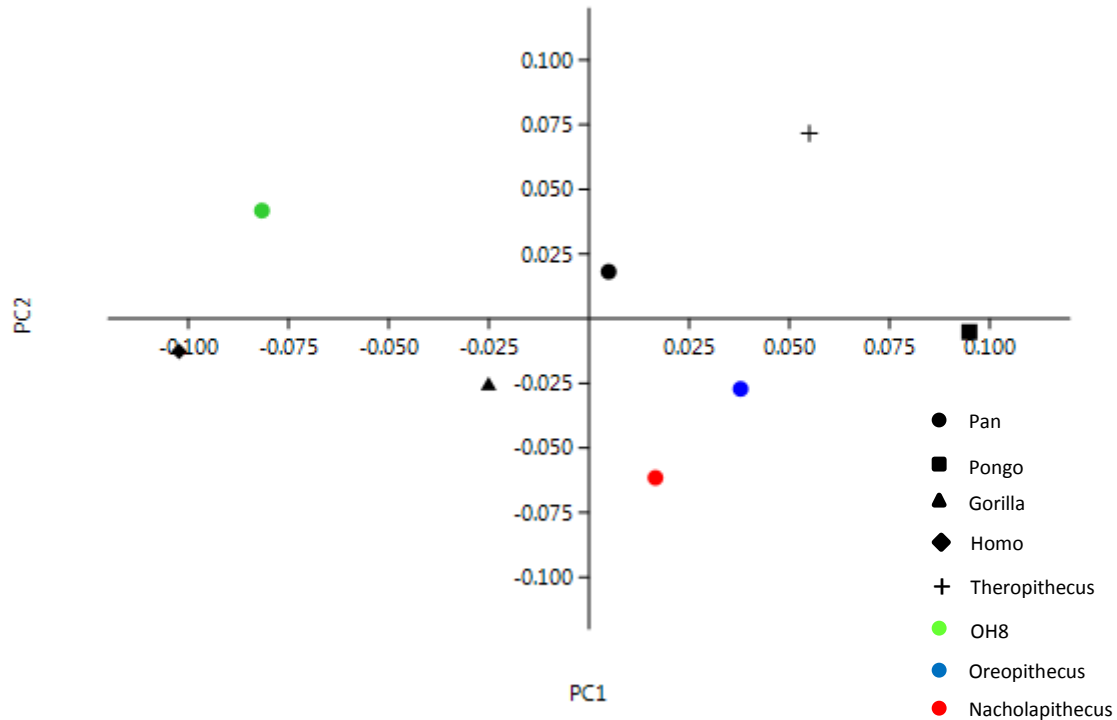


Figure 3.1.6. Principal component 1 vs. principal component 2 of species means and fossils for the talus.

Principal component 3 strongly distinguishes *Nacholapithecus* on the positive extent from the other species. *Pongo* and *Homo* occupy the negative extreme of the axis while the rest of the species are situated close to the average value. *Oreopithecus* and *Gorilla* share approximately the same value just inside the negative range; *Pan* and OH8 are both marginally inside the positive range. *Theropithecus* has a slightly higher positive value, but this is not as extreme as that seen in *Nacholapithecus*. Principal component 4 strongly distinguishes *Oreopithecus*, which occupies the most negative part of the axis, from other species. The closest species to *Oreopithecus* is *Gorilla*, but it does not display the same pronounced value on this principal component. Instead it has a very modest position on the axis lying closest to *Pan*. *Pongo* occupies the most positive part of the axis while OH8 and *Nacholapithecus* share roughly the same value situated between *Pongo* and the African apes. None of the higher principal components were found to provide any revealing distinctions among species.

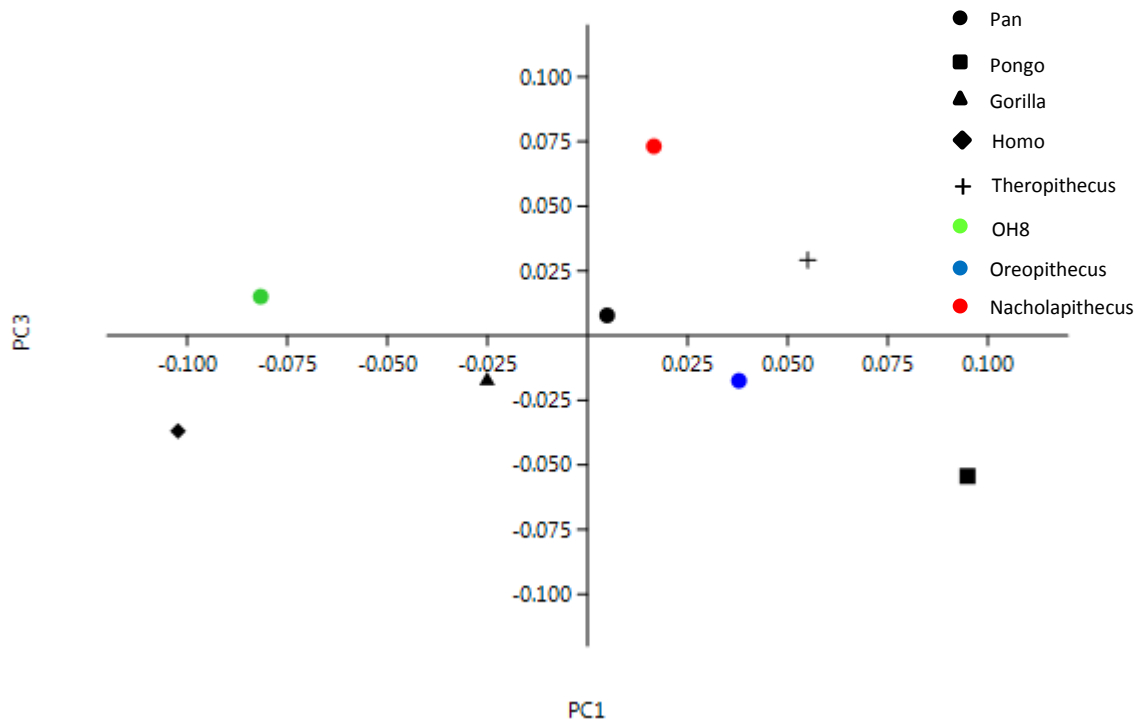


Figure 3.1.7. Principal component 1 vs. principal component 3 of species means and fossils for the talus.

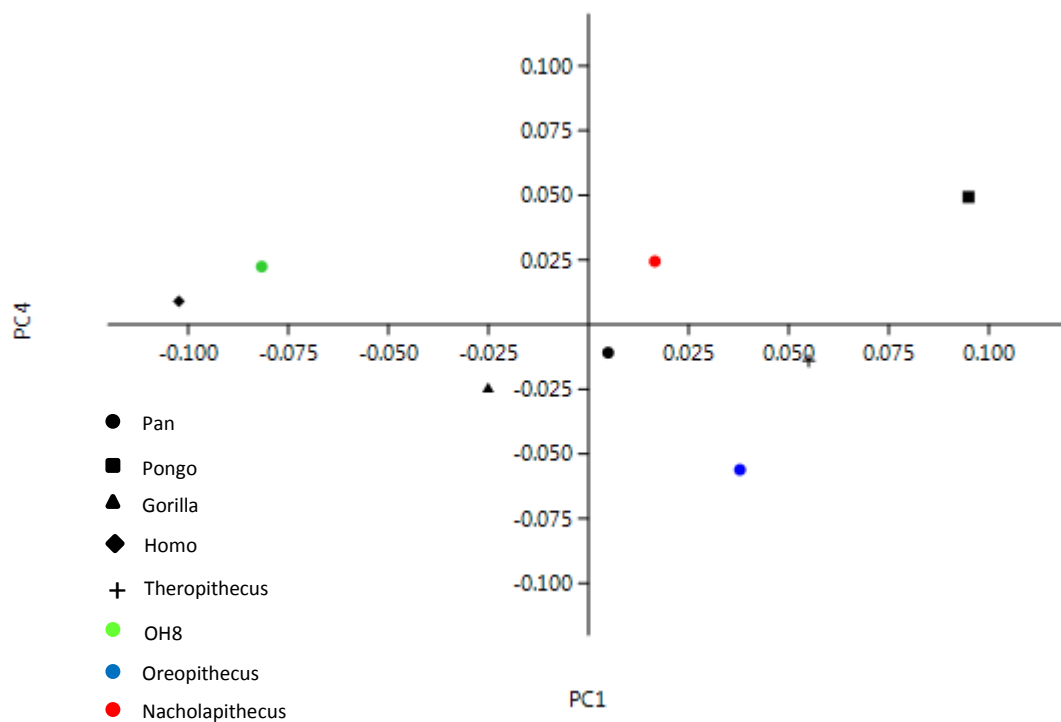


Figure 3.1.8. Principal component 1 vs. principal component 3 of species means and fossils for the talus.

3.1.2. Statistical tests

To assess the similarities and differences in shape between species the full Procrustes distances between extant species means and fossils were calculated and examined. The Procrustes distances are presented in Table 3.1.1. *Pan* and *Gorilla* are mutually closest to each other, therefore hypothesis 1 is confirmed; *Pan* and *Gorilla* are most similar in talus morphology. The shared similarity of the African apes is expected due to their similar ecology and locomotor behaviour, as well as their recent common ancestry. Both species are subsequently closest to *Oreopithecus*. *Pongo* is closest to *Oreopithecus* and then slightly more distant from *Pan*. Considering only the extant species means, *Pongo* is closest to *Pan* and then to *Theropithecus*. It is also apparent that the non-human apes are not more similar to one another to the exclusion of *Homo* and *Theropithecus*. *Gorilla* is closer to *Homo* than to *Pongo*, *Pan* is closer to *Theropithecus* than to *Pongo*, and *Pongo* is closer to *Theropithecus* than to *Gorilla*. Therefore hypothesis 2 is rejected for the talus. The morphology of the talus clearly varies significantly among the apes as *Homo* and *Theropithecus* were found to be closer to *Gorilla* and *Pan*, respectively, than either of the African apes were to *Pongo*. This implies that *Pongo* is more strongly derived in its talar morphology, to a similar degree to that seen in *Homo* and *Theropithecus*. *Theropithecus* is not consistently strongly different in shape from the other extant species, therefore hypothesis 3 is rejected for the talus.

	Pan	Pongo	Gorilla	Homo	Thero	OH8	Nacho	Oreo
Pan	0	0.137464	0.08574	0.150438	0.117379	0.110983	0.126081	0.103736
Pongo	0.137464	0	0.153719	0.207603	0.143002	0.199869	0.162514	0.131163
Gorilla	0.08574	0.153719	0	0.113232	0.146895	0.12163	0.126196	0.102476
Homo	0.150438	0.207603	0.113232	0	0.192567	0.109064	0.173058	0.165225
Thero	0.117379	0.143002	0.146895	0.192567	0	0.162577	0.153543	0.13128
OH8	0.110983	0.199869	0.12163	0.109064	0.162577	0	0.160182	0.165072
Nacho	0.126081	0.162514	0.126196	0.173058	0.153543	0.160182	0	0.131937
Oreo	0.103736	0.131163	0.102476	0.165225	0.13128	0.165072	0.131937	0

Table 3.1.1. Procrustes distances amongst species mean shapes and fossils for the talus. Reading across the rows, the two lowest Procrustes distances to each species/fossil are represented. The closest is highlighted in bold red, the second closest in bold black.

Oreopithecus is closest in shape to *Gorilla* and then marginally more distant from *Pan*. However, *Oreopithecus* is more distant from both *Gorilla* and *Pan* than the two species are from each other.

Nevertheless, *Oreopithecus* is closest to the African apes by quite a margin and therefore hypothesis 4 is confirmed for the talus; *Oreopithecus* is not cercopithecoid-like and this hypothesis has been justifiably discarded. This also means that hypothesis 5 is confirmed for the talus, *Oreopithecus* is similar to the African apes indicating that it is a member of the Miocene Hominoidea of Europe. Notably, *Oreopithecus* is furthest from *Homo*. Thus, *Oreopithecus* bears the greatest similarity to the climbing, arboreally adapted, knuckle-walking apes and is distinct from the bipedal representatives in this study. OH8 is most similar to *Homo* followed by its proximity to *Pan*, this confirms hypothesis 6 although the close proximity of OH8 to the apes is indicative of a mosaic morphology. It would seem to support the view that OH8 was a committed biped with reasonably close phylogenetic links to *Homo*, but that the ankle retains some primitive features. *Nacholapithecus* was most similar in shape to *Pan*, and minutely less similar to *Gorilla*, therefore hypothesis 7 is rejected; *Nacholapithecus* is not most similar to *Theropithecus*. This suggests that *Nacholapithecus* had diverged somewhat from the cercopithecoid condition towards the hominoid condition in its ankle morphology.

The relationships discussed above based on Procrustes distance were tested for significance by calculating the Mahalanobis distance from the fossil specimen to the species of interest. It was found that *Oreopithecus* was significantly different in shape from *Gorilla*, with a Mahalanobis distance of 24.57, 4.956 Standard deviation units and a p value of <0.01. Therefore, it is necessary to explore the exact nature of these differences in more detail to ascertain whether or not the differences are of a sort which could potentially indicate a drastically different function of the foot, such as that of bipedal behaviour, for example. OH8 was also found to be significantly different from *Homo*, with a Mahalanobis distance of 21.198, 4.604 standard deviation units and a p value of <0.02. Therefore, the exact nature of these differences was also examined further. *Nacholapithecus* was found to be significantly different from *Pan* in terms of the talus morphology under study. It was found to have a Mahalanobis distance of 36.335 from the *Pan* sample, 6.027 standard deviation units with a p value of <0.0005. To calculate whether extant species were significantly different from one another permutation tests were conducted on the pairwise Procrustes distances between individuals in the complete dataset. It was found that all extant species were significantly different from each other with values of $p = <0.0001$.

Differences in size were calculated using permutation tests based on individual centroid sizes. The relevance of size of the pedal elements in the investigation of possible bipedal behaviour in a fossil species is important. One might expect that the mechanical requirements imposed on the foot due to frequent bipedal behaviour would manifest in the skeleton through increased robusticity and size

of the bones, particularly the talus. Of the extant species *Homo* and *Gorilla* were not found to have a significantly different mean centroid size ($p = 0.175$), although the *Gorilla* mean (266) was higher than that of *Homo* (256.1). Both *Gorilla* and *Homo* were also found to have significantly higher means than all other species at $p = <0.0001$. Therefore, hypothesis 8 was confirmed for the talus, *Homo* and *Gorilla* are the largest of the extant species. *Pan* and *Pongo* were not found to have significantly different means ($p = 0.0265$) after Bonferroni correction for multiple comparisons adjusted the p value to 0.005, however, the mean centroid size for *Pongo* (209.6) was substantially larger than *Pan* (192.5). *Theropithecus* was found to have a significantly smaller mean centroid size (124.3) than all extant species at $p = <0.0001$. Therefore, hypothesis 9 was confirmed for the talus, *Theropithecus* is the smallest of the extant species in the study. To sum up, the hierarchy of size for the talus of extant species can be represented as follows *Gorilla/Homo* > *Pongo/Pan* > *Theropithecus*.

It was found that *Oreopithecus* was significantly smaller than all ape species but was not significantly larger than *Theropithecus* ($z = 1.025$; $p = 0.153$). Therefore, hypothesis 10 is rejected for the talus. *Oreopithecus* is not comparable in size to *Pan* but is rather found to be similar in size to a cercopithecoid. This finding suggests that the trochlea, medial malleolar facet and head of the talus were in fact rather gracile. This finding has to be taken with some caution, however, since the entire talus was not available for study and may have given a different result if it were. OH8 was found to be significantly smaller than both *Homo* ($z = -3.554$; $p = 0.0002$) and *Gorilla* ($z = -3.141$; $p = 0.0008$). However, OH8 was not found to be significantly different in size from either *Pan* ($z = -0.351$; $p = 0.363$) or *Pongo* ($z = -0.857$; $p = 0.196$). Therefore, hypothesis 11 is confirmed for the talus, and thus OH8 was not found to have an especially robust talus, but nor one that was gracile. This is apparent when reconstructions of the body size of *Homo habilis* place it in the range of extant bonobos (McHenry 1992). *Nacholapithecus* was found to be significantly smaller than all ape species but significantly larger than *Theropithecus*. Therefore, hypothesis 12 is confirmed for the talus, *Nacholapithecus* is intermediated in size between *Theropithecus* and the extant apes. This would support the notion that stem hominoids had begun a general increase in body size but that this process was slow.

3.1.3. Visualisation of shape differences

In order to describe the differences in shape it is necessary to use some technical terminology. Figures 3.1.9 and 3.1.10 illustrate what these terms are referring to.

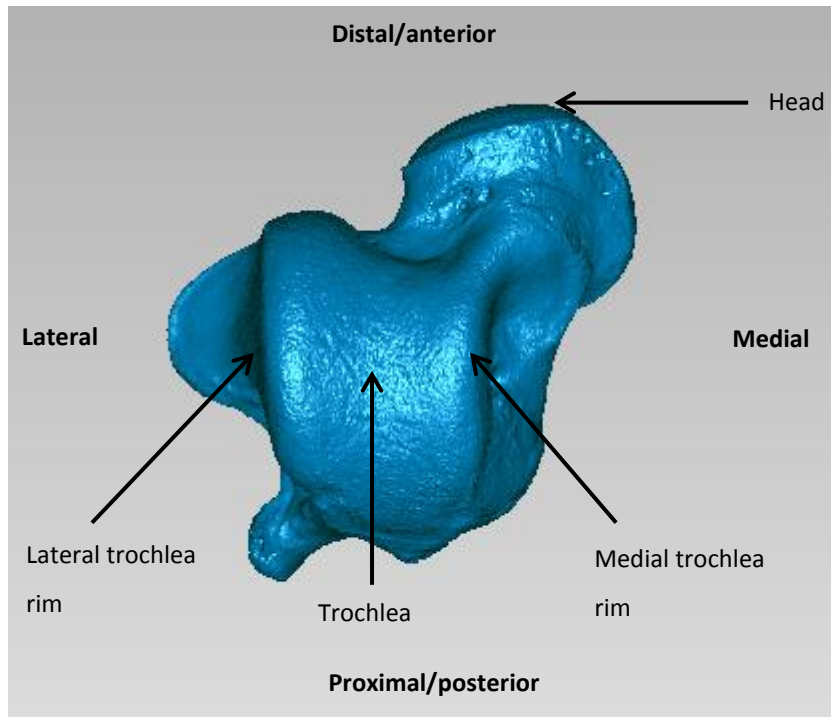


Figure 3.1.9. Superior view of the talus displaying terminology used to describe shape differences.

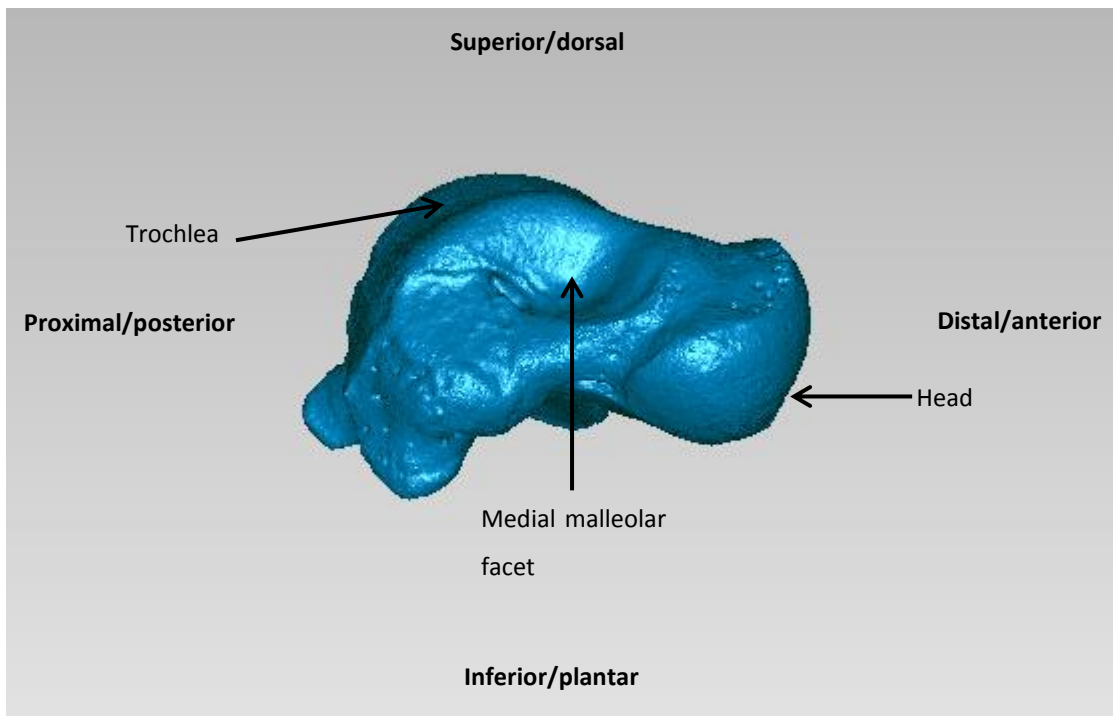


Figure 3.1.10. Medial view of the talus displaying terminology used to describe shape differences.

From *Gorilla* to *Oreopithecus*

Oreopithecus bears noteworthy differences from the *Gorilla* talar morphology. The neck of the talus is slightly elongated in *Oreopithecus* (Figure 3.1.11A). This feature is coincident with a shortening of the medial and lateral malleolar rims. This is due to the fact that the trochlea itself is clearly reduced in relative size in *Oreopithecus*. The lateral trochlear rim is clearly elevated relative to the medial trochlear rim, relative to the head of the talus (Figure 3.1.11B). This feature is expressed to a similar degree in both *Gorilla* and *Oreopithecus*. The head of the talus is deviated more medially and angled more plantarly in *Oreopithecus*. Additionally, the head of the talus is significantly more curved in *Oreopithecus* but is also much smaller. The medial malleolar facet is larger in *Gorilla* but the difference in size is slight. The inferior border of the facet also flares medially to roughly the same extent in both species, however, the anterior border does not flex medially in *Oreopithecus* to the degree seen in *Gorilla*. Thus, the key differences in medial malleolar facet morphology between the two species relate to the greater flexion of the facet from the body of the talus in *Gorilla*.

Oreopithecus bears differences to *Pan* which are roughly equivalent to the differences between it and *Gorilla*. The trochlea is relatively smaller in *Oreopithecus* than it is in *Pan* and the trochlear rims are both shortened. The shortening of the medial malleolar rim has the consequence that the neck of the talus is longer in *Oreopithecus* relative to *Pan*. The head of the talus diverges medially and has a more pronounced plantar inflection in *Oreopithecus*. Additionally, the head of the talus is more tightly curved in *Oreopithecus* but the difference in size of the head is not as pronounced between *Pan* and *Oreopithecus*. The medial malleolar facet is slightly smaller than in *Pan*, too, but as is the case in the comparison between *Oreopithecus* and *Gorilla* the differences are slight. *Oreopithecus* also displays less pronounced flaring of the facet than in *Pan*.

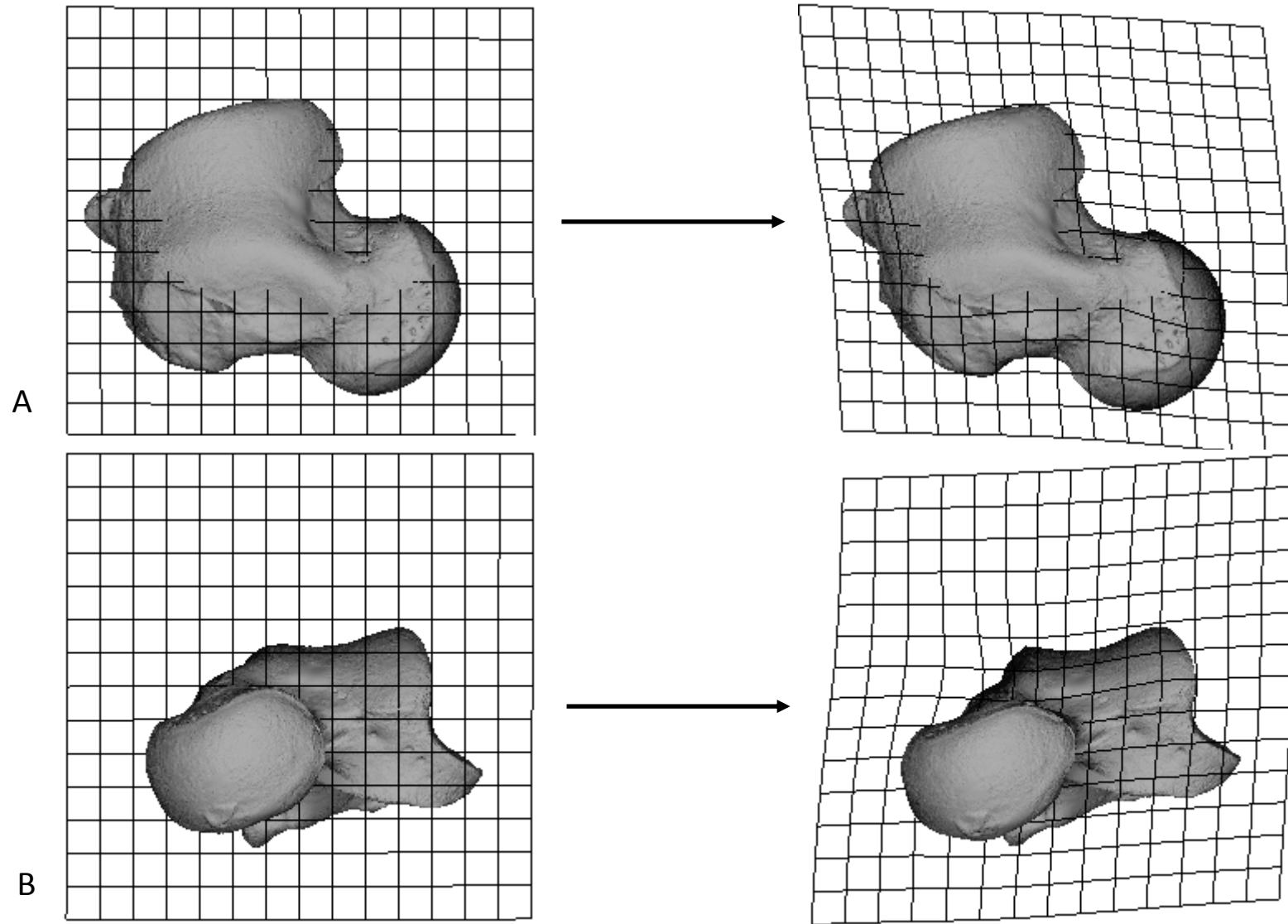


Figure 3.1.11. Demonstration of the warp from the *Gorilla* mean talus (left) to *Oreopithecus* (right). A) superior view. B) Distal view.

From *Homo* to OH8

Homo and OH8 share many similarities but there are some features of the talus that align OH8 more closely with the African apes than *Homo*. The trochlea is large in both *Homo* and OH8 and both the medial and lateral trochlea rims appear longer than they do in the apes. This has the consequence that the talar neck is short in *Homo* and OH8. The medial malleolar facet is large in both species relative to the size of the trochlea. In both species the head of the talus is large and bears a degree of torsion relative to the plane of the trochlea which exceeds that in apes. However, there are clear differences between *Homo* and OH8 in their talar morphology. There is a distinct keel along the midline of the trochlea in OH8 while the trochlea is much flatter in *Homo* (Figure 3.1.12). This keeling is a feature found amongst the apes and thus distinguishes OH8 from *Homo*. The head of the talus of OH8 deviates more medially than does that of *Homo*. The medial deviation is not as pronounced as it is in African apes but is clearly noticeable. This deviation of the head in OH8 is linked to a pronounced medial deviation of the anterior border of the medial malleolar facet. This is markedly different to the flat and straight medial malleolar facet of *Homo*.

From *Pan* to *Pongo*

The talus of *Pongo* is unlike that of African apes as illustrated in Figure 3.1.13. The wedging of the trochlea is absent in *Pongo*. From superior view the medial and lateral rims appear parallel, similar to *Homo*. However, the lateral trochlear rim is strongly elevated relative to the medial in *Pongo* and this feature is expressed to a greater degree than it is in the African apes, and the medial trochlear rim extends further anteriorly. The medial malleolar facet is greatly reduced in size in *Pongo* relative to *Pan*. The facet is narrow across its dorsoplantar dimension throughout its entire length, lacking the cup formed on the anterior aspect of the bone in *Pan*. Additionally, the facet also lacks the strong flaring of its inferior and anterior borders away from the body of the talus. Instead the facet is relatively vertically aligned, in which regard it is rather like *Homo*. The neck is longer in *Pongo* than it is in *Pan* and the head is angled to face more medially, while the divergence from the body is roughly the same. The head lacks the same inferior inflection and torsion seen in *Pan* and has a more tightly curved surface. However, the head of the talus is vastly reduced in size in *Pongo*.

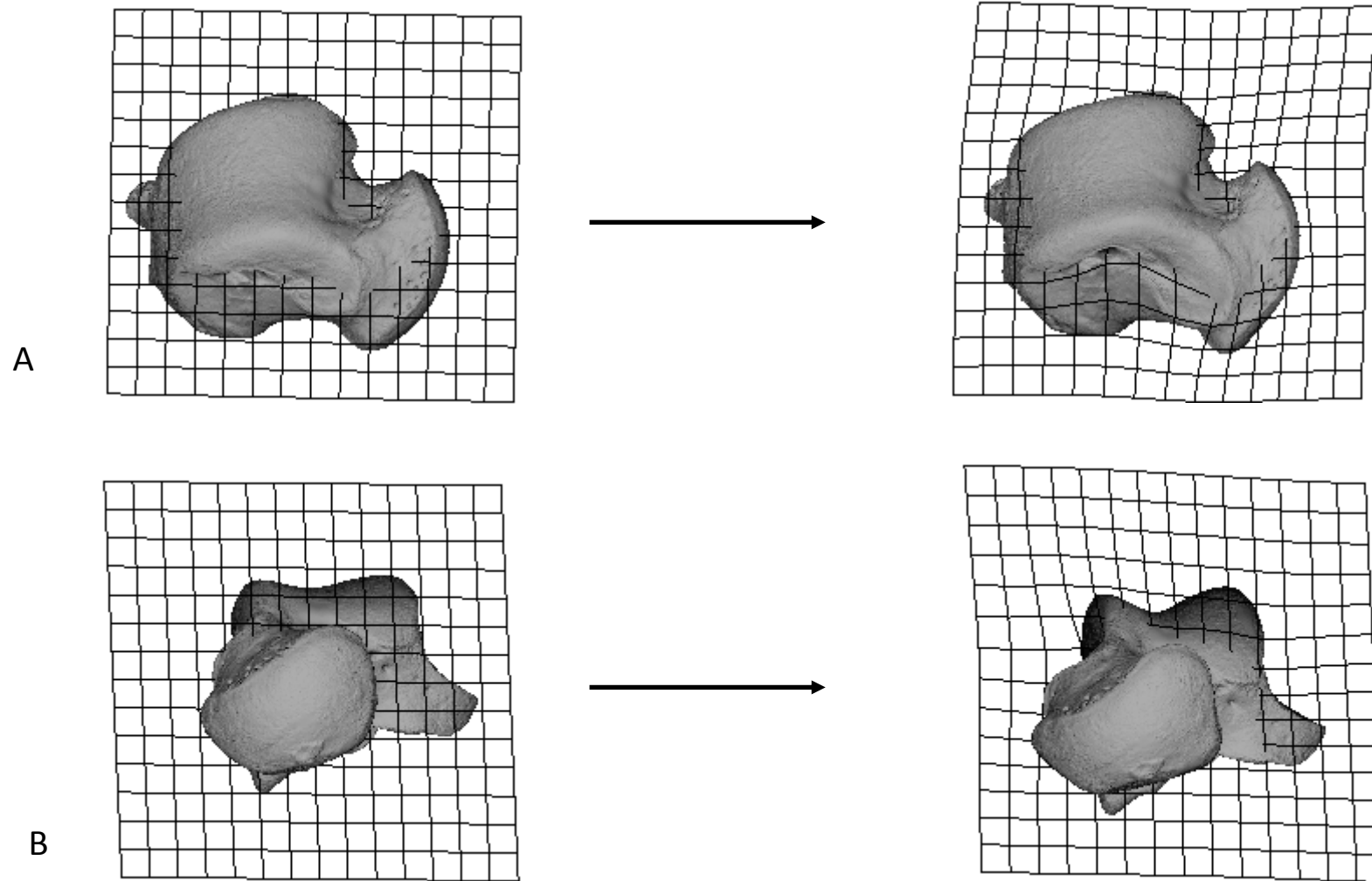


Figure 3.1.12. Demonstration of the warp from the *Homo* mean talus (left) to OH8 (right). A) Superior view. B) Distal view

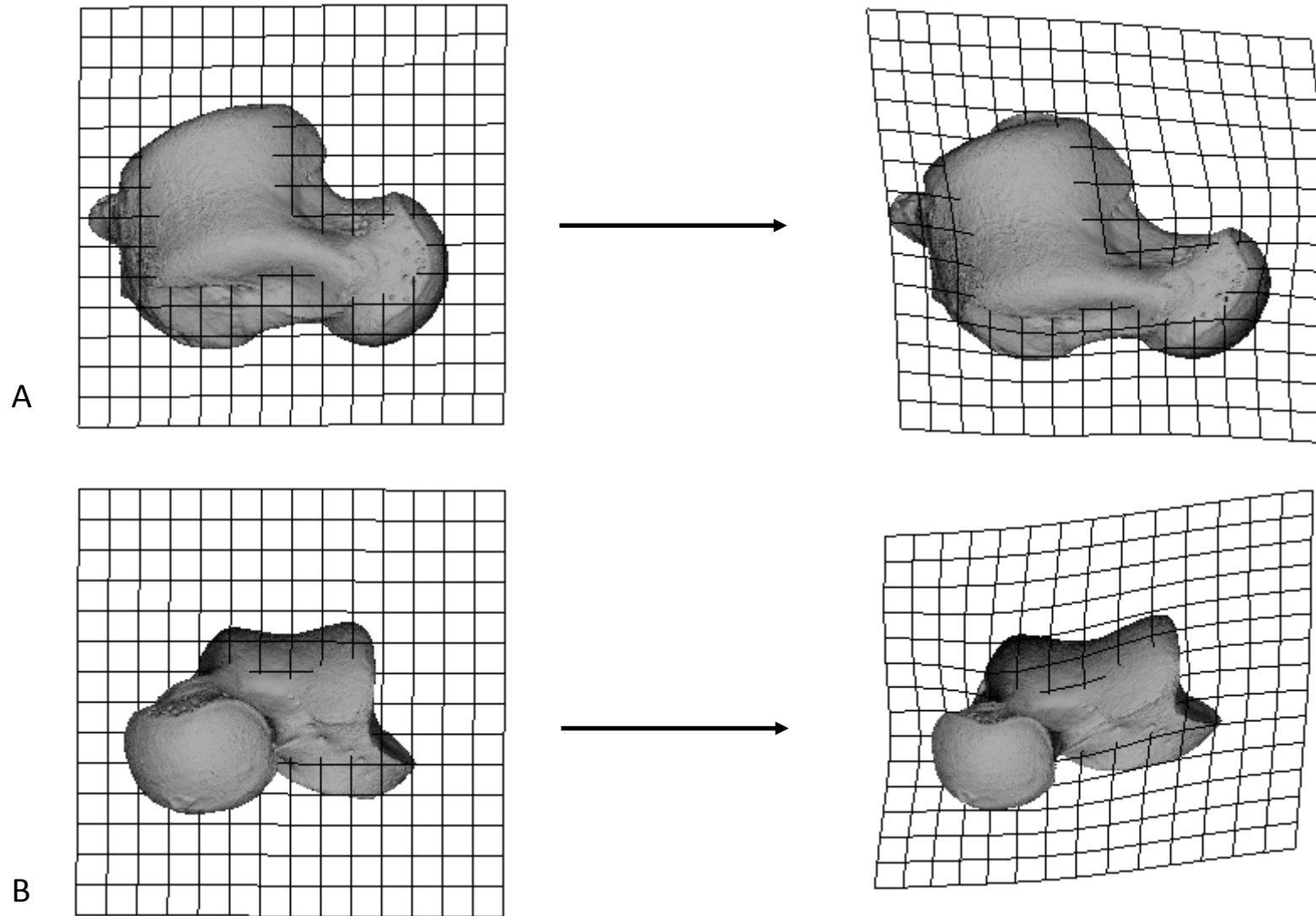


Figure 3.1.13. Demonstration of the warp from the *Pan* mean talus (left) to the *Pongo* mean (right). A) Superior view. B) Distal view

From *Pan* to *Nacholapithecus*

Nacholapithecus presents an unclear mosaic of features. It was most similar to *Pan* in terms of Procrustes distance. Compared to *Pan*, *Nacholapithecus* has a trochlea that is wider anteriorly than posteriorly. This is caused by rotation of the posterior borders of the malleolar facets towards one another. Thus, the wider anterior trochlear border is in fact due to a narrower posterior border, although, there is a more pronounced medial deviation of the anterior border of the medial malleolar facet in *Nacholapithecus*. The trochlea in general has a broad appearance in *Nacholapithecus*, similar to *Pan*. The medial malleolar facet is much shorter in *Nacholapithecus* and the medial trochlear rim is noticeably shorter than the lateral. Furthermore, the lateral trochlear rim is elevated considerably higher relative to the head and neck than the medial trochlear rim is. This gives the midline of the trochlea a much deeper groove in *Nacholapithecus* than in *Pan* (Figure 3.1.14). The head of the talus appears to be approximately equivalent in size, torsion, and deviation from the talar body between *Nacholapithecus* and *Pan*.

From *Theropithecus* to *Nacholapithecus*

Nacholapithecus represents a pronograde stem hominoid and shares many features of its postcranium with extant cercopithecoids. Therefore, despite the fact that *Nacholapithecus* and *Theropithecus* were separated by a relatively large Procrustes distance, the differences between them were visualised in an attempt to better understand these differences. However, as noted above, the revealed differences are somewhat confusing. For example, *Nacholapithecus* appear to have a narrower trochlea than *Theropithecus* (Figure 3.1.15), despite having a trochlea which is broadly similar in relative size to *Pan*. The lateral trochlear rim is also significantly higher than the medial rim in *Nacholapithecus* compared to *Theropithecus*. From personal observation, the elevation of the lateral trochlear rim relative to the medial was expected to distinguish *Nacholapithecus* from *Pan* but simultaneously approximate the morphology of *Theropithecus*. To find that this elevation in fact distinguishes *Nacholapithecus* from both species is unusual. There are differences between *Nacholapithecus* and *Theropithecus*, however, which are concordant with the comparison of *Nacholapithecus* and *Pan*. For example, the longer lateral trochlear rim and short, broad medial malleolar facet. Additionally the head of the talus is slightly broader and more curved in *Nacholapithecus*, as well as being slightly less divergent.

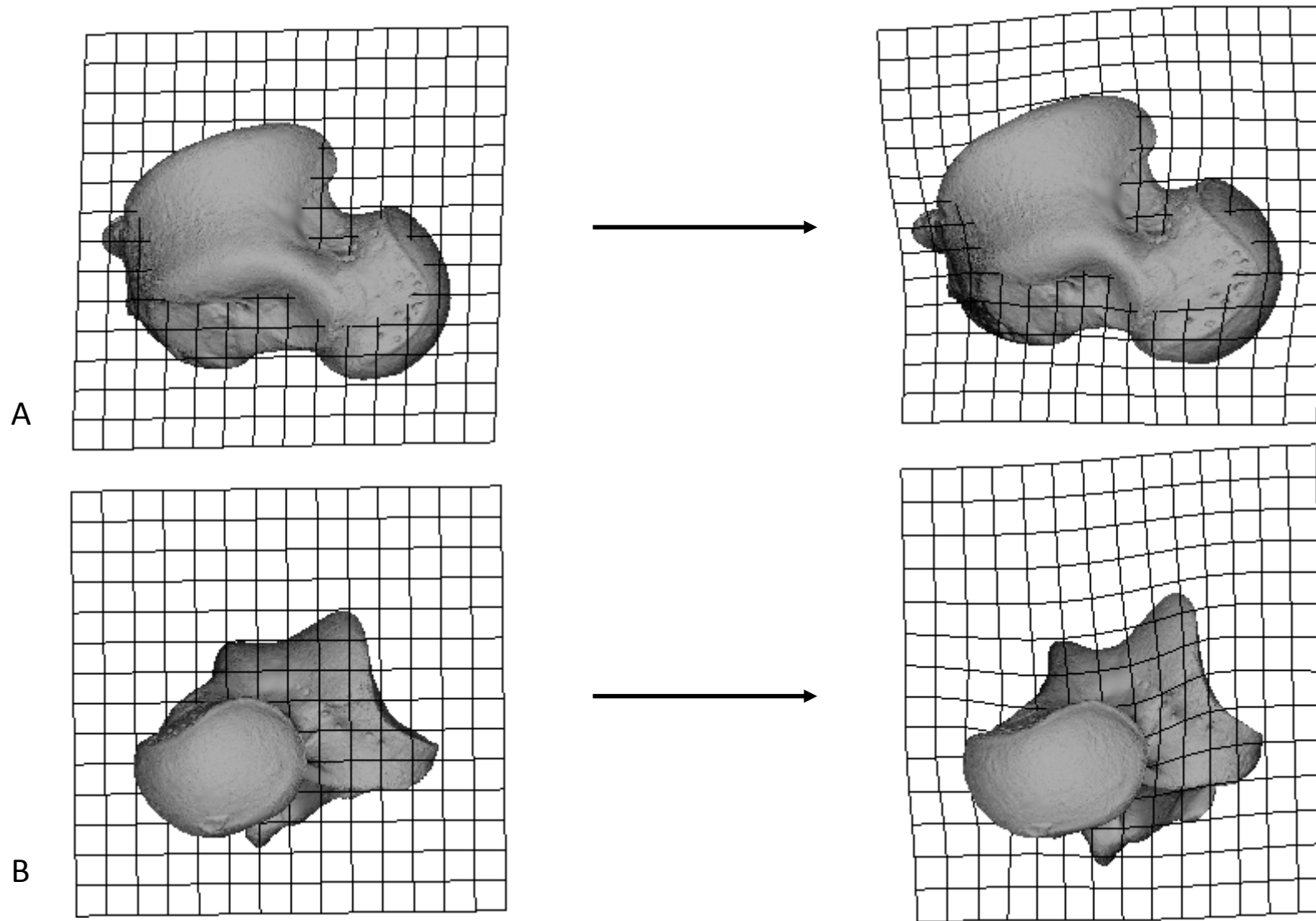


Figure 3.1.14. Demonstration of the warp from the *Pan* mean talus (left) to *Nacholapithecus* (right). A) Superior view. B) Distal view

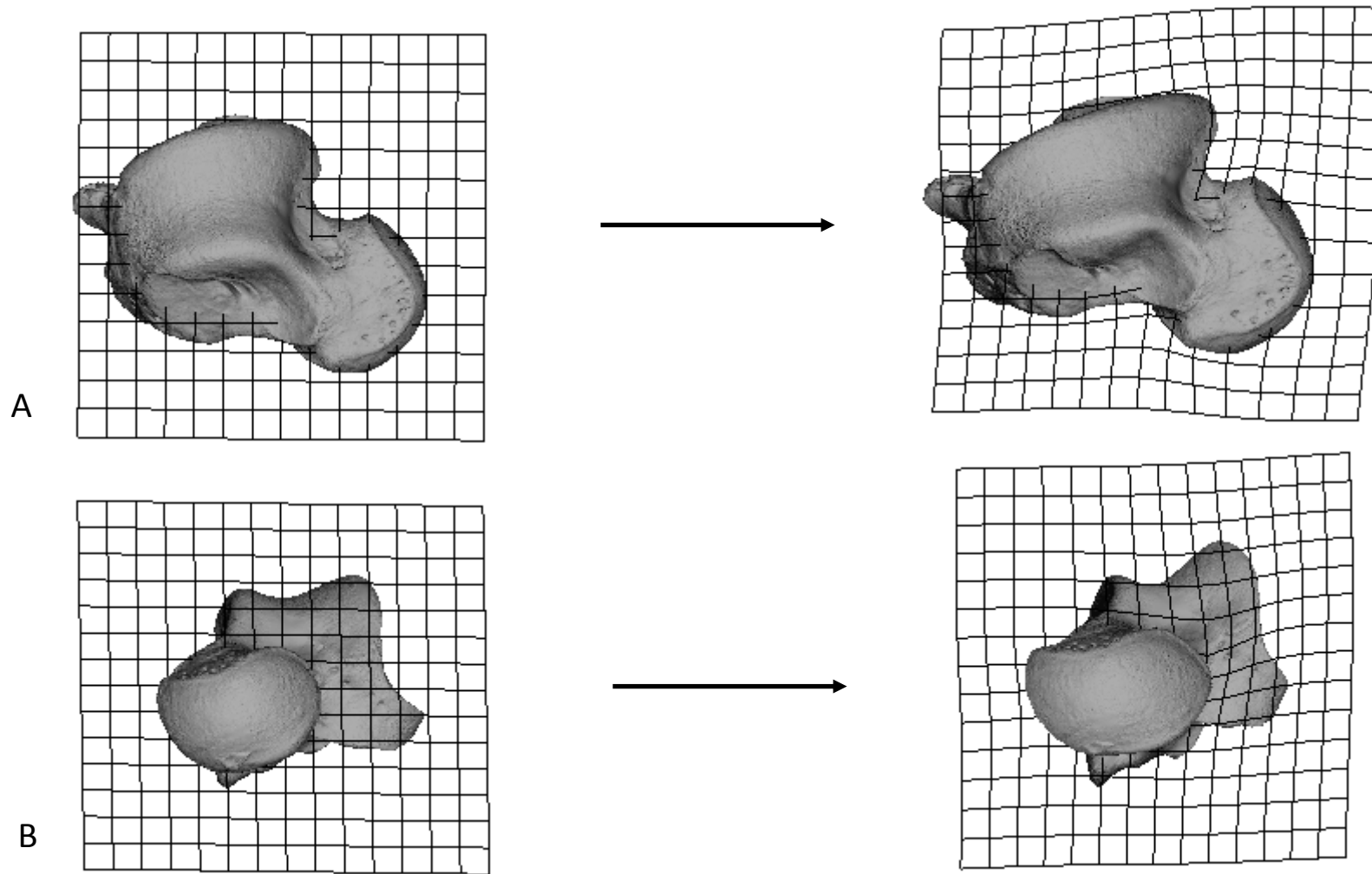


Figure 3.1.15. Demonstration of the warp from the *Theropithecus* mean talus (left) to *Nacholapithecus* (right). A) Superior view. B) Distal view

3.2. Navicular

3.2.1. Principal components analysis

3.2.1.1. Full sample

A principal components analysis was conducted on the Procrustes aligned landmarks for the navicular using all individuals in the study. The first three principal components accounted for 67.61% of the variance in the sample, the first five accounted for 75.5%, and the first thirteen PCs accounted for 90.31% of the variance. The remaining 9.7% of the variance was explained by PCs 14-78 (Figure 3.2.1.)

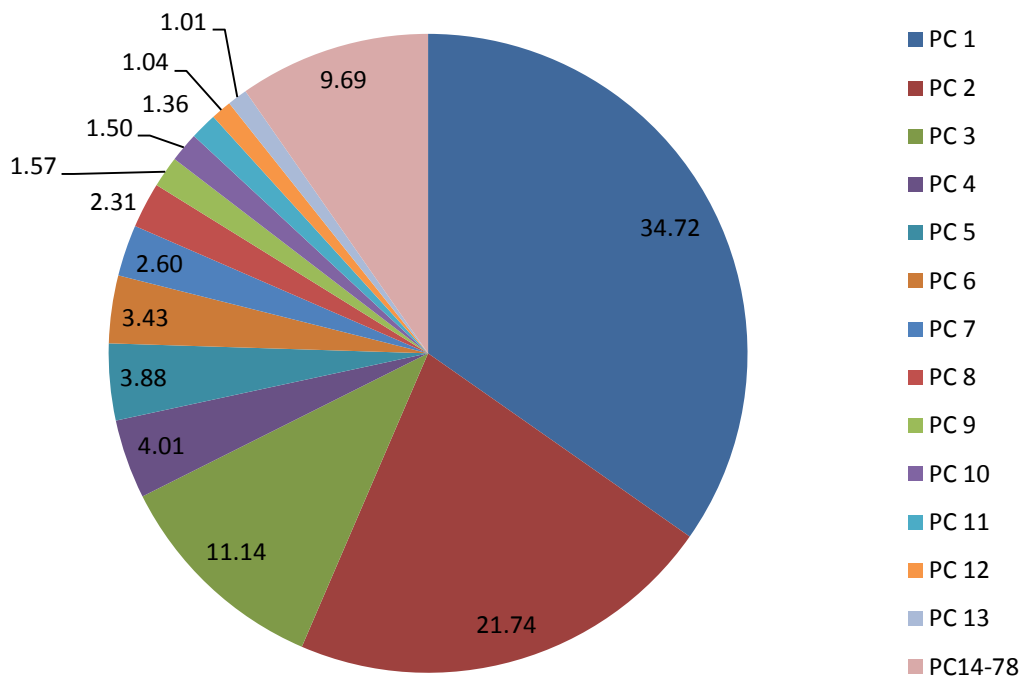


Figure 3.2.1. Percentage of the overall variance explained by each principal component for the navicular.

The first two principal components give a distribution for the navicular which is similar to that reported by Harcourt-Smith (2002). However, that study did not include any monkey species and the slight differences between the present study and that of Harcourt-Smith are attributed to that fact.

PC1 strongly separates the non-human apes from *Homo* and *Theropithecus*. All three species of non-human ape have very similar mean values in the negative range of the PC1 axis (Figure 3.2.2) as well as having similar ranges, whereas in the Harcourt-Smith study *Pongo* was situated more intermediate between *Homo* and African apes. The range of *Pan* exceeds that of both *Pongo* and *Gorilla*. *Homo* and *Theropithecus* both have high positive scores along PC1, with the *Theropithecus* mean lying close to the higher end of the *Homo* range. OH8 lies close to the *Homo* mean with a slightly more positive score but comfortably within the *Homo* range, and *Oreopithecus* is well within the range of all the non-human apes but with a value closest to the *Pan* mean for PC1.

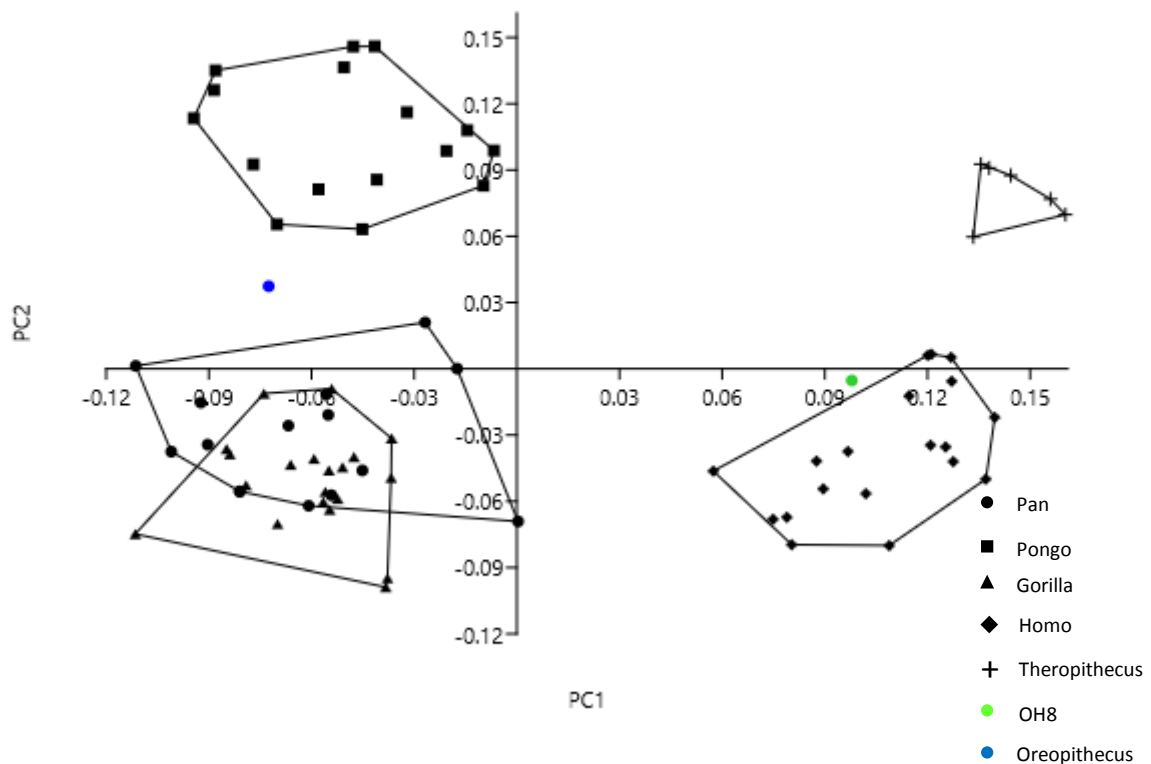


Figure 3.2.2. Principal component 1 vs. principal component 2 of all individuals for the navicular.

A split between *Homo*/African apes and *Pongo*/*Theropithecus* is apparent on PC2. The means of the African apes and *Homo* are all negative on the PC2 axis. *Pan* has a value that is noticeably less negative than that of *Gorilla* and a distribution that is noticeably more positive also. Conversely *Gorilla* has a more negative mean value and distribution. The mean and distribution of *Homo* is

roughly intermediate between that of *Pan* and *Gorilla*. *Pongo* and *Theropithecus* both have positive scores on the axis. The *Theropithecus* mean is lower than that of *Pongo* but most of its distribution is concurrent with the lower end of the *Pongo* distribution. OH8 has a value close to the mean for PC2, substantially less negative than the *Homo* mean but still within the *Homo* range of variation, although OH8 actually lies closest to the *Pan* mean. *Oreopithecus* has a positive score on the axis but lies outside the ranges of any represented species, closest to the mean of *Theropithecus*, but midway between the African apes and *Pongo*. Together PC1 and PC2 separate the species into four distinct clusters; humans, African apes, *Pongo* and *Theropithecus*. It is tempting to presume that old world monkeys would group together, more or less, with *Theropithecus*, but this would be unsupported. However, it would be an interesting area for future investigation. OH8 lies within the *Homo* distribution for both PC1 and PC2, though it is situated relatively far from the mean. *Oreopithecus* is located approximately mid-way between the African apes and *Pongo*; PC2 alone accounts for this, while PC1 places *Oreopithecus* in a general non-human ape group.

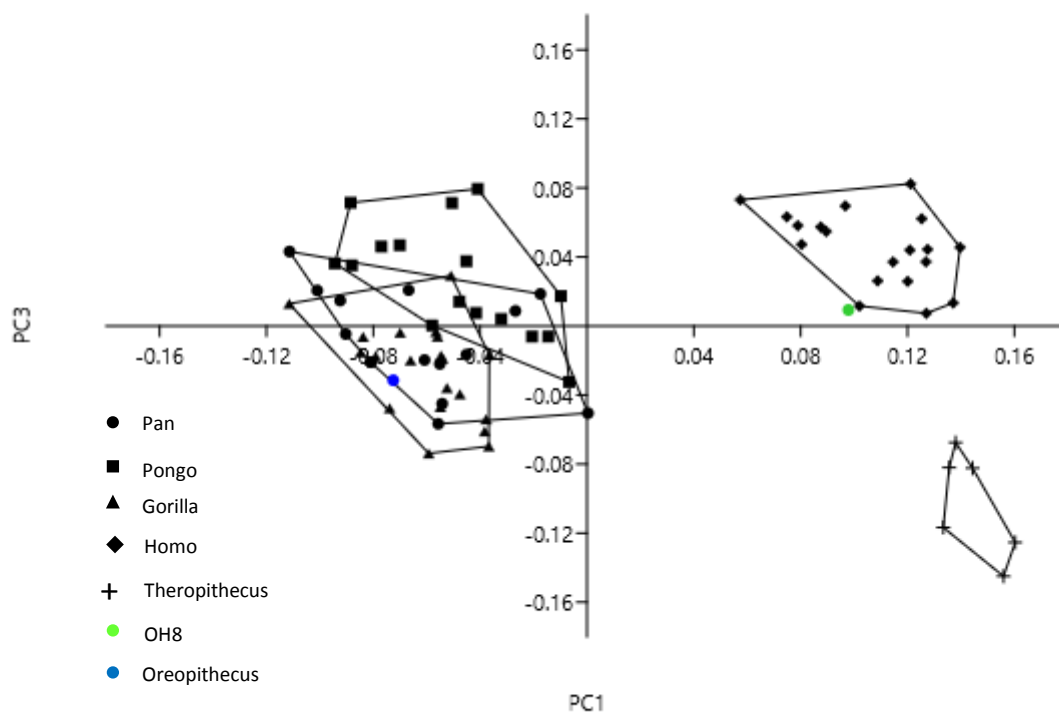


Figure 3.2.3. Principal component 1 vs. principal component 3 of all individuals for the navicular.

Pan and *Gorilla* are almost indistinguishable on both PC3 and PC1 (Figure 3.2.3). *Gorilla* has a slightly more negative mean value and distribution than does *Pan*, whose mean lies approximately at 0 on the PC3 axis. *Pongo* and *Homo* have average values in the positive range of the axis, with *Homo* having the slightly more positive mean. Both, however, appear to have noticeably more positive distributions than the African apes despite *Pongo* having some overlap with both African ape means. The mean value for *Theropithecus* is significantly more negative than for any other species but its least negative values do overlap with the more negative range of the *Gorilla* distribution. OH8 again lies on the periphery of the human range with a value close to 0 on the PC3 axis. *Oreopithecus* is very close to the average *Gorilla* score and well within the ranges of both *Gorilla* and *Pan*, but on the extreme periphery of the *Pongo* range.

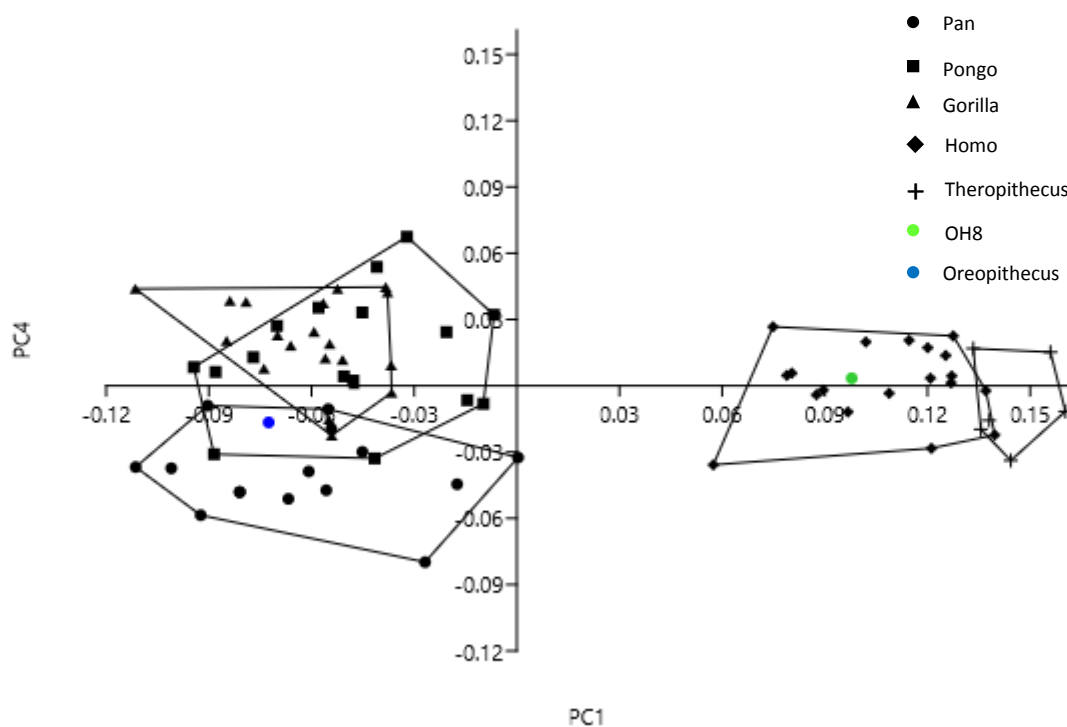


Figure 3.2.4. Principal component 1 vs. principal component 4 of all individuals for the navicular.

Principal component 4 discriminates between specimens very weakly (Figure 3.2.4), although there is an apparent separation of *Pan* but there is still broad overlap with other species. The higher principal components are ineffective at distinguishing between species although principal component 5 and principal component 12 show clear separation of fossil species. Principal component 5 (Figure 3.2.5) separates *Oreopithecus* on its negative range from the extant species, while principal component 12 (Figure 3.2.6) separates both *Oreopithecus* and OH8 on its positive range from the rest of the sample.

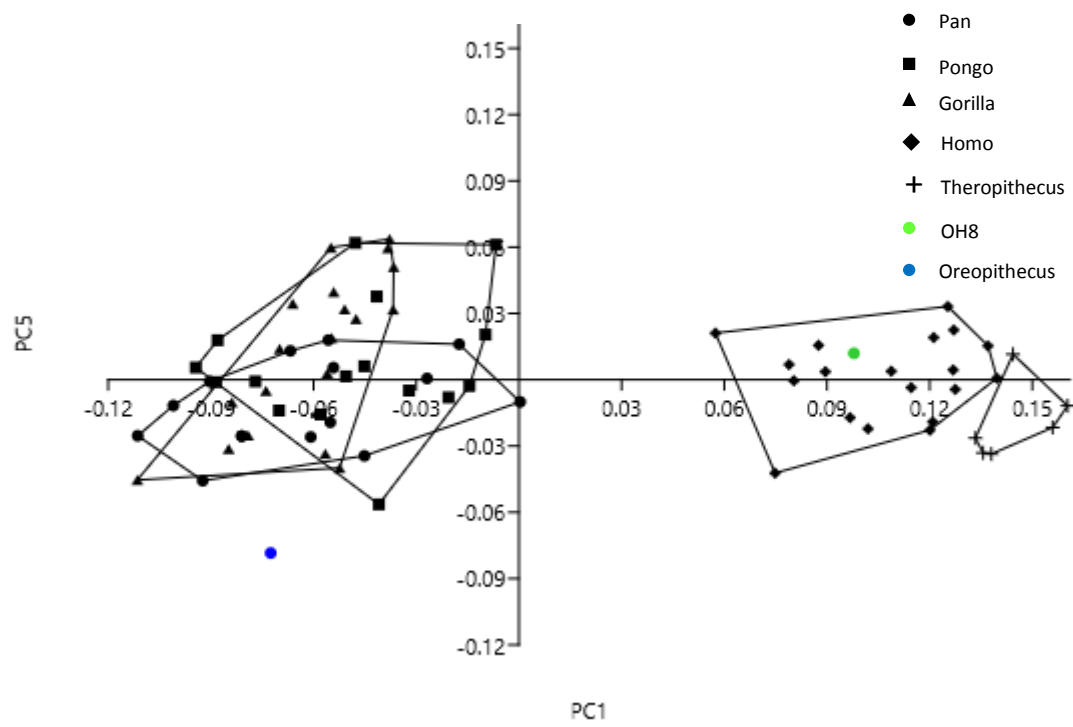


Figure 3.2.5. Principal component 1 vs. principal component 5 of all individuals for the navicular.

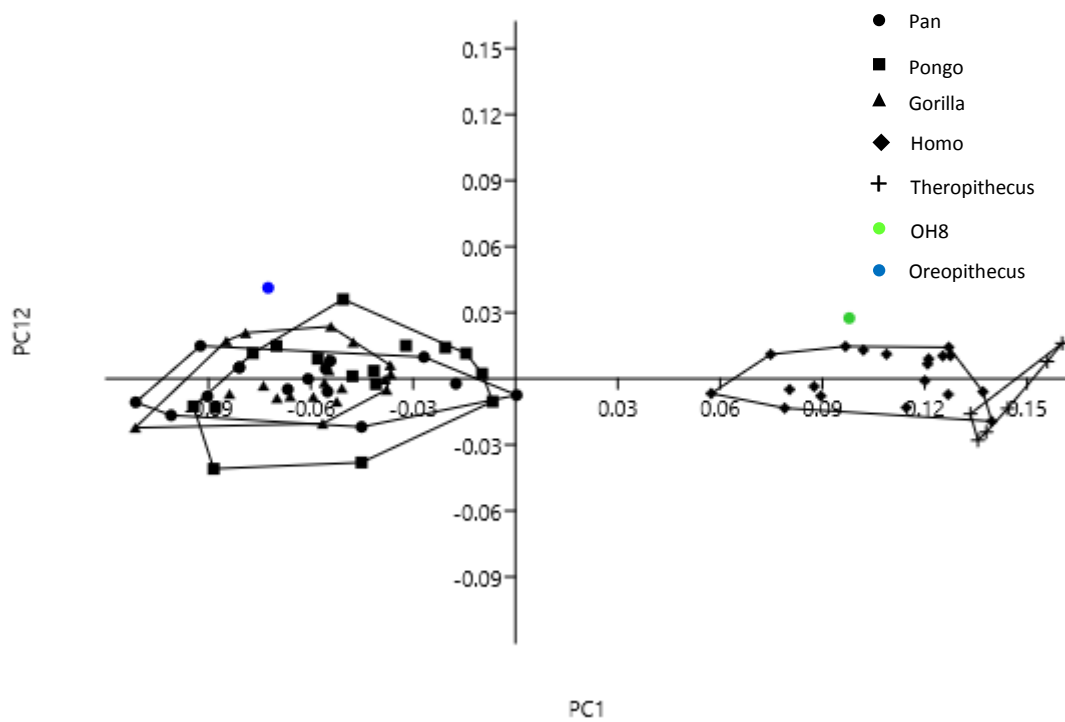


Figure 3.2.6. Principal component 1 vs. principal component 12 of all individuals for the navicular.

3.2.1.2. Extant species means vs. fossils

A principal components analysis was conducted on the Procrustes aligned landmarks for the navicular using the extant species mean shapes and fossils only. The first principal component explains 50.81% of the variance, the first two explain 73.64%, and the first three explain 84.8%, with 97.84% of the variance explained by the first five principal components (Figure 3.2.7).

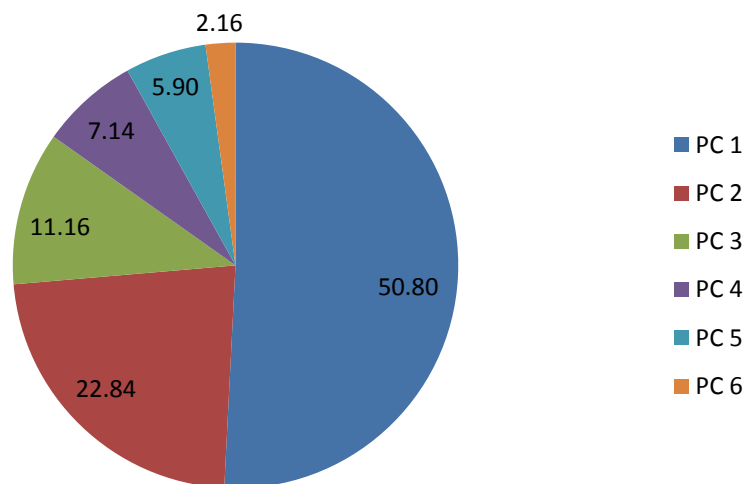


Figure 3.2.7. Percentage of the variance explained by each PC using only species mean shapes.

The first principal component for the extant species means data is comparable to that for the full data set. The non-human apes are grouped together on the negative part of the axis while *Homo* and *Theropithecus* occupy the positive half of the axis (Figure 3.2.8). *Theropithecus* is more distant from the non-human apes than *Homo*. On the negative part of the axis there is little to separate the African apes and *Pongo*, although the African apes do have slightly more negative values than *Pongo*. The fossil specimens correspond roughly to their distribution in the principal components analysis conducted on the full sample. *Oreopithecus* falls on the negative half of the axis with the non-human apes. It has a more negative value than all species, making it closest to the African apes along this axis, although there is not much to separate the ape species. OH8 lies on the positive half of the axis, closest to *Homo*.

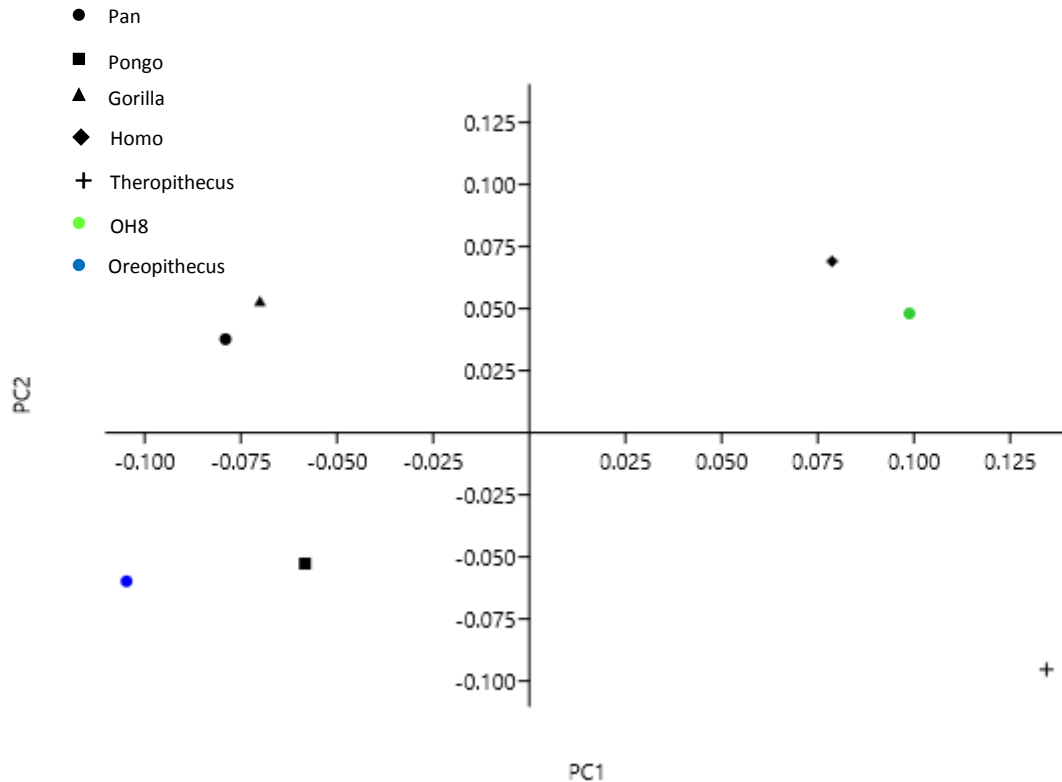


Figure 3.2.8. Principal component 1 vs. principal component 2 of species means and fossils for the navicular.

Principal component 2 is also similar when using only species means, although the axis is inverted. The axis creates a distinction between *Homo* and the African apes positively while *Pongo* and *Theropithecus* occupy the negative aspect of the axis. One notable difference when examining the species means only is that *Oreopithecus* is clearly separated from the African apes and appears very similar to *Pongo* on this axis, as opposed to being placed midway between the African apes and *Pongo* on this axis when the full sample is used. OH8 is more similar to the African apes than *Homo* with respect to PC2, but there is very little difference between African apes and *Homo* on this axis. The third principal component most obviously separates *Pongo*, on the extreme positive end, from all other groups (Figure 3.2.9). There are minor differences between the remaining groups, but these are eclipsed by the clear separation of *Pongo*. Principal component 4 reveals very little, while PC5 clearly separates *Homo* and OH8 (Figure 3.2.10).

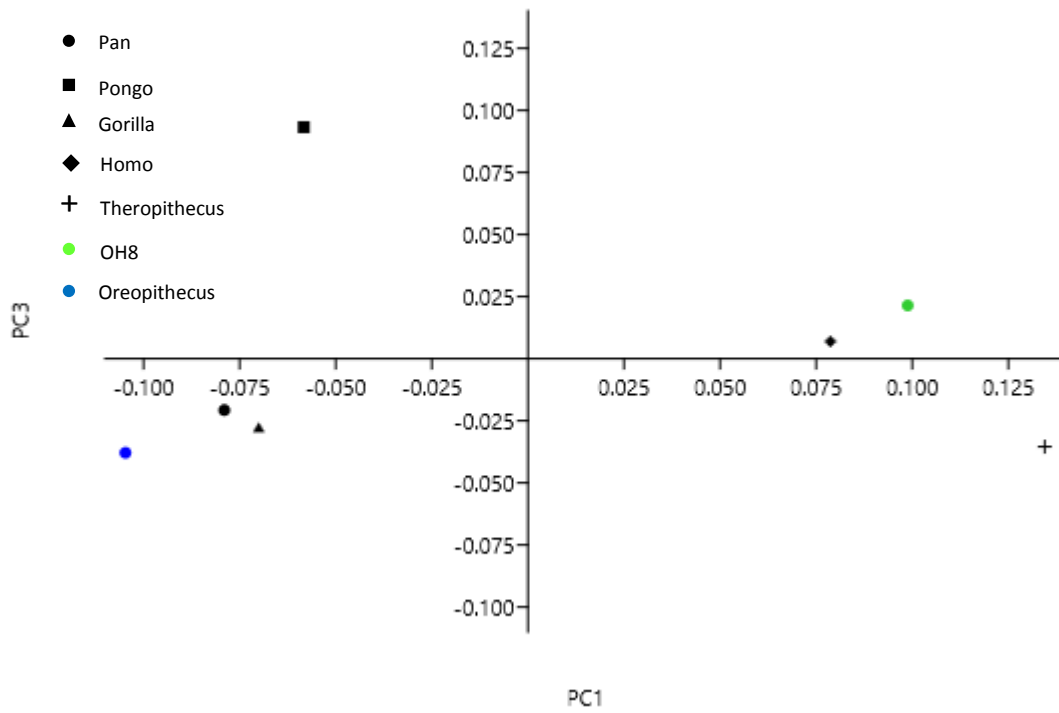


Figure 3.2.9. Principal component 1 vs. principal component 3 of species means and fossils for the navicular.

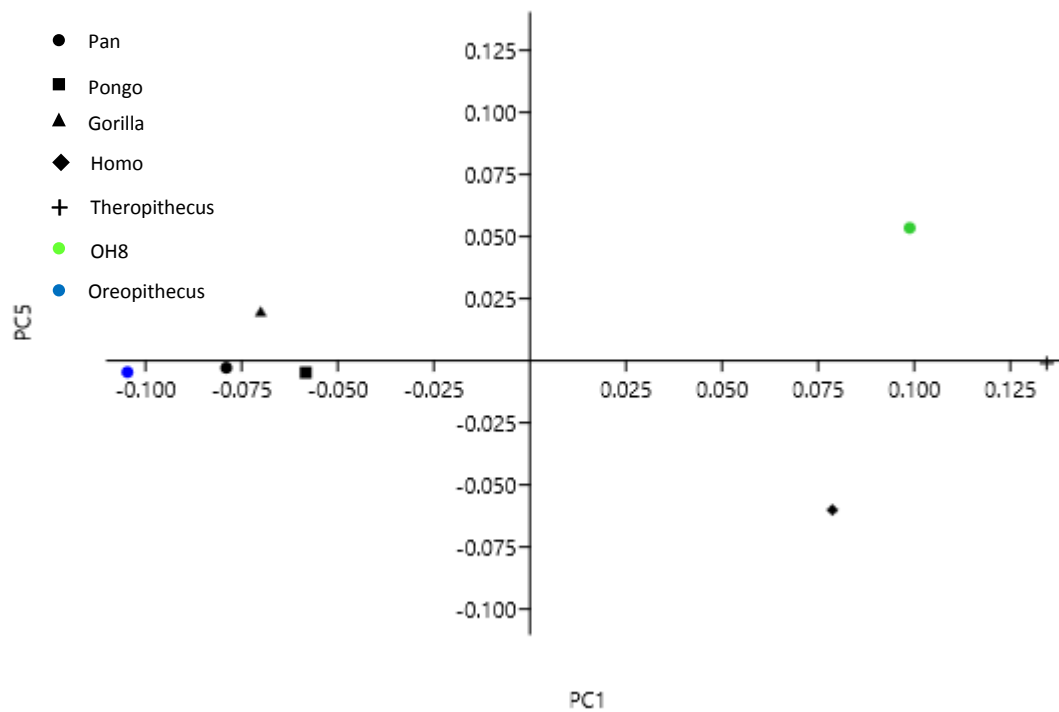


Figure 3.2.10. Principal component 1 vs. principal component 5 of species means and fossils for the navicular.

3.2.2. Statistical tests

The full Procrustes distances between species means and fossils for the navicular are presented in Table 3.2.1. The Procrustes distances for the navicular gave similar results to the talus for both *Pan* and *Gorilla*. Here also *Pan* and *Gorilla* are closest to each other and each subsequently closest to *Oreopithecus*. Therefore hypothesis 1 is accepted for the navicular; the African ape species are most similar to each other of all the extant species included in the study. This reflects their similar ecology and locomotion, as well as their close phylogenetic link. *Pongo* is closest to *Pan* and then to *Oreopithecus*. However, if only extant species are considered then *Pongo* is next closest to *Gorilla* after *Pan*. Similarly, both *Pan* and *Gorilla* are next closest to *Pongo* after each other if fossil taxa are excluded. Therefore hypothesis 2 is accepted for the navicular; the non-human apes are more similar to each other than any is to either *Homo* or *Theropithecus*. As for hypothesis 1, this reflects the similar ecology and locomotion among the non-human apes compared to the more specialized species of *Homo* and *Theropithecus*. Hypothesis 3 is also accepted for the navicular. *Theropithecus* is consistently the furthest from the other extant species included in the study. The fact that it is closest in shape to *Homo* of all the extant species may be related to the higher terrestriality of *Theropithecus* and *Homo* relative to the non-human apes.

	Pan	Pongo	Gorilla	Homo	Thero	OH8	Oreo
Pan	0	0.153004	0.076649	0.183441	0.254981	0.20345	0.139468
Pongo	0.153004	0	0.167161	0.212305	0.236435	0.214315	0.157492
Gorilla	0.076649	0.167161	0	0.183633	0.25601	0.197421	0.158286
Homo	0.183441	0.212305	0.183633	0	0.194471	0.120154	0.239077
Thero	0.254981	0.236435	0.25601	0.194471	0	0.180333	0.258254
OH8	0.20345	0.214315	0.197421	0.120154	0.180333	0	0.246241
Oreo	0.139468	0.157492	0.158286	0.239077	0.258254	0.246241	0

Table 3.2.1. Procrustes distances amongst species mean shapes and fossils for the navicular. The smallest and second smallest distances are shown on each row. The bold red shows the closest relationship and bold black the second closest.

The data for the navicular reveal that *Oreopithecus* is most similar to *Pan* and then *Pongo* is a good way more distant (although *Gorilla* is only marginally more distant from *Oreopithecus* than *Pongo* is). *Oreopithecus* is most distant from *Theropithecus* in Procrustes distance indicating that *Oreopithecus*

bears very little similarity to old world monkeys and is instead more closely aligned with ape species. *Oreopithecus* is also clearly more similar in morphology to *Pan* than any other ape species. Therefore hypothesis 4 is accepted for the navicular; *Oreopithecus* is unlike *Theropithecus* in its navicular morphology. Similarly, hypothesis 5 is also accepted for the navicular; *Oreopithecus* is most similar to one of the African apes (in this case *Pan*). OH8 is closest to *Homo* in terms of its navicular morphology. The next closest species to OH8 is *Theropithecus*, although this is somewhat more distant than *Homo*. Therefore hypothesis 6 is accepted for the navicular; OH8 is most similar in shape to *Homo*. The significance of these Procrustes distances was assessed by calculating the Mahalanobis distance between the fossil and nearest extant species mean. It was discovered that *Oreopithecus* was significantly different from *Pan* in terms of navicular shape with a Mahalanobis distance of 28.526, 5.34 standard deviation units and a p value of <0.0005. OH8 was not found to be significantly different from *Homo* with respect to navicular shape with a Mahalanobis distance of 15.685, 3.96 standard deviation units and a p value of 0.1. The significance of differences between extant species means was calculated using permutation tests on the pairwise Procrustes distances between individuals in the sample. It was found that all extant species were significantly different from one another at $p = <0.0001$.

The difference in mean centroid size was calculated between the extant species. The results for the navicular were similar to those obtained for the talus. *Gorilla* and *Homo* were not found to be significantly different in size following t tests ($p = 0.0589$), although *Gorilla* (217.4) was larger than *Homo* (205.4). Both *Gorilla* and *Homo* were found to have significantly higher means than all other extant species at $p = <0.0001$. Therefore, hypothesis 8 is accepted for the navicular; *Homo/Gorilla* will consistently be the largest in size of the extant species. *Pan* and *Pongo* were not found to have significantly different means ($p = 0.162$), although *Pongo* (162.9) was larger than *Pan* (155.2). The centroid size of *Theropithecus* (100) was found to be significantly smaller than all other extant species at $p = <0.0001$. Therefore, hypothesis 9 is confirmed for the navicular; *Theropithecus* is the smallest of the extant species. For the navicular the hierarchy of size for the extant species can be represented in the same way as it is for the talus. *Gorilla/Homo* > *Pongo/Pan* > *Theropithecus*.

The difference in size of the fossil species from the extant species was also assessed using the centroid size of all individuals used in the study. *Oreopithecus* was found to be significantly smaller than all ape species with a significance threshold of $p=0.01$ following Bonferroni correction. The results were as follows: *Oreopithecus* vs. *Pan* ($z = -3.548$, $p = 0.0002$); *Oreopithecus* vs. *Pongo* ($z = -2.436$, $p = 0.0074$); *Oreopithecus* vs. *Gorilla* ($z = -4.261$, $p = <0.0001$); *Oreopithecus* vs. *Homo* ($z = -$

6.296, $p = <0.000$). *Oreopithecus* was found not to be significantly larger than *Theropithecus* ($z = 1.847$, $p = 0.0324$). Therefore, hypothesis 10 is rejected for the navicular; *Oreopithecus* is not comparable in size to *Pan*. This result matches that for the talus and suggests that the foot of *Oreopithecus* was not as robust as that of extant apes and would seem to constitute an argument against a significant bipedal component to the positional repertoire. The results for OH8 also resemble those for the talus. OH8 is significantly larger than *Theropithecus* ($z = 5.806$, $p = <0.0001$), which is an unsurprising result. OH8 is larger than the *Pan* mean, but not significantly ($z = 0.341$, $p = 0.3664$) and is smaller than the *Pongo* mean, but also not significantly ($z = -2.436$, $p = 0.4095$). OH8 is significantly smaller than both *Gorilla* ($z = -2.533$, $p = 0.0057$) and *Homo* ($z = -3.389$, $p = 0.0004$), which, as for the talus, must be viewed in the context of its small body size. Therefore, hypothesis 11 is confirmed for the navicular; OH8 is smaller in size than *Homo*.

3.2.3. Visualisation of shape differences

In order to describe the differences in shape it is necessary to use some technical terminology. Figures 3.2.11 and 3.2.12 illustrate what these terms are referring to.

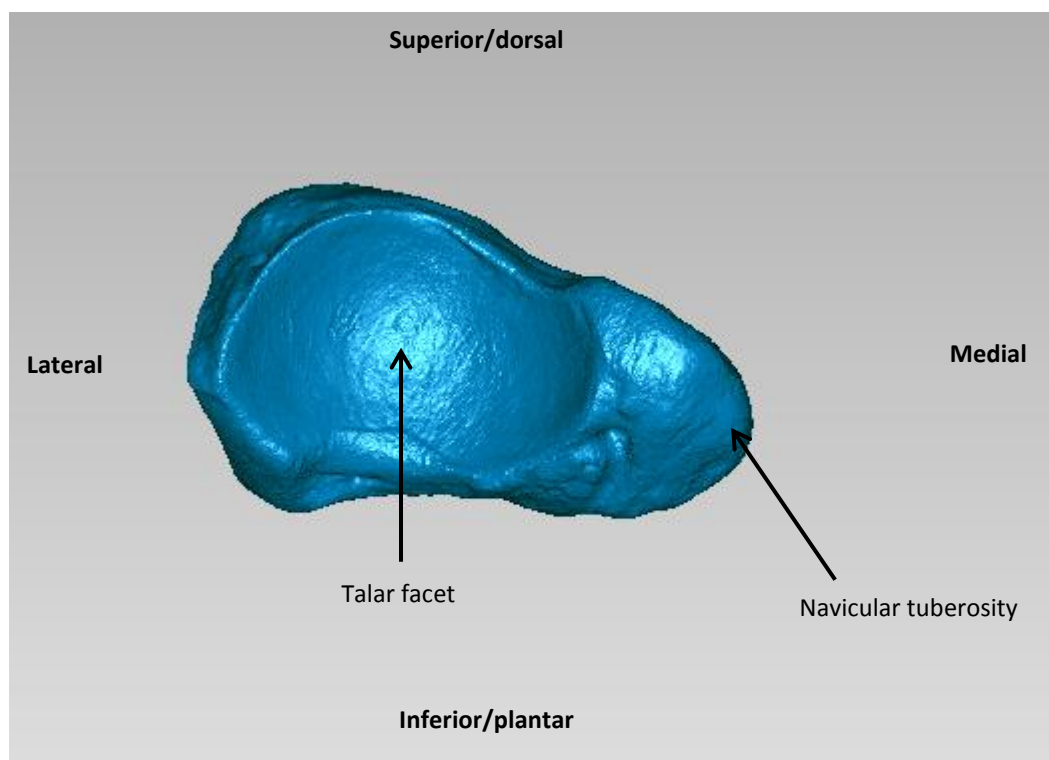


Figure 3.2.11. Proximal view of the navicular displaying terminology used to describe shape differences.

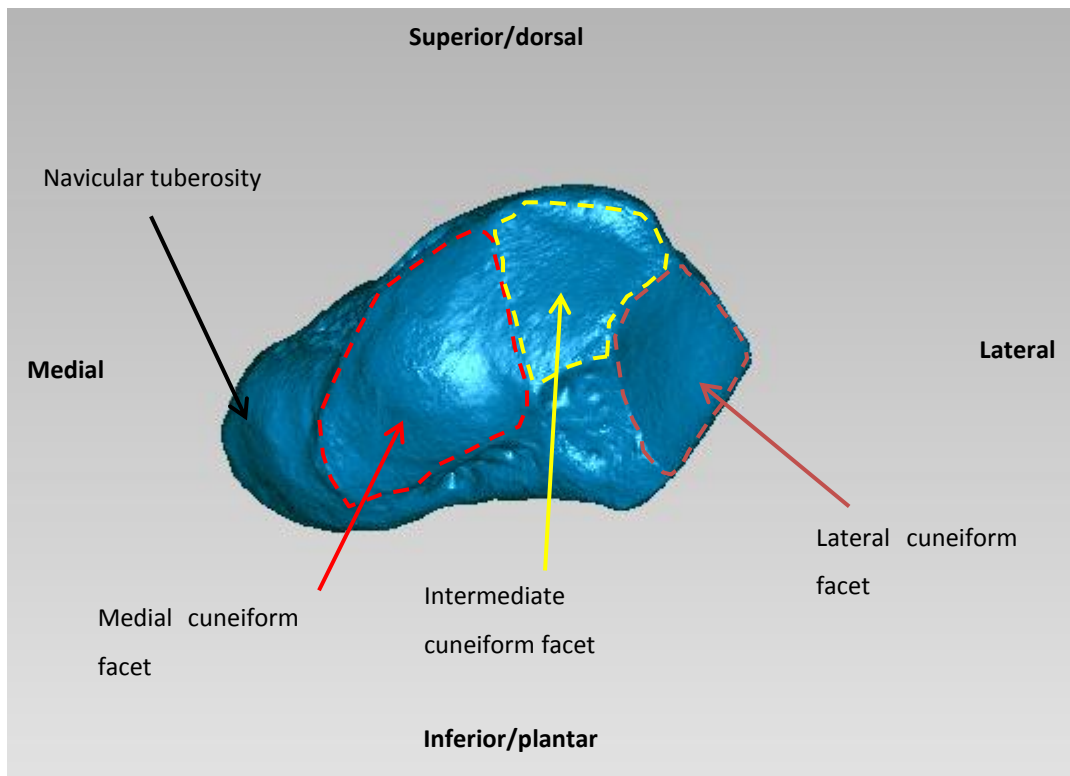


Figure 3.2.12. Distal view of the navicular displaying terminology used to describe shape differences.

From *Pan* to *Gorilla*

Pan and *Gorilla* were separated by a low Procrustes distance despite being significantly different from one another. The close proximity of the mean shapes of *Pan* and *Gorilla* is reflected in the scant observable differences between the two. The most obvious difference is the more robust navicular of *Gorilla*. This is most obvious from superior view (Fig 3.2.13B). It is clear that the anteroposterior breadth of the bone is greater in *Gorilla* than it is in *Pan*, though this difference is not pronounced. Both *Pan* and *Gorilla* have an expansion to the medial third of the talar facet, which is also oriented inferiorly, though this is slightly more pronounced in *Gorilla* (Fig. 3.2.13A). Similarly, both species have a constriction of the inferior border of the talar facet but this is much more strongly expressed in *Gorilla* than *Pan*. The surface area of the talar facet is comparable to the overall surface area of the three cuneiform facets combined in both species. The features of the talar facet are largely the same in *Pan* and *Gorilla*. The cuneiform facets also have roughly the same configuration in both *Pan* and *Gorilla*. There is a clear flexion of the lateral cuneiform facet away from the other two. The degree of flexion is comparable in both species. The lateral and medial cuneiform facets are rotated against each other in both species and to a comparable degree. This gives the distal facets an inferiorly directed concavity when viewed distally. The result of this is that the intermediate cuneiform facet is smallest and wedged between the other two facets. The medial cuneiform facet is the largest of the three in both species. In summary, it is clear that the two species are highly similar in terms of navicular morphology.

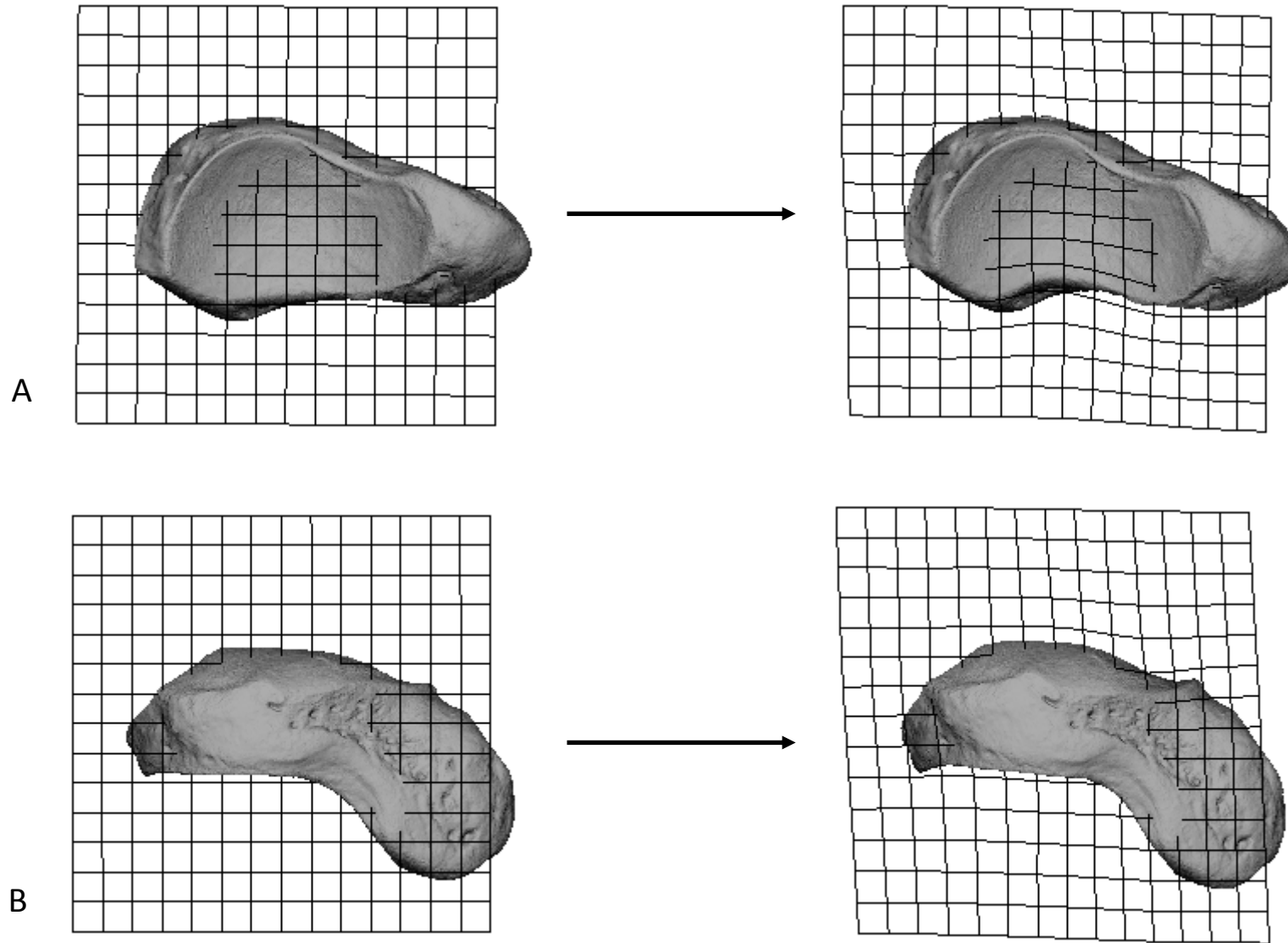


Figure 3.2.13. Demonstration of the warp from the *Pan* mean navicular (left) to *Gorilla* mean (right). A) Proximal view. B) Superior view

The warp from *Homo* to *Theropithecus* is included because *Homo* was the closest extant species to *Theropithecus*, although the Procrustes distances between *Theropithecus* and any other species are largest for the navicular so the fact that *Homo* is its nearest neighbor among the extant species does not imply a great deal of similarity. The talar facet of *Theropithecus* has a reduced mediolateral dimension in proximal view. However, the curvature of the facet is high with the medial and lateral halves roughly forming a 90° angle. The distal facets are directly opposite the lateral half of the talar facet and therefore the medial half of the talar facet forms a medial border (Fig. 3.2.14A). *Theropithecus* shares with *Homo* an expansion rather than constriction of the inferior border of the talar facet but bears a dorsoplantar expansion rather than constriction of the medial half of the talar facet. From superior view it is apparent that *Theropithecus* as a proximodistally broad navicular, in which it is similar to *Homo*. However, the proximodistal breadth of the medial side of the bone is significantly greater due to the extreme proximal projection of the medial border of the talar facet described above. From superior view it is also clear that the intermediate cuneiform facet extends much further superiorly and proximally than either of the other two cuneiform facets. The distal surface of the navicular is unique in *Theropithecus* among the extant species. It is clear that the medial cuneiform facet is vastly reduced in size while the lateral cuneiform facet is the largest by quite a margin (Fig. 3.2.14B). The intermediate cuneiform facet is larger than it is in other species and notably has an inferior border which extends some way beyond the inferior border of the two neighbouring facets. There is also mediolateral constriction of the intermediate cuneiform facet at its midpoint, unlike in any other extant species.

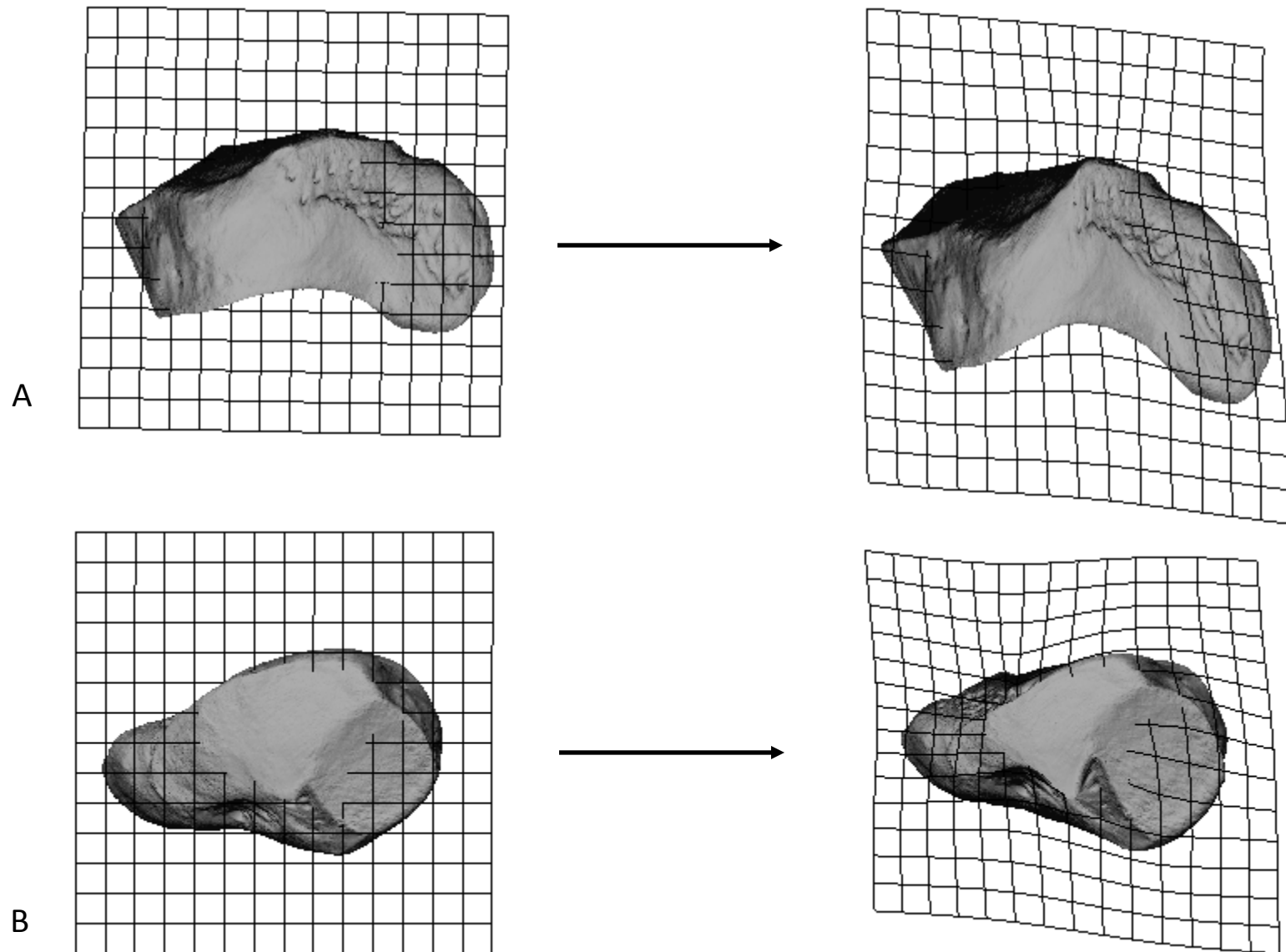


Figure 3.2.14. Demonstration of the warp from the *Homo* mean navicular (left) to *Theropithecus* mean (right). A) Superior view. B) Distal view

From *Pan* to *Oreopithecus*

The navicular of *Oreopithecus* differs in shape from *Pan* in a number of interesting ways, but also bears some similarities. The navicular facet is narrower across both its superoinferior and mediolateral dimensions (Fig. 3.2.15A). The inferior border is similarly constricted projecting superiorly and the medial third of the facet is extended medially tapering to a narrow medial border from the expanded superior border, similar to *Pan*. However, the expansion of the medial and superior borders is less pronounced in *Oreopithecus* giving the overall impression of a relatively smaller navicular facet in this species. The medial border of the navicular facet is flexed towards the superior aspect of the bone in *Oreopithecus* unlike the more inferior orientation found in *Pan* and the bone is also narrower across its anteroposterior dimension on the medial side. However, this is simultaneous with relative broadening of the lateral side of the bone. In *Pan* the lateral cuneiform facet is strongly flexed away from the intermediate and lateral cuneiform facets which results in a very narrow anteroposterior breadth of the lateral side of the bone. In contrast *Oreopithecus* has a less strongly flexed lateral cuneiform facet giving it a relatively wider lateral half of the navicular (Fig. 3.2.15B), although the bone itself is relatively narrower overall in *Oreopithecus*. The proximal and distal articular surfaces are more parallel in *Oreopithecus* due to these facts. The superior border of the intermediate cuneiform facet extends further onto the dorsal surface of the bone in *Oreopithecus*, possibly indicating a greater degree of flexion at the midfoot than is found in *Pan*. The medial cuneiform facet is constricted across its short axis, which lies roughly along the dorsoplantar axis of the bone. The reduced size of the facet in *Oreopithecus* may indicate that it was poorly adapted to transmitting and supporting high levels of force through this joint.

From *Pongo* to *Oreopithecus*

The salient differences between the navicular morphology of *Oreopithecus* and *Pongo* are also considered despite the notably greater difference in shape between them than *Oreopithecus* and *Pan*. This is an attempt to better understand the functional relationships of *Oreopithecus*. *Oreopithecus* is more similar to *Pan* than *Pongo* in terms of talar facet morphology. The inferior border of the talar facet is more constricted, similar to *Pan*, unlike the flat medial to lateral inferior border in *Pongo* (Figure 3.2.16A). The medial third of the talar facet is more expanded than it is in *Pongo*, as is the superior border, which gives the proximal facet a greater area which is roughly comparable to that of the distal facets. From superior view, the proximal facet is also more tightly

curved from medial to lateral in *Pongo* while it is flatter in *Oreopithecus* (Fig. 3.2.16B). This fact, coupled with the expansion of the medial portion of the facet, directs the plane of the talar facet more towards the medial cuneiform facet in *Oreopithecus*, while it is directed more closely towards the intermediate cuneiform facet in *Pongo*. The inferior border of the intermediate cuneiform facet is narrower in *Oreopithecus* than it is in *Pongo*, in which it is broader than in any other species. This is linked to the extreme flexion of the lateral cuneiform facet in *Pongo*. This facet is more distally directed in *Oreopithecus*, which gives the lateral side of the bone a greater anteroposterior breadth. The medial cuneiform facet is narrower than *Pongo* across its smaller axis, similar to the comparison with *Pan*, but is longer across its main axis than *Pongo* is. This bears implications for mobility and weight-bearing along the first ray. The intermediate cuneiform facet is expanded onto the dorsal aspect of the bone, a feature which is less strongly expressed in *Pongo* as well as *Pan*.

From *Homo* to OH8

OH8 was found not to be significantly different in shape from the *Homo* mean (see above), however, it is still useful to talk about how OH8 is similar to *Homo* so that the implications of these similarities can be discussed in the context of foot function. OH8 shares with *Homo* a talar facet which is substantially smaller in area than the combined area of the cuneiform facets, and notably with a reduced mediolateral dimension caused by a constricted medial third of the talar facet. OH8 shares an inferior projection of the midpoint of the inferior border of the talar facet with both *Homo* and *Theropithecus*, unlike the constricted inferior border found in the apes. The anteroposterior breadth of the navicular is large in OH8 as it is in *Homo*, and this is in part due to the morphology of the lateral side of the bone. The lateral cuneiform facet lies roughly in the same plane as the intermediate and lateral cuneiform facets, unlike non-human apes in which the facet is flexed laterally. This has the effect of broadening the lateral side of the bone, although the bone is generally broader from anterior to posterior in *Homo* and OH8. The size of the cuneiform facets are relatively larger in *Homo* and OH8, especially in the dorsoplantar dimension. The medial cuneiform facet has a greatly reduced mediolateral dimension and lacks the curved articular surface found in non-human apes. The inferior border of the intermediate cuneiform facet is extremely narrow compared to the superior border resulting in the intermediate cuneiform being firmly wedged between the medial and lateral cuneiform inferiorly.

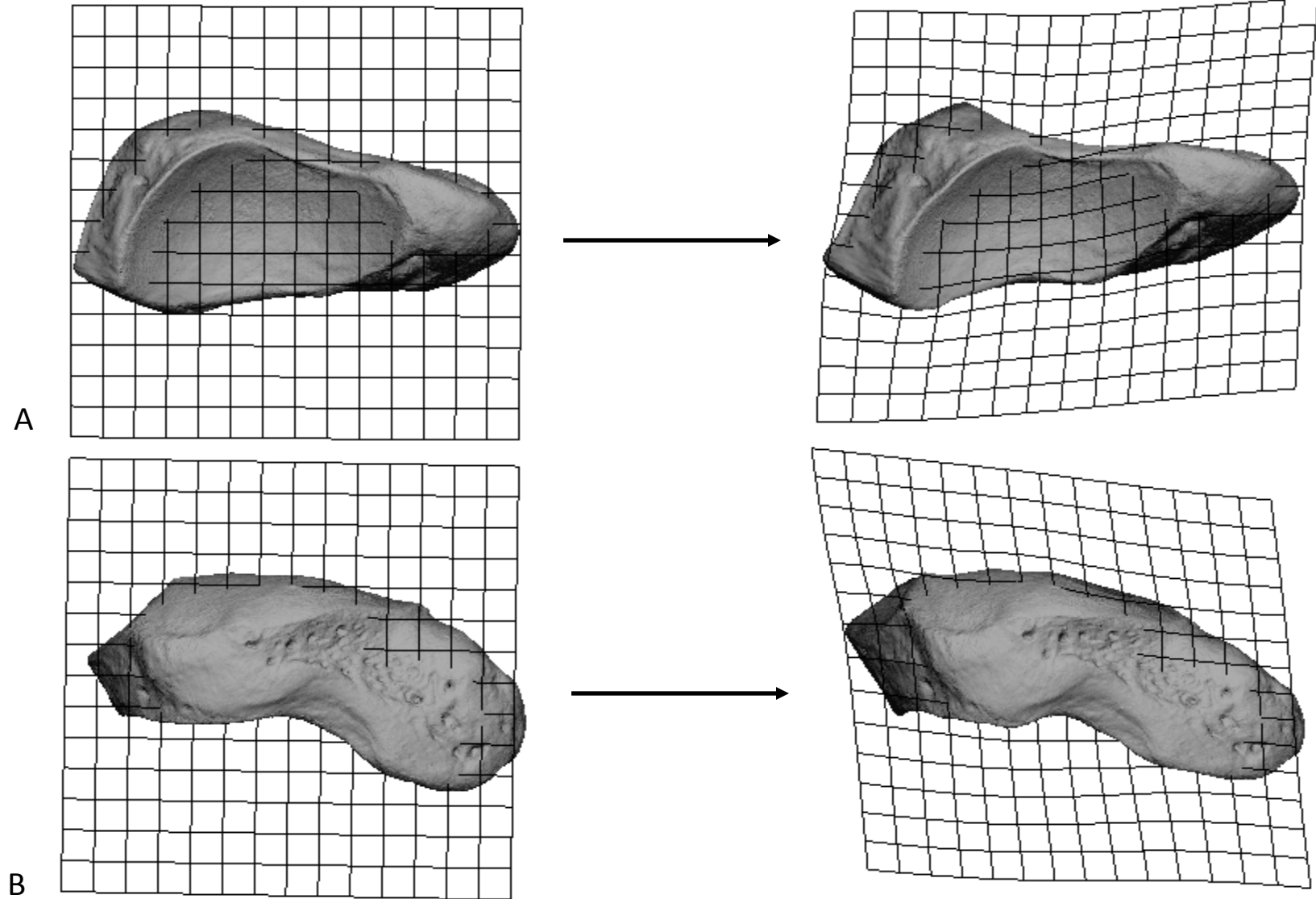


Figure 3.2.15. Demonstration of the warp from the *Pan* mean navicular (left) to *Oreopithecus* (right). A) Proximal view. B) Superior view

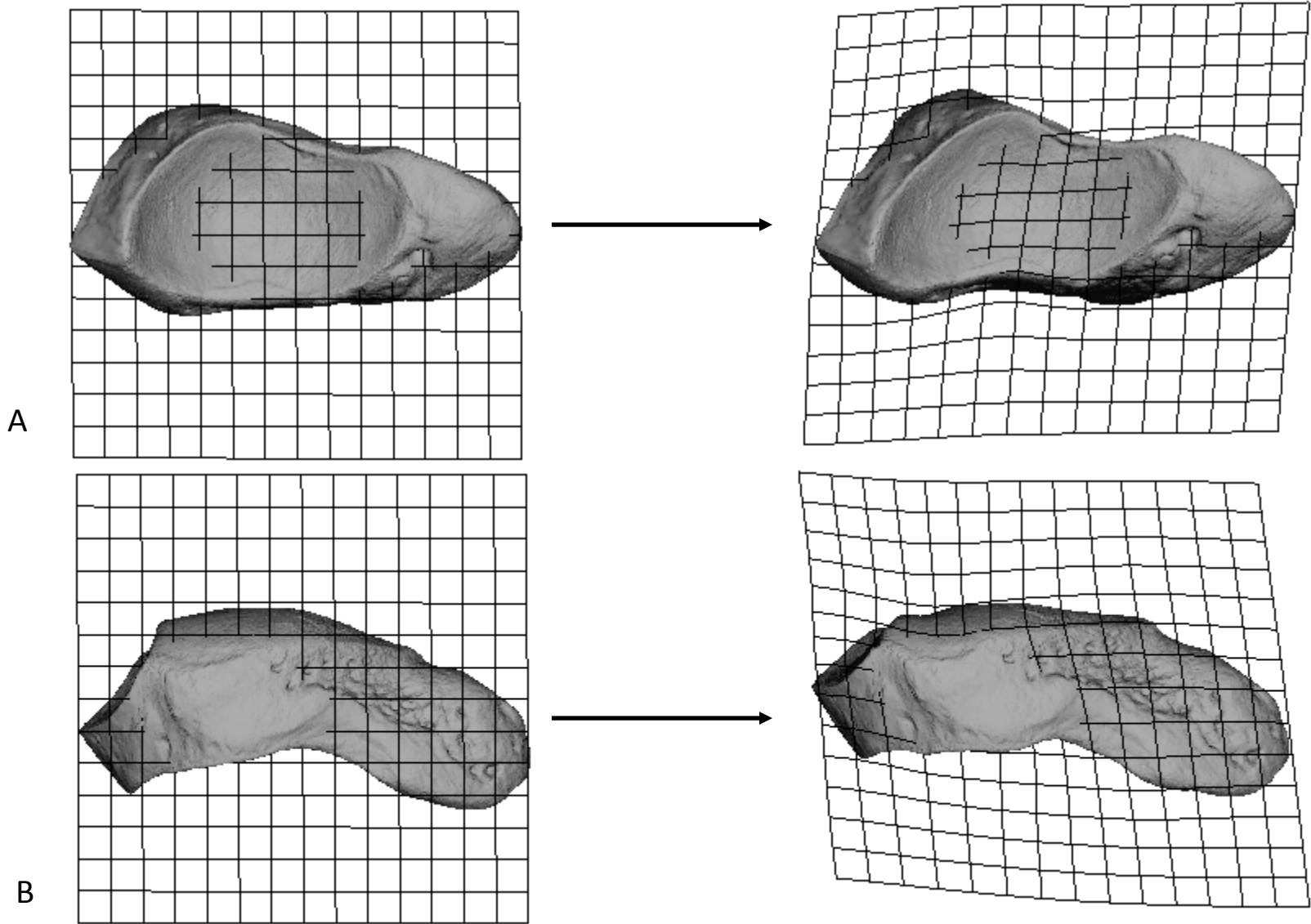


Figure 3.2.16. Demonstration of the warp from the *Pongo* mean (left) to *Oreopithecus* (right). A) Proximal view. B) Superior view

3.3. Medial cuneiform

3.3.1. Principal components analysis

3.3.1.1. Full sample

A principal components analysis was conducted on the Procrustes aligned landmarks of the medial cuneiform for all specimens used in the study (Fig. 3.3.1). The first three principal components explain 65.72% of the variance, the first five principal components explain 77.41% of the variance, and the first twelve explain 90.07% of the variance. The remaining 9.93% is explained by principal components 13-82.

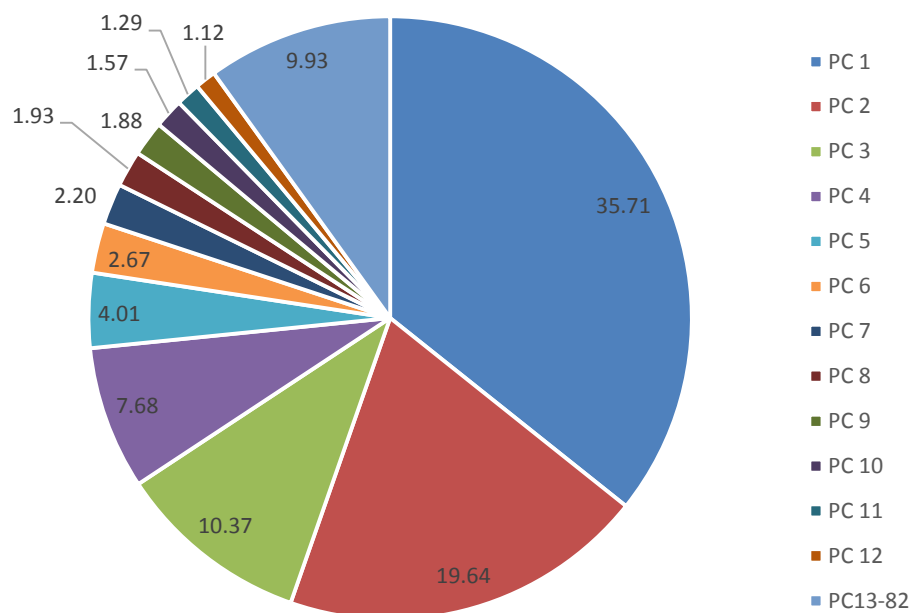


Figure 3.3.1. Percentage of the overall variance explained by each principal component for the medial cuneiform.

The first two principal components combined explain more than half of the variance in the data set. The first principal component most strongly distinguishes *Theropithecus* at the extreme positive end of the axis and *Gorilla* at the extreme negative end (Fig. 3.3.2). There is a good deal of overlap

between the distributions of *Pan* and *Gorilla* on the negative aspect of the axis but the *Pan* distribution is noticeably less negative. *Theropithecus* does not overlap with any other species on PC1. *Pongo* and *Homo* share roughly the same distribution along PC1, both occupying the lower end of the positive aspect of the axis. Both species are closer to *Pan* than to *Theropithecus*. *Nacholapithecus* falls firmly within the *Homo* range on PC1, lying marginally outside the range of *Pongo* on the higher end of its distribution, in the direction of *Theropithecus*. OH8 also falls well within the range of *Homo*, at the lower limit of its range, and also within the range of *Pongo* on PC1. The *Oreopithecus* specimens lie roughly intermediate between *Pan* and *Gorilla* on PC1 and all cluster together fairly tightly.

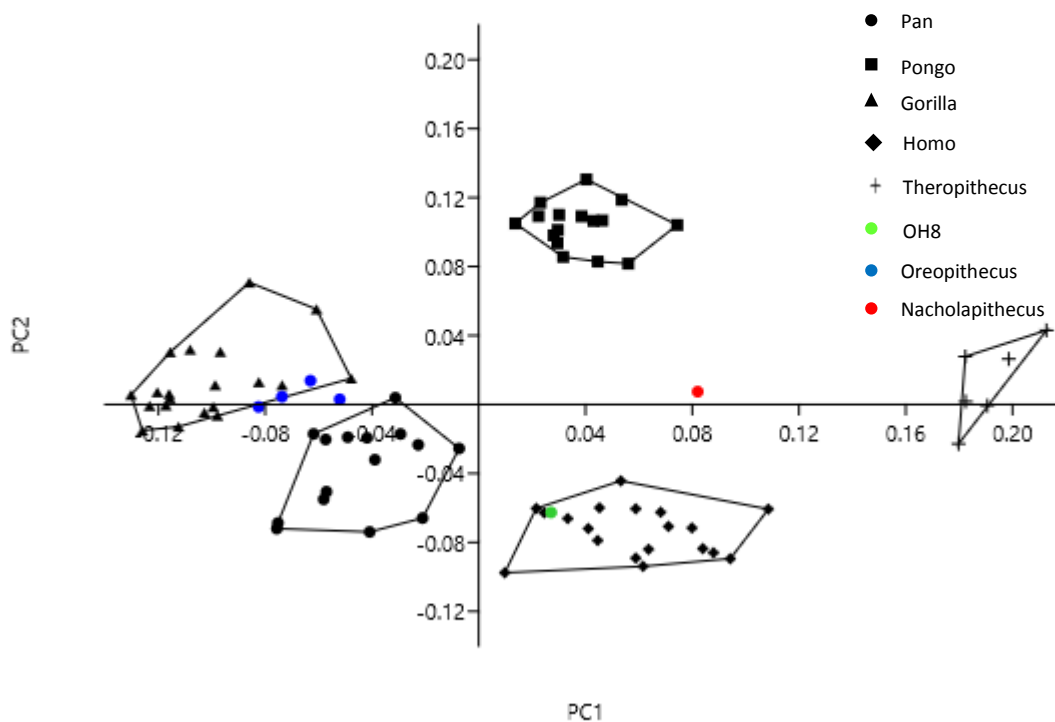


Figure 3.3.2. Principal component 1 vs. principal component 2 of all individuals for the medial cuneiform.

Principal component 2 most strongly separates *Homo* on the negative half of the axis and *Pongo* on the positive half. *Theropithecus* and the African apes all lie intermediate between *Homo* and *Pongo* and each of their ranges cross the x axis. *Pan* is the most negative of the three, having considerable overlap with the *Homo* distribution and only one individual crossing the x axis into the positive half.

The *Gorilla* and *Theropithecus* distributions are both mostly in the positive half of the axis and overlap broadly with one another. *Nacholapithecus* lies in the ranges of *Gorilla* and *Theropithecus* on PC2, close to the x axis. OH8 is within the *Homo* range, but is also within the more negative range of *Pan*. The *Oreopithecus* specimens are within the ranges of *Pan*, *Gorilla*, and *Theropithecus*. Taken together, PC1 and PC2 provide four broad groups; the African apes, *Homo*, *Pongo*, and *Theropithecus*. However, the African ape clusters are clearly distinct and clearly closer to each other than to any other group. The *Oreopithecus* specimens lie closer to the *Gorilla* overall distribution but are also close to that of *Pan*. OH8 lies at the periphery of the *Homo* range while *Nacholapithecus* lies central to all groups on its own.

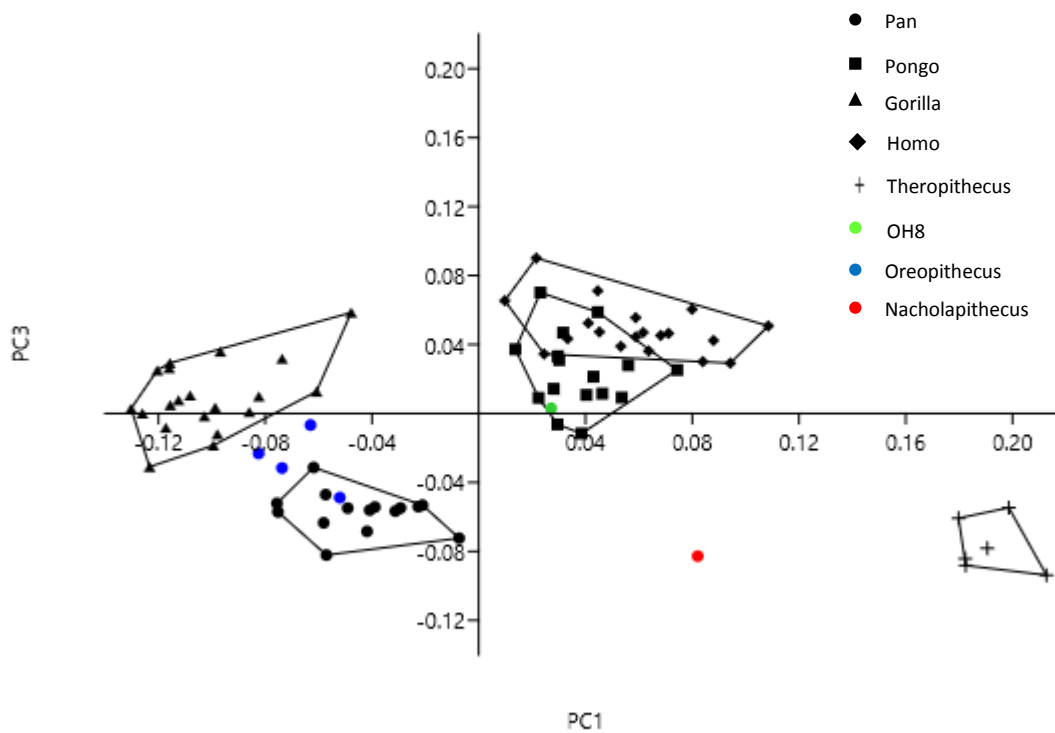


Figure 3.3.3. Principal component 1 vs. principal component 3 of all individuals for the medial cuneiform.

The distributions of *Homo*, *Pongo*, and *Gorilla* are broadly similar on PC3 (Fig. 3.3.4), although the distribution of *Homo* is higher on the positive aspect of the axis and does not cross the x axis, unlike *Pongo* and *Gorilla*. The ranges of *Pan* and *Theropithecus* are practically coincident on the negative aspect of the axis. *Nacholapithecus* lies squarely in the *Theropithecus* range on PC3 and close to the

negative extreme of the *Pan* range. OH8 lies close to the x axis on PC3 in the ranges of *Pongo* and *Gorilla* but outside the range of *Homo*. The *Oreopithecus* specimens are distributed between *Pan* and *Gorilla*, but all *Oreopithecus* individuals fall on the negative aspect of the axis. The higher principal components are not as effective at discriminating between species, but some fossil species are separated from extant groups on PC4 and 5 (Figs 3.3.4 & 3.3.5), although this effect is small.

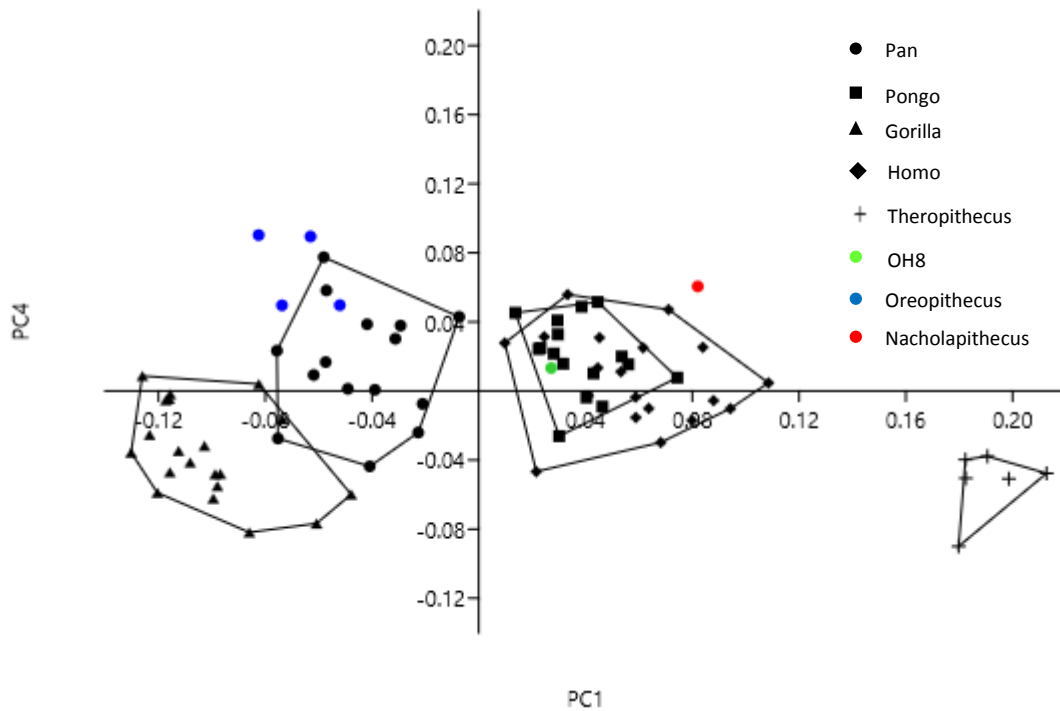


Figure 3.3.4. Principal component 1 vs. principal component 4 of all individuals for the medial cuneiform.

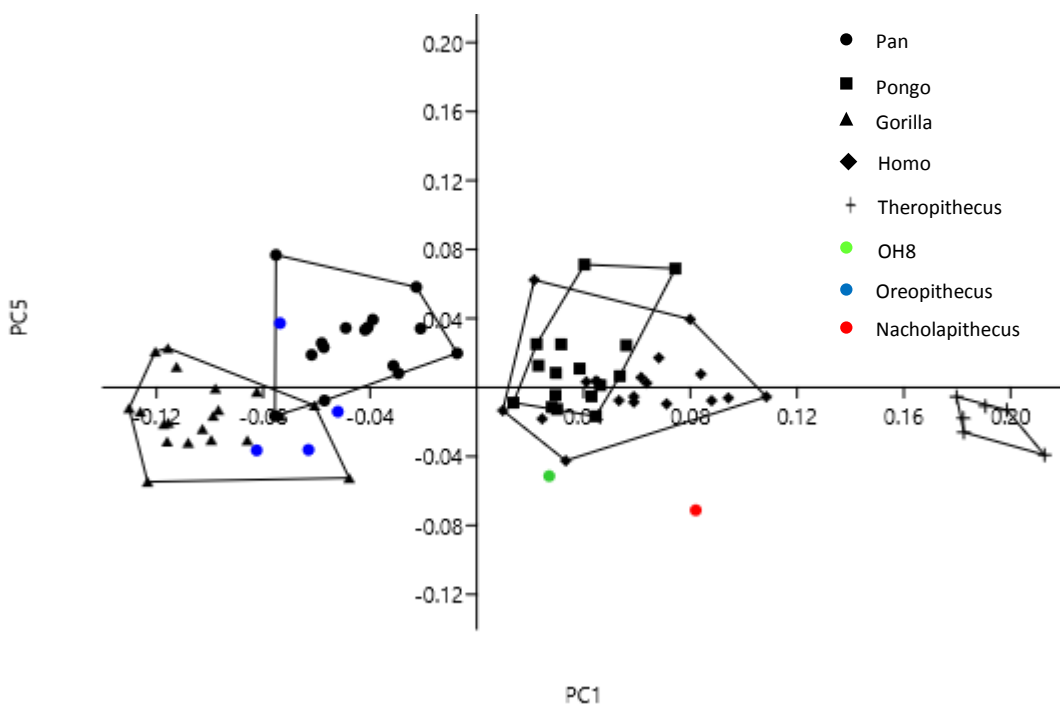


Figure 3.3.5. Principal component 1 vs. principal component 5 of all individuals for the medial cuneiform.

3.3.1.2. Extant species means vs. fossils

A principal components analysis was conducted on the Procrustes aligned landmarks of the medial cuneiform for the extant species mean shapes and the fossils. There were eleven principal components. The first three explained 72.98% of the variance, the first four explained 80.85% of the variance, and the first nine explain practically 100% of the variance in the data set (Fig. 3.3.6).

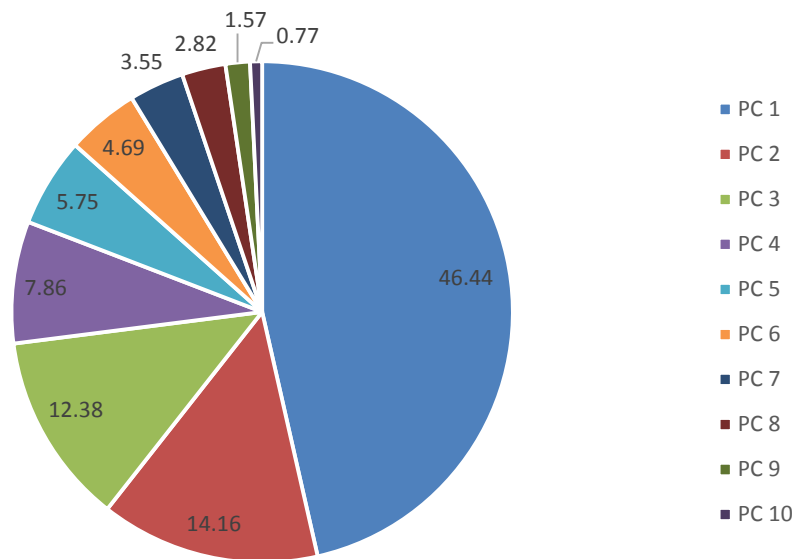


Figure 3.3.6. Percentage of the variance explained by each PC using only species mean shapes for the medial cuneiform.

The first principal component provides a distribution of species and fossils similar to the one extracted from the full sample, although the axis is flipped when only species means are used (Fig. 3.3.7). *Gorilla* has the highest value on the positive aspect of the axis. *Pan* also lies on the positive part of the axis but is more modestly placed than *Gorilla*. *Pongo* and *Homo* each have values close to 0 on PC1 but both lie in the negative range of the axis; *Homo* has a slightly higher negative value than *Pongo*. *Theropithecus* is distinct from all other extant species means, having an extremely high value on the negative aspect of the axis. *Oreopithecus* is grouped with *Gorilla* and *Pan*, it has a value approximately midway between the two. OH8 has a value slightly inside the negative range of the axis, extremely close to 0, aligning it closely with *Homo* and *Pongo* on PC1. *Nacholapithecus* is situated midway between *Homo/Pongo* and *Theropithecus* with a moderately high value on the negative aspect of the PC1 axis.

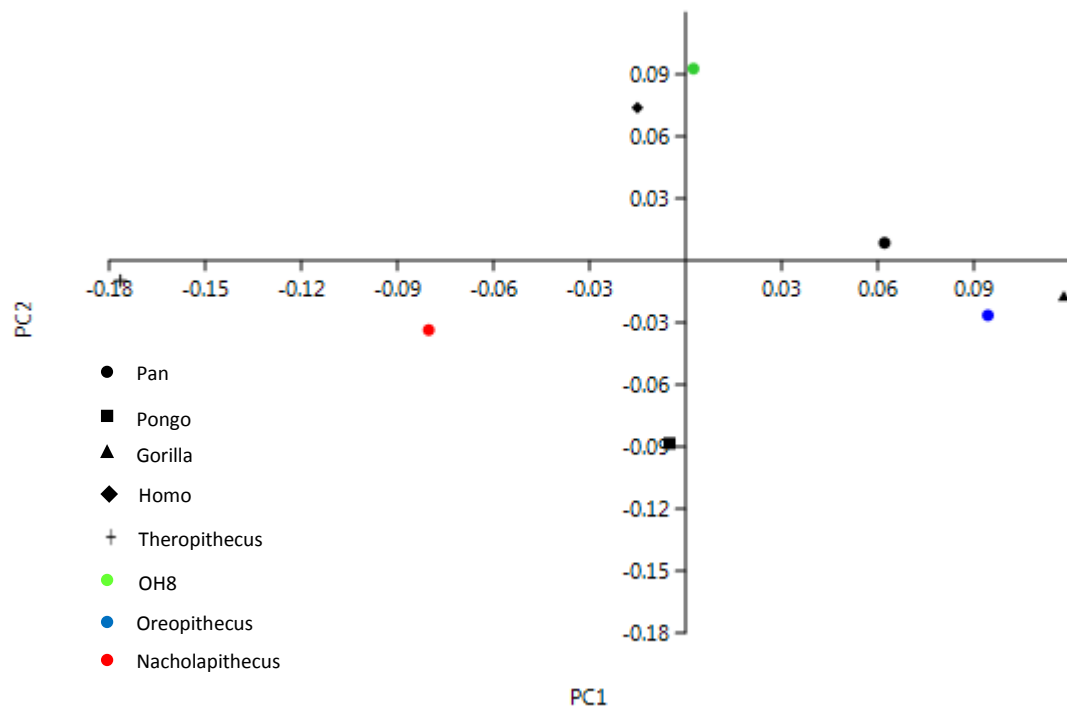


Figure 3.3.7. Principal component 1 vs. principal component 2 of species means and fossils for the medial cuneiform.

PC2 also presents a distribution which is reminiscent of that extracted from the full dataset, although the axis has been inverted. The clearest differentiation along the axis is between *Homo* and *Pongo*. *Homo* occupies the extreme end of the positive half of the axis while *Pongo* occupies the extreme end of the negative half of the axis. Of the remaining extant species, PC2 does little to separate them. Each has a value close to 0 on the axis, with *Pan* marginally located on the positive half and *Gorilla* and *Theropithecus* slightly positioned in the negative half. *Oreopithecus* has a value close to that of *Gorilla*, with a slightly higher negative value, but not approaching the *Pongo* mean. OH8 has a value on the positive half of the axis in excess of the *Homo* mean. *Nacholapithecus* has a value which is approximately the same as that for *Oreopithecus*. Thus, taken together, PC1 and PC2 offer a broadly comparable distribution of species means and fossils, and the distribution of the full dataset. The higher principal components are much less informative. PC3 clearly separates *Nacholapithecus* on the extreme positive half of the axis from all other species (Fig. 3.3.8), while PC5 strongly separates *Homo* and OH8 (Fig. 3.3.9).

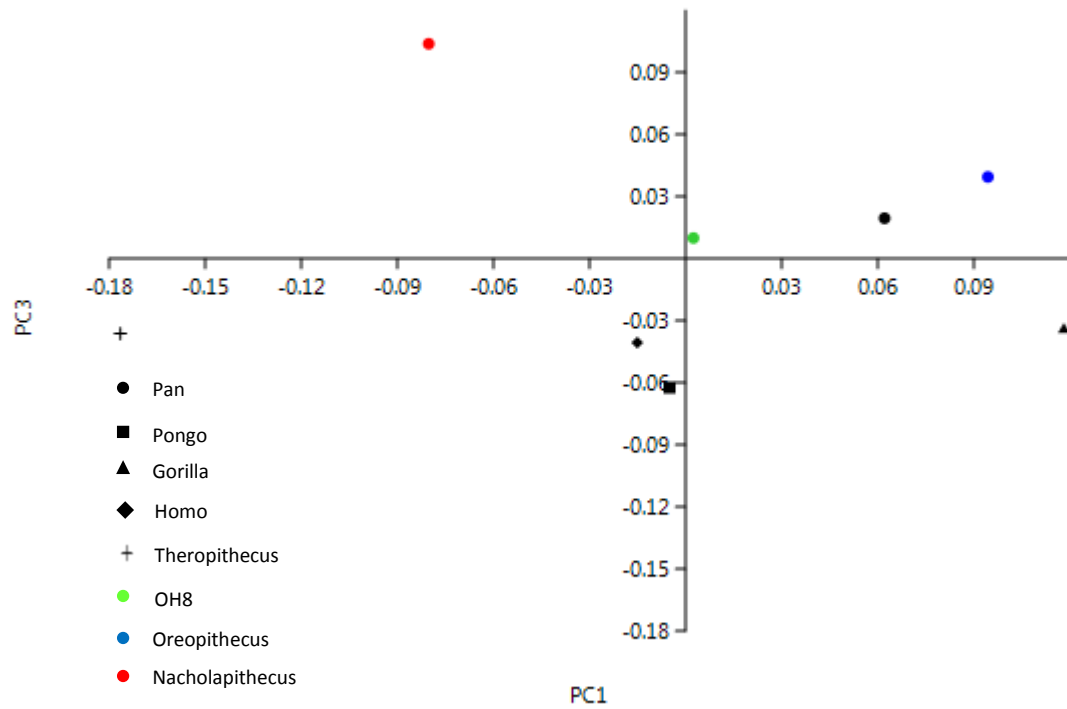


Figure 3.3.8. Principal component 1 vs. principal component 3 of species means and fossils for the medial cuneiform.

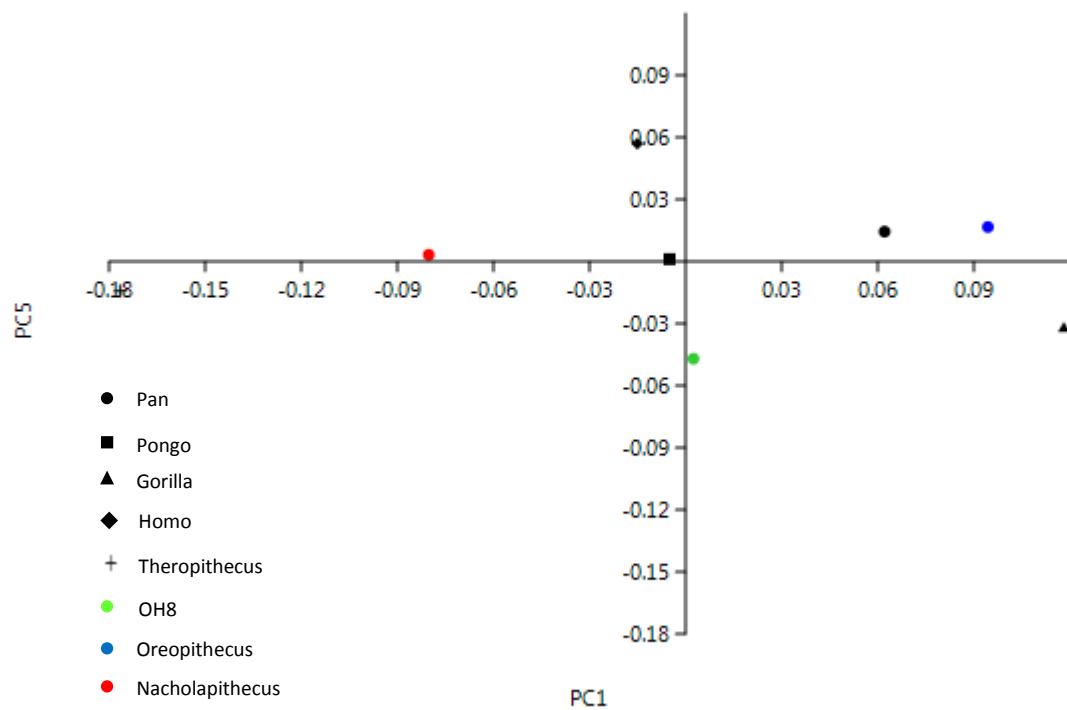


Figure 3.3.9. Principal component 1 vs. principal component 5 of species means and fossils for the medial cuneiform.

3.3.2. Statistical tests

There were four *Oreopithecus* medial cuneiforms available for study and therefore it was first established whether or not it is reasonable to conclude that the four medial cuneiforms belong to a single species. This was done by calculating the mean shape for all of the extant species and for *Oreopithecus* and then calculating the average Procrustes distance of all the individuals from the mean of their species. It was found that the *Oreopithecus* specimens differed from their mean to a similar degree to that seen in known extant species. The average Procrustes distances of individuals from the species mean and the range of values is presented in Table 3.3.1. *Oreopithecus* has an average distance of individuals from the species mean which is lower than that of both *Pan* and *Gorilla* and similar to *Homo* and *Pongo*. *Oreopithecus* also has the smallest range, which is likely linked to its small sample size but also gives some confidence in the result. Therefore it was concluded that the four *Oreopithecus* medial cuneiforms probably represent a single species.

Species	Average Procrustes distance	Range
<i>Pan</i>	0.083579	0.050807
<i>Pongo</i>	0.074108	0.051412
<i>Gorilla</i>	0.087945	0.061893
<i>Homo</i>	0.075105	0.063923
<i>Theropithecus</i>	0.059697	0.033981
<i>Oreopithecus</i>	0.077422	0.017465

Table 3.3.1. Average Procrustes distance of individuals from species mean and range of Procrustes distances.

To assess the similarities and differences between extant species and fossils the full Procrustes distances were calculated between the extant species and *Oreopithecus* mean shapes, and fossil representatives. The full Procrustes distances between each group/fossil are presented in Table 3.3.2. Of the extant species, *Pan* and *Gorilla* are closest to one another confirming hypothesis 1 for the medial cuneiform; the African apes are most similar and this reflects their similar ecology and locomotor behaviour, as well as their close evolutionary relationship. However, *Pan* is actually more similar in shape to *Oreopithecus* than to *Gorilla*, the implications of which will be discussed in greater detail below. *Oreopithecus* is the closest neighbour of *Pongo* while *Gorilla* is slightly more distant. However, the Procrustes distances of both species from *Pongo* are large implying marked differences

in shape between these groups. Notably, the Procrustes distance between *Pan* and *Homo* is lower than that between *Pan* and *Pongo*. Therefore, hypothesis 2 is rejected for the medial cuneiform; the non-human apes do not express broadly similar morphology reflecting their use of an arboreal habitat. *Pan* is more similar in shape to the terrestrial *Homo*. *Theropithecus* consistently has the greatest Procrustes distance between itself and all other extant species. Therefore, hypothesis 3 is confirmed for the medial cuneiform; *Theropithecus* is most markedly different in shape reflecting its status as an outgroup among the extant species.

Oreopithecus is most similar in shape to *Pan*. It is closer to *Pan* than *Pan* is to *Gorilla* by quite a margin and then vastly further from *Pongo*. Therefore, hypothesis 4 is rejected for the medial cuneiform; *Oreopithecus* bears very little similarity to a cercopithecoid. Simultaneously hypothesis 5 is confirmed; *Oreopithecus* is most similar to the African apes, specifically *Pan* in this instance. The considerably greater similarity between *Oreopithecus* and *Pan* suggests that the first digit likely functioned in a manner similar to *Pan* rather than *Gorilla*. OH8 was found to be most similar in shape to *Homo*, confirming hypothesis 6 for the medial cuneiform and suggesting that the first digit of OH8 lacked the mobility found in the African apes. *Nacholapithecus* was found to be most similar to *Theropithecus*, confirming hypothesis 7 for the medial cuneiform. However, the Procrustes distance is large and therefore the similarity may not necessarily reflect similar function.

	Pan	Pongo	Gorilla	Homo	Thero	Oreo	OH8	Nacho
Pan	0	0.182421	0.121944	0.154754	0.252612	0.107613	0.157604	0.194903
Pongo	0.182421	0	0.178361	0.180351	0.217679	0.172918	0.201885	0.197826
Gorilla	0.121944	0.178361	0	0.190797	0.301268	0.128727	0.189121	0.249219
Homo	0.154754	0.180351	0.190797	0	0.208808	0.185923	0.126452	0.199381
Thero	0.252612	0.217679	0.301268	0.208808	0	0.289956	0.231795	0.190877
Oreo	0.107613	0.172918	0.128727	0.185923	0.289956	0	0.175324	0.203549
OH8	0.157604	0.201885	0.189121	0.126452	0.231795	0.175324	0	0.191976
Nacho	0.194903	0.197826	0.249219	0.199381	0.190877	0.203549	0.191976	0

Table 3.3.2. Procrustes distances amongst species mean shapes and fossils for the medial cuneiform. Reading across the rows, the two closest species to each species/fossil are represented. The closest is highlighted in bold red, the second closest in bold black.

To calculate whether extant species (and *Oreopithecus*) were significantly different from one another permutation tests were conducted on the pairwise Procrustes distances between all individuals in the dataset. It was found that all species (including *Oreopithecus*) were significantly

different from each other, all recording p values of <0.0001. Therefore, *Oreopithecus* and *Pan* were significantly different in shape, despite having the lowest Procrustes distance between their means. Therefore, the differences between the two are examined in greater detail below. To assess whether the other fossils were significantly different from the extant species to which they were closest the Mahalanobis distance between them was calculated. OH8 was found to be significantly different in shape from *Homo* with a Mahalanobis distance of 21.198, which is 4.6 standard deviation units obtaining a p value of 0.02. *Nacholapithecus* was found to be significantly different from *Theropithecus* with a Mahalanobis distance of 111.772, which is 10.572 standard deviation units obtaining a p value of 0.0005.

The significance of difference in size between extant species (and *Oreopithecus*) were calculated using permutation tests based on centroid size for the medial cuneiform. Among the extant species it was found that *Homo* and *Gorilla* had significantly larger mean centroid sizes than all other species ($p = <0.0001$). It was also found that the two did not have significantly different means from one another ($p = 0.0248$ (significance value set to 0.00333 following Bonferroni correction for multiple comparisons)) although the mean value of *Homo* (211.1) was larger than that of *Gorilla* (198.3). Therefore, hypothesis 8 was accepted for the medial cuneiform; *Homo/Gorilla* are the largest of the extant species. *Pan* and *Pongo* were not found to have significantly different mean centroid sizes for the medial cuneiform ($p = 0.743$) although *Pongo* (159) had a slightly larger mean centroid size than did *Pan* (157.5). *Theropithecus* was consistently found to have a smaller mean centroid size than the other extant species ($p = <0.0001$) and therefore hypothesis 9 was accepted for the medial cuneiform. The size relationships of the extant species for the medial cuneiform could be summarised as *Homo/Gorilla* > *Pongo/Pan* > *Theropithecus*.

Oreopithecus was found to be significantly smaller than all extant ape species with p values of <0.001 in each instance. However, *Oreopithecus* was not found to be significantly larger than *Theropithecus* at the $p = 0.00333$ threshold following Bonferroni correction for multiple comparisons ($p = 0.0238$). Therefore, hypothesis 10 is rejected for the medial cuneiform; *Oreopithecus* is not comparable in size to *Pan*, suggesting that the foot of *Oreopithecus* is much more gracile than would be expected for a habitually bipedal primate. The other fossils were compared to the extant species by calculating the z score of their centroid size from the species mean and converting this into a p value. OH8 (146.1) was found to be significantly smaller than *Gorilla* ($z = -2.509$; $p = 0.006$) and

Homo ($z = -5.54$; $p = <0.0001$). However, OH8 was not found to be significantly smaller than *Pan* ($z = -1.074$; $p = 0.141$) or *Pongo* ($z = -0.929$; $p = 0.176$), but was, predictably, found to be significantly larger than *Theropithecus* ($z = 5.186$; $p = <0.0001$). Therefore, hypothesis 11 was accepted for the medial cuneiform; OH8 is smaller than *Homo* reflecting its position as an early example of bipedalism in an ape with small stature. *Nacholapithecus* (142.3), like OH8, was found to be significantly smaller in size than *Gorilla* ($z = -2.693$; $p = 0.0035$) and *Homo* ($z = -5.866$; $p = <0.0001$). It was also found not to be significantly smaller than *Pan* ($z = -1.435$; $p = 0.076$) and *Pongo* ($z = -1.205$; $p = 0.114$). *Nacholapithecus* was also found to be significantly larger than *Theropithecus* ($z = 4.775$; $p = <0.0001$). Therefore, hypothesis 12 is disconfirmed for the medial cuneiform; *Nacholapithecus* is not intermediate in size between *Theropithecus* and *Pan/Pongo*, it instead falls on the lower end of the *Pan* range showing a marked increase in size of the medial cuneiform early in hominoid evolution.

3.3.3. Visualisation of shape differences

In order to describe the differences in shape it is necessary to use some technical terminology. Figures 3.3.10 and 3.3.11 illustrate what these terms are referring to.

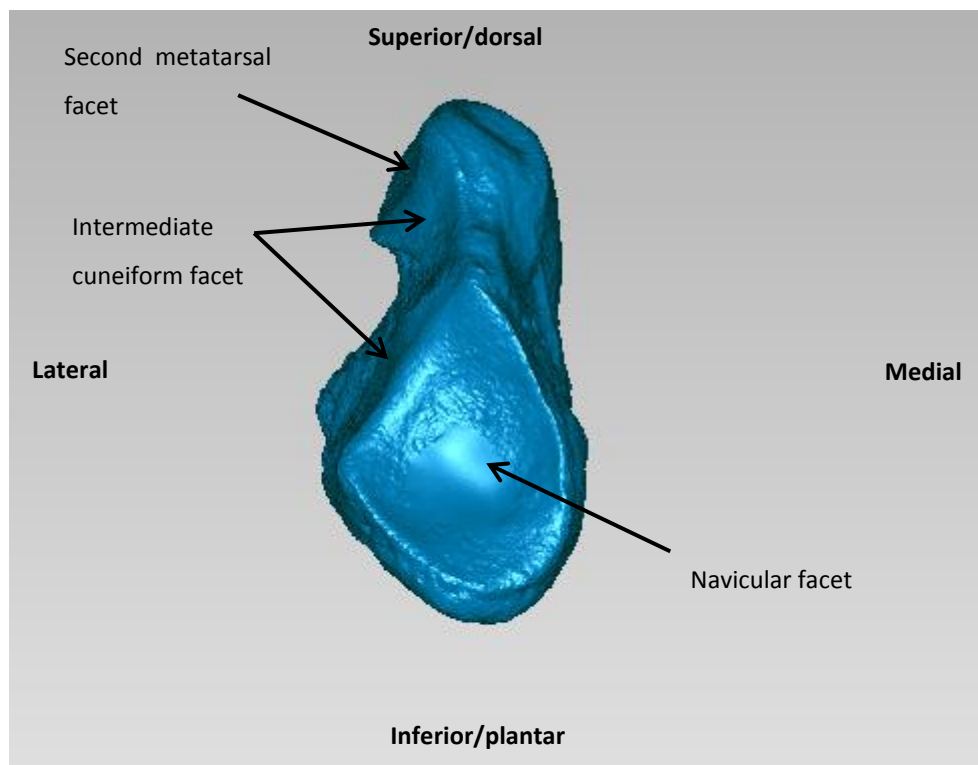


Figure 3.3.10. Proximal view of the medial cuneiform displaying terminology used to describe shape differences.

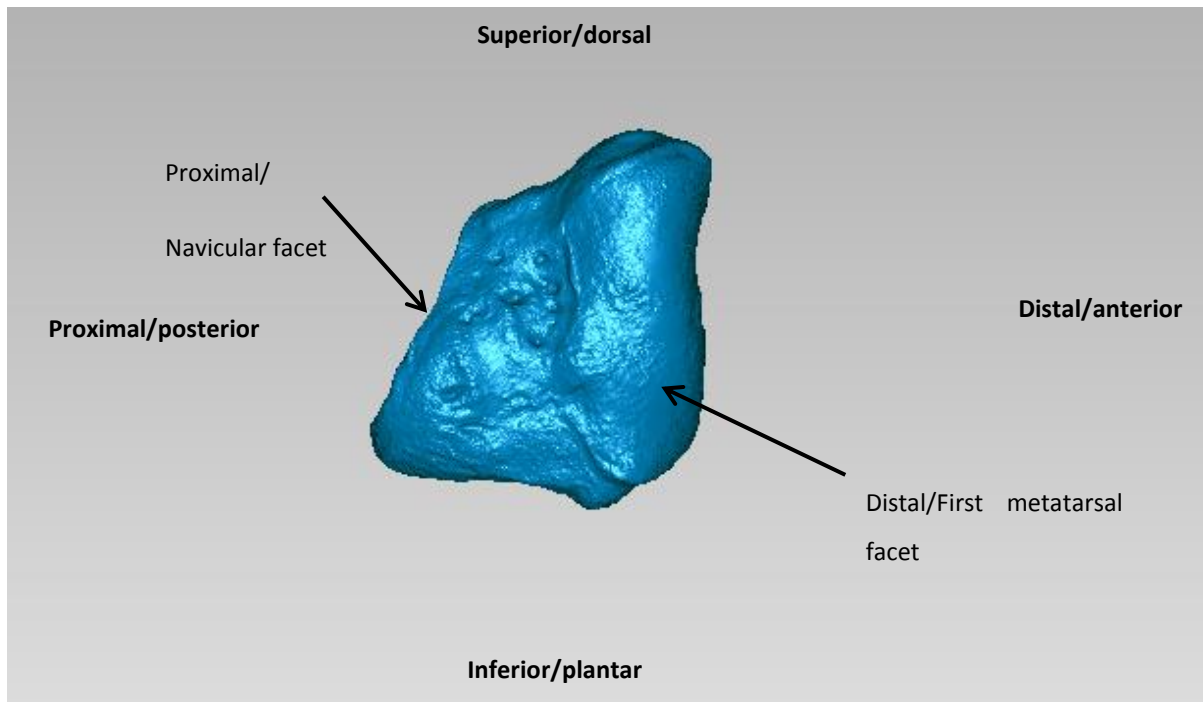


Figure 3.3.11. Medial view of the medial cuneiform displaying terminology used to describe shape differences.

From *Pan* to *Oreopithecus*

The differences between *Pan* and *Oreopithecus* are subtle, which is to be expected given the small Procrustes difference between their means. The navicular facet is comparable in size in both species (Figure 3.3.12 A) and there is very little noticeably different in terms of the shape of the facet between the two. The facet is more even-sided in *Oreopithecus* approximating more closely a rectangle. Thus, compared to *Pan* the superior corner of the facet does not extend as far superiorly and the medial corner is slightly more elevated, giving a rectangular appearance compared to the slightly more tear-drop shape of *Pan*, additionally, the orientation of the long axis of the facet is roughly the same in both species. The proximodistal breadth of the bone is roughly the same in both species, although the bone is slightly narrower mediolaterally in *Oreopithecus*. The length of the facet for the second metatarsal is greater in *Oreopithecus* indicating that the articulation with the intermediate cuneiform may be relatively less extensive in *Oreopithecus*. However, the relative increase in the size of the facet for the second metatarsal could also be explained by the relatively much larger superior half of the distal facet in *Oreopithecus*. The superior half of the distal facet extends further distally in *Oreopithecus* to a notable degree (Figure 3.3.12.B), it is also somewhat wider mediolaterally. The distal facet exhibits a similar degree of encroachment onto the medial side of the bone in *Oreopithecus* indicating that the degree of abduction of the hallux may have been comparable, the facet is also helical in nature indicating that internal rotation occurred with flexion.

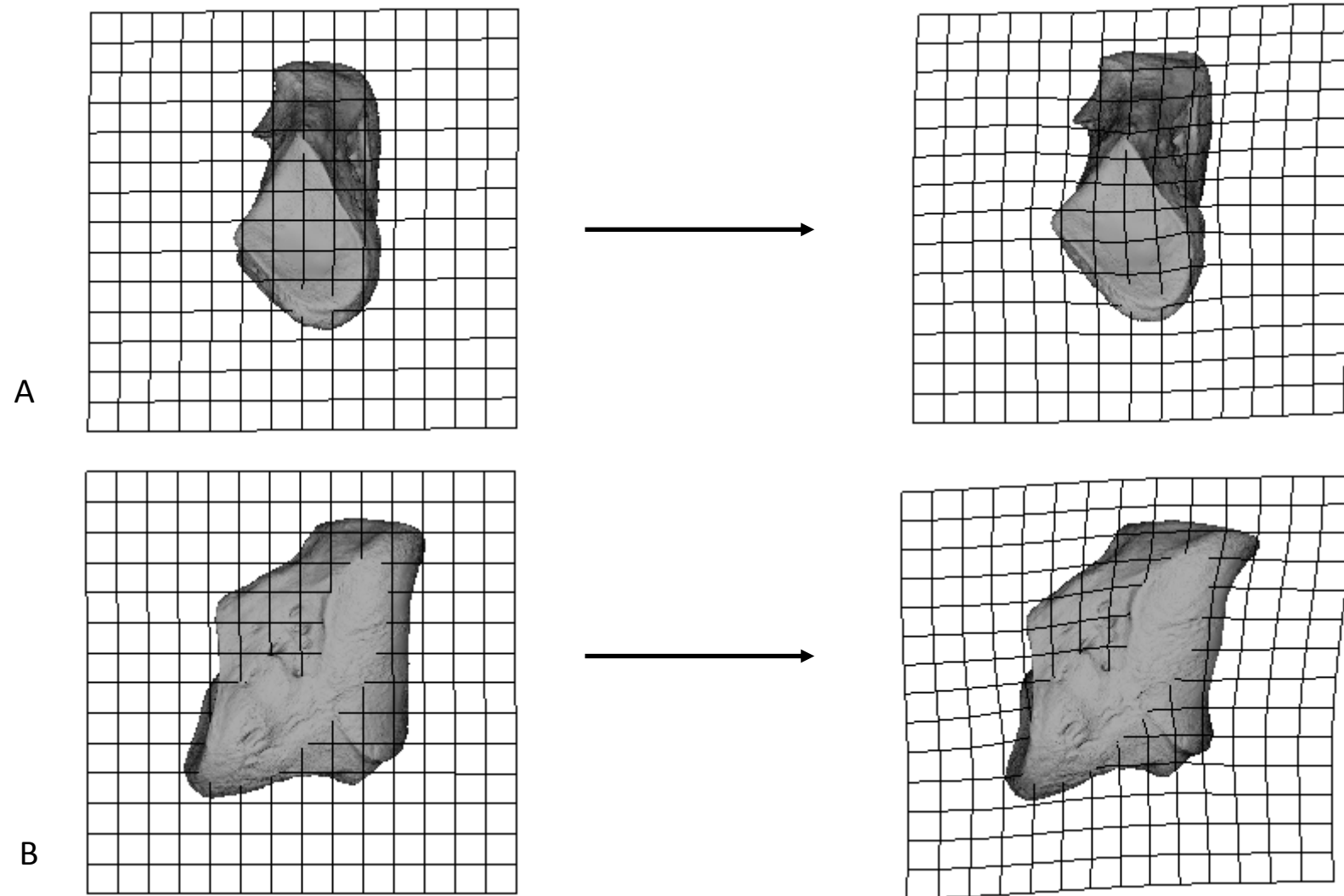


Figure 3.3.12. Demonstration of the warp from the *Pan* mean medial cuneiform (left) to *Oreopithecus* (right). A) Proximal view. B) Medial view

The shape differences between the medial cuneiform of *Gorilla* and *Oreopithecus* are slight, but clearly discernible. The most obvious distinctions lie in the overall dimensions of the bone. The mediolateral width of the medial cuneiform is clearly substantially lower in *Oreopithecus* (Figure 3.3.13.A) while the proximodistal length of the bone is noticeably greater (3.3.13.B). The navicular facet of *Oreopithecus* is more rectangular than that of *Gorilla*, a difference which mirrors that between *Oreopithecus* and *Pan*. The facet is relatively smaller in *Oreopithecus* relative to the overall size of the bone and this is mainly due to the less well-developed superior portion of the facet compared to *Gorilla*. *Gorilla* and *Oreopithecus* share a similar orientation of the navicular facet which therefore overall aligns *Oreopithecus* with the African ape condition in this regard. The facet for the second metatarsal also extends further from the distal surface of the bone in *Oreopithecus* compared to *Gorilla*, a result similar to the comparison with *Pan*. This fact could also be linked to the expansion of the superior half of the distal facet in *Oreopithecus*. The superior half of the facet extends further distally and is mediolaterally wider compared to *Gorilla*, although this difference is not as marked in *Pan*, which is likely linked to the greater overall size and robusticity of *Gorilla*. The distal facet appears to encroach onto the medial side of the bone to a greater extent in *Oreopithecus*, indicating that the degree of abduction of the hallux in *Oreopithecus* is likely slightly greater than that found in *Gorilla*. The curvature of the first metatarsal facet has a similar form in *Oreopithecus* and *Gorilla*. The facet is helical in shape in both species.

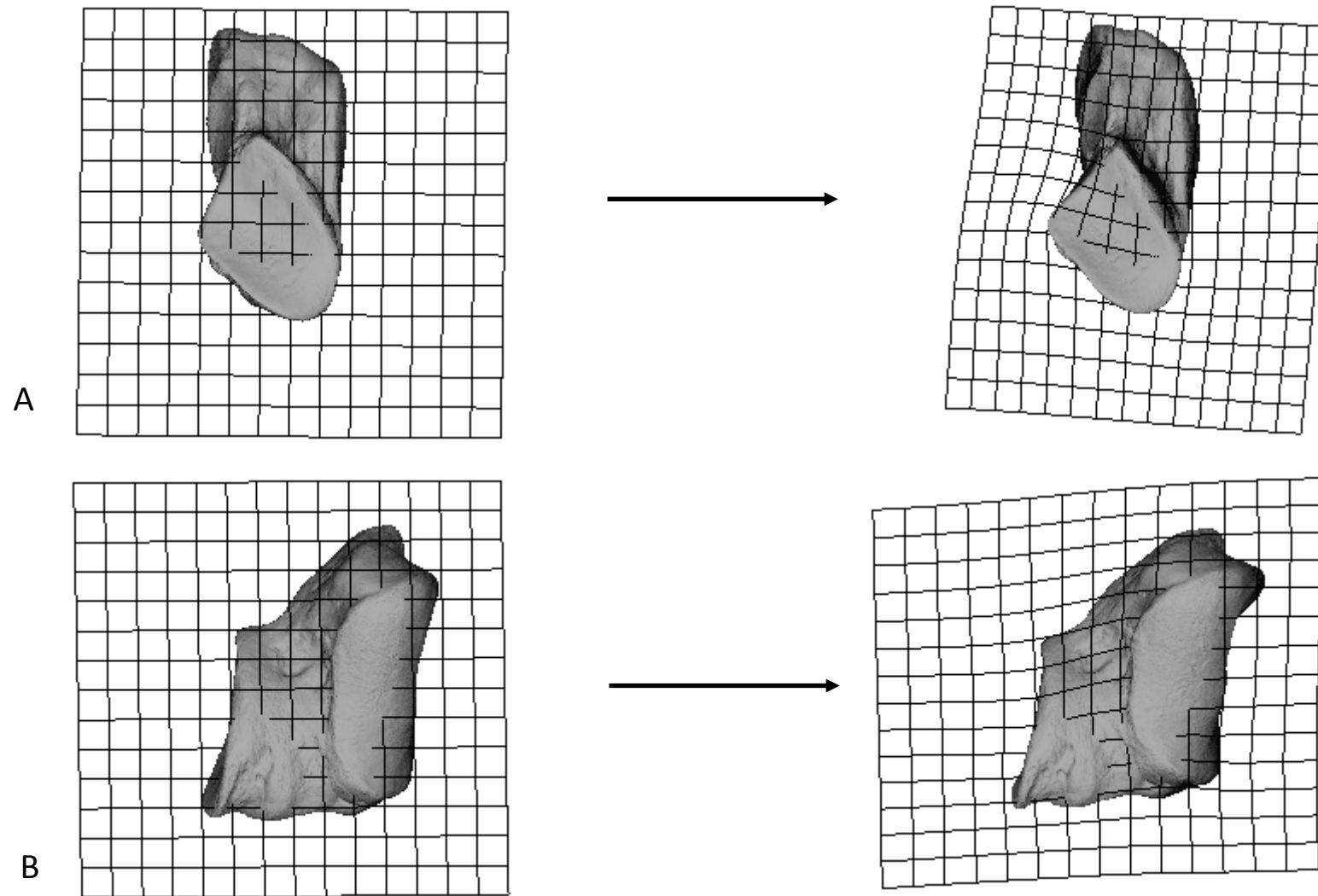


Figure 3.3.13. Demonstration of the warp from the *Gorilla* mean medial cuneiform (left) to *Oreopithecus* (right). A) Proximal view. B) Medial view

The Procrustes distance between *Pongo* and *Oreopithecus* is substantially greater than that between *Oreopithecus* and either of the African apes. This fact is reflected in the greater dissimilarity between *Pongo* and *Oreopithecus*. The long axis of the navicular facet of *Oreopithecus* lies close to a dorsoplantar orientation, more parallel to the first metatarsal facet. In contrast, the long axis of the *Pongo* navicular facet lies closer to a mediolateral orientation (Fig. 3.3.14A). In this respect *Oreopithecus* is similar to the African apes. The first metatarsal facet exhibits extreme encroachment onto the medial side of the bone in *Pongo* (Fig. 3.3.14B). The facet also encroaches onto the medial side of the bone in *Oreopithecus* but to a much lesser degree, making *Oreopithecus* clearly more like the African apes. The alignment of the long axis of the navicular facet mediolaterally and the severe encroachment of the distal facet onto the medial side of the bone result in the medial cuneiform of *Oreopithecus* being considerably narrower mediolaterally. However, this relative narrowness is for reasons entirely different than the narrowness of *Oreopithecus* relative to *Gorilla*. *Gorilla* is generally more robust than *Oreopithecus*, being both mediolaterally wider and proximodistally shorter. However, *Pongo* has a proximodistally longer medial cuneiform (Fig. 3.3.14B). Therefore, the apparent narrowness of the medial cuneiform of *Oreopithecus* to that of *Pongo* is not a consequence of difference in robusticity. The surface area of the distal facet is considerably larger in *Oreopithecus*, particularly with respect to the superior portion of the facet.

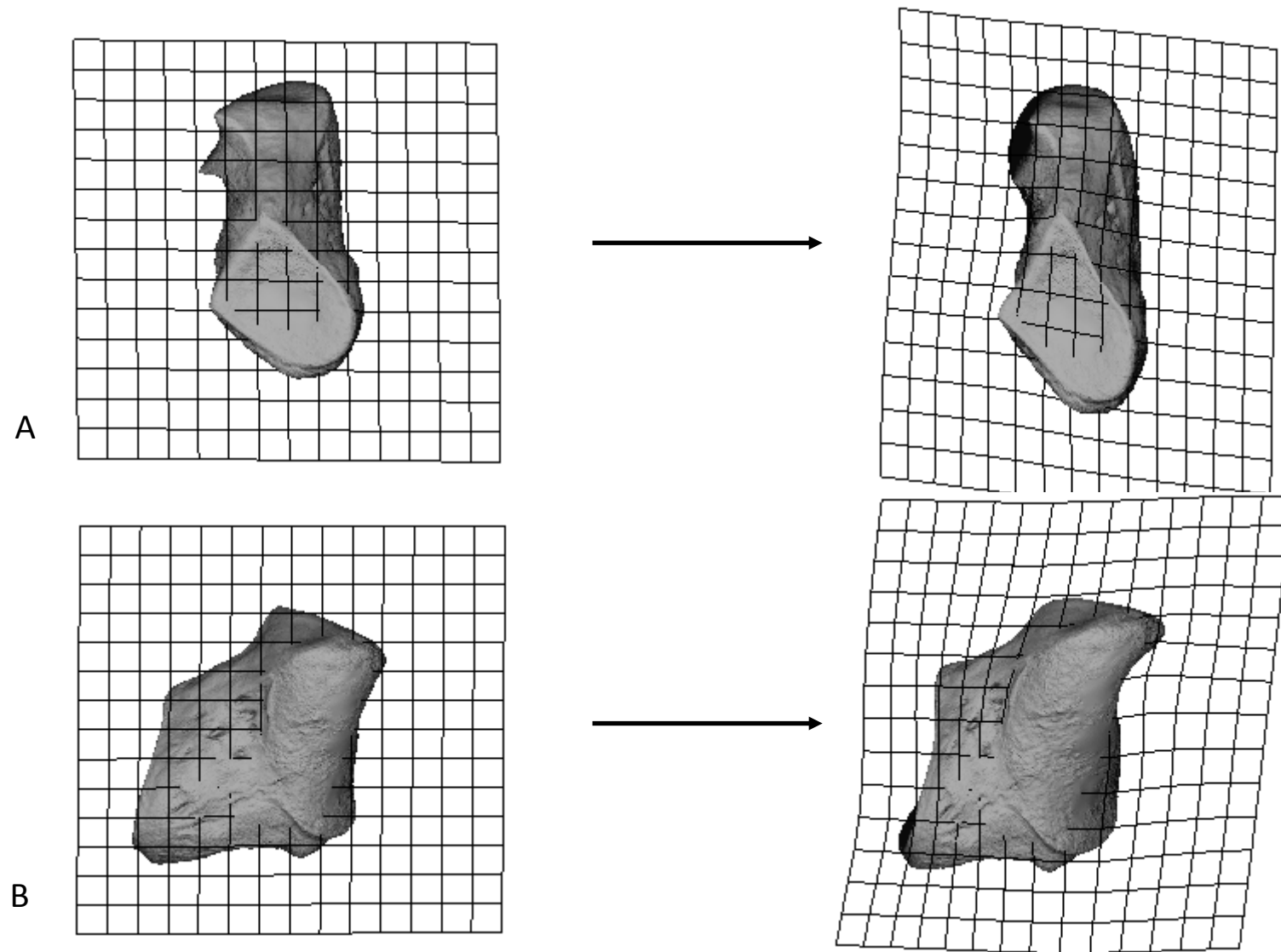


Figure 3.3.14. Demonstration of the warp from the *Pongo* mean medial cuneiform (left) to *Oreopithecus* (right). A) Proximal view. B) Medial view

From *Theropithecus* to *Nacholapithecus*

The dimensions of the medial cuneiform distinguish *Nacholapithecus* from *Theropithecus*. It is clear that the bone is mediolaterally wider (Figure 3.3.15A) and proximodistally shorter (Figure 3.3.15B) in *Nacholapithecus* than its counterpart. This shows that the bone is stouter in *Nacholapithecus*, a finding that suggests *Nacholapithecus* was more like the hominoids in terms of robusticity of the medial cuneiform. The navicular facet is noticeably larger across both its mediolateral and superoinferior dimensions in *Nacholapithecus*. This is caused by considerable expansion of the entire medial border of the facet and the superior corner of the facet. The lateral border of the facet is not as well-developed in *Nacholapithecus* but this does not detract from the overall increase in size of the facet from *Theropithecus* to *Nacholapithecus*. The navicular facet also exhibits less of a distally directed sloping from inferior to superior when viewed either medially or laterally. This feature also aligns *Nacholapithecus* in the direction of the African apes and distinguishes it from the distally sloping facet found in *Theropithecus*. The facet for the first metatarsal is more well-developed in *Nacholapithecus*, particularly the inferior half and the projection of the superior half away from the proximal side of the bone. The surface of the distal facet is more cylindrical in *Nacholapithecus*, resembling African apes in this regard. The first metatarsal facet also lacks the strong constriction at its midpoint found in *Theropithecus* and encroaches further onto the medial side of the bone.

From *Pan* to *Nacholapithecus*

Nacholapithecus is markedly distinct from *Pan* in a number of ways. The bone is mediolaterally quite narrow (Figure 3.3.16.A) whilst being proximodistally broad (Figure 3.3.16.B) giving a gracile appearance which resembles *Theropithecus* in comparison to *Pan*. Similarly, the navicular facet is small relative to the size of the bone and is significantly smaller in superoinferior height relative to the first metatarsal facet when compared to *Pan*. The shape of the distal facet is similar in *Nacholapithecus* but there are two pronounced borders to the facet on both its superomedial and inferomedial corners. The facet surface is otherwise similarly cylindrically shaped in both species. However, the encroachment of the facet onto the medial side of the bone is considerably less extensive in *Nacholapithecus*.

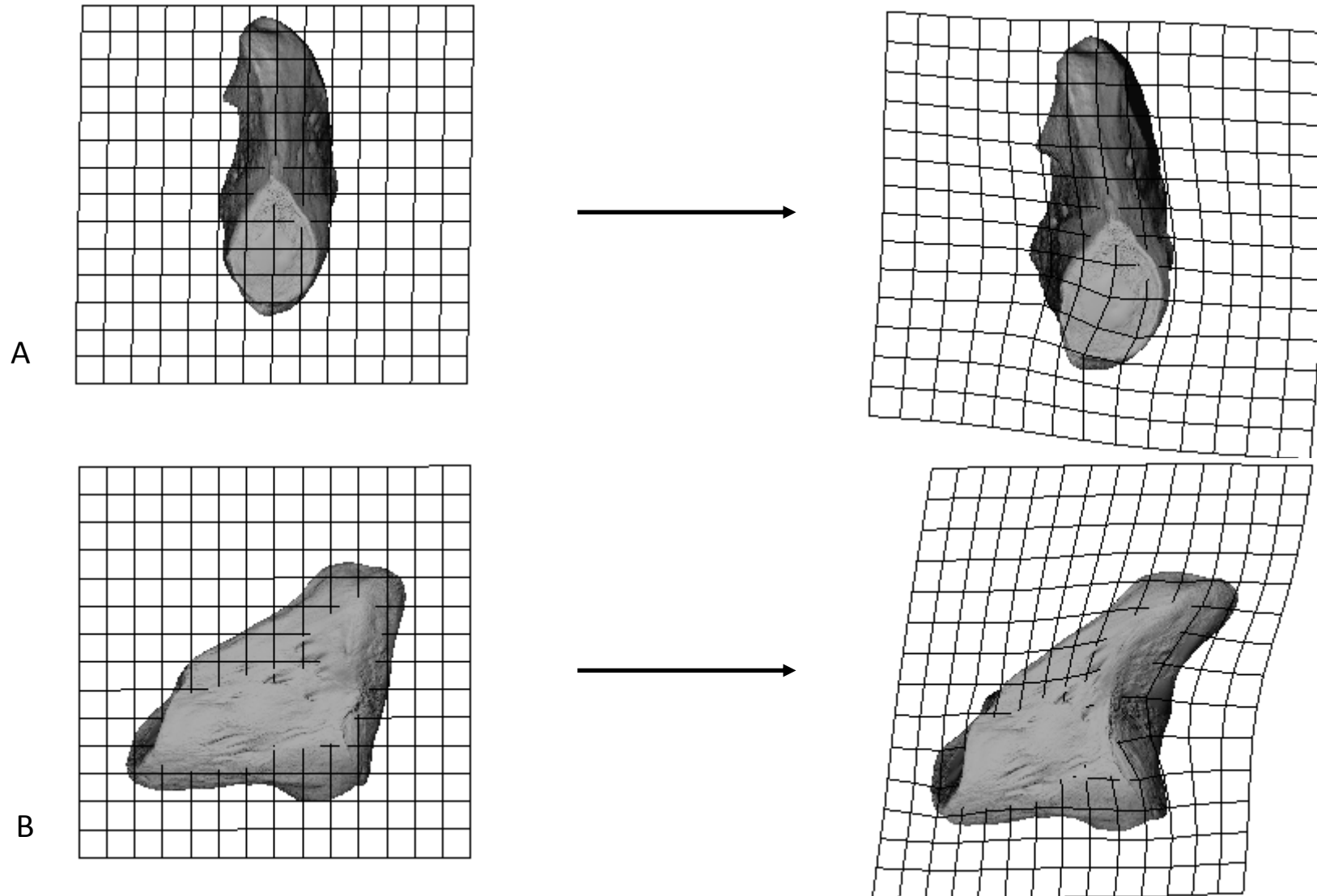


Figure 3.3.15. Demonstration of the warp from the *Theropithecus* mean (left) to *Nacholapithecus* (right). A) Proximal view. B) Medial view

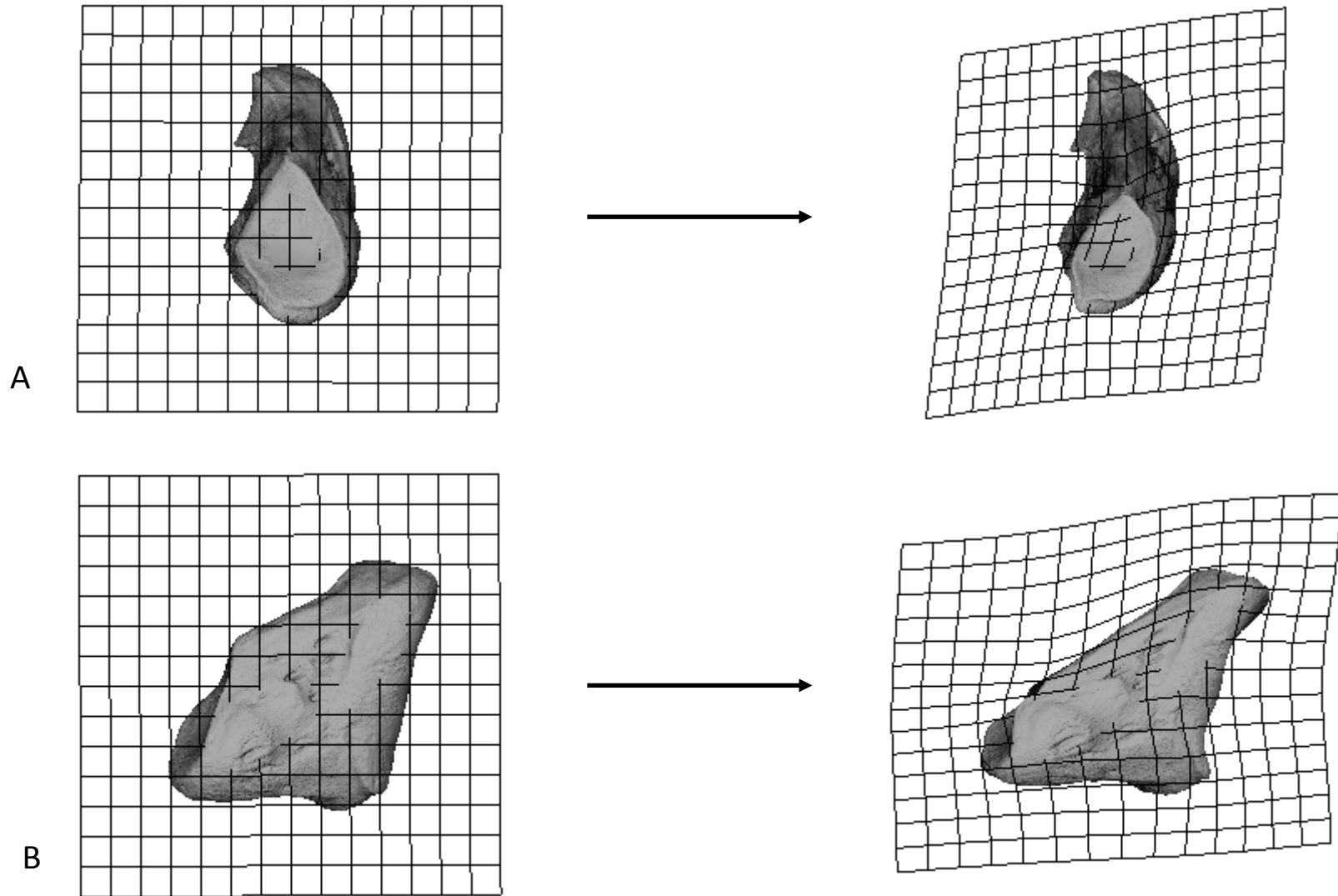


Figure 3.3.16. Demonstration of the warp from the *Pan* mean (left) to *Nacholapithecus* (right). A) Proximal view. B) Medial view

The medial cuneiform of OH8 has general dimensions that are comparable to those of *Homo*. The bone is fairly broad mediolaterally and relatively short proximodistally lending the bone a stout appearance. The navicular facet is roughly the same shape in both *Homo* and OH8, having a more triangular outline than a rectangular one like the apes. In *Homo* the inferior corner of the triangle is gently rounded whereas it comes to a pronounced point in OH8. For this reason the navicular facet is not as extensive in OH8, although it is similar in shape. The smaller size of this facet is also evident in the small superoinferior length of the facet relative to the overall superoinferior height of the bone (Figure 3.3.17.A). The navicular facet resembles *Homo* in having its superoinferior axis aligned parallel with the facet for the first metatarsal from medial view (Figure 3.3.17.B). The mediolateral axis of the facet is also more or less parallel with the mediolateral axis of the distal facet further resembling *Homo* in the orientation of the proximal and distal facets. The distal facet encroaches more onto the medial side of the bone in OH8 than in *Homo*, but not to the degree found in other taxa. The first metatarsal facet is also not as flat as it is in *Homo*, having a moderately curved surface which is visible from medial view. The facet also lacks the reniform appearance of the *Homo* distal facet, instead being roughly oblong in outline. It lacks the cylindrical appearance of the facet in African apes, however.

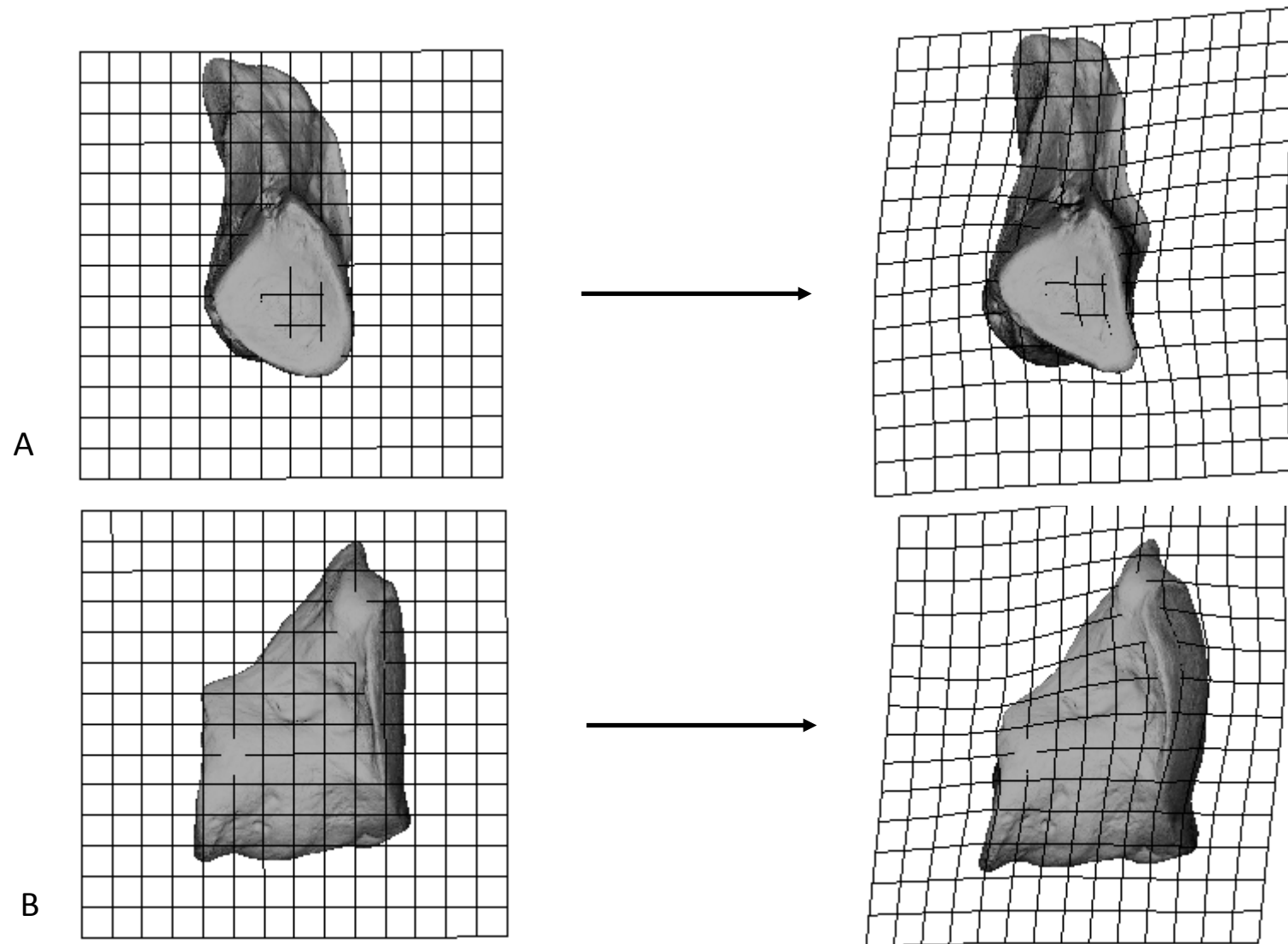


Figure 3.3.17. Demonstration of the warp from the *Homo* mean medial cuneiform (left) to OH8 (right). A) Proximal view. B) Medial view

3.4. Intermediate cuneiform

3.4.1. Principal components analysis

3.4.1.1. Full sample

A principal components analysis was conducted on the Procrustes aligned landmarks of all individual specimens for the intermediate cuneiform. The first three principal components account for 57.89% of the variance, the first five explain 69.96% of the variance, and the first fifteen explain 91.04% of the variance. The remaining 9% of the variance is explained by principal components 16-78 (Figure 3.4.1).

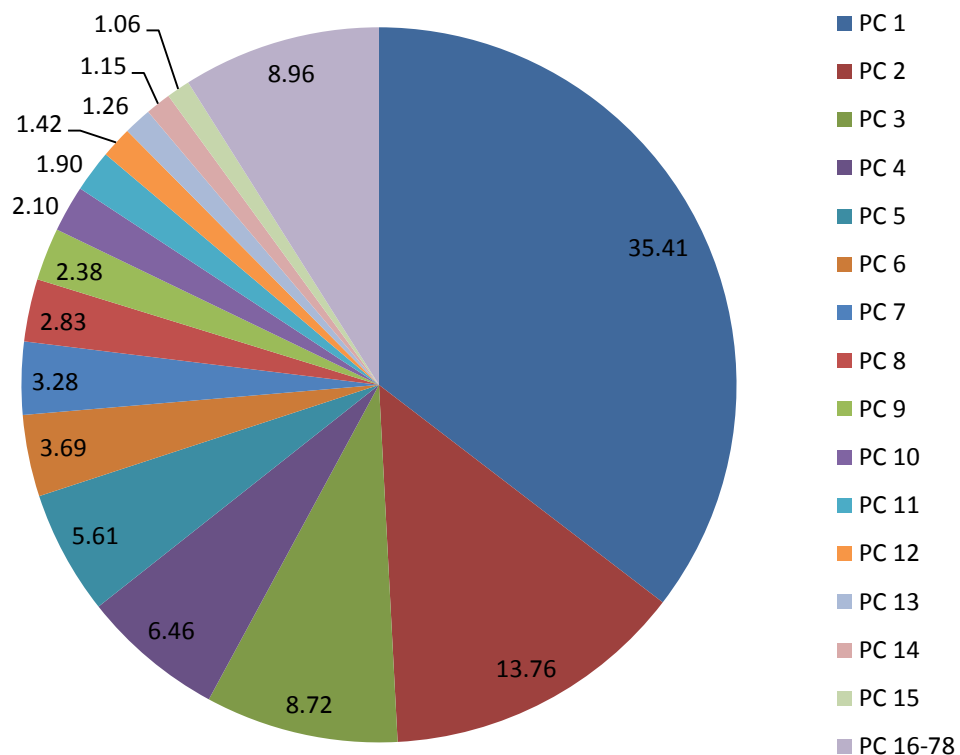


Figure 3.4.1. Percentage of the overall variance explained by each principal component for the medial cuneiform.

The first principal component groups *Homo* and *Theropithecus* together on the positive side of the axis (Figure 3.4.2). *Theropithecus* lies at the lower end of the *Homo* range, which is quite broad, and

also within the more positive end of the *Pongo* range. There is considerable overlap between *Homo* and *Pongo*, although only two *Pongo* specimens actually overlap with the *Homo* distribution, the majority of *Pongo* individuals lie beyond the lower extreme of the *Homo* range. *Pan* also has a large range on PC1 overlapping considerably with the distributions of *Pongo* and *Gorilla*. *Gorilla* has the most negative range on the first principal component. OH8 falls on the lower periphery of *Homo* on the first principal component, within the range of *Theropithecus*. *Oreopithecus* lies on the extreme negative end of the axis, just at the lower limit of the *Gorilla* range.

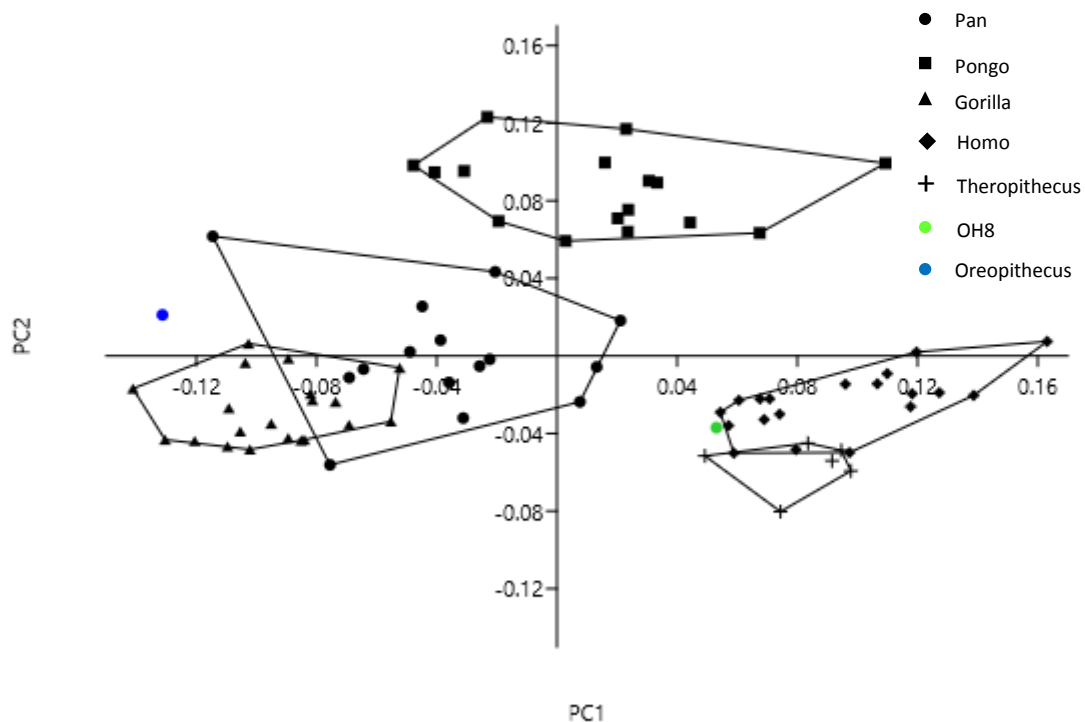


Figure 3.4.2. Principal component 1 vs. principal component 2 of all individuals for the intermediate cuneiform.

The second principal component clearly separates *Pongo* on the positive half of the axis and other species more on the negative half of the axis. There is some small excursion of the ranges of *Homo* and *Gorilla* into the positive half of the axis but this is minor. *Pan* has a large range across the axis with approximately half of the distribution on each half of the axis. *Theropithecus* has the most negative distribution of any species but does show limited overlap with *Homo* and *Pan*. OH8 is within the *Homo* range on the PC2 axis, but its location is also encompassed by the ranges of *Pan* and *Gorilla*. *Oreopithecus* is within the *Pan* range on PC2 but outside the ranges of all other species. Taken together PC1 and PC2 provide a rough grouping of the African apes away from other species,

although *Pan* is much more widely distributed on the graph. *Pongo* is a unique group on these two principal components. *Homo* and *Theropithecus* form a grouping but their overlap is minimal. OH8 lies just outside of the *Homo* distribution on the graph, but very close to it. *Oreopithecus* lies outside the distribution of any species but closest to the African apes.

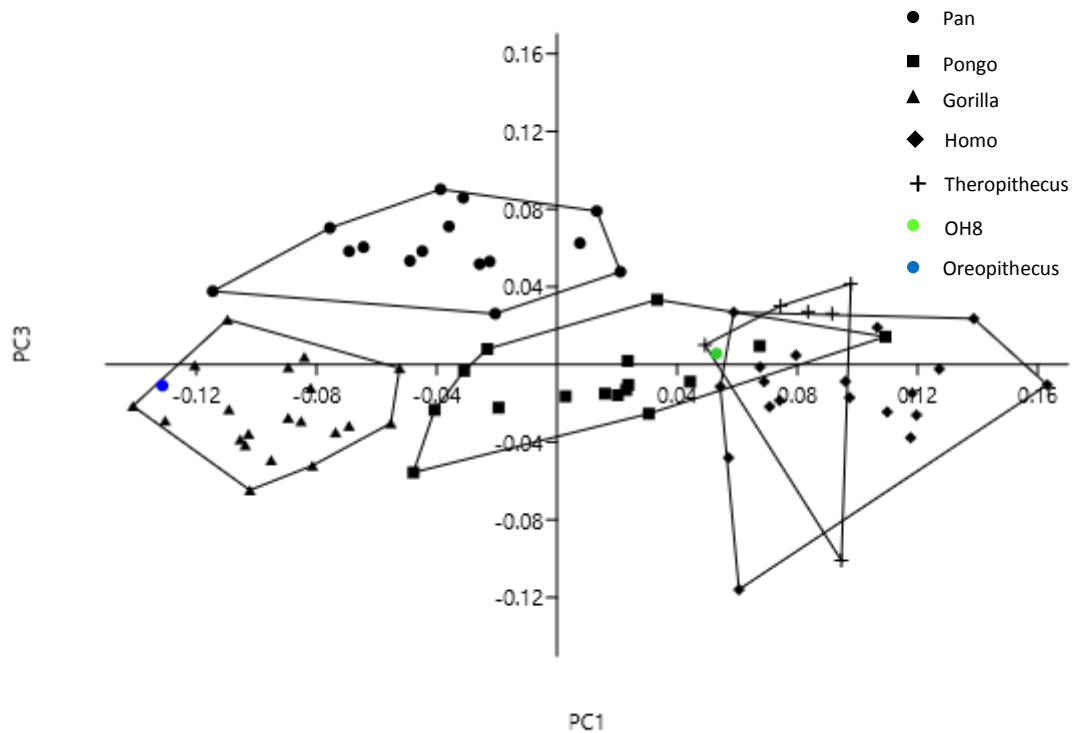


Figure 3.4.3. Principal component 1 vs. principal component 3 of all individuals for the intermediate cuneiform.

The third principal component (Fig. 3.4.3) separates *Pan* from other species, although there is a slight overlap with the lower aspect of its range and the other species. The axis is ineffective at distinguishing any other species from one another. *Pongo*, *Gorilla*, *Homo*, and *Theropithecus* are all broadly similar in terms of their distribution, although the *Homo* and *Theropithecus* ranges extend further into the negative half of the axis than *Pongo* or *Gorilla*. Both OH8 and *Oreopithecus* lie close to 0 on PC3, within the ranges of all species except *Pan*. PC4 (Fig. 3.4.4) separates *Theropithecus* from all other species on the positive half of the axis while all other species are indistinguishable; *Oreopithecus* has a high value also, close to the *Theropithecus* distribution. PC 5 distinguishes *Oreopithecus* on the positive half of the axis (Fig. 3.4.5), but there is some overlap with one *Theropithecus* individual. PC7 (Fig. 3.4.6) and PC9 (Fig. 3.4.7) offer little to discriminate between

species but *Oreopithecus* is noticeably distinct lying in the negative half of the axis. The other principal components do not appreciably discriminate between species or fossils.

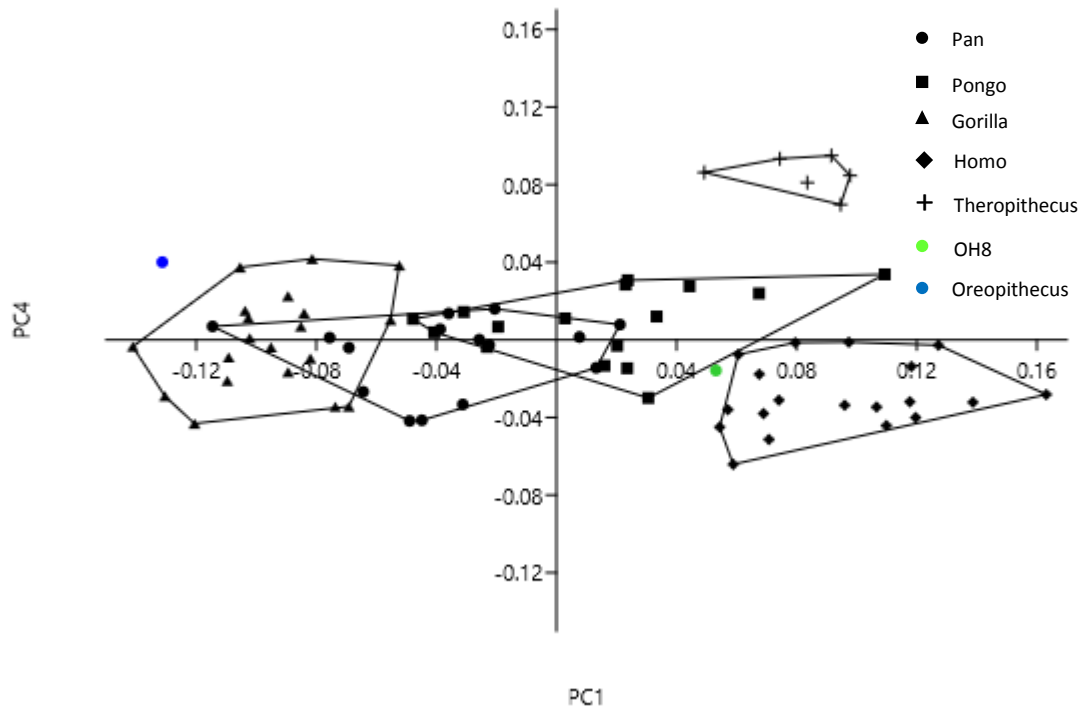


Figure 3.4.4. Principal component 1 vs. principal component 4 of all individuals for the intermediate cuneiform.

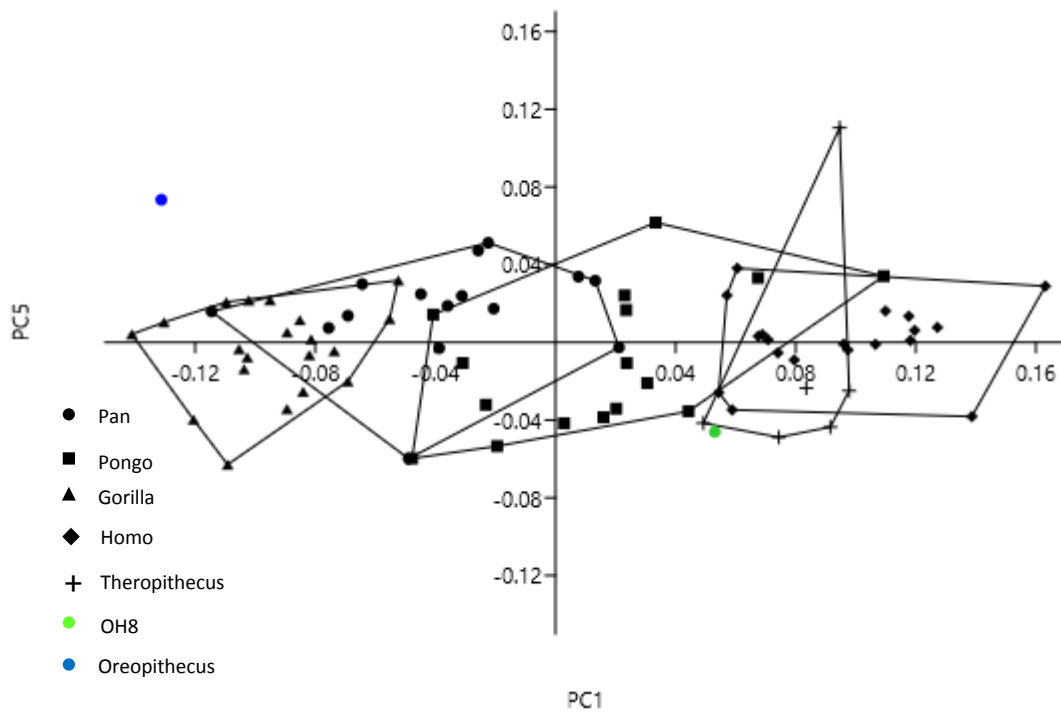


Figure 3.4.5. Principal component 1 vs. principal component 5 of all individuals for the intermediate cuneiform.

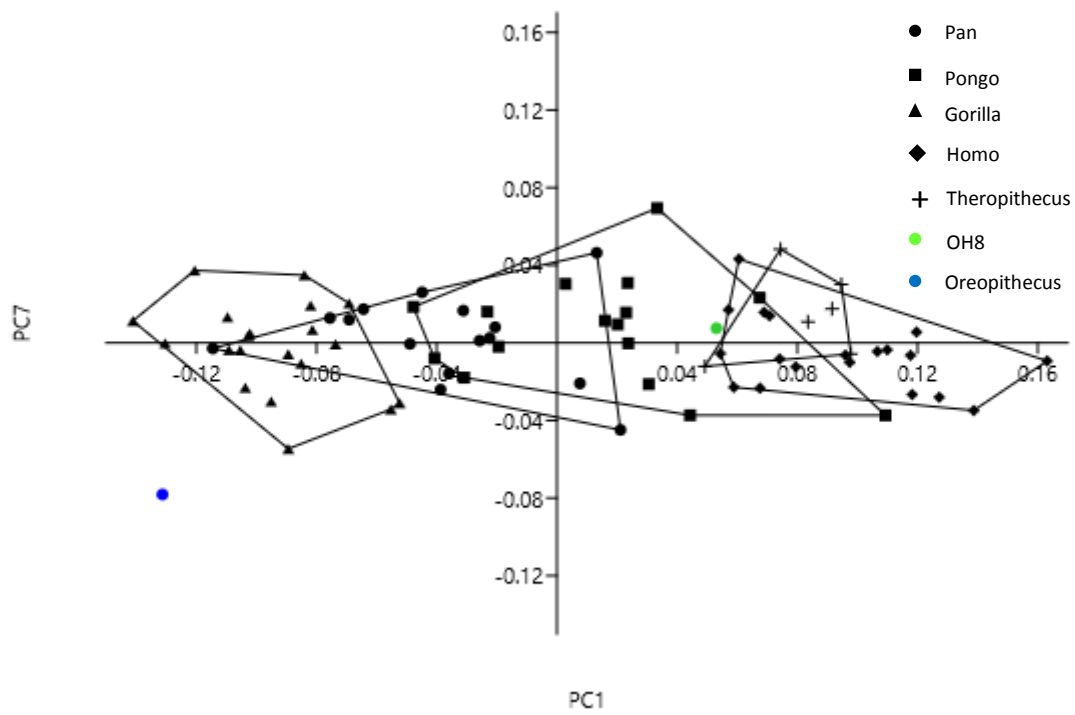


Figure 3.4.6. Principal component 1 vs. principal component 7 of all individuals for the intermediate cuneiform.

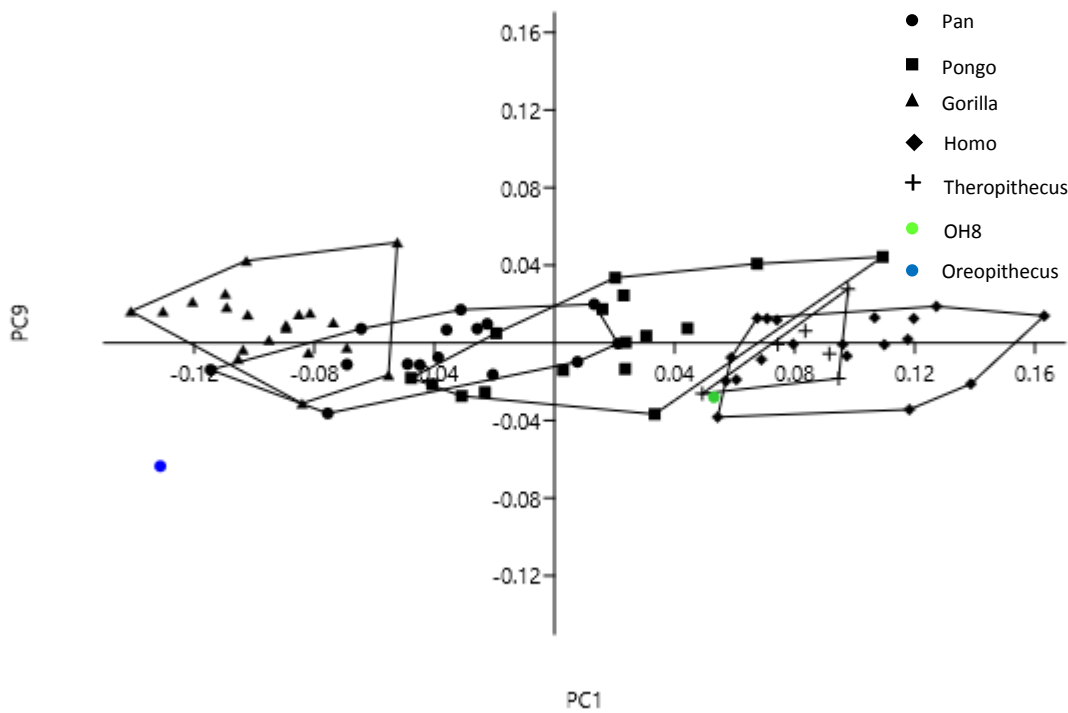


Figure 3.4.7. Principal component 1 vs. principal component 9 of all individuals for the intermediate cuneiform.

3.4.1.2. Extant species means vs. fossils

A principal components analysis was conducted on the Procrustes aligned landmarks for the intermediate cuneiform using the species means and fossils only. The analysis generated seven principal components. The first three explained 81.13% of the variance, the first five explained 95.76% of the variance, and the first six explained practically 100% of the variance while the variance explained by the seventh principal component was negligible ($1.5 \times 10^{-29}\%$). The information is presented in Figure 3.4.8.

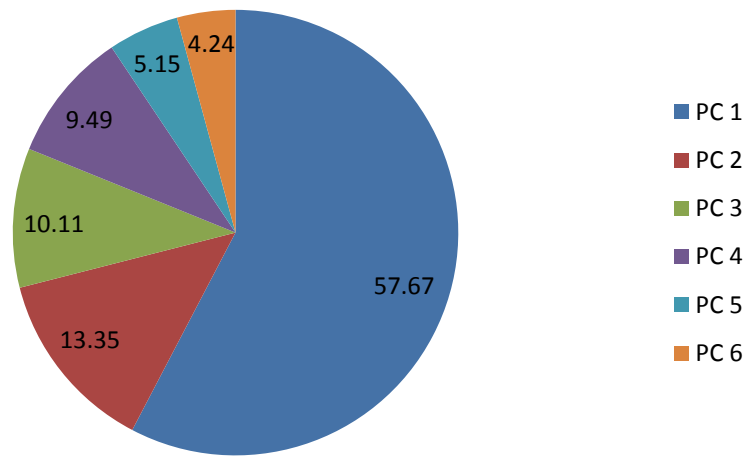


Figure 3.4.8. Percentage of the variance explained by each PC using only species mean shapes.

The distribution of the species means and fossils on the first principal component (Fig. 3.4.9) is broadly comparable to the distribution when the full sample is used (Fig. 3.4.2). *Homo* and *Theropithecus* are grouped together with the highest values on the positive range of the axis while *Gorilla* is situated with the highest negative value on the first principal component. Between these two extremes lie *Pan* and *Pongo*, the former on the negative range of the axis closer to *Gorilla* and the latter in the positive range of the axis closer to *Homo* and *Theropithecus*. However, *Pongo* is clearly closer to the African apes than it is to *Homo* and *Theropithecus*. The fossils are also distributed similarly in relation to the species means as they are to groups using the full sample. OH8 has a high positive value but not as high as *Homo* and *Theropithecus*. *Oreopithecus* has a high negative value giving it a considerably more negative placement than *Gorilla*. It differs from the full sample analysis in this respect; *Oreopithecus* is clearly distinct from *Gorilla*.

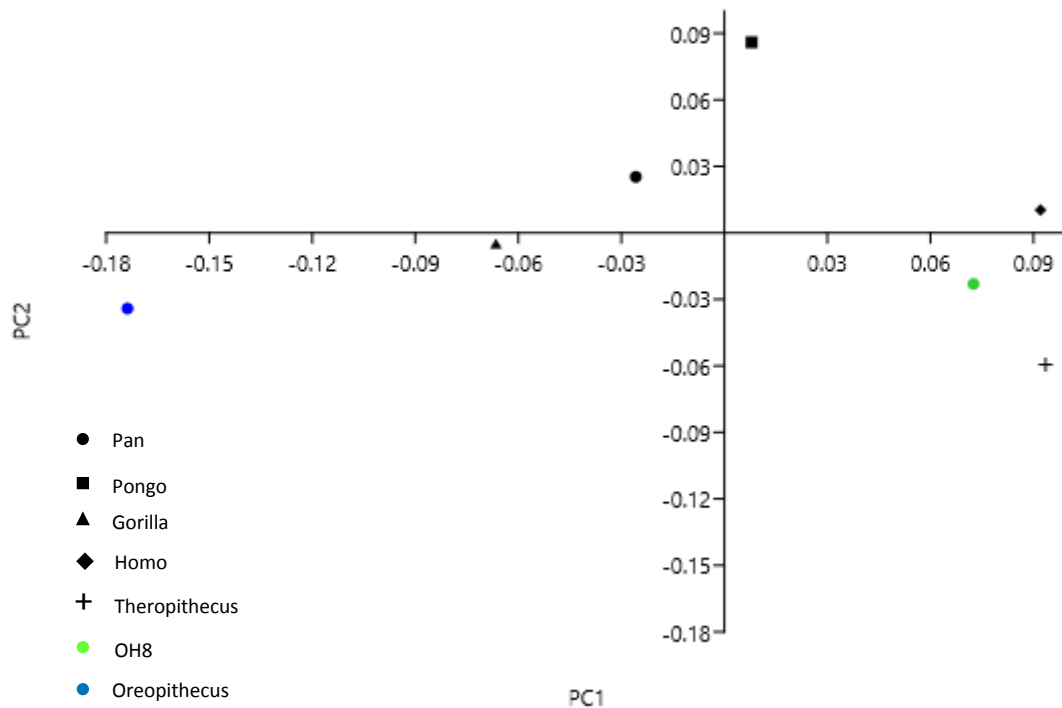


Figure 3.4.9. Principal component 1 vs. principal component 2 of species means and fossils for the intermediate cuneiform.

Principal component 2 provides a similar distribution to the axis extracted using the full dataset. The most clearly distinct species is *Pongo* with a high value on the positive end of the axis. This is followed by *Pan* with a more modest value on PC2. *Homo* and *Gorilla* each have values close to 0 on the axis. *Theropithecus* has a highly negative value on the axis distinguishing it from the other extant species. OH8 has a value intermediate between *Homo* and *Theropithecus*, close to *Gorilla*, which is also true of *Oreopithecus*. However, the positioning of *Oreopithecus* is in contrast to that for the full sample in which it is more closely associated with *Pan*. The two principal components combined provide a distribution of species which is similar to the one observed for the full sample. *Homo* and *Theropithecus* group together closely and OH8 is clearly grouped along with them. *Pan* and *Gorilla* are also quite closely linked while *Pongo* is the most distinct of any extant species. The most notable difference between the two analyses is the clear distinction of *Oreopithecus* from all other species means in contrast to its closer affinities to *Gorilla* in the analysis using the full sample. This is due to the fact that a single *Oreopithecus* specimen is compared to numerous individuals in the full sample analysis, weakening its signal.

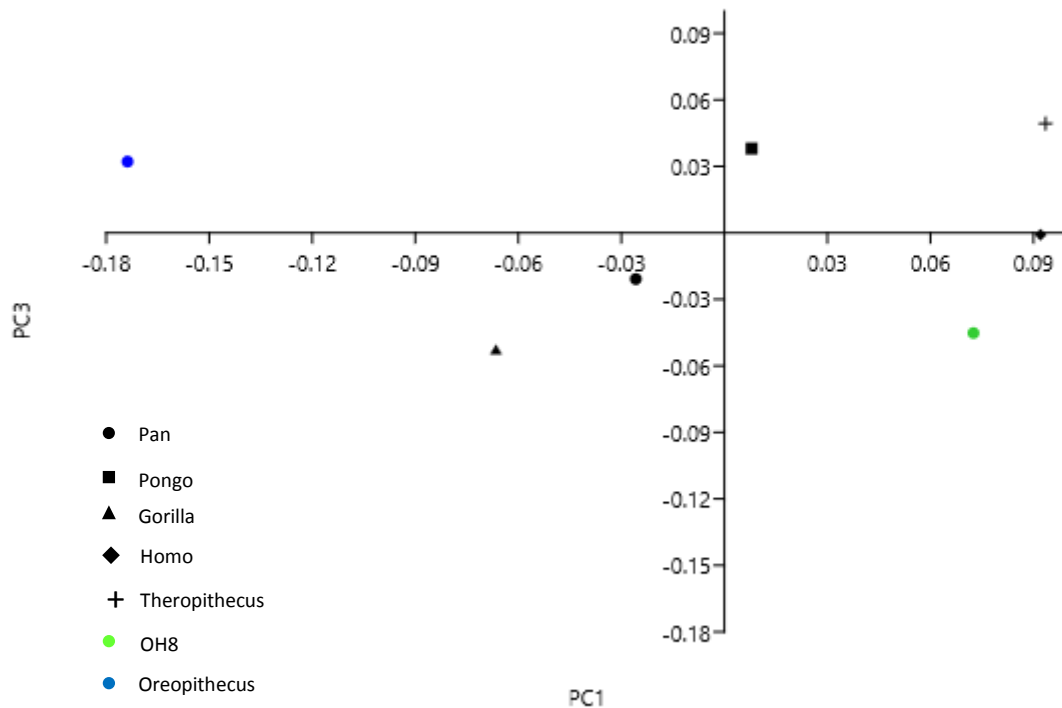


Figure 3.4.10. Principal component 1 vs. principal component 3 of species means and fossils for the intermediate cuneiform.

The third principal component departs considerably from the distribution found in the full sample (Fig. 3.4.10). In the full sample analysis the axis for the third principal component is poor at discriminating amongst the groups with the exception of *Pan*. When only the extant species means were used *Pan* is not clearly separated from other species on the axis. In contrast, *Gorilla* has the most negative value while *Pongo* and *Theropithecus* have the most positive values. OH8 has a value similar to *Gorilla* on this axis and *Oreopithecus* has a value similar to *Pongo* and *Theropithecus*. The fourth principal component separates the fossil species in the negative range of the axis from the African apes and *Theropithecus* in the positive range of the axis, but the separation is weak. The higher principal components are poor at discriminating between species, although PC5 separates the African apes from one another weakly, while the sixth principal component separates *Homo* from the other species but the effect is not large.

3.4.2. Statistical tests

In order to understand the relationships in shape between species the full Procrustes distances were calculated between all species means and fossils. The distances are tabulated below (Table 3.4.1) and discussed. With respect to the African apes the results for the intermediate cuneiform are consistent with those for the talus, navicular, and medial cuneiform. *Pan* and *Gorilla* are each other's closest neighbours confirming hypothesis 1 for the intermediate cuneiform; the African apes share similar ecology and evolutionary history and exhibit similar locomotory behaviour, and this results in the strongest morphological similarity among extant species. Both species are then next closest to *Pongo*, however, the Procrustes distance between *Pan* and *Pongo* is considerably lower than that between *Gorilla* and *Pongo*, and *Pongo* is closer in shape to *Homo* than it is to *Gorilla*. Therefore, hypothesis 2 is rejected for the intermediate cuneiform; the African apes do not represent a group that is similarly adapted to an arboreal habitat. There are clearly pronounced differences in morphology of the intermediate cuneiform among the apes indicative of their considerably different locomotor habits. The Procrustes distances among the extant species are difficult to interpret and do not offer any clear pattern. As noted above, *Pongo* is closer in shape to *Homo* than to *Gorilla*, a result which has no immediately obvious explanation. Similarly, *Theropithecus* has a lower Procrustes distance from *Homo* than any of the other apes and this distance is closer to *Homo* than *Pongo* is to any other extant species. This also has no immediately obvious explanation, however, it disconfirms hypothesis 3 for the intermediate cuneiform; *Theropithecus* does not represent an out-group among the extant species in morphology and locomotion. There appear to be some similarities between the digitigrade cercopithecoid foot and that of the obligate biped *Homo*.

	Pan	Pongo	Gorilla	Homo	Thero	OH8	Oreo
Pan	0	0.127664	0.112932	0.156059	0.173601	0.156973	0.191085
Pongo	0.127664	0	0.159165	0.142259	0.176232	0.160423	0.222978
Gorilla	0.112932	0.159165	0	0.190705	0.201193	0.178202	0.166271
Homo	0.156059	0.142259	0.190705	0	0.125258	0.105922	0.275978
Thero	0.173601	0.176232	0.201193	0.125258	0	0.140555	0.280329
OH8	0.156973	0.160423	0.178202	0.105922	0.140555	0	0.261884
Oreo	0.191085	0.222978	0.166271	0.275978	0.280329	0.261884	0

Table 3.4.1. Procrustes distances amongst species mean shapes and fossils for the intermediate cuneiform. The smallest and second smallest distances are shown on each row. The bold red shows the closest relationship and bold black the second closest.

Of the extant species, *Oreopithecus* was closest to *Gorilla* and then to *Pan*, although the distance between *Oreopithecus* and *Pan* was substantially greater than that between *Oreopithecus* and *Gorilla*. *Oreopithecus* was furthest from *Theropithecus* of the extant species. These facts confirm hypothesis 4; *Oreopithecus* is not cercopithecoid-like and therefore the proposition that *Oreopithecus* represents a Miocene cercopithecoid has rightfully been abandoned. The Procrustes distances also provide support for hypothesis 5. *Oreopithecus* is most similar to one of the African apes and therefore there is good reason to believe that it had a foot which functions similarly. However, the Procrustes distance between *Oreopithecus* and *Gorilla* is quite high compared to other instances in which *Oreopithecus* was closest to one of the African apes. Therefore, although the intermediate cuneiform is closest to *Gorilla* by some way, there are still likely to be marked differences between the two which could have significant implications for the foot of *Oreopithecus*, these will be explored in the comparison of shape between the two. *Homo* and OH8 are closest to each other and are in fact more similar in shape than *Pan* and *Gorilla*. This confirms hypothesis 6; OH8 is most similar in intermediate cuneiform morphology to *Homo* indicating that the OH8 foot likely belonged to an obligate biped.

The differences described were tested for significance. The extant species were compared using permutation tests on the pairwise Procrustes distances between individual specimens. It was found that all extant species were significantly different from one another with a p value of <0.0001. The difference in shape of the fossils from their nearest neighbour were tested for significance by calculating the Mahalanobis distance of the fossil from the species mean. *Oreopithecus* was found to be significantly different in shape from *Gorilla* with a Mahalanobis distance of 59.273, which was 7.698 standard deviation units from the mean to give a p value of 0.0005. It was also significantly different in shape from *Pan* with a Mahalanobis distance of 62.893, 7.93 standard deviation units from the *Pan* mean and a p value of <0.0005. In contrast OH8 was not found to be significantly different from *Homo* with respect to intermediate cuneiform shape. It was found to have a Mahalanobis distance of 15.512, which is 3.938 standard deviation units from the mean with a p value of 0.1.

Using the centroid sizes of all individuals in the study the significance of differences in size between the fossils and extant species were calculated. Differences in size between extant species were calculated using permutation tests of the individual centroid sizes to compare species means. It was found that *Homo* (158.6) was significantly larger than *Gorilla* (143.3) with a p value of 0.0031 (below the 0.005 value following Bonferroni correction for multiple comparisons). However, *Gorilla* (and

Homo) was significantly larger than all other extant species with a p value of <0.0001. Therefore, hypothesis 8 is confirmed for the intermediate cuneiform; *Homo/Gorilla* are the largest of all extant species. *Pan* and *Pongo* were not found to be significantly different in size ($p = 0.127$) but *Pongo* (114.2) had a larger intermediate cuneiform than *Pan* (108) on average. *Theropithecus* was consistently found to be significantly smaller than all other extant species with a p value of <0.0001. Therefore, hypothesis 9 is confirmed for the intermediate cuneiform; *Theropithecus* is the smallest of the extant species.

Oreopithecus was found to have a significantly smaller intermediate cuneiform than all ape species, including *Homo*; the significance threshold was set to 0.01 following Bonferroni correction for multiple comparisons. *Oreopithecus* vs *Pan* ($z = -3.137$; $p = 0.0009$); *Oreopithecus* vs *Pongo* ($z = -3.248$; $p = 0.0006$); *Oreopithecus* vs *Gorilla* ($z = -3.821$; $p = 0.0001$); *Oreopithecus* vs *Homo* ($z = -7.014$; $p = <0.0000$). *Oreopithecus* was not found to be significantly greater in size than *Theropithecus* with respect to its intermediate cuneiform ($z = -0.359$; $p = 0.36$). This constitutes another result pointing to the fact that the pedal skeleton of *Oreopithecus* was significantly less robust than that of extant apes, and similar in size to that of extant cercopithecoids. Therefore, hypothesis 10 is rejected for the intermediate cuneiform; *Oreopithecus* is not comparable in size to *Pan* or any other ape. The OH8 intermediate cuneiform was not found to be significantly smaller than any non-human ape species; the p value was set to 0.01 following Bonferroni correction for multiple comparisons. OH8 vs *Pan* ($z = 0.372$; $p = 0.3549$); OH8 vs *Pongo* ($z = -0.207$; $p = 0.4182$); OH8 vs *Gorilla* ($z = -1.797$; $p = 0.0362$). OH8 was, however, found to be significantly smaller than *Homo* ($z = -3.99$; $z = <0.000$). Therefore, hypothesis 11 is supported by the findings here; OH8 is smaller than *Homo*. This is argued to reflect its small body size and position as one of the earliest obligate bipeds.

3.4.3. Visualisation of shape differences

In order to describe the differences in shape it is necessary to use some technical terminology. Figures 3.4.11 and 3.4.12 illustrate what these terms are referring to.

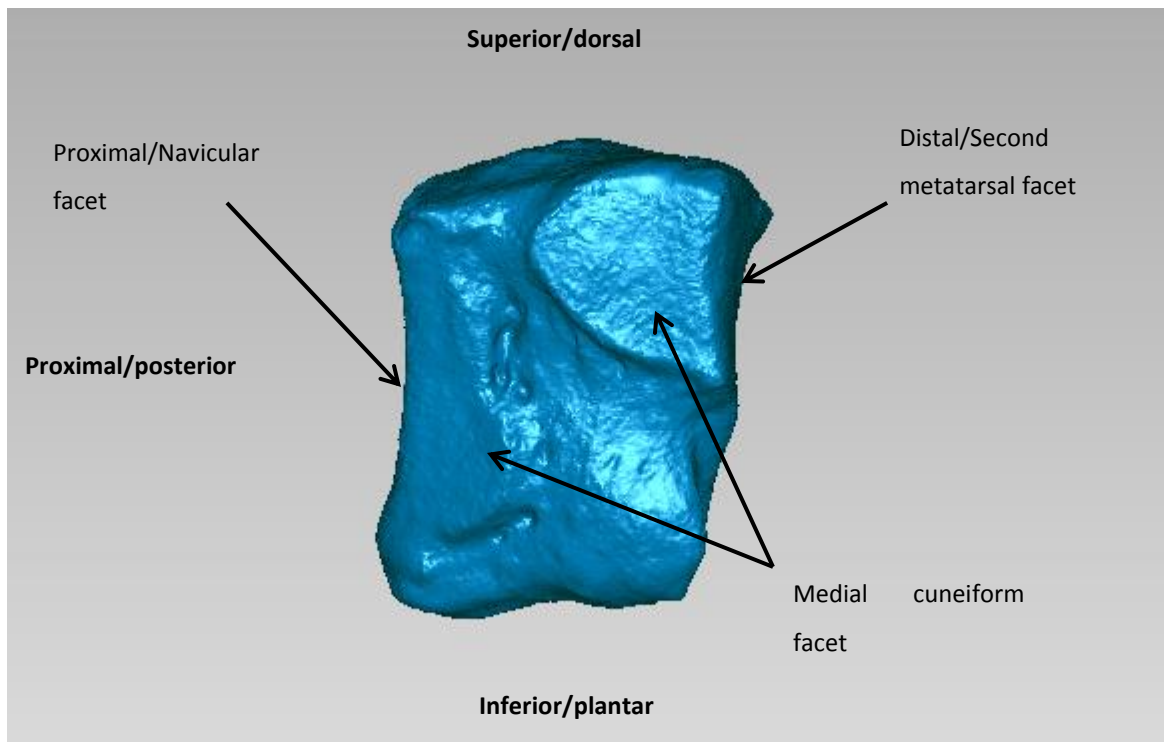


Figure 3.4.11 Medial view of the Intermediate cuneiform displaying terminology used to describe shape differences.

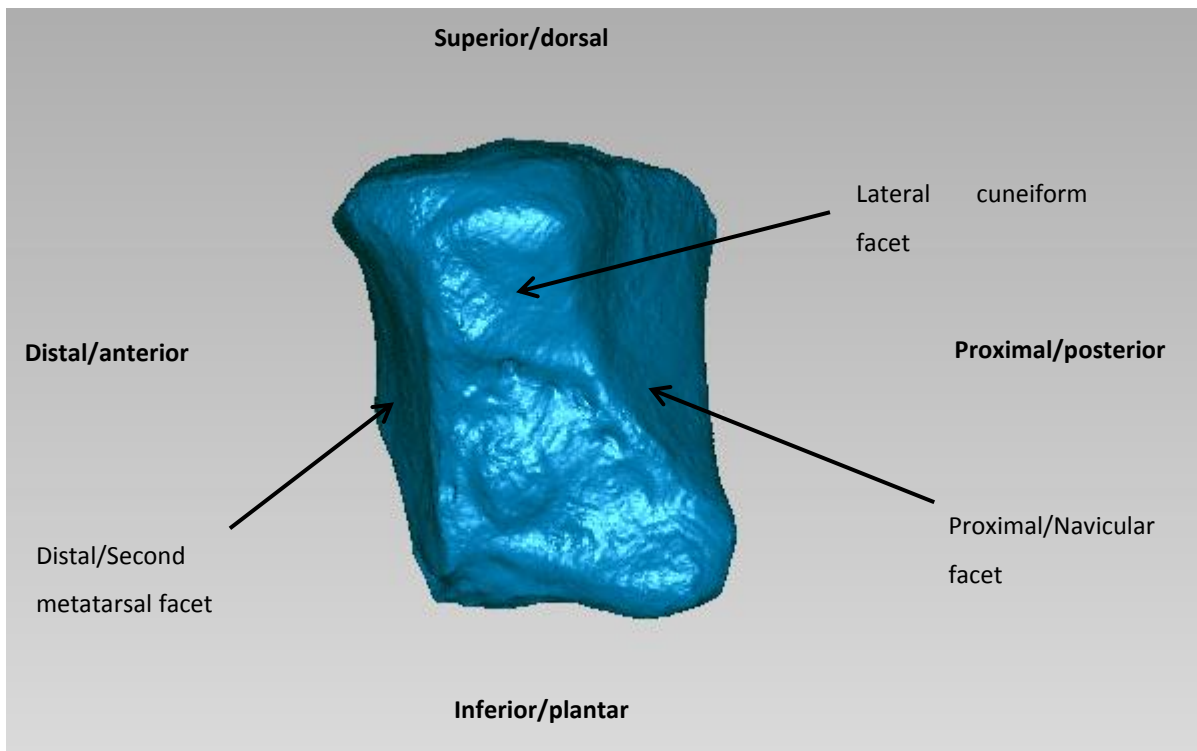


Figure 3.4.12. Lateral view of the Intermediate cuneiform displaying terminology used to describe shape differences.

From *Gorilla* to *Oreopithecus*

The *Oreopithecus* intermediate cuneiform is different in shape from that of *Gorilla* in a number of notable ways. The navicular facet is much smaller in size in *Oreopithecus*. It is reduced in breadth across both its mediolateral and superoinferior axes (Fig. 3.4.13A). However, the bone overall has a greater dorsoplantar dimension than *Gorilla*. The reduction in mediolateral breadth of the superior half of the navicular facet is especially pronounced in comparison to *Gorilla*. In both species the inferior portion of the facet tapers to a finer point than the superior portion, though this effect is stronger in *Gorilla*. The narrower inferior portion is angled laterally giving a bend to the lateral border of the facet in both species but this feature is exaggerated in *Oreopithecus*. The superomedial corner of the facet lacks the inferior sloping found in *Gorilla*, giving the superior borders of the proximal and distal facets a more parallel alignment in the transverse plane. The navicular facet is flatter when viewed medially or laterally in *Oreopithecus*. In *Gorilla* there is a distinct protrusion of the inferior border of the facet proximally, giving the facet a clearly concave surface from either medial or lateral view (Fig. 3.4.13B).

Oreopithecus shares with *Gorilla* a mediolaterally narrower superior border of the proximal articular surface compared to the distal surface when viewed superiorly (Figure 3.4.14A). However, this feature is much more strongly expressed in *Oreopithecus*. It is also clearly apparent from superior view that the lateral side of the bone has a shorter proximodistal breadth than the medial side in *Gorilla*. The consequence of this is that the proximal and distal articular surfaces are not parallel. This effect is much more pronounced in *Oreopithecus* than *Gorilla*. The lateral side of the bone in *Oreopithecus* is excessively shortened giving a considerably more trapezoidal outline to the bone in superior view than is the case in *Gorilla*. From this view it can also clearly be seen that the bone has a shorter proximodistal dimension in *Oreopithecus*. The distal facet is roughly similar in shape in both species, resembling a T shape. The superior half of the facet has a greater surface area in *Gorilla* while the inferior half of the facet is larger in *Oreopithecus*, however, these differences are not excessive. The superomedial corner of the distal facet slopes toward the posterior side of the bone in both *Gorilla* and *Oreopithecus* but this is clearly more strongly expressed in *Gorilla* (Fig. 3.4.14B).

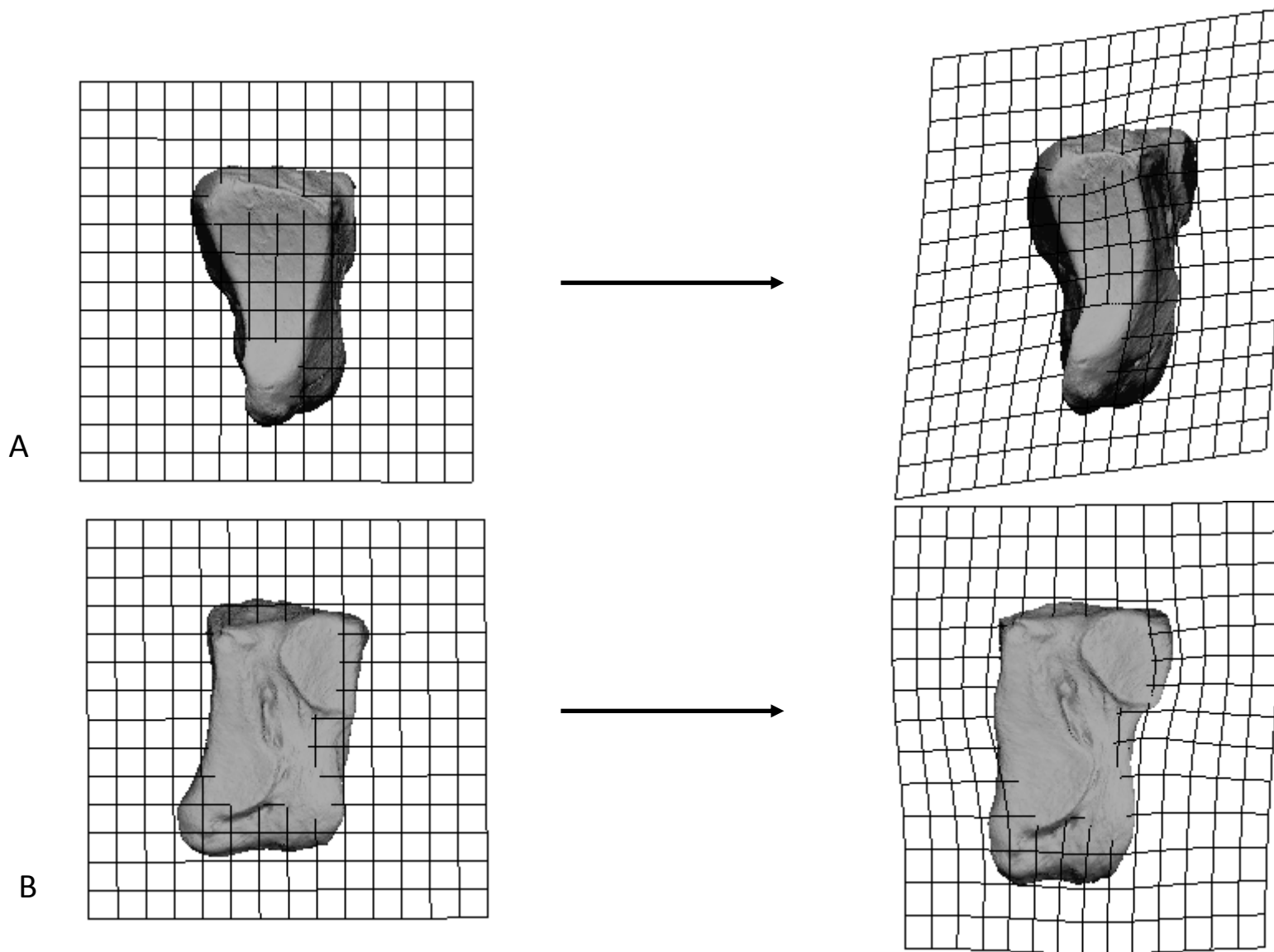


Figure 3.4.13. Demonstration of the warp from the *Gorilla* mean intermediate cuneiform (left) to *Oreopithecus* (right). A) Proximal view B) Medial view

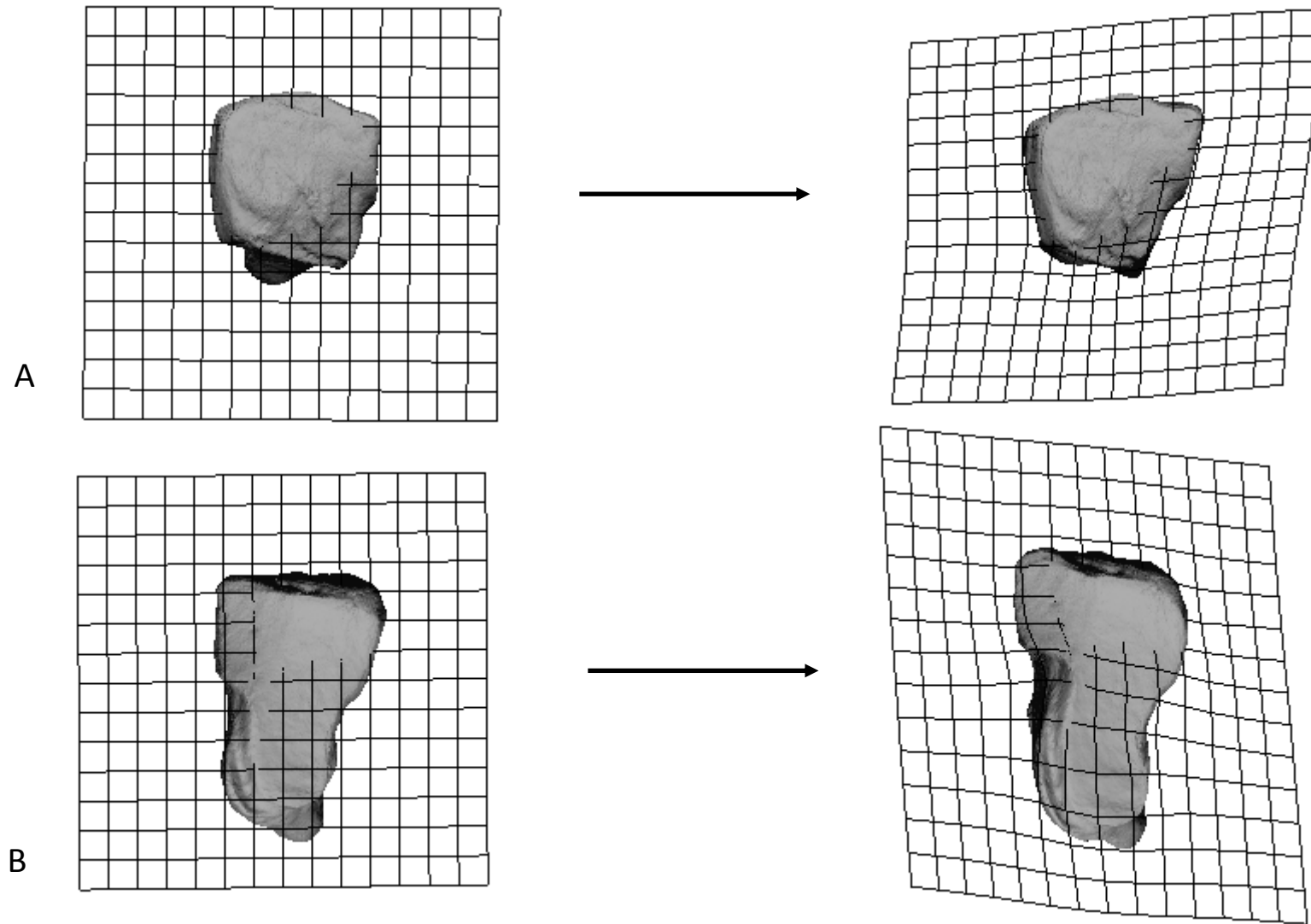


Figure 3.4.14. Demonstration of the warp from the *Gorilla* mean intermediate cuneiform (left) to *Oreopithecus* (right). A) Superior view B) Distal view

From *Pan* to *Oreopithecus*

Warping from the *Pan* mean shape to *Oreopithecus* revealed that the differences in shape between *Oreopithecus* and *Pan* are similar to those between *Oreopithecus* and *Gorilla*. The navicular facet is smaller across both its superoinferior and mediolateral axes in *Oreopithecus*, and has a particularly narrow superior border. But *Oreopithecus* has an intermediate cuneiform which is elongated across its superoinferior dimension (Fig. 3.4.15A) relative to *Pan*, which is relatively short in this dimension. The superomedial corner of the superior border of the navicular facet of *Oreopithecus* does not slope towards the inferior side of the bone, differing from *Pan* in this respect (Fig. 3.4.15A). The inferior border of the facet tapers to a narrow point in both *Pan* and *Oreopithecus*, and has a noticeable lateral inflection. From medial or lateral view it is clear that the inferior border navicular facet in *Pan* projects proximally beyond the superior border, giving the facet a concavity from medial or lateral view. However, this feature is not as strongly expressed in *Pan* and the facet is therefore flatter than it is in *Gorilla*. In contrast, the navicular facet of *Oreopithecus* is flat from medial or lateral view.

The medial and lateral sides of the bone are subequal in length from superior view in *Pan* (Fig. 3.4.15B), with the lateral side slightly shorter. Consequently, the proximal and distal facets are not parallel in the coronal plane. However, this feature is not as extreme as it is in *Gorilla*. The discrepancy in length of the medial and lateral sides of the bone is more marked in *Oreopithecus* than either African ape giving the bone a trapezoidal outline from superior view in comparison to the sub-rectangular shape found in the African apes. Additionally, the bone is clearly proximodistally shorter in *Oreopithecus* than *Pan*. The posterior sloping of the superomedial corner of the intermediate cuneiform is more pronounced in *Oreopithecus* than *Pan*, accounting for its greater similarity to *Gorilla*. The distal facet outline is comparable to *Pan* in a manner similar to its similarity with *Gorilla*, resembling a T shape. The superior half of the facet has a relatively smaller surface area than the inferior half in *Oreopithecus*. Thus, although *Oreopithecus* is closer in shape to *Gorilla*, the differences between it and each African ape are comparable. The key features linking it to *Gorilla* are the pronounced proximodistal shortening of the bone, clear trapezoidal outline from superior view, and more pronounced posterior sloping of the superomedial corner of the distal facet.

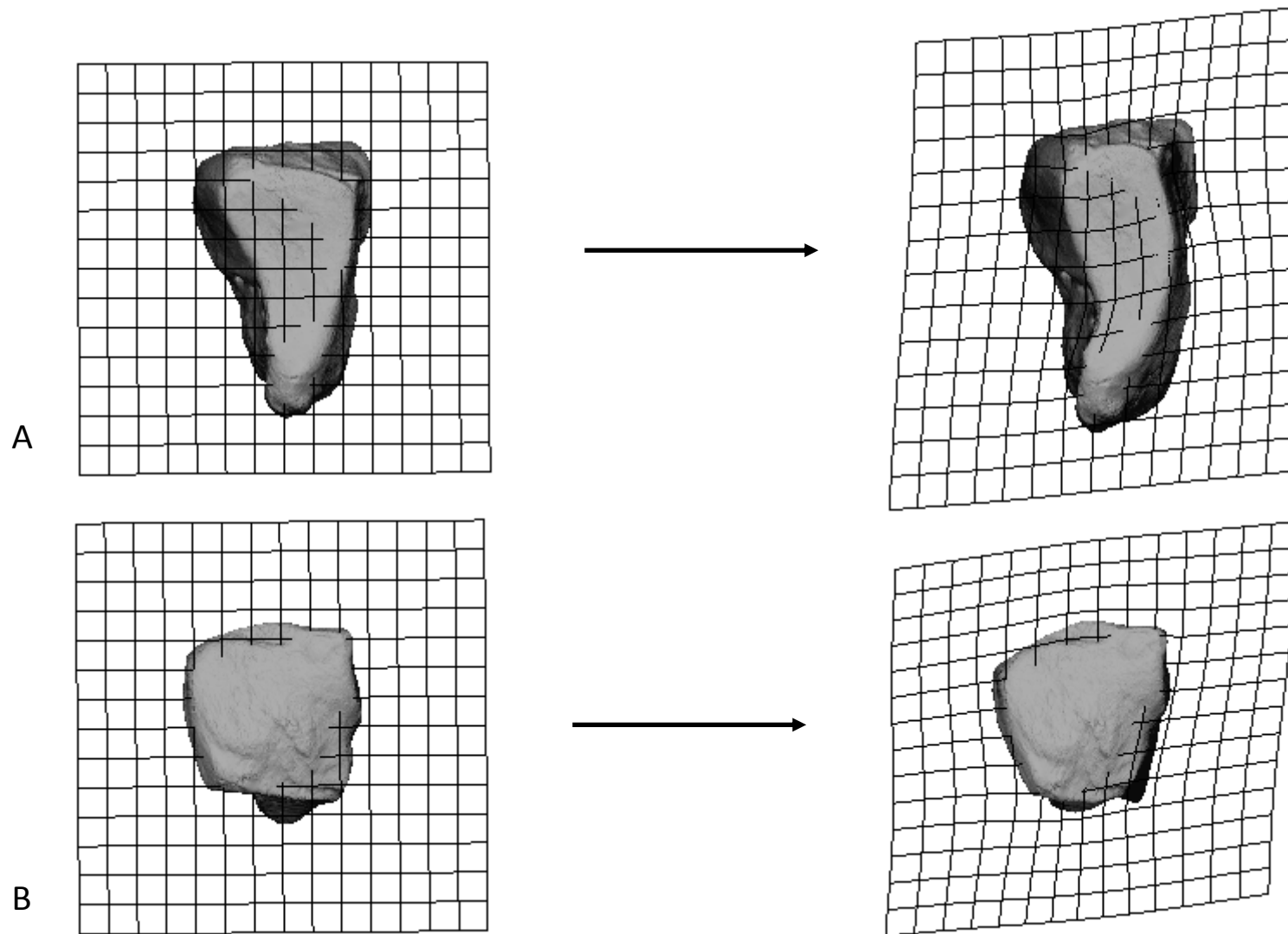


Figure 3.4.15. Demonstration of the warp from the *Pan* mean intermediate cuneiform (left) to *Oreopithecus* (right). A) Proximal view B) Superior view

Homo and OH8 were not found to be statistically significantly different in shape. However, the *Homo* mean shape was warped to OH8 to demonstrate these similarities and how the two differed from the other species included in the study. The proximal facet is broadly reminiscent of the proximal facet of the African apes. It is roughly triangular in outline with an inferiorly sloping superomedial corner (Fig. 3.4.16A). The facet is broader across its superior half while the inferior border tapers to a narrower point. However, in both *Homo* and OH8 the inferior half of the facet is well-developed compared to the African apes giving the facet a more robust appearance. There is a slight lateral inflection of the inferior border of the navicular facet but this is much less pronounced than the condition in the African apes or *Oreopithecus*. From medial view it is apparent that the proximal facet is flat in both *Homo* and OH8, lacking the proximal projection of the inferior border found in *Pan* and *Gorilla*. It is also clear from medial view in both *Homo* and OH8 that the distal facet slopes anteriorly relative to the proximal facet. Thus, in relation to the articulation between the navicular and intermediate cuneiform the articulation between intermediate cuneiform and second metatarsal is oriented inferiorly.

From superior view the medial and lateral sides of the bone are parallel. However, the medial side of the bone is longer because the superomedial corner of the navicular facet projects further proximally than the superolateral corner (Fig. 3.4.16B). However, the proximal and distal facets are more parallel overall in *Homo* and OH8 than in the African apes. Because of this, the superior border of the distal facet is markedly shorter than the superior border of the proximal facet (Fig. 3.4.16B); the bone narrows considerably from proximal to distal in *Homo* and OH8. *Homo* and OH8 clearly also have a proximodistally broader bone than is the case in the African apes or *Oreopithecus*. Both OH8 and *Homo* have a distal facet which lacks the T shape characteristic of the African apes. Instead the facet is roughly triangular in shape, narrowing inferiorly and with relatively equal medial and lateral borders. There is an absence of the posterior sloping of the superomedial corner of the facet giving the distal facet a flat appearance.

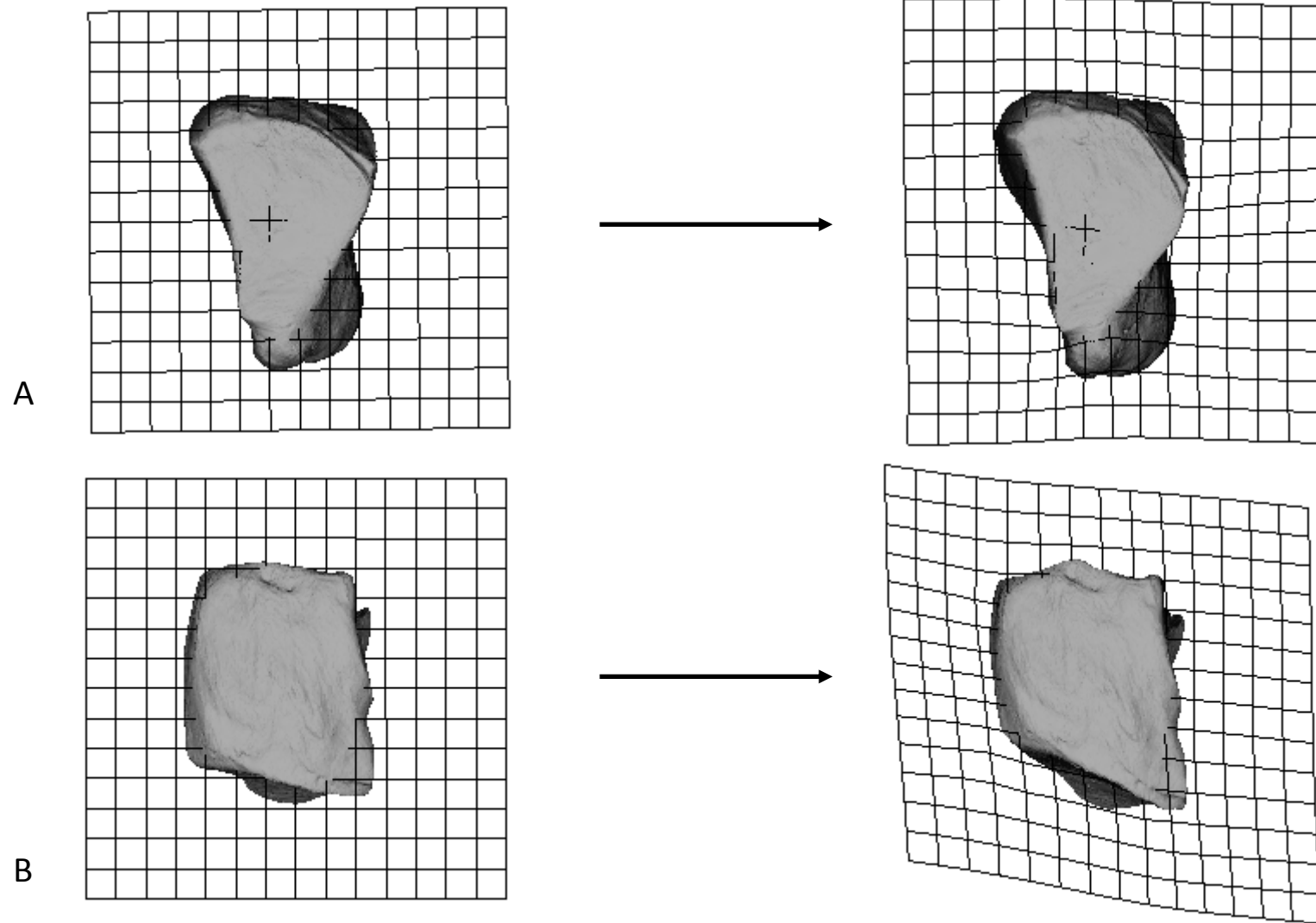


Figure 3.4.16. Demonstration of the warp from the *Homo* mean intermediate cuneiform (left) to OH8 (right). A) Proximal view B) Superior view

There are a number of pronounced differences between the intermediate cuneiform of *Pan* and *Pongo*. The navicular facet has a smaller surface area in *Pongo* and a vastly different shape. The most striking difference is the wider inferior half of the facet in *Pongo* giving the bone a sub-rectangular as opposed to triangular outline in proximal view (Fig. 3.4.17A). The inferior border of the facet is flexed medially in this view instead of the lateral orientation found in the other apes. The more rectangular outline of the *Pongo* navicular facet has the effect that the superomedial corner of the facet does not slope inferiorly like it does in other species. The navicular facet has a proximally directed concavity when viewed from the medial or lateral side as it does in the African apes. However, because the facet is reduced in size, thereby having a smaller superoinferior dimension, the radius of curvature is lower in *Pongo*. From medial and lateral view it can also be seen that the proximal and distal surfaces of the bone are parallel, running along a dorsoplantar axis.

From superior view it is clear that the intermediate cuneiform of *Pongo* has a substantially shorter lateral side than medial. The result is that the proximal and distal facets are rotated externally about the sagittal axis and are angled to face slightly laterally. For this reason the medial side of the superior border of the navicular facet projects further proximally than the lateral side from superior view. The bone becomes wider distally from this view and it is clear that the posterior sloping of the superomedial corner of the distal facet is extreme in *Pongo*. The distal facet of *Pongo* is unlike that of any other species. The lateral side of the facet resembles the T shape form of the African apes. However, the medial side of the facet is extremely well developed and expanded medially from the body of the bone. There is no constriction of the inferior half of the facet, instead the superior and inferior halves blend together (Fig. 3.4.17B).

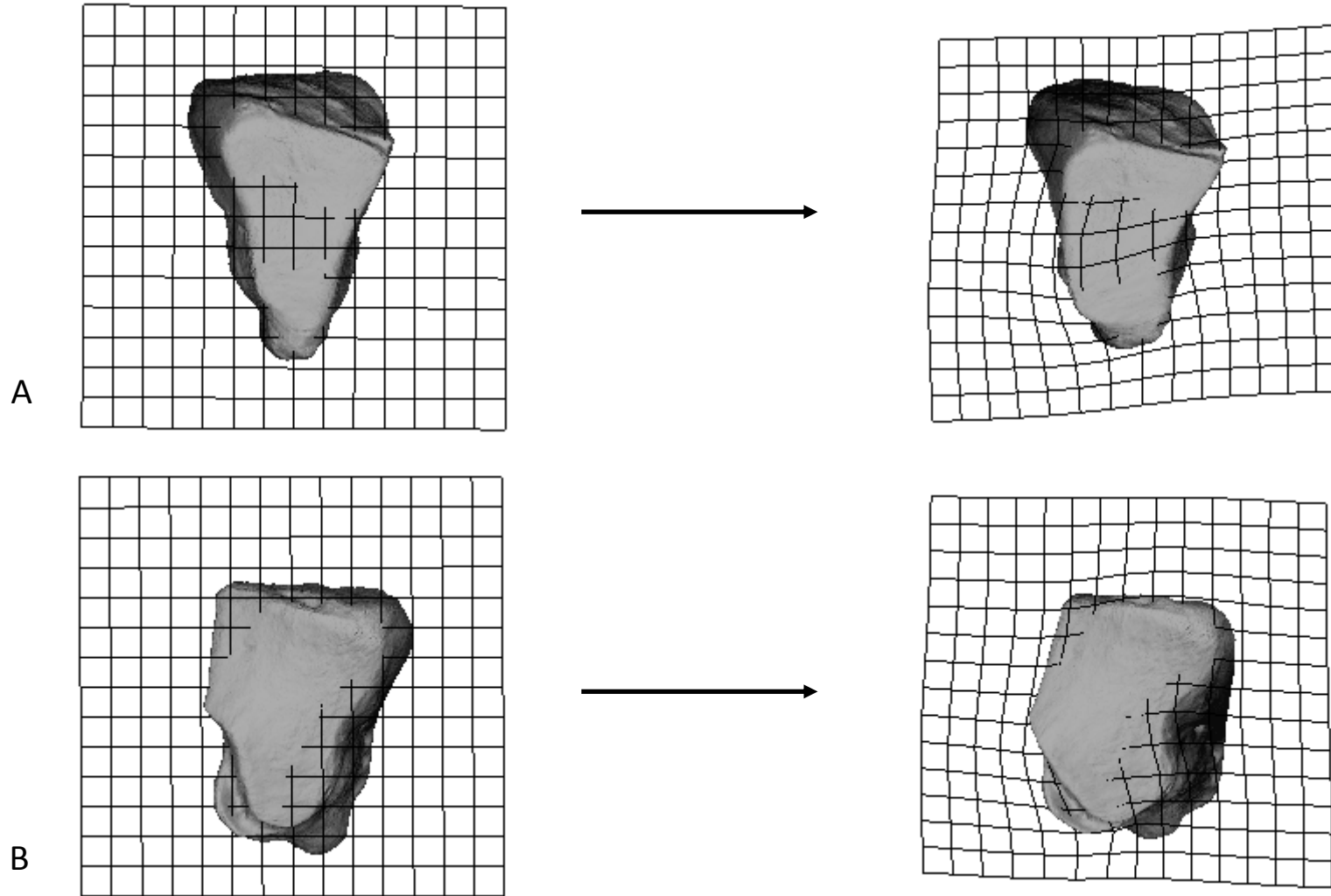


Figure 3.4.17. Demonstration of the warp from the *Pan* mean intermediate cuneiform (left) to the *Pongo* mean (right). A) Proximal view B) Distal view

Homo had the lowest Procrustes distance from *Theropithecus*. In the interest of presenting the morphology of all species a warp was conducted from the *Homo* mean shape to the *Theropithecus* mean to visualise the differences between the two. From proximal view it is clear that the intermediate cuneiform of *Theropithecus* is considerably mediolaterally narrower than that of *Homo*. However, the navicular facet of *Theropithecus* has a roughly similar outline. The facet is broad across its superior border and tapers inferiorly into a narrow point. The superomedial corner of the facet slopes inferiorly, as it does in *Homo* and the African apes. This feature is expressed more strongly in *Theropithecus* than *Homo*. *Theropithecus* is unlike *Homo* in having a sharp narrowing of the navicular facet resulting in strong mediolateral constriction of the facet. Unlike *Homo*, the inferior border of the facet has a strong proximal projection giving the facet a concavity from medial or lateral view (Fig. 3.4.18A). The expression of this feature in *Theropithecus* exceeds that in the African apes. However, from both medial and lateral view it is clear that *Theropithecus* has a proximodistally broad intermediate cuneiform, a feature aligning it more closely with *Homo* than with the African apes.

The bone has parallel and roughly equal sided medial and lateral sides in *Theropithecus* from superior view (Fig.3.4.18B). The superomedial corner of the navicular facet projects more proximally than the superolateral corner, as it does in *Homo*. These features have the effect that the proximal and distal facets are aligned parallel to each other in the coronal plane. The clear difference between *Homo* and *Theropithecus* is the narrowness of the intermediate cuneiform in *Theropithecus* despite its proximodistal length. The distal facet of *Theropithecus* is unique among the extant species in this study. It forms a T shape which is superficially like that of the African apes but has a pronounced constriction at its midpoint unlike the more modest narrowing found in *Pan* and *Gorilla*. The inferior portion of the distal facet is therefore roughly less than half of the size of the superior half in *Theropithecus*. There is a flexion between the superomedial corner of the distal facet and the rest of the facet, however, this does not extend onto the dorsal surface of the bone as it does in the non-human apes. This is because the distal facet is tilted anteriorly in a *Homo*-like manner giving the distal facet an inferior set relative to the proximal facet.

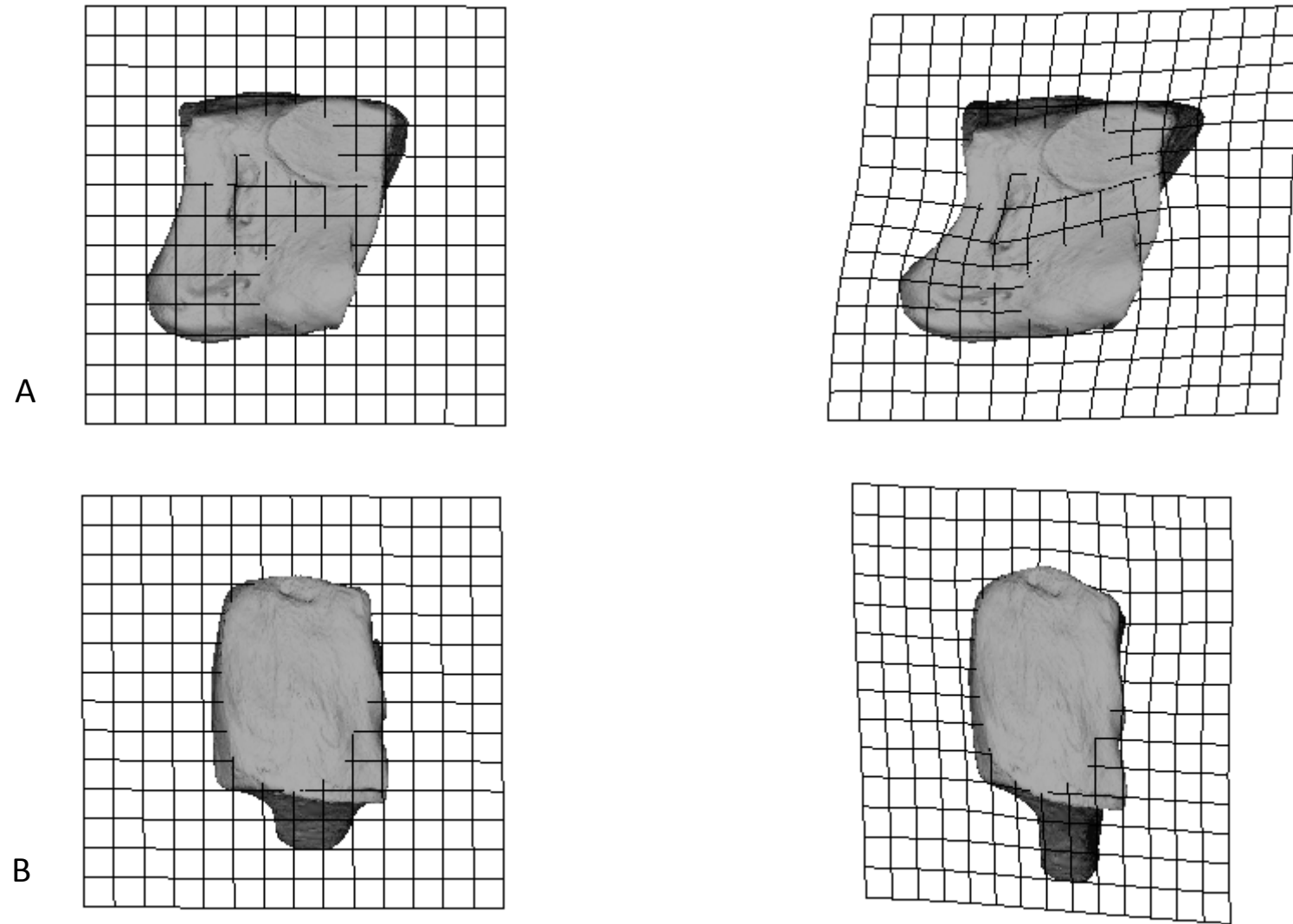


Figure 3.4.18. Demonstration of the warp from the *Homo* mean intermediate cuneiform (left) to the *Theropithecus* mean (right). A) Medial view B) Superior view

3.5. Lateral cuneiform

3.5.1. Principal components analysis

3.5.1.1. Full sample

The percentage of variance explained by each principal component following a principal components analysis conducted on the Procrustes aligned landmarks of all specimens for the lateral cuneiform are presented in Figure 3.5.1. The first three principal components explained 63.02% of the variance; the first five principal components explained 74.43% of the variance, and the first fourteen explained 90.42% of the variance. The remaining 9.52 percent of the variance was explained by principal components 15-78.

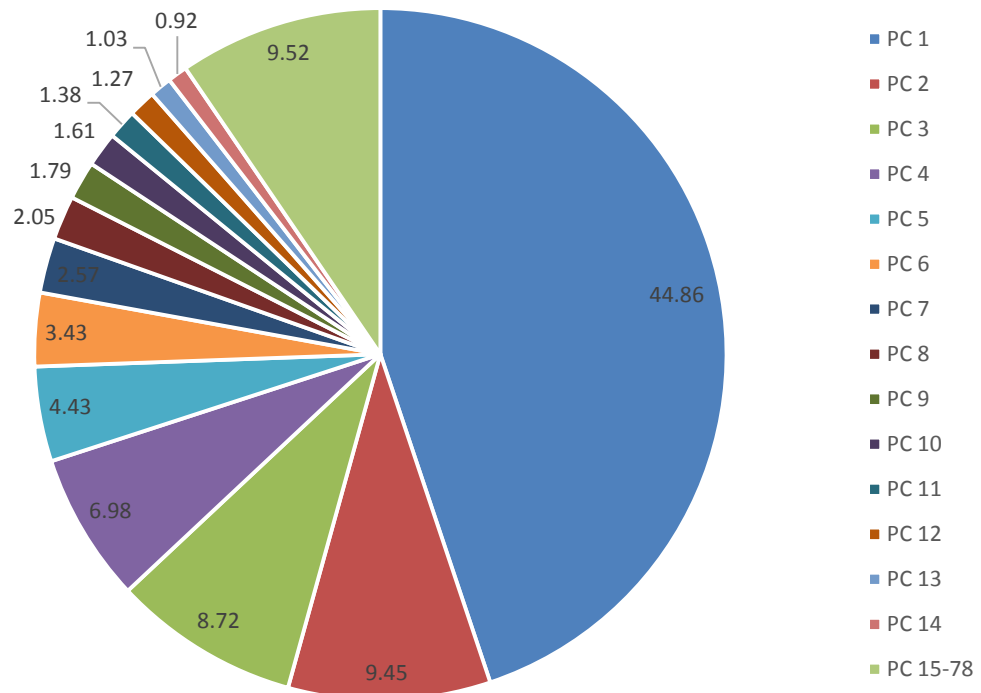


Figure 3.5.1. Percentage of the overall variance explained by each principal component for the lateral cuneiform.

Principal component 1 and principal component 2 are plotted against each other and presented in Figure 3.5.2. Principal component 1 separates *Homo* from *Pongo* at the negative and positive extremes of the axis, respectively. *Pan*, *Gorilla* and *Theropithecus* cluster around the average PC1

value. There is no overlap between the range of *Homo* and any other species on PC1, while there is some minor overlap between the lower values of *Pongo* and the higher values of *Gorilla*, however, the *Pongo* distribution is the most broadly distributed. There is considerable overlap between the *Pan* and *Gorilla* ranges. The *Pan* mean value lies roughly at 0 on the PC1 axis while the mean *Gorilla* value is located higher in the positive range of the axis. The *Theropithecus* mean is slightly below 0 on the PC1 axis and the values are tightly clustered, varying very little and falling entirely within the *Pan* range. *Oreopithecus* has a value close to the *Gorilla* mean, well within the range of *Gorilla* variation and on the periphery of the *Pongo* distribution. OH8 has a negative PC1 value on the periphery of the *Homo* range, and closest to the *Homo* mean.

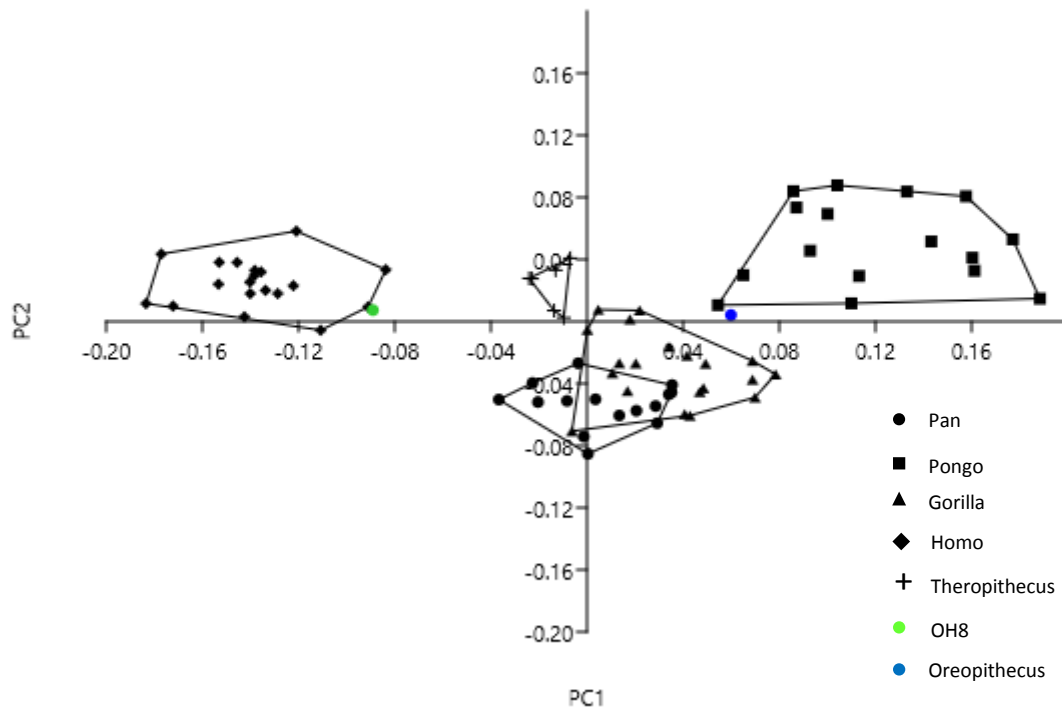


Figure 3.5.2. Principal component 1 vs. principal component 2 of all individuals for the lateral cuneiform.

Principal component 2 most clearly separates the African apes from the other species. *Pan* occupies the most negative range of the PC2 axis of any species. There is considerable overlap with *Gorilla* but the *Pan* mean lies at the periphery of the range of *Gorilla*. The *Gorilla* distribution has slightly lower values than *Pan* but still has predominantly negative values on the PC2 axis. However, there is a degree of overlap with all other species due to the *Gorilla* specimens with positive PC2 values. The *Pongo* distribution has the highest positive values on the PC2 axis. The *Pongo* mean has a higher

positive value than that of *Homo* but there is a large degree of overlap between the two distributions. It should be noted, however, that the range of the *Pongo* distribution is high on this axis. The *Theropithecus* mean has a positive value on PC2 and is very similar to the *Homo* mean; the range of *Theropithecus* is encompassed entirely by that of *Homo*. There is also considerable overlap between the ranges of *Theropithecus* and *Pongo*, and some slight overlap between the lower extreme of *Theropithecus* and the specimens of *Gorilla* with positive values. *Oreopithecus* has a value on PC2 between the means of *Pongo/Gorilla*, but also overlaps with *Homo* and *Theropithecus*. OH 8 has a value on PC2 close to the *Homo/Theropithecus* means.

Taken together PC1 and PC2 account for more than 50% of the variance explained and separate the specimens into *Homo*, *Pongo* and African ape clusters. *Theropithecus* lies closest to the African apes but is distinct from them. The overall shape of the distribution is similar to that observed for the talus. *Oreopithecus* lies in the extreme periphery of the *Pongo* distribution but closer to the *Gorilla* centroid. OH8 lies on the *Homo* periphery and is situated closest to the *Homo* centroid.

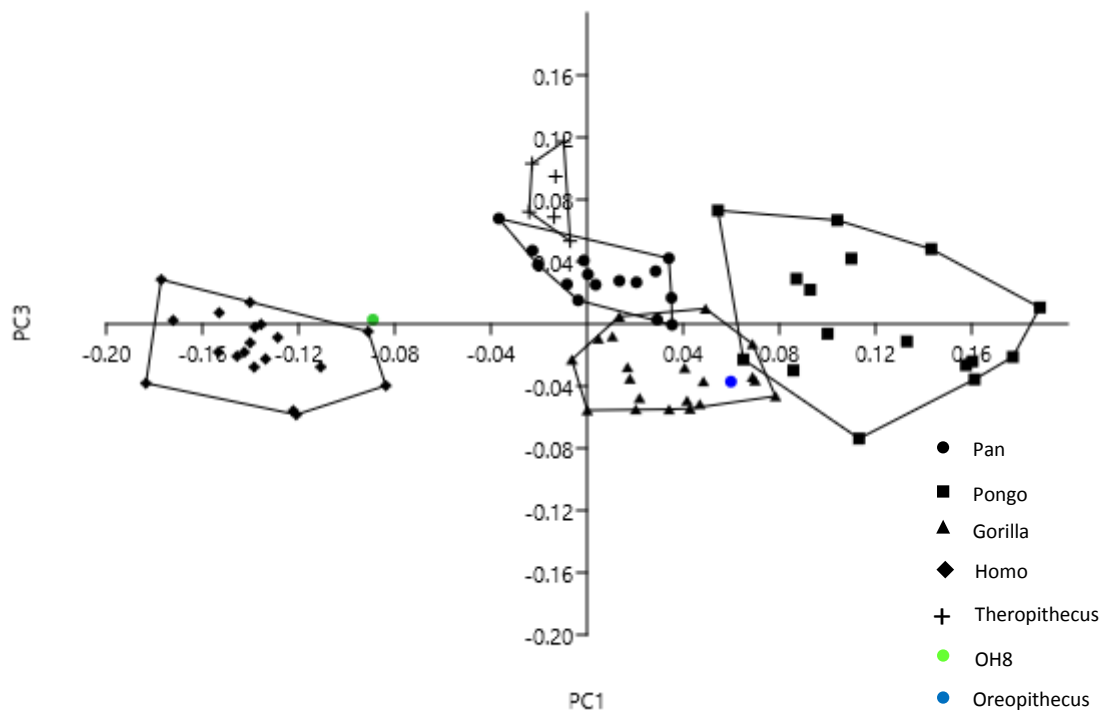


Figure 3.5.3. Principal component 1 vs. principal component 3 of all individuals for the lateral cuneiform.

PC3 is plotted against PC1 in Figure 3.5.3; PC3 most noticeably separates *Theropithecus* from the other groups. There is a significant degree of overlap between some groups because the ranges are very high. The *Gorilla* distribution has predominantly negative values on the axis and has the most negative mean value slightly below 0 on the PC3 axis. The value of the *Homo* mean is slightly closer to 0 than the *Gorilla* mean but still clearly has a negative value on the axis; there is a considerable overlap between the distributions of the two species. *Pan* has a mean on the axis with a positive value and the lower extreme of its distribution has some minor overlap with the range of *Gorilla*, and also with the *Homo* distribution. The *Pongo* mean value is slightly above 0 on the PC3 axis but not as high as the mean value of *Pan*. The range of the *Pongo* distribution on PC3 also encompasses all of the *Pan*, *Gorilla* and *Homo* ranges as well as some of that of *Theropithecus*. *Theropithecus* has the most positive distribution of any species. The lower periphery of its distribution overlaps slightly with both *Pan* and *Pongo*. OH8 has a value on PC3 roughly the same as the *Pongo* mean slightly greater than 0 on the PC3 axis, although OH8 is within the distributions of *Pongo*, *Homo*, *Pan*, and *Gorilla*. *Oreopithecus* is located closest to the *Gorilla* mean on the PC3 axis but also falls within the *Homo* and *Pongo* distributions.

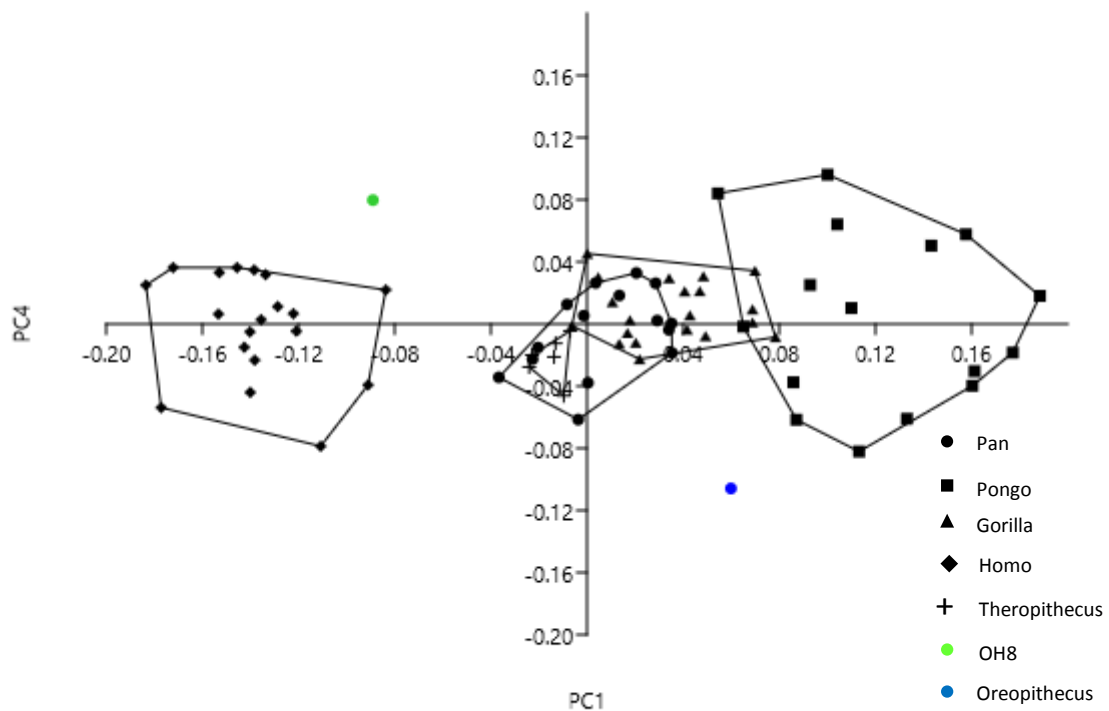


Figure 3.5.4. Principal component 1 vs. principal component 4 of all individuals for the lateral cuneiform.

Principal component 4 (Fig. 3.5.4) is not effective at distinguishing between extant species groups. The range of *Pongo* is particularly large, encompassing the entire distribution of all other species on this axis. *Homo* also has a large range on PC4, though it is somewhat smaller than the *Pongo* range. There are some differences between the distributions of *Pan* and *Gorilla* but these are minor in relation to the vast ranges of *Pongo* and *Homo* on PC4. The axis does clearly distinguish OH8 and *Oreopithecus*, however. OH8 has a high positive value on the axis while *Oreopithecus* has a high negative value on the axis.

Principal component 5 separates *Theropithecus* from all other extant species, although the effect is relatively small. However, OH8 is also separated from other extant species and falls within the range of *Theropithecus* on this axis (Fig. 3.5.5). All subsequent higher principal components were ineffective at distinguishing between extant species or fossil specimens.

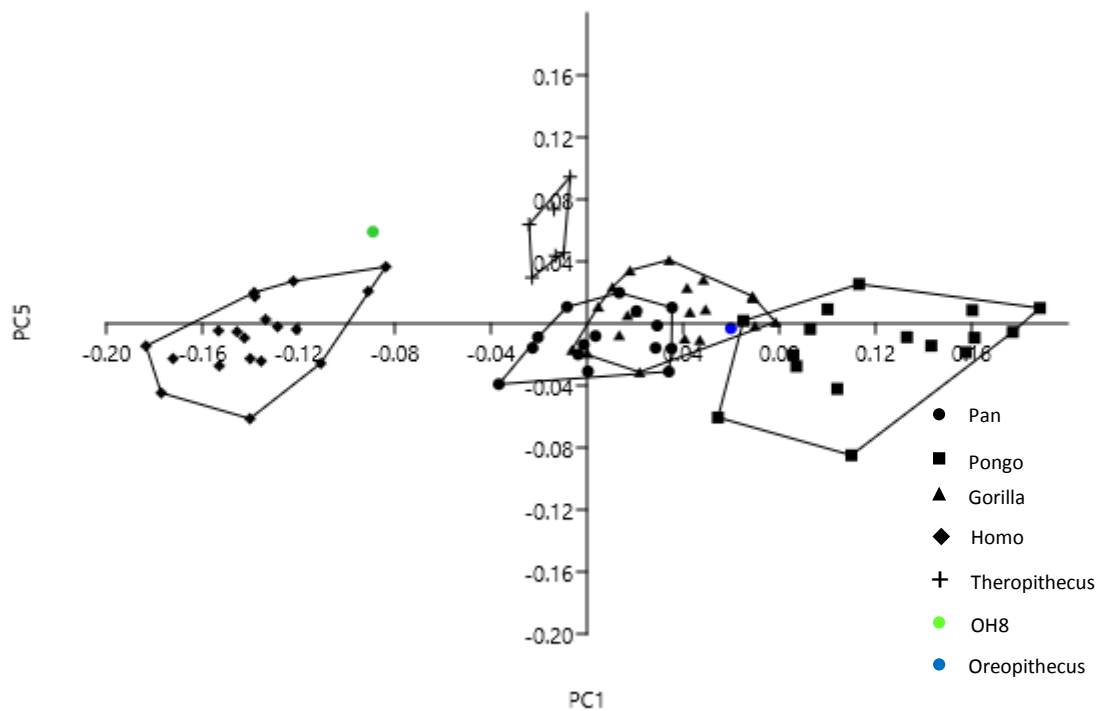


Figure 3.5.5. Principal component 1 vs. principal component 5 of all individuals for the lateral cuneiform.

3.5.1.2. Extant species means vs. fossils

A principal components analysis was conducted on the Procrustes aligned landmarks for the lateral cuneiform using only the species mean shapes and fossils. Of seven principal components the first three explained 82.16% of the variance, the first five explained 97.75% of the variance and the first six explained practically 100%. This information is presented in Figure 3.5.6. The seventh principal component explained a negligible portion of the overall variance in the data.

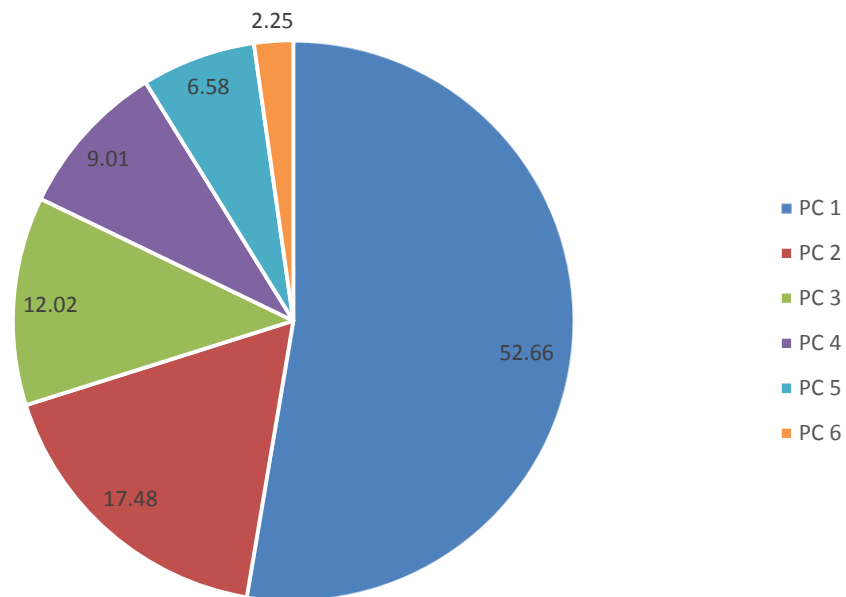


Figure 3.5.6. Percentage of the variance explained by each PC using only species mean shapes for the lateral cuneiform.

The first principal component provides a distribution which is roughly the same as the first principal component extracted from the full dataset (Figure 3.5.7). Of the extant species, the axis most strongly separates *Homo* and *Pongo* at the negative and positive extremes of the axis, respectively. *Pan* is located closest to 0 on the axis which is also true of the first principal component using the full sample. *Gorilla* has a positive value on the axis while *Theropithecus* has a negative value. *Gorilla*, *Pan* and *Theropithecus* are all clustered close to 0 on the axis with *Homo* and *Pongo* occupying the extremes of the axis. The similarity of the first principal component between the two analyses extends to the fossil specimens also. OH8 has an extreme negative value on the axis, close to that of *Homo*, and *Oreopithecus* has an extreme positive value placing it close to *Pongo*.

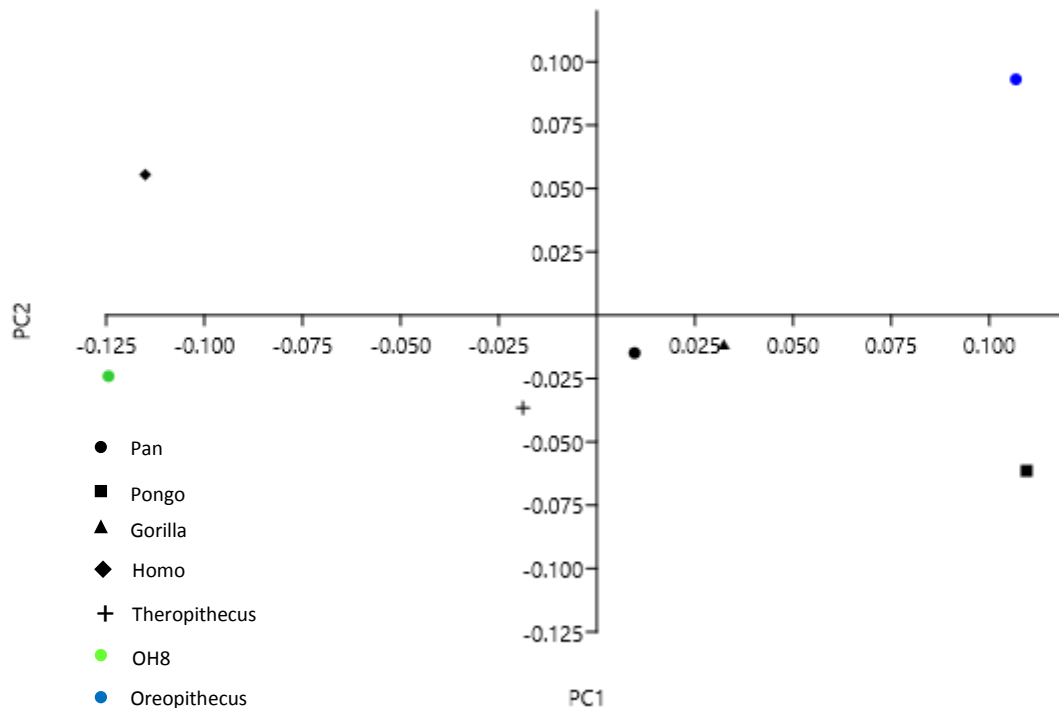


Figure 3.5.7. Principal component 1 vs. principal component 2 of species means and fossils for the lateral cuneiform.

The second principal component corresponds broadly to the second principal component extracted from the full sample, but there are clear differences. In the analysis using only the extant species mean shapes *Homo* and *Pongo* are clearly separated along principal component 2. This is in stark contrast to their distributions on the previous axis (Fig. 3.5.2), on which they are roughly coincident and separated from the African apes. The African apes have very similar negative values on the PC2 axis close to 0. *Theropithecus* has a slightly greater value in the negative range of the axis, closer to *Pongo*. The fossils also bear little similarity to their placement on the second principal component extracted from the full sample. OH8 is situated noticeably closer to the African apes and *Theropithecus*, lying a considerable distance from *Homo* in the negative range of the axis. Similarly, *Oreopithecus* is located at a distance from *Pongo* and the other non-human apes and in the positive range of the axis, sitting closer to *Homo* on PC2. Taken together PC1 and 2 reveal an African ape and *Theropithecus* grouping close to the origin of the graph, and then subsequently separates *Homo*, *Pongo*, *Oreopithecus* and OH8 into each of the four quadrants on the graph.

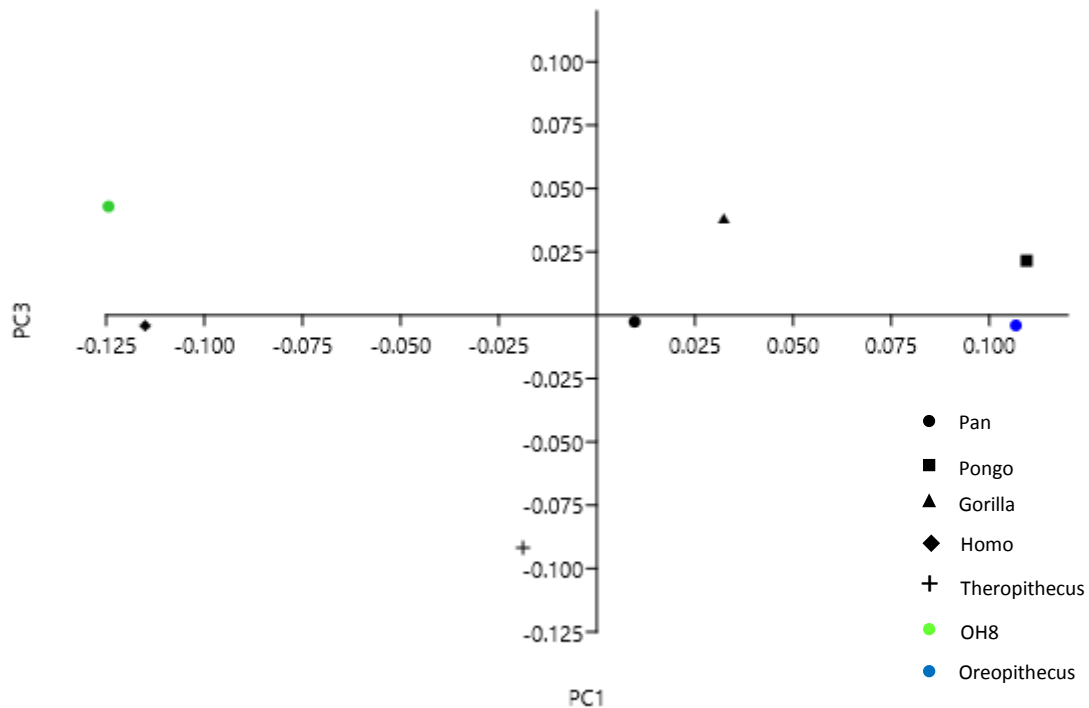


Figure 3.5.8. Principal component 1 vs. principal component 3 of species means and fossils for the lateral cuneiform.

Principal component 3 provides a distribution which is broadly comparable to the third principal component extracted using the full dataset. The axis most obviously separates *Theropithecus* from *Gorilla*, although the effect is much larger when only the extant species mean shapes are used. *Theropithecus* occupies the negative range of the axis almost entirely alone. While *Homo*, *Pan*, and *Oreopithecus* do all have negative values on the axis, they all have values extremely close to 0. Of the extant species, *Gorilla* and *Pongo* occupy the positive range of the PC3 axis. *Gorilla* has the higher value further emphasising the difference between it and *Theropithecus*. OH8 is clearly most closely linked to *Gorilla* on this axis and actually has a value in excess of that of *Gorilla*. *Oreopithecus* is most similar to *Homo* but the difference between the two and *Pan* is incredibly small. No other plots are shown, but principal component 4 separates OH8 from other species quite clearly in the negative range of the axis while the African apes and *Homo* group together in the positive range of the axis. PC5 separates *Homo* and *Pongo* in the negative range of the axis from all other species, but the effect is weak. PC6 offers little information separating species.

3.5.2. Statistical tests

The full Procrustes distances between species mean shapes and fossils were calculated to assess similarities and differences between extant species means and fossils; the results are presented in Table 3.5.1. The significance of difference between extant species means were calculated based on permutation tests of pairwise Procrustes distances. The results showed that all extant species means were significantly different from one another with p values of <0.0001, a result which is concordant with findings for the other bones. The Procrustes distances revealed that *Pan* and *Gorilla* were mutually closest to each other of all the extant species. Therefore hypothesis 1 is confirmed for the lateral cuneiform; the African apes share a similar morphology which likely reflects their similar ecology and locomotor behaviour as well as their closely shared evolutionary history. *Pan* is subsequently closest to *Theropithecus*. Therefore, hypothesis 2 is rejected for the lateral cuneiform; the non-human apes do not form a grouping which reflects their arboreality compared to the terrestrial species of *Homo* and *Theropithecus*. This suggests that there is considerable variation in the morphology and function of the lateral cuneiform and that it cannot be predicted on the basis of increased arboreality/terrestriality. There is a lower Procrustes distance between *Theropithecus* and either of the African apes than there is between *Pongo* and either of the African apes. Therefore, hypothesis 3 is rejected for the lateral cuneiform; *Theropithecus* is not the most different in shape for the lateral cuneiform indicating that differences in morphology of this bone between *Theropithecus* and the hominoids are not related to digitigrady/plantigrady.

Oreopithecus is most distant in shape from *Homo* and then *Theropithecus*. Its distance from *Theropithecus* is considerably greater than its distance from non-human ape species. Therefore, hypothesis 4 is accepted for the lateral cuneiform; there is no evidence to support the proposal that *Oreopithecus* represents a cercopithecoid. *Oreopithecus* shares its lowest Procrustes distance with *Gorilla*, followed by *Pongo*. However, the Procrustes distances between *Oreopithecus* and these species are quite large. Therefore, there is some evidence to support hypothesis 5 for the lateral cuneiform: that *Oreopithecus* is most similar in shape to one of the African ape species, but the large Procrustes distance between *Oreopithecus* and its closest neighbours necessitates caution in the interpretation of this result. OH8 is closest to *Homo* and then to *Theropithecus*, although the Procrustes distances are relatively large. Therefore, there is some evidence to support hypothesis 6: that OH8 is most similar to *Homo* which reflects its status as an obligate biped. However, the large Procrustes distance indicates that there are important differences between the two. *Oreopithecus* is found to be significantly different in shape from *Gorilla* with a Mahalanobis distance of 64.133, which

is 8.008 standard deviation units and obtaining a p value of 0.0005. Therefore, the details of this difference are explored below to ascertain any functionally relevant information. OH8 is significantly different in shape from *Homo* with a Mahalanobis distance of 28.348, 5.324 standard deviation units and associated with a p value of 0.001. Therefore, the shape differences between *Homo* and OH8 are examined in detail to better understand the implications of these differences for understanding the function of the OH8 foot.

	Pan	Pongo	Gorilla	Homo	Thero	OH8	Oreo
Pan	0	0.156613	0.085081	0.170566	0.129286	0.18022	0.173483
Pongo	0.156613	0	0.128555	0.258152	0.181957	0.25051	0.169135
Gorilla	0.085081	0.128555	0	0.182656	0.151936	0.183166	0.15494
Homo	0.170566	0.258152	0.182656	0	0.174933	0.142335	0.241737
Thero	0.129286	0.181957	0.151936	0.174933	0	0.177006	0.202211
OH8	0.18022	0.25051	0.183166	0.142335	0.177006	0	0.264234
Oreo	0.173483	0.169135	0.15494	0.241737	0.202211	0.264234	0

Table 3.5.1. Procrustes distances amongst species mean shapes and fossils for the lateral cuneiform. The smallest and second smallest distances are shown on each row. The bold red shows the closest relationship and bold black the second closest.

Differences in size were assessed using centroid sizes of fossils and individuals from each species group. The size relationships of extant species were addressed by using permutation tests. For each species comparison the probability that the samples of centroid sizes were drawn from the same population was calculated. There were ten comparisons overall so Bonferroni correction for multiple comparisons adjusted the significance threshold to 0.005. It was found that *Homo* (176.7) was significantly larger than *Gorilla* (154.4) with a p value of <0.0001. Both *Homo* and *Gorilla* were also larger than all other extant species with a consistent p value of <0.0001. Therefore, hypothesis 8 is confirmed for the lateral cuneiform; either *Gorilla* or *Homo* will be the largest of any extant species. *Pan* and *Pongo* were not found to be significantly different in size ($p = 0.691$), however, *Pan* (121) was marginally larger than *Pongo* (119.4) on average. *Theropithecus* (85.3) was found to be significantly smaller than all other extant species with a consistent p value of <0.0001. Therefore, hypothesis 9 is confirmed for the lateral cuneiform; *Theropithecus* is the smallest of the extant species. The size hierarchy for the lateral cuneiform can be expressed as follows *Homo* > *Gorilla* > *Pan/Pongo* > *Theropithecus*.

Oreopithecus was found to be significantly smaller than all ape species. The results were as follows: *Oreopithecus* vs. *Pan* ($z = -4.35$; $p = <0.0001$); *Oreopithecus* vs. *Pongo* ($z = 2.594$; $p = 0.0047$); *Oreopithecus* vs. *Gorilla* ($z = -3.912$; $p = <0.0001$); *Oreopithecus* vs. *Homo* ($z = -8.299$; $p = <0.0001$). However, *Oreopithecus* was not found to be significantly larger than *Theropithecus* with respect to its lateral cuneiform ($z = 0.022$; $p = 0.491$), a result which is concordant with the results for other bones and rejecting hypothesis 10 for the lateral cuneiform; *Oreopithecus* was not similar in size to *Pan*. This indicates that the foot of *Oreopithecus* was gracile relative to extant ape species. OH8 was not found to be significantly smaller than non-human apes. OH8 vs. *Pan* ($z = 0.979$; $p = 0.164$); OH8 vs. *Pongo* ($z = 0.732$; $p = 0.232$); OH8 vs. *Gorilla* ($z = -1.439$; $p = 0.075$). OH8 was found to be significantly smaller than *Homo*, however ($z = -4.333$; $p = <0.0001$). Therefore, hypothesis 11 is accepted for the lateral cuneiform; OH8 is smaller than *Homo*. This result is concordant with the results for other bones presented earlier.

3.5.3. Visualisation of shape differences

In order to describe the differences in shape it is necessary to use some technical terminology. Figures 3.5.9 and 3.5.10 illustrate what these terms are referring to.

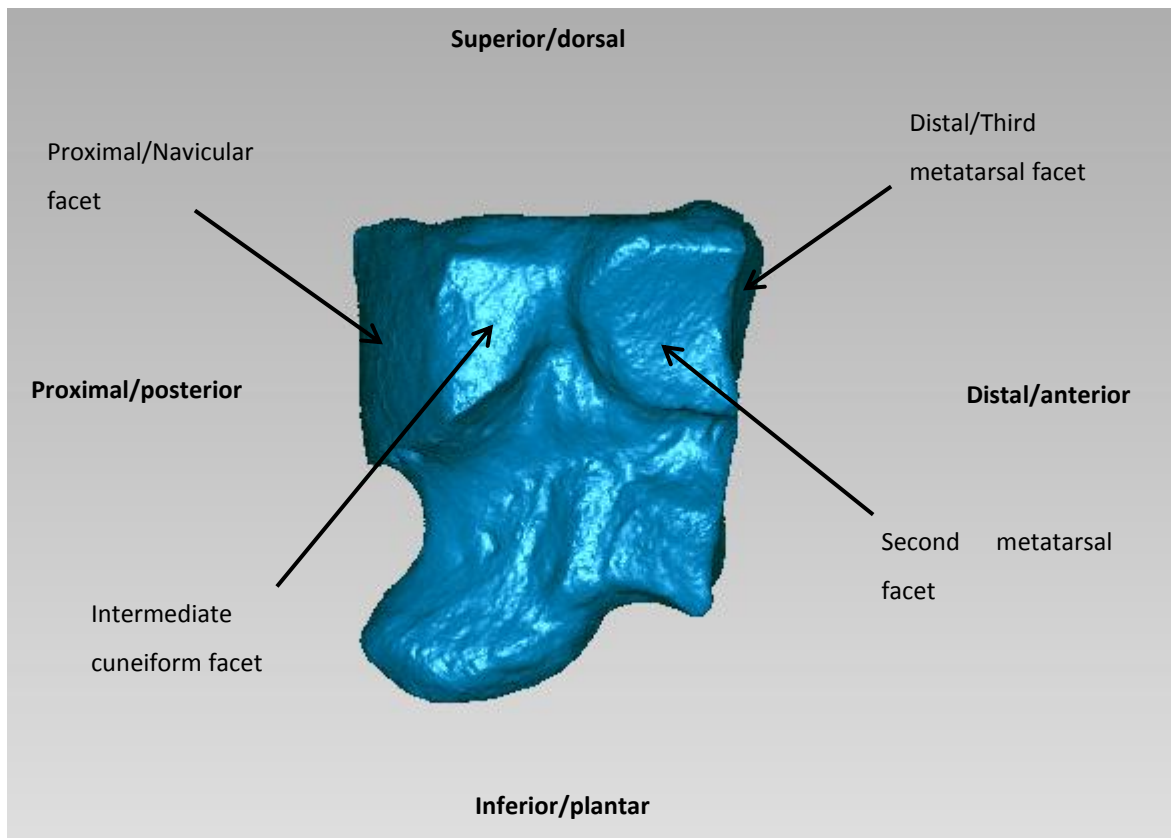


Figure 3.5.9. Medial view of the lateral cuneiform displaying terminology used to describe shape differences.

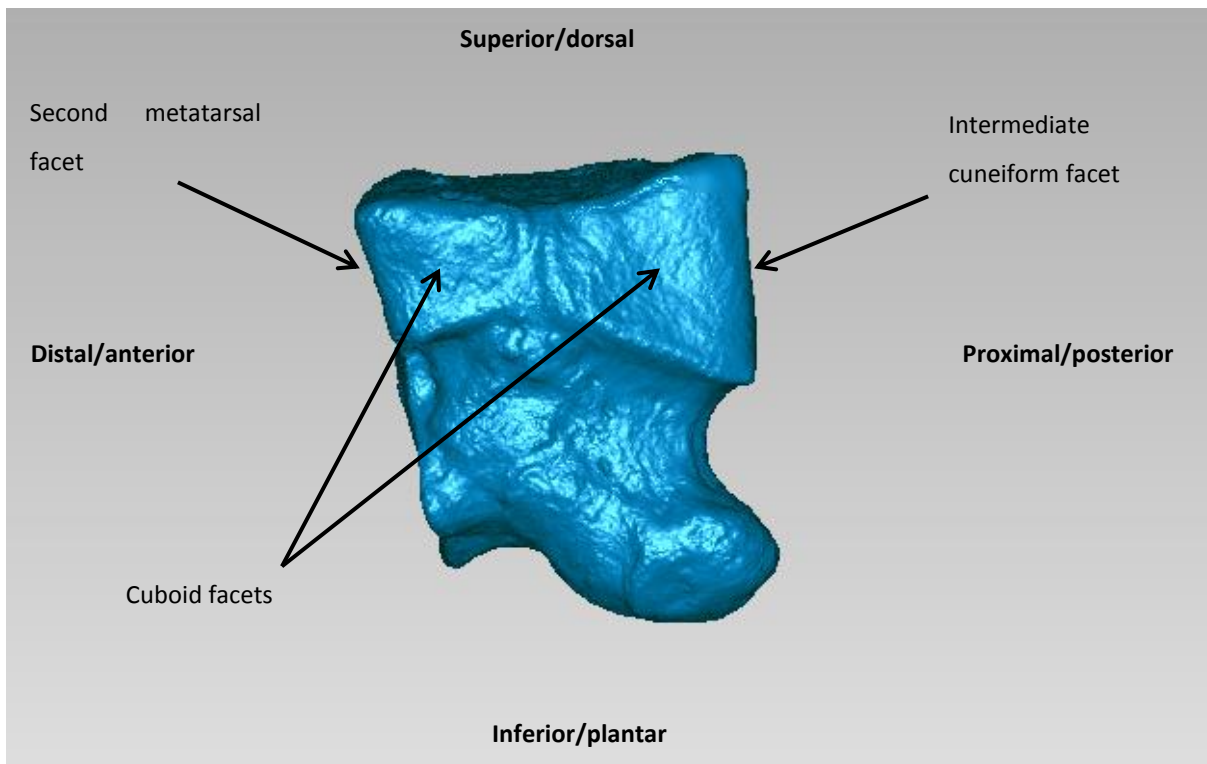


Figure 3.5.10. Lateral view of the lateral cuneiform displaying terminology used to describe shape differences.

From *Gorilla* to *Oreopithecus*

The navicular facet of the lateral cuneiform is broadly similar in appearance in *Oreopithecus* and *Gorilla*. However, there are clear differences relating to its form between the two. The medial border of the facet is much narrower than the lateral border, which is caused by a sharp superiorly directed slope of the inferior border of the facet from lateral to medial. The medial border of the facet is also located closer to the distal surface of the bone in both *Oreopithecus* and *Gorilla*, but this is more strongly expressed in *Oreopithecus* making the medial side of the bone proximodistally relatively shorter than it is in *Gorilla*. The proximal facet is not as large relative to the overall size of the bone in *Oreopithecus*. This can be seen from the shortening of the lateral and medial borders of the facet and general compression of the surface in comparison to *Gorilla* (Figure 3.5.11A). The convexity of the facet surface is greater in *Oreopithecus*, particularly along its mediolateral axis. The facet for the third metatarsal has superomedial and superolateral corners that are diminished in size relative to *Gorilla*. In *Gorilla* the entire superior portion of the distal facet is more expansive. Similarly, the inferior portion is mediolaterally narrow in *Oreopithecus*, which is true of the facet overall. The bone is generally reduced in its superoinferior and mediolateral dimensions in *Oreopithecus* relative to *Gorilla*. This reduction in size is especially pronounced on the proximal side of the bone.

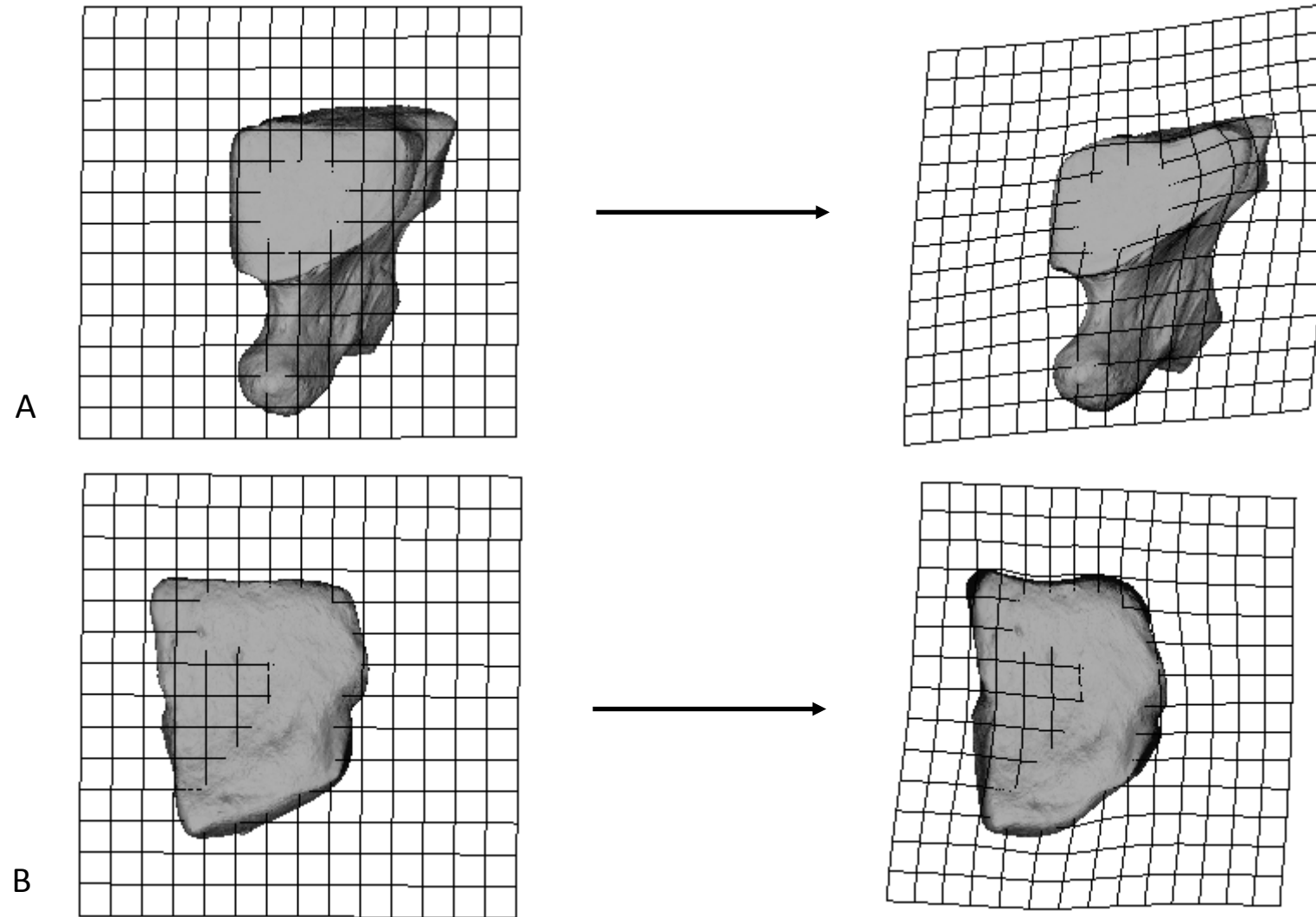


Figure 3.5.11. Demonstration of the warp from the *Gorilla* mean lateral cuneiform (left) to *Oreopithecus* (right). A) Proximal view B) Superior view

From *Pongo* to *Oreopithecus*

The navicular facet of the lateral cuneiform is also similar in shape between *Oreopithecus* and *Pongo*. Warping from the *Pongo* mean to *Oreopithecus* reveals that the differences in shape between the two are actually similar to those noted between *Oreopithecus* and *Gorilla*. The facet is smaller in *Oreopithecus* than it is in *Pongo*, however, this difference is not as marked as it is between *Oreopithecus* and *Gorilla*. The medial and lateral borders of the navicular facet are shorter in *Oreopithecus*, contributing to the overall smaller facet compared to *Pongo* (Figure 3.5.12A). However, these differences are not as markedly different as they are between *Oreopithecus* and *Gorilla*. This reflects the fact that the navicular facet is much narrower on its medial half in *Pongo* than *Gorilla*. The convexity of the facet is similar in both *Pongo* and *Oreopithecus*. The medial border of the navicular facet slopes superiorly in *Oreopithecus* compared to *Pongo*, in which it is directed more directly medially. The difference in length of the medial side of the bone is not as marked between *Pongo* and *Oreopithecus*, reflecting that the medial side of the bone is shorter in *Pongo* than *Gorilla*. The facet for the third metatarsal also bears similar differences. The superior portion of the facet is greatly diminished in size in *Oreopithecus* relative to *Pongo*, and this is more pronounced than the same difference observed against *Gorilla*. However, the superomedial corner of the facet of *Pongo* is relatively smaller than that of *Gorilla* and bears a slight posterior slope. This morphology is also found in *Oreopithecus*. The distal facet has a greater reduction in superoinferior length compared to *Pongo*. The superior border of the medial side of the facet is relatively elevated compared to *Pongo* also, which may be related to the great shortening of the medial side of the bone. The bone is generally superoinferiorly short and mediolaterally narrow compared to *Pongo*.

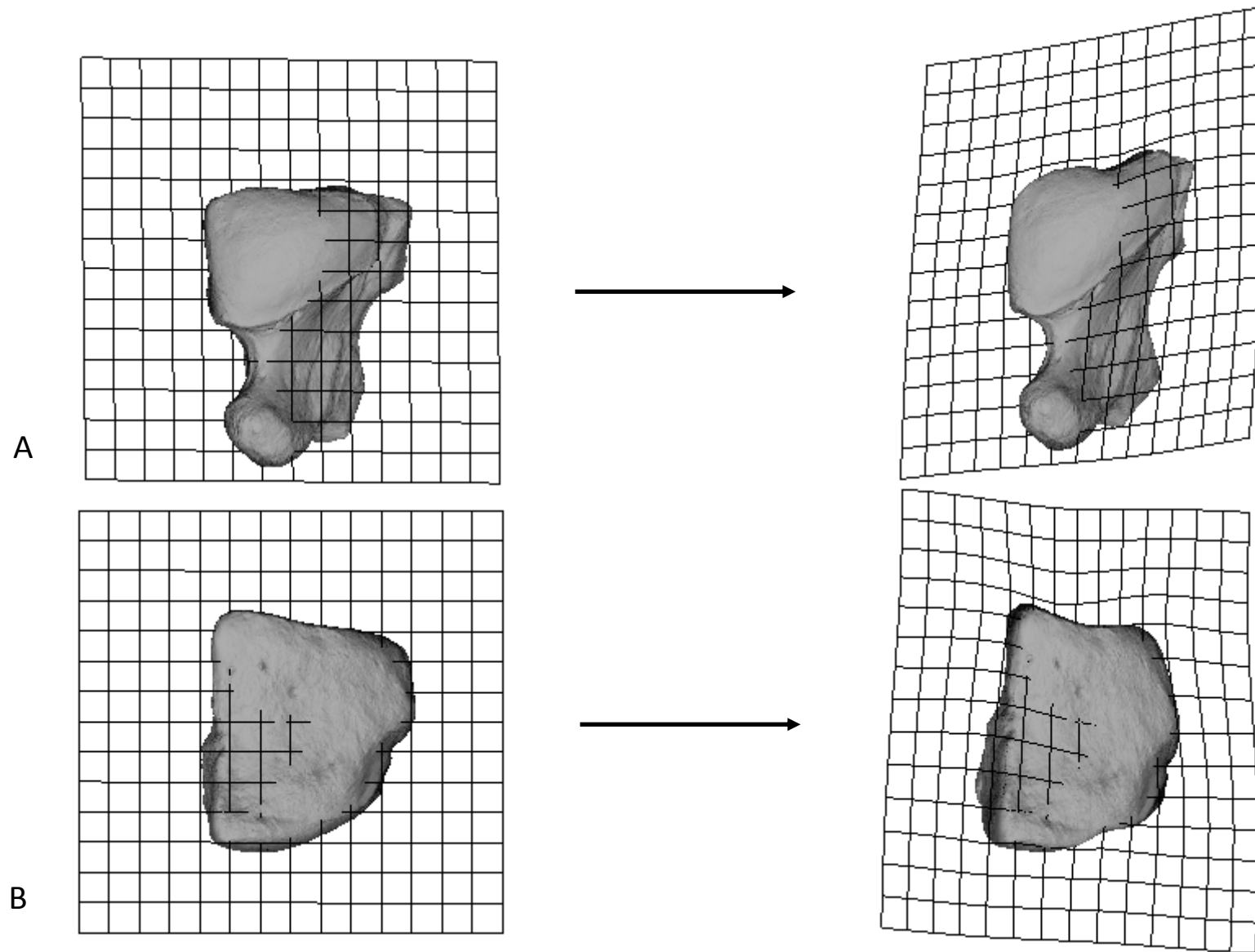


Figure 3.5.12. Demonstration of the warp from the *Pongo* mean lateral cuneiform (left) to *Oreopithecus* (right). A) Proximal view B) Superior view

There are a number of similarities and differences between the lateral cuneiforms of *Homo* and OH8. The navicular facet is mediolaterally narrow in both and superoinferiorly long, although the facet is actually relatively longer superoinferiorly in OH8 (Figure 3.5.13). The facet is flat in OH8 as it is in *Homo*, and the medial border of the facet does not lie excessively close to the distal facet making the medial and lateral sides of the bone approximately the same length (although the medial side of the bone is fractionally shorter in both *Homo* and OH8). The distal facet is flat in OH8 as it is in *Homo*. However, the inferior border of the distal facet extends further from the proximal surface of the bone in OH8 lending the facet a parallel alignment with the proximal facet from either medial or lateral view. In contrast the facet is tilted anteriorly in *Homo* relative to the proximal facet because the inferior border of the distal facet lies closer to the proximal surface than does the superior border. The lateral side of the bone in OH8 does not project laterally from superior view, as it does in *Homo*. Instead the lateral side of the bone is approximately straight from proximal to distal from superior view, resembling the African apes in this regard.

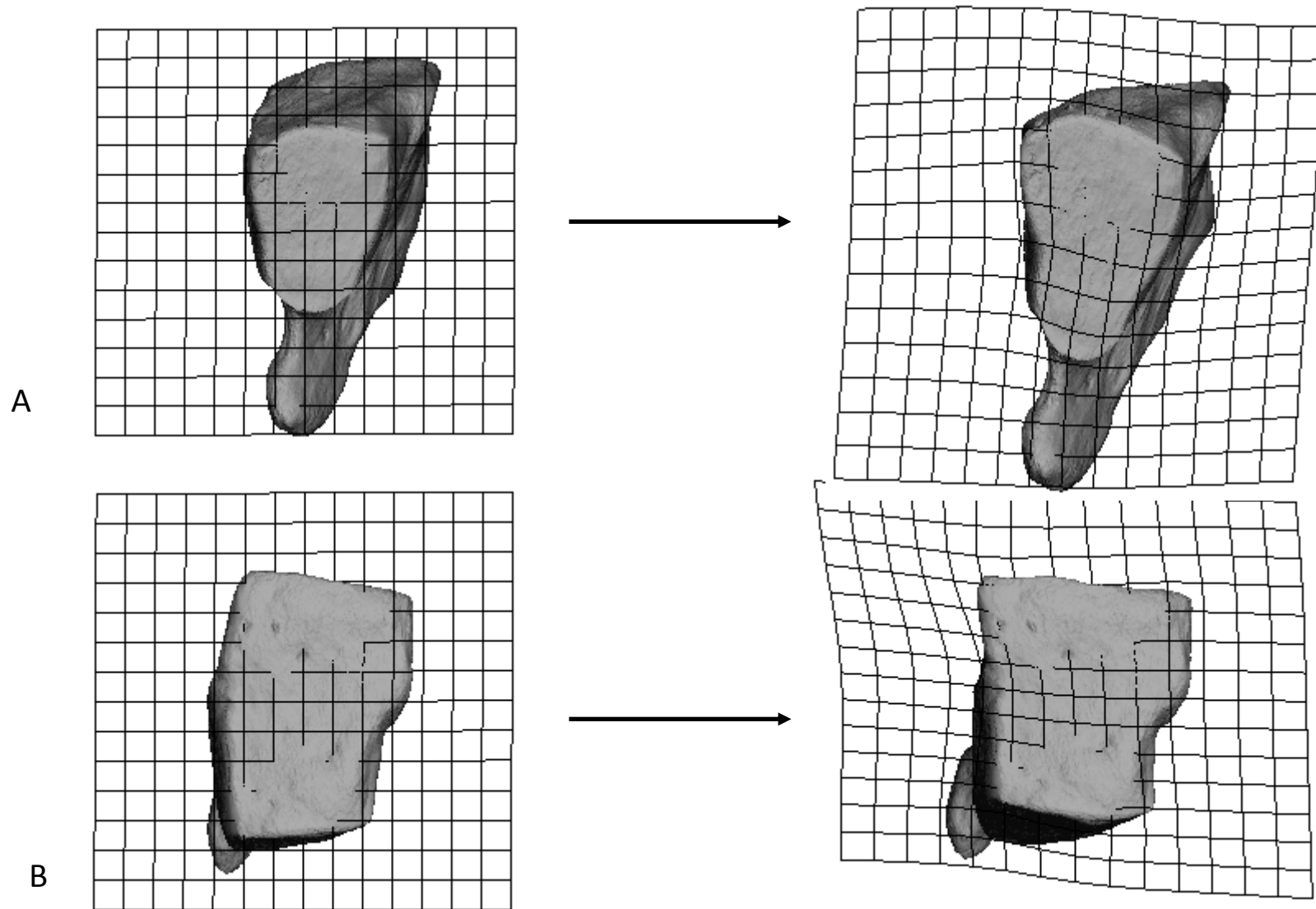


Figure 3.5.13. Demonstration of the warp from the *Homo* mean lateral cuneiform (left) to OH8 (right). A) Proximal view B) Superior view

The warp from *Pan* to *Theropithecus* was included to provide some insight into the morphology of these two species, it is especially pertinent because *Pan* has the lowest Procrustes distance from *Theropithecus*. The navicular facet of *Pan* is roughly rectangular in outline, unlike the form in other non-human apes in which the medial border is noticeably shorter than the lateral. *Theropithecus* is unlike *Pan* in this respect, but also unlike the other non-human apes. The medial border of the navicular facet is roughly relatively the same size in *Theropithecus* as in *Pan*, but the lateral border is excessively reduced in length. This causes both the superior and inferior borders to slope from the medial border and gives the facet an approximately triangular outline (Fig. 3.5.14A). The navicular facet has a moderate degree of curvature aligning it with *Pan*, unlike the flat surface of *Homo* and the highly curved surface of *Pongo*. From superior view it is clear that the medial side of the bone is slightly shorter than the lateral but is not greatly shortened compared to *Pan*. However, the lateral side of the bone does not extend as far distally in *Theropithecus* giving the bone a shorter lateral side relative to *Pan*. Thus, *Theropithecus* has a more even-sided bone from superior view, appearing almost rectangular. From lateral view it is clear that the articulation with the cuboid does not extend as far distally as it does in *Pan* by a large margin (Fig. 3.5.14B). This is also linked with the excessive reduction of the lateral side of the navicular facet. Similarly, the articulation with the intermediate cuneiform facet does not extend as far distally as it does in *Pan*. Therefore it seems there is a general reduction in size of the proximal aspect of the bone. The distal facet has a form which is like *Pan* in general. The most notable difference is the extreme mediolateral narrowness of the facet in *Theropithecus*, particularly the inferior portion of the facet. However, the facet is T-shaped in outline, roughly matching *Pan*.

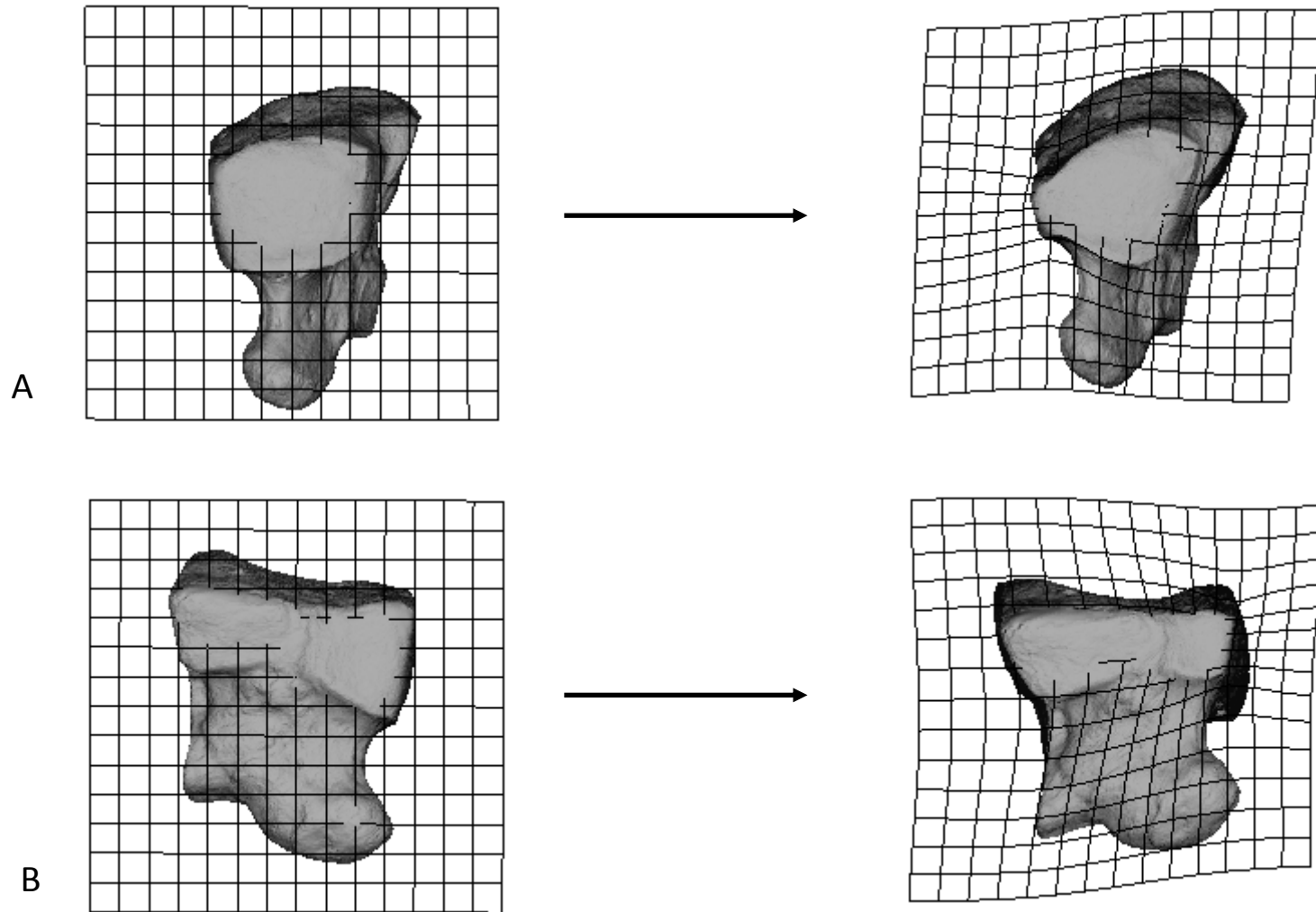


Figure 3.5.14. Demonstration of the warp from the *Pan* mean lateral cuneiform (left) to the *Theropithecus* mean (right). A) Proximal view B) Lateral view

3.6. First metatarsal

There were no complete first metatarsals for *Oreopithecus*, but there were a proximal and distal first metatarsal of *Oreopithecus* available for study, which were compared to the proximal and distal landmarks of the first metatarsal for all extant species. The complete first metatarsal was examined amongst the extant species to provide a comparative framework against which to assess the proximal and distal first metatarsal of *Oreopithecus*. The principal components analysis is first conducted on the complete bone, then the proximal, and then the distal metatarsal. This is repeated for the statistical tests and again for the visualisation of shape differences. This allows each section of the analysis for the complete bone to be compared readily with the proximal and distal first metatarsal without being too widely separated in the document.

3.6.1. Principal components analysis

3.6.1.1. Complete first metatarsal: full sample

A principal components analysis was conducted on the Procrustes aligned landmarks of the entire first metatarsal using all individuals from the extant species groups. The first three principal components explained 78.05% of the variance in the dataset, the first five principal components explained 84.03% of the variance, and the first nine explained 90.05% of the variance. The remaining 9.95% of the variance was explained by principal components 10-76 (Fig. 3.6.1.)

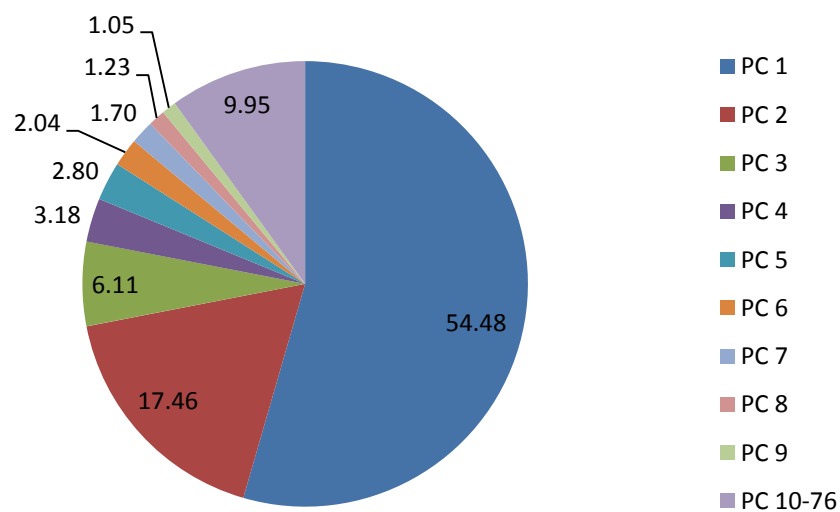


Figure 3.6.1. Percentage of the overall variance explained by each principal component for the first metatarsal.

PC1 clearly separates *Homo* from the other species (Fig. 3.6.2). *Homo* is located on the positive end of the axis and does not overlap with the distribution of any other species. Situated around 0 on the PC1 axis is *Gorilla*. The mean of *Gorilla* is slightly above 0 on this axis but its range includes this value. The negative part of the *Gorilla* range overlaps slightly with the lower end of the range of *Pan*, however, the entire *Pan* distribution is on the negative side of the PC1 axis. The mean of *Pan* is closer to the mean PC1 value than that of *Pongo* which is located more negatively. However, the range of *Pan* contains the mean of *Pongo* and, similarly, the range of *Pongo* contains the centroid of *Pan*; the mean values are located on the periphery of the respective ranges. Finally *Theropithecus* is located in the negative range of the PC1 axis, its distribution falls entirely within the *Pongo* range and has some minor overlap with that of *Pan*. The mean of *Theropithecus* has a similar value to that of *Pongo*.

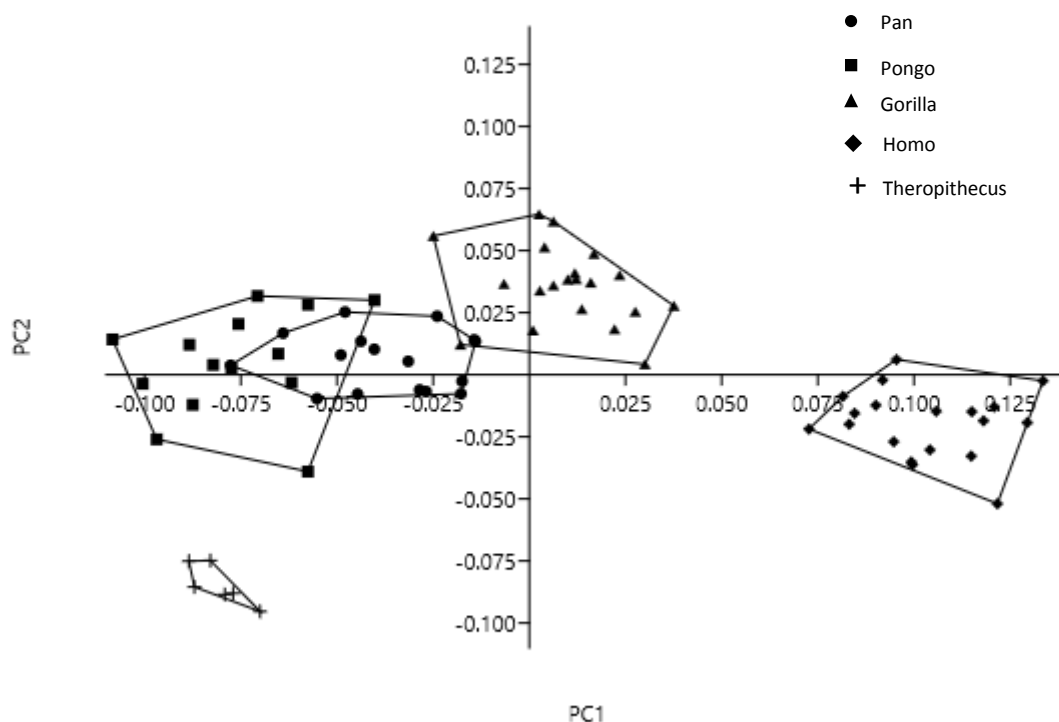


Figure 3.6.2. Principal component 1 vs. principal component 2 of all individuals for the first metatarsal.

PC2 most clearly separates *Theropithecus* from the other species, although there are some differences between the ape species. *Gorilla* occupies the most positive part of the PC2 axis. The mean of *Gorilla* is beyond the range of all other species. However, the negative range of the *Gorilla* distribution overlaps considerably with both *Pan* and *Pongo*, and marginally with that of *Homo*. *Pan* and *Pongo* have similar distributions to each other, and their means are situated fractionally above

the mean PC2 value; the range of *Pongo* is greater along PC2 and contains the entire *Pan* range within it. Of the apes *Homo* is situated most negatively on the PC2 axis. Its mean is below the mean PC2 value but the distribution of *Homo* overlaps with the distributions of all other apes. *Theropithecus* is situated on the extreme negative aspect of the PC2 axis and does not overlap with any other species. The higher principal components offer no revealing information about species distributions as all species ranges overlap with means around 0 on the axis.

3.6.1.2. Complete first metatarsal: species means

A principal components analysis was conducted on the Procrustes aligned landmarks of the species mean first metatarsal shapes. Only five principal components were extracted and the first four explain practically 100% of the variance. The first two account for 93.21% and the first three for 97.62%. These proportions are represented in figure 3.6.3.

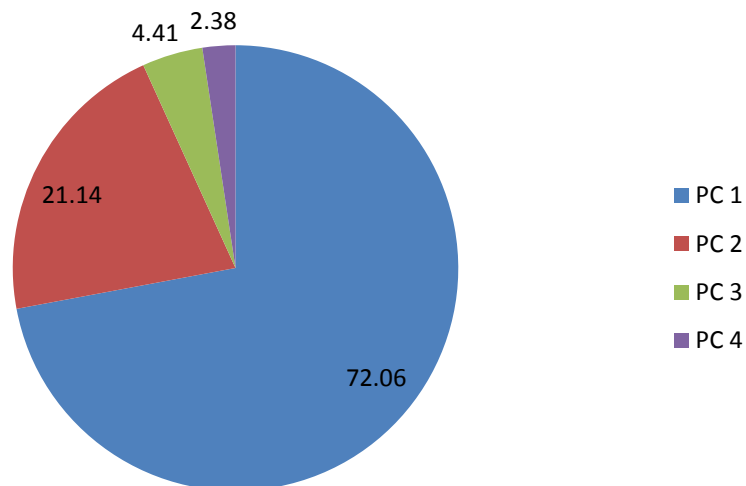


Figure 3.6.3. Percentage of the variance explained by each PC using only species mean shapes for the first metatarsal.

The first principal component extracted from analysis of the species mean shapes provides a similar distribution to that extracted for the complete dataset. *Homo* occupies the highest part of the axis in the positive range and is quite clearly distinct from all other species. *Theropithecus* occupies the extreme negative range of the axis but is not as clearly distinct from other species as *Homo*. All of the

non-human ape species cluster relatively close to 0 on the axis. Notably, *Gorilla* has a positive value which makes it the closest of the apes to *Homo* on this axis. *Pan* and *Pongo* each have negative values on PC1, although *Pongo* has a higher value than *Pan*. The second principal component also provides a distribution that is roughly the same when using species mean shapes as for the full dataset, although the axis is inverted. The axis most clearly separates *Theropithecus* from other species, occupying the extreme part of the positive range. *Homo* also lies in the positive range, thus *Homo* and *Theropithecus* are separated from the non-human apes on this axis. All of the non-human apes have values in the negative range. *Gorilla* has the highest value on the axis, while *Pan* and *Pongo* are more or less identical and lie closer to 0. The overall distribution of species mean shapes on PC1 v PC2 therefore corresponds well to the distribution presented earlier for the full sample. The higher principal components were not effective at distinguishing among species means, as all species means lay close to 0 for PC3 and PC4.

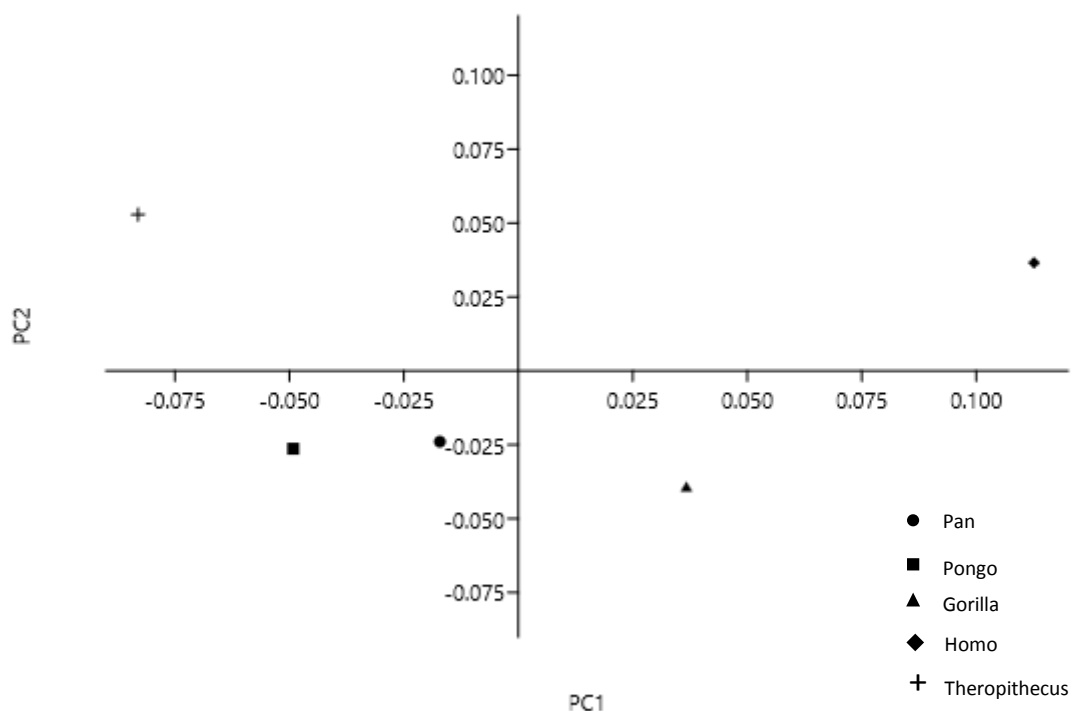


Figure 3.6.4. Principal component 1 vs. principal component 2 of species means for the first metatarsal.

3.6.1.3. Proximal first metatarsal: full sample

A principal components analysis was conducted using the Procrustes aligned landmarks of the proximal first metatarsal for all specimens. The first three principal components explained 59.03% of the variance in the dataset, the first five explained 73.86% and the first 11 explained 91.1% of the total variance. The remaining 8.9% of the variance was explained by principal components 12-76. The proportions of variance explained by each principal component are shown in Figure 3.6.5.

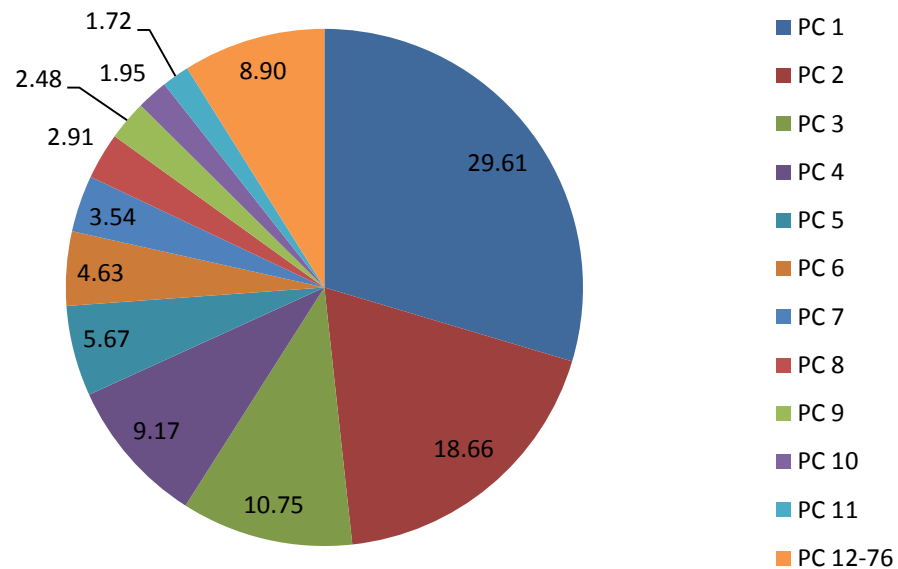


Figure 3.6.5. Percentage of the overall variance explained by each principal component for the proximal landmarks of the first metatarsal.

All species have relatively high ranges on the PC1 axis making it difficult to locate fine differences between groups (Fig. 3.6.6). However, some broad trends are apparent. *Homo* is located on the positive extreme of the axis overlapping slightly with *Pongo* and considerably with *Theropithecus*. *Pan* is located at the negative extreme of the PC1 axis but overlaps considerably with both *Pongo* and *Gorilla*, including the means of both species within its range. *Pongo* and *Gorilla* overlap considerably, though the *Gorilla* mean is located more negatively than the *Pongo* mean, lying approximately midway between the *Pan* and *Pongo* means. The *Theropithecus* distribution is located more positively than that of the African apes and *Pongo* but does overlap to a small degree with both *Pongo* and *Gorilla*. However, there is substantially greater overlap between the *Theropithecus* and *Homo* distributions. The *Oreopithecus* specimen is located on the negative end of the axis between the *Gorilla* and *Pongo* means.

The distribution of the sample when considering only the proximal first metatarsal differs somewhat from the distribution found when the entire bone was analysed. This is not an unexpected result as the shapes under consideration are markedly different (i.e. whole MT1 vs. proximal MT1). However, it is still useful to compare the differences. *Homo* is still separated from the other species quite clearly, however, whereas *Theropithecus* was located on the extreme opposite end of the axis when the entire bone was studied, it is the most closely associated with *Homo* when only the proximal articular surface is considered. *Gorilla* is not closest to *Homo* on the first principal component, indicating that the proximal facet in isolation differs somewhat between the two. Finally the ranges appear much larger when only the proximal landmarks are considered, and they overlap to a far greater extent, than when the entire bone is considered.

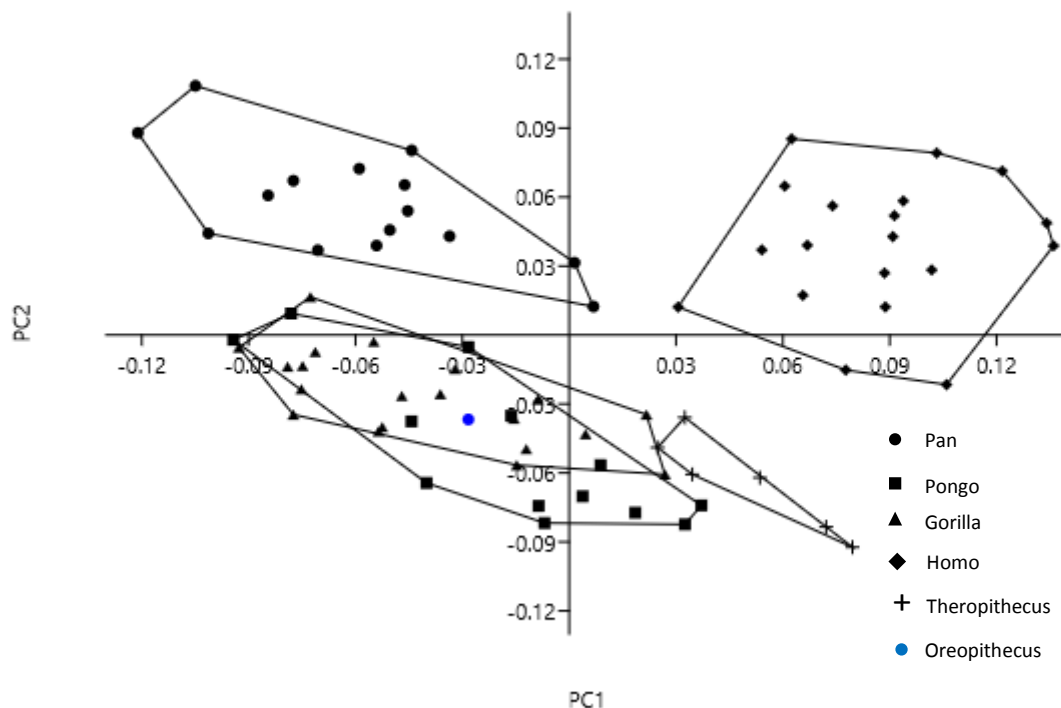


Figure 3.6.6. Principal component 1 vs. principal component 2 of all individuals for the proximal landmarks of the first metatarsal.

The ranges of the groups are narrower on the PC2 axis and this provides a clearer separation of species. *Pan* and *Homo* are distributed on the positive end of the PC2 axis. The mean of *Pan* has a higher value than that of *Homo* but there is substantial overlap between the two species. The distributions of *Pan* and the remaining ape species are adjacent, while *Homo* overlaps both groups.

The *Gorilla* distribution is located mainly on the negative aspect of the axis, its mean has a value just below 0 on the PC2 axis. The *Pongo* mean is relatively more negative than that of *Gorilla* but there is substantial overlap between the two distributions. The *Theropithecus* distribution overlaps considerably with that of *Pongo* and their means are also similar. However, the *Theropithecus* distribution is clearly furthest from 0. The *Oreopithecus* specimen is located in the negative region of the PC2 axis between the *Gorilla* and *Pongo* means. The second principal component thus gives a different distribution to the one found when the entire bone was analysed. The second principal component for the proximal landmarks fails to clearly separate *Theropithecus* and *Gorilla* from the other species and instead separates *Homo* and *Pan* from the other groups. The higher principal components are poor at illuminating differences between species or *Oreopithecus*. The ranges of the distributions are high and all overlap with low values close to 0 on the axis.

3.6.1.4. Proximal first metatarsal: species means and *Oreopithecus*

A principal components analysis was conducted on the Procrustes aligned landmarks of the proximal first metatarsal using the species mean shapes only. Six principal components were extracted. The first three explained 87.98% of the total variance in the dataset, the first four explained 95.82% of the variance and the first five explained practically 100% of the variance. The amount of variance explained by the sixth principal component was negligible. The proportions of the variance explained by each principal component are shown in Figure 3.6.7.

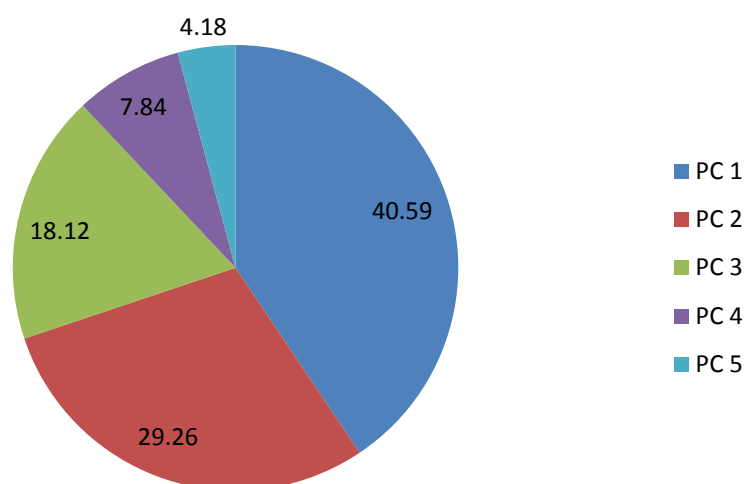


Figure 3.6.7. Percentage of the variance explained by each PC using only species mean shapes for the proximal landmarks of the first metatarsal.

The distribution of species means on PC1 is roughly similar to the distribution using all individuals for the proximal landmarks of the first metatarsal, although the axis has been inverted (Figure 3.6.8). *Homo* occupies the extreme part of the negative range of the axis and its closest neighbour is *Theropithecus*. All other species are located on the positive aspect of PC1. *Gorilla*, *Pongo*, and *Pan* are very similar on PC1, as they are when all individuals are analysed together. Furthermore, *Pan* has the highest value and is located furthest from *Homo*. The position of *Oreopithecus* is markedly different when compared to the species mean shapes. It occupies the extreme positive aspect of the PC1 axis, clearly separated from all non-human ape species and, indeed, all species.

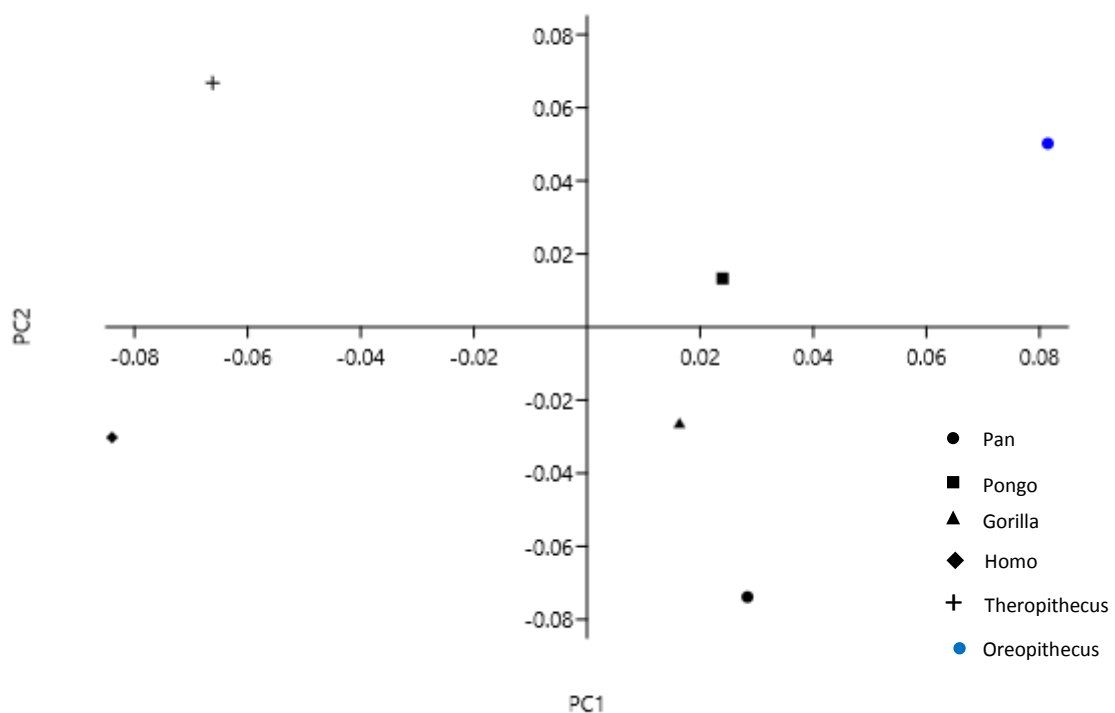


Figure 3.6.8. Principal component 1 vs. principal component 2 of species means for the proximal landmarks of the first metatarsal.

The second principal component also offers a broadly similar distribution to the one extracted when the full dataset was used, although its axis is also inverted. *Pan* has the highest value in the negative range of the axis while *Theropithecus* has the highest value in the positive range, but this is much clearer when only species means are taken into account. *Homo* is the closest species to *Pan*, but the two are more distinct when compared only by their mean shapes. *Gorilla* is located somewhat differently when only species means were analysed. It has a similar value to *Homo* and is clearly

positioned on the negative aspect of the axis away from *Pongo*, whereas it was closely associated with *Pongo* and separated from *Homo* and *Pan* when the full sample was analysed. *Pongo* is located similarly in this analysis, in the opposite half of the axis to *Homo* and *Pan*, although somewhat more distinct from *Oreopithecus*. *Oreopithecus* has a high value on the positive aspect of the axis, close to that of *Theropithecus*.

3.6.1.5. Distal first metatarsal: full sample

A principal components analysis was conducted using the Procrustes aligned landmarks of the distal first metatarsal for all specimens. The first three principal components explained 54.97% of the variance in the dataset, the first five explained 66.6%, the first 10 explained 82.41%, and the first sixteen explained 90.38% of the total variance. The remaining 9.62% of the variance was explained by principal components 17-76. The proportions of variance explained by each principal component are shown in Figure 3.6.9.

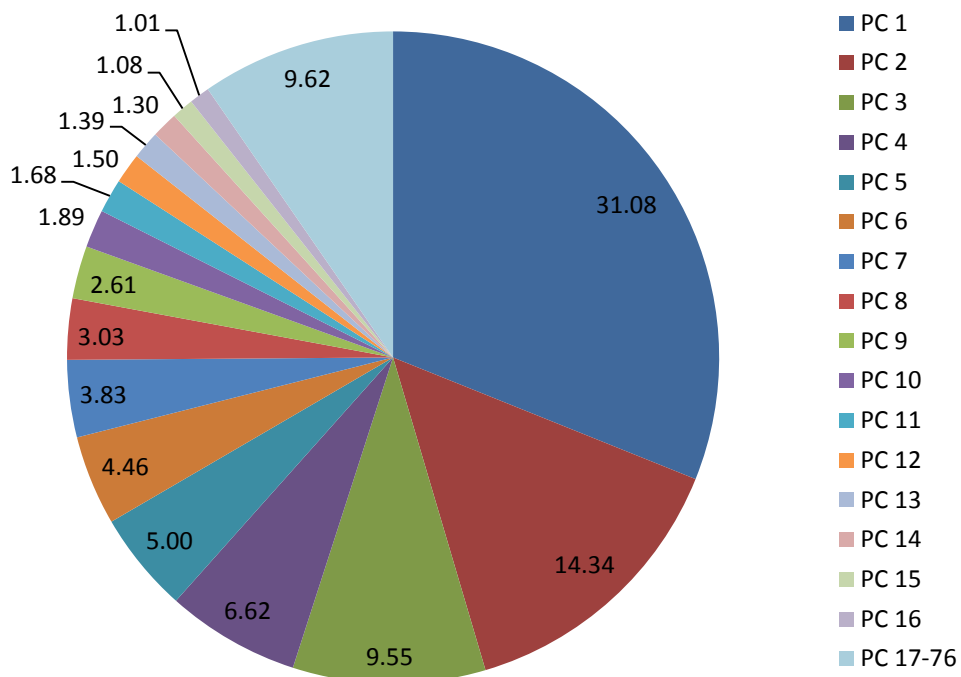


Figure 3.6.9. Percentage of the overall variance explained by each principal component for the distal landmarks of the first metatarsal.

The first principal component reveals a distribution which is quite unlike the distribution found when the entire bone was analysed. The first two principal components are plotted against each other in Figure 3.3.10. *Homo* is not clearly distinct from other species on the first principal component, instead overlapping considerably with *Pan* and slightly with *Gorilla* and *Theropithecus* at the lower and upper ends of its range respectively. PC1 one most clearly differentiates *Theropithecus*, with the highest distribution on the positive aspect of the axis, from *Pongo*, with the highest distribution on the negative aspect of the axis. However, neither species is clearly distinct and both overlap with the distributions of other species. *Gorilla* and *Pan* have broadly similar values around 0 on the PC1 axis making them intermediate between *Pongo* and *Theropithecus*. *Homo* has a distribution which is entirely on the positive aspect of the axis, although it overlaps considerably with the African apes, and a little with *Theropithecus*. *Oreopithecus* has a value on the positive aspect of the axis, well within the ranges of both *Pan* and *Homo* and clearly outside the ranges of *Pongo* and *Theropithecus*.

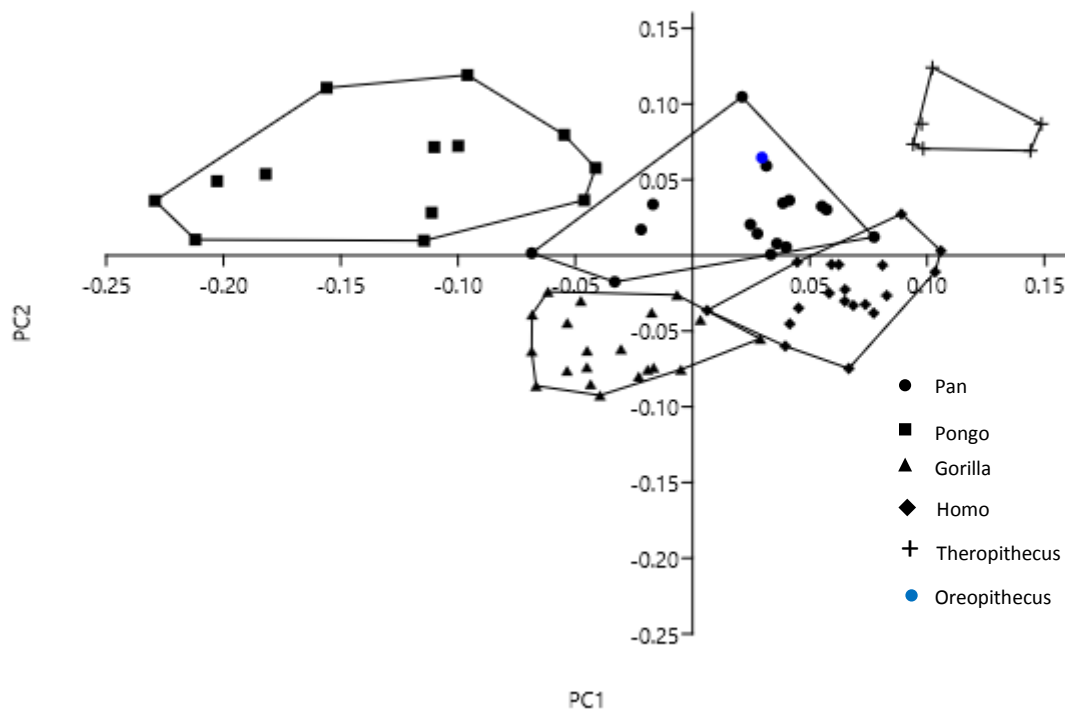


Figure 3.6.10. Principal component 1 vs. principal component 2 of all individuals for the distal landmarks of the first metatarsal.

The second principal component is also quite different from the second principal component extracted for the entire first metatarsal. However, there is one notable similarity. The axis clearly separates *Gorilla* from *Theropithecus*. However, this distinction is not as clear when only the distal landmarks are used. There is considerable overlap between *Theropithecus* and *Pan* and *Pongo* on the positive aspect of the axis, and considerable overlap between *Gorilla* and *Homo* on the negative aspect of the axis. The axis does seem to show a general separation of *Homo* and *Gorilla* from the other species and taken together the first two principal components do separate each species into distinct groups. *Oreopithecus* lies within the ranges of both *Pan* and *Gorilla* on PC2, and overall lies in the range of *Pan* when both axes are considered together. The higher principal components offer poor distinction between species, as all groups cluster around 0 on the axes and exhibit considerable overlap of their ranges.

3.6.1.6. Distal first metatarsal: species means and *Oreopithecus*

A principal components analysis was conducted on the Procrustes aligned landmarks of the distal first metatarsal using the species mean shapes only. Six principal components were extracted. The first three explained 90.36% of the total variance in the dataset, the first four explained 96.44% of the variance and the first five explained practically 100% of the variance. The amount of variance explained by the sixth principal component was negligible. The proportions of the variance explained by each principal component are shown in Figure 3.6.11.

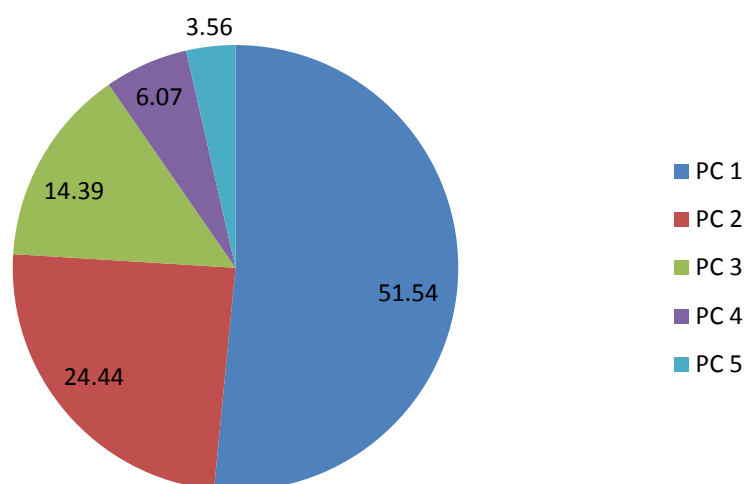


Figure 3.6.11. Percentage of the variance explained by each PC using only species mean shapes for the distal landmarks of the first metatarsal.

The first principal component approximates the first principal component extracted from the full sample (Figure 3.6.12). *Theropithecus* and *Pongo* occupy the positive and negative extremes respectively, although they are more clearly distinct from other species when only species means are examined. *Pan* has a value close to 0 on PC1 but lies just inside the positive range of the axis. *Homo* has a slightly higher value, lying between *Pan* and *Theropithecus* but clearly closer to *Pan*. *Gorilla* lies in the negative range of the axis roughly midway between *Pan* and *Pongo*. *Oreopithecus* has a higher value than *Homo* on the positive aspect of the PC1 axis, unlike its location when the full sample is analysed. However, it is clearly closer to *Homo* and *Pan* than it is to *Theropithecus*.

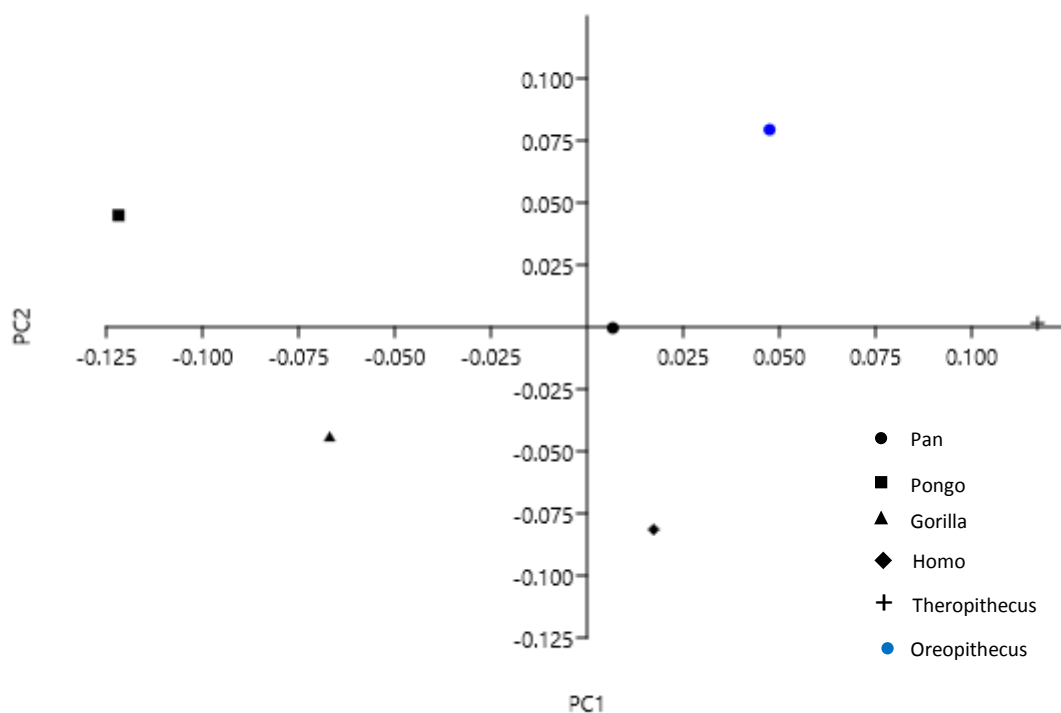


Figure 3.6.12. Principal component 1 vs. principal component 2 of species means for the distal landmarks of the first metatarsal.

The second principal component is similar to the second principal component extracted from the full data set in that it clearly separates *Homo* and *Gorilla* from the other species in the negative range of the axis, although in the case of species means *Homo* is more obviously distinct. *Pongo* is the most distinct of the extant species on the positive aspect of the axis, while *Pan* and *Theropithecus* have values at 0 on the axis, unlike the full sample when *Theropithecus* is relatively distinct. *Oreopithecus* lies on the extreme positive part of the axis, clearly distinct from other species, but closest to *Pongo*

on this axis. PC3 clearly separates *Pongo* and *Theropithecus* on the negative aspect of the axis from *Gorilla* and *Oreopithecus* on the positive half of the axis (Fig. 3.6.13), while *Pan* and *Homo* both lie close to 0. The higher principal components are of little value in differentiating between species as all species means lie close to 0.

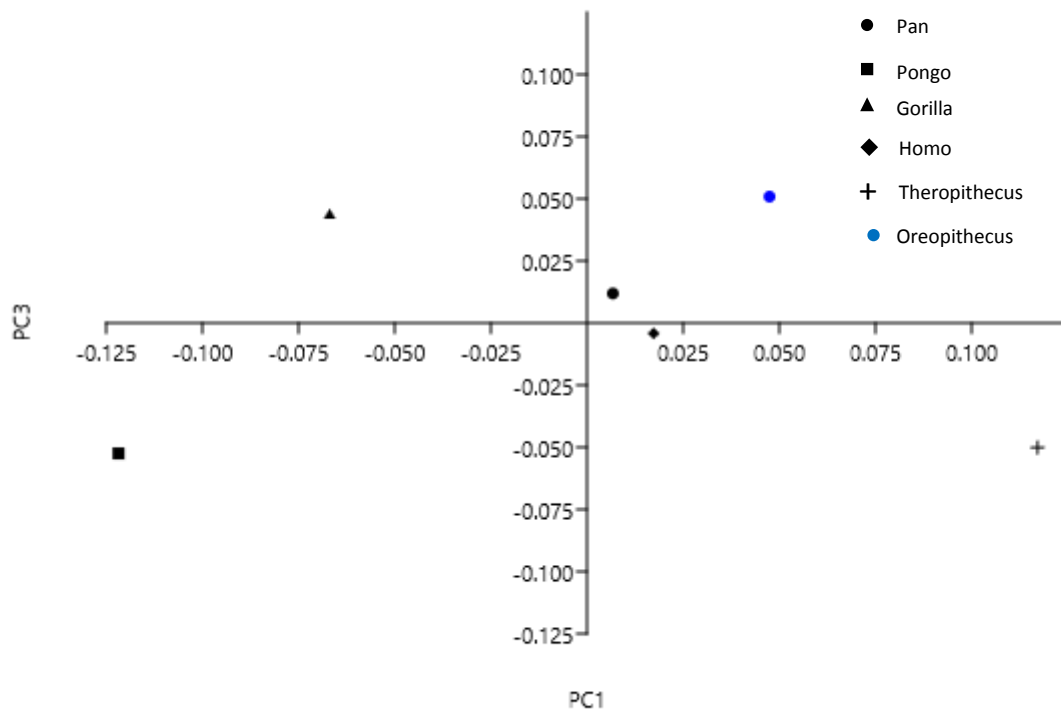


Figure 3.6.13. Principal component 1 vs. principal component 3 of species means for the distal landmarks of the first metatarsal.

3.6.2. Statistical tests

3.6.2.1. Complete first metatarsal

To assess the similarities and differences between extant species complete first metatarsals the full Procrustes distances between species mean shapes were calculated and examined. The Procrustes distances are presented in Table 3.6.1. *Pan* and *Pongo* were mutually closest to one another, and both were subsequently closest to *Gorilla*. Therefore, hypothesis 1 is disconfirmed for the first metatarsal; the African apes are not most similar to one another of all extant species. This indicates that the morphology of the first metatarsal varies substantially between them despite their similar ecology, locomotion and evolutionary history. The reasons for this will be considered along with warps between the mean shapes. The African apes and *Pongo* were mutually closest to one another to the exclusion of *Homo* and *Theropithecus*. Therefore, hypothesis 2 was accepted for the first metatarsal; the non-human apes are morphologically similar, likely reflecting their considerable arboreality in contrast to the terrestriality of *Homo* and *Theropithecus*. *Theropithecus* was found to be more similar to both *Pan* and *Pongo* than *Homo* was. This disconfirms hypothesis 3 providing no support to the proposition that the cercopithecoid species will be substantially more different than the hominoid species studied. The reasons for the closer similarity of *Homo* and *Gorilla* will be considered below. Following permutation tests of the pairwise distances between individuals each comparison was associated with a p value of <0.0001 and therefore all species can be considered to be significantly different from one another in shape of the first metatarsal.

	Pan	Pongo	Gorilla	Homo	Thero
Pan	0	0.05807	0.067542	0.145467	0.104359
Pongo	0.05807	0	0.09862	0.174107	0.093926
Gorilla	0.067542	0.09862	0	0.111389	0.150797
Homo	0.145467	0.174107	0.111389	0	0.196178
Thero	0.104359	0.093926	0.150797	0.196178	0

Table 3.6.1. Procrustes distances amongst species mean shapes for the complete first metatarsal. Reading across the rows, the two closest species to each species are represented. The closest is highlighted in bold red, the second closest in bold black.

Differences in size were assessed using permutation tests to compare the likelihood that two species were drawn from the same sample (and therefore have the same mean). This resulted in ten consecutive tests and therefore the significance threshold was set to 0.005 following Bonferroni correction for multiple comparisons. It was found that *Homo* and *Gorilla* were not significantly

different from one another in size with an associated p value of 0.6031. However, the *Gorilla* mean (386.5) was slightly higher than that of *Homo* (380.5). This result means that hypothesis 8 is confirmed for the first metatarsal; *Gorilla* and *Homo* are the largest of the extant species. *Gorilla* and *Homo* were larger than all other species at $p = <0.0001$. *Pan* (341.1) was found to be significantly larger than *Pongo* (305.2) with an associated p value of 0.0007. *Theropithecus* (219.5) was significantly smaller than all other species with associated p values of <0.0001 . Thus, the hierarchy of size relationships can be presented as follows: *Gorilla/Homo* > *Pan* > *Pongo* > *Theropithecus*.

3.6.2.2. Proximal first metatarsal

The pairwise Procrustes distances between species mean and fossil proximal first metatarsal shape are presented in Table 3.6.2. *Pan* and *Pongo* are each closest in shape to *Gorilla*. However, the proximity of *Pongo* to *Gorilla* is marginally closer than between *Pan* and *Gorilla*. Therefore hypothesis 1 is disconfirmed for the proximal first metatarsal; the African apes do not share the closest morphology among the extant species indicating that there is some substantial difference in function of the hallux between the two species. However, the African apes and *Pongo* do form a morphologically similar grouping to the exclusion of *Homo* and *Theropithecus*. Therefore, hypothesis 2 is accepted for the proximal first metatarsal; the non-human apes are mutually more similar to one another than to any other extant species. One possible explanation for this is that the non-human apes spend considerable time in an arboreal setting compared to *Homo* and *Theropithecus*, which are exclusively terrestrial. *Theropithecus* was found to be closer to *Pongo* and *Gorilla* than *Homo* was, and closer to *Homo* than either *Pan* or *Gorilla* was. Therefore, hypothesis 3 was rejected for the proximal first metatarsal; *Theropithecus* is not the most different of the extant species indicating that the differences observed in all extant species cannot be explained in terms of plantigrady vs. digitigrady. For example, the fact that *Homo* is uniquely derived to bipedalism, and the effect this has on the pedal skeleton, will have profound effects on the shape relationships beyond plantigrady/digitigrady or hominoid/cercopithecoid.

Oreopithecus is closest to *Pongo* and then to *Gorilla*, although its distance from *Gorilla* was substantially greater than its distance from *Pongo*. The distance of *Oreopithecus* from *Pongo* was in the range of distances found amongst the extant ape species. *Oreopithecus* was further from *Theropithecus* than from any non-human ape. Thus, hypothesis 4 is confirmed for the proximal first metatarsal; *Oreopithecus* is not cercopithecoid-like in its pedal anatomy. Hypothesis 5 is rejected for

the proximal first metatarsal; *Oreopithecus* is not most similar in shape to one of the African apes. The close proximity of *Oreopithecus* to *Pongo* is interesting because the medial cuneiform was most similar in shape to *Pan*. The implications of this are difficult to comprehend and are considered below. Permutation tests were conducted on the pairwise Procrustes distances between individual specimens and revealed that all extant species were significantly different from one another with p values of <0.0001. The significance of the Procrustes distance from *Oreopithecus* to its closest neighbours was assessed by calculating the Mahalanobis distance of the specimen from the species means. It was found that *Oreopithecus* was significantly different from *Gorilla* with a Mahalanobis distance of 39.585, which is 6.29 standard deviation units from the *Gorilla* mean with an associated p value of 0.0005. *Oreopithecus* was not found to be significantly different in shape from *Pongo* with a Mahalanobis distance of 7.472, which is 2.73 standard deviation units from the mean with a p value of 0.25.

	Pan	Pongo	Gorilla	Homo	Thero	Oreo
Pan	0	0.114558	0.091427	0.14678	0.171992	0.149278
Pongo	0.114558	0	0.084496	0.138853	0.128769	0.105077
Gorilla	0.091427	0.084496	0	0.146365	0.136017	0.139624
Homo	0.14678	0.138853	0.146365	0	0.140594	0.185852
Thero	0.171992	0.128769	0.136017	0.140594	0	0.169796
Oreo	0.149278	0.105077	0.139624	0.185852	0.169796	0

Table 3.6.2. Procrustes distances amongst species mean shapes for the proximal first metatarsal. Reading across the rows, the two closest species to each species are represented. The closest is highlighted in bold red, the second closest in bold black.

Differences in the size of the proximal surface of the first metatarsal were compared using permutation tests to compare the means of extant species groups. It was found that *Homo* and *Gorilla* were not significantly different size ($p = 0.1367$, although *Gorilla* (97.6) had a marginally larger mean than *Homo* (92.9). Both species had significantly larger means than all other extant species with associated p values of <0.0001. Therefore, hypothesis 8 was confirmed for the proximal first metatarsal; *Homo* and *Gorilla* are the largest of the extant species. *Pan* (73.2) was found to be significantly larger than *Pongo* (61.2) with a p value of <0.0001. *Theropithecus* (33) was found to have a significantly smaller mean centroid size than each other extant species with consistent p values of <0.0001. Therefore, hypothesis 9 was accepted for the proximal first metatarsal; *Theropithecus* is the smallest extant species in the study. The hierarchy of size can be presented as follows: *Gorilla/Homo* > *Pan* > *Pongo* > *Theropithecus*. The *Oreopithecus* specimen was assessed by calculating its z score in comparison to each species mean, and from this calculating the associated p value. It was found that

the proximal first metatarsal of *Oreopithecus* was significantly smaller than *Homo* ($z = 5.382$; $p = <0.00001$), *Gorilla* ($z = 4.353$; $p = <0.00001$), and *Pan* ($z = 4.812$; $p = <0.00001$). *Oreopithecus* was also found to be significantly larger than *Theropithecus* ($z = 7.666$; $p = <0.00001$). *Oreopithecus* and *Pongo* were not found to be significantly different in size of the proximal first metatarsal ($z = 2.14$; $p = 0.0162$) with a significance threshold of $p=0.01$ following Bonferroni correction for multiple comparisons. Therefore, hypothesis 10 is rejected for the proximal first metatarsal; *Oreopithecus* is smaller than *Pan*. However, *Oreopithecus* falls on the lower end of the *Pongo* range of centroid sizes again making its pedal bones unusually small.

3.6.2.3. Distal first metatarsal

Table 3.6.3 presents the Procrustes distances between all species means and *Oreopithecus*. The closest species to *Gorilla* was *Pan*, while in contrast the closest species to *Pan* was *Homo* (though it was narrowly followed by *Gorilla*). Therefore, hypothesis 1 is not accepted for the distal first metatarsal; the African apes are not more similar to each other than to any other extant species. However, there is still a great deal of similarity between the two which will be discussed below. Both *Pan* and *Gorilla* are more similar in shape to *Homo* than either is to *Pongo*. Therefore, hypothesis 2 is rejected for the distal first metatarsal; the non-human apes do not share a closer morphology to one another excluding *Homo* and *Theropithecus*. These differences most likely relate to the reduced function and size of the first metatarsal in *Pongo*. It indicates that the morphology of the distal first metatarsal is not a good indicator of more arboreal vs. more terrestrial species in this study. *Pongo* is also more different in shape to either *Pan* or *Homo* than either is to *Theropithecus*. Therefore, hypothesis 3 is rejected for the distal first metatarsal; *Theropithecus* is not more different in shape than any other extant species.

Pan is the closest neighbour of *Oreopithecus*, and the Procrustes distance between them is similar to that separating the African apes and *Homo*. However, its next closest neighbour (*Theropithecus*) was substantially further away. Therefore, hypothesis 4 is confirmed for the distal first metatarsal; *Oreopithecus* does not resemble a cercopithecoid. Simultaneously, hypothesis 5 is confirmed; *Oreopithecus* is most similar in distal first metatarsal shape to *Pan*. Permutation tests of pairwise Procrustes distances between extant groups revealed that all extant species were significantly different from one another with p values of <0.0001 . *Oreopithecus* was not found to be significantly different in distal first metatarsal shape from *Pan*. The Mahalanobis distance of the *Oreopithecus*

specimen from the *Pan* mean was 11.252, which is 3.354 standard deviation units and a p value of 0.2.

	Pan	Pongo	Gorilla	Homo	Thero	Oreo
Pan	0	0.159806	0.111669	0.111105	0.138668	0.117072
Pongo	0.159806	0	0.14896	0.197118	0.24515	0.201794
Gorilla	0.111669	0.14896	0	0.129483	0.211967	0.176926
Homo	0.111105	0.197118	0.129483	0	0.153187	0.17418
Thero	0.138668	0.24515	0.211967	0.153187	0	0.152029
Oreo	0.117072	0.201794	0.176926	0.17418	0.152029	0

Table 3.6.3. Procrustes distances amongst species mean shapes for the distal first metatarsal. Reading across the rows, the two closest species to each species are represented. The closest is highlighted in bold red, the second closest in bold black.

Differences in size between species were assessed using permutation tests to find significant differences in mean centroid size. It was found that *Homo* (118.8) had a significantly larger mean than *Gorilla* (101.2) with a p value of <0.0001. Both *Homo* and *Gorilla* had significantly larger means than all other extant species with associated p values of <0.0001. Therefore, hypothesis 8 was confirmed for the distal first metatarsal; *Homo* and *Gorilla* are the largest of the extant species. *Pan* (81) was found to be significantly larger than *Pongo* (65.8) with a p value of <0.0001. *Theropithecus* (38.3) had a significantly smaller mean than all other extant species with associated p values of <0.0001. Therefore, hypothesis 9 was confirmed for the distal first metatarsal; *Theropithecus* is the smallest of all extant species. The z score of the *Oreopithecus* specimen from the species means was calculated and converted to a p value expressing the likelihood that the *Oreopithecus* specimen is significantly different from the mean of each species. It was found that *Oreopithecus* was significantly smaller than *Homo* ($z = 6.016$; $p = <0.0001$), *Gorilla* ($z = 3.757$; $p = <0.0001$), and *Pan* ($z = 4.433$; $p = <0.0001$). *Oreopithecus* was also found to be significantly larger than *Theropithecus* ($z = 7.12$; $p = <0.0001$). However, *Oreopithecus* was not found to be significantly smaller in size than *Pongo* ($z = 0.83$; $p = 0.2$). Therefore, hypothesis 10 is rejected for the distal first metatarsal; *Oreopithecus* is not comparable in size to *Pan*. However, it was found to be of a similar size to *Pongo* which may be indicative of more robust hallux compared to the size of the tarsals.

3.6.3. Visualisation of shape differences

In order to describe the differences in shape it is necessary to use some technical terminology. Figures 3.6.14 and 3.6.15 illustrate what these terms are referring to.

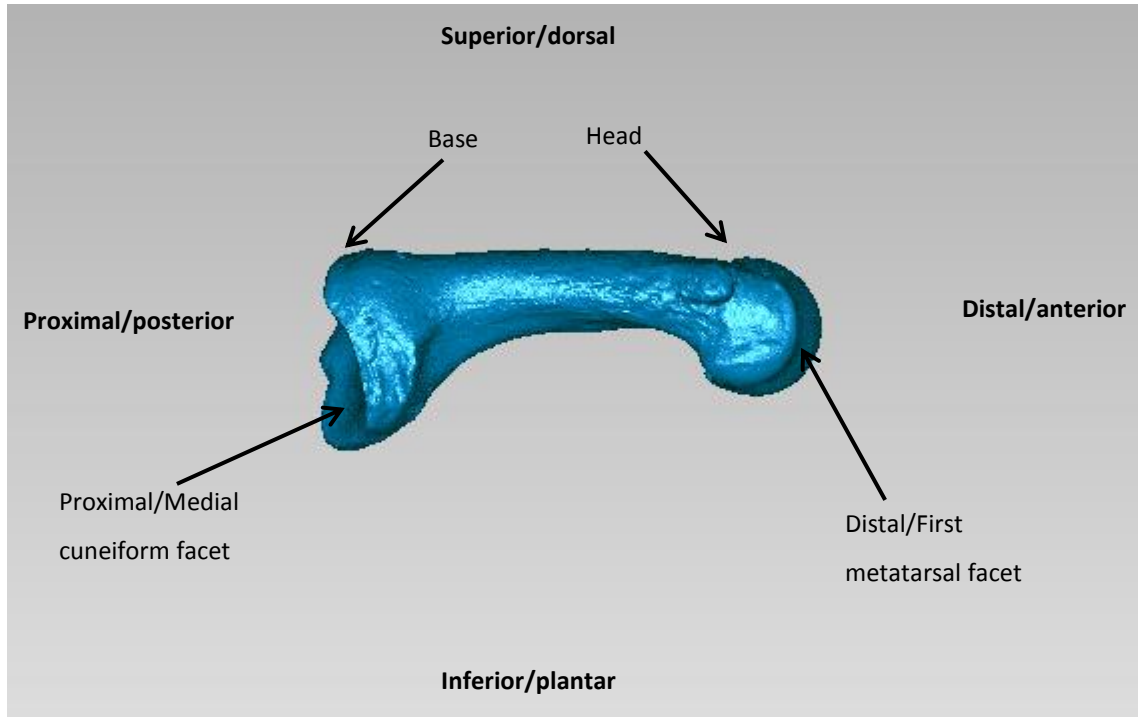


Figure 3.6.14. Medial view of the first metatarsal displaying terminology used to describe shape differences.

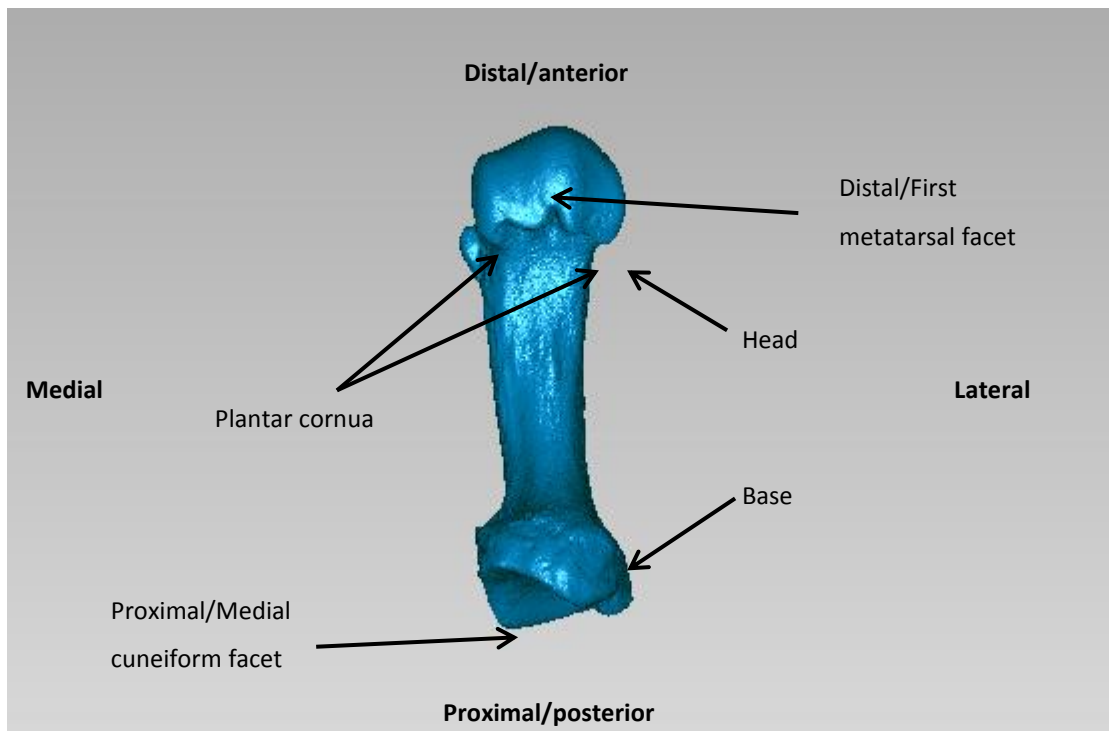


Figure 3.6.15. Inferior view of the first metatarsal displaying terminology used to describe shape differences.

3.6.3.1. Complete first metatarsal

From *Pan* to *Gorilla*

There are numerous differences between the two species, the most obvious of which relate to the stout appearance of the bone in *Gorilla*. The first metatarsal is wider, deeper, and shorter at both its proximal and distal ends in *Gorilla* than is the case in *Pan* (Figure 3.6.16A). Although no landmarks were placed on the diaphysis, these differences in overall bone dimensions are apparent from the relative sizes of, and distances between, the proximal and distal facets. The medial cuneiform facet is narrower across its mediolateral, but larger across its superoinferior, dimension in *Gorilla* relative to the overall size of the bone. However, the facet retains its helical form and is not noticeably flatter in *Gorilla*, indicating that the articulation between the first metatarsal and medial cuneiform is conducive to considerable flexion and extension with conjunct internal and external rotation. The medial cuneiform facet is rotated externally in *Gorilla* (Figure 3.6.16B), bringing the long axis of the proximal facet closer to parallel with the long axis of the distal facet, while in *Pan* these facets are more oblique to one another. The head of the first metatarsal has a much greater surface area in *Gorilla* and the plantar cornua are more extensive and well-defined (Figure 3.6.16A). The medial and lateral edges of the distal facet are not as tightly curved in *Gorilla* as they are in *Pan* giving the head of the first metatarsal a less tightly curved profile from superior to inferior. The head of the bone is also moderately elevated towards the dorsal side of the bone and rotated in the same direction suggesting that the degree of curvature of the first metatarsal from proximal to distal is slightly lower in *Gorilla* than *Pan*.

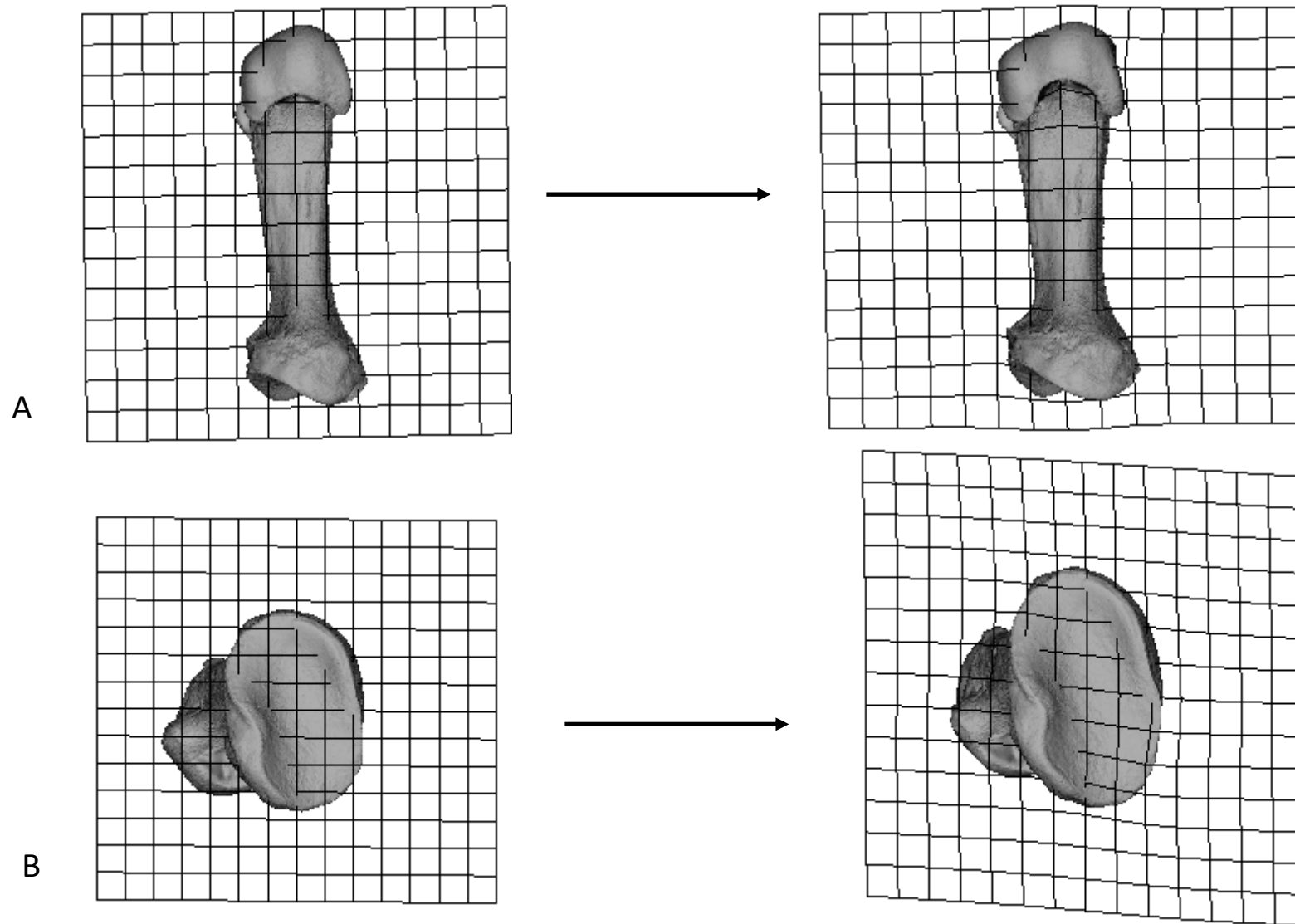


Figure 3.6.16. Demonstration of the warp from the *Pan* mean first metatarsal (left) to the *Gorilla* mean (right). A) Inferior view. B) Proximal view

From *Pan* to *Pongo*

There are marked differences between the first metatarsal of *Pan* and *Pongo*. Most notably the overall size of the bone in *Pongo* is somewhat reduced; the bone is shorter, narrower and shallower than it is in *Pan*. Therefore, by inference from the warping from *Pan* to *Gorilla*, the first metatarsal of *Pongo* is more distinct from *Gorilla* in these same attributes. The proximal facet is greatly reduced in size in *Pongo*, its inferolateral corner is particularly poorly developed relative to *Pan*, as is the inferior half of the facet overall (Figure 3.6.17A). However, the facet does retain its general helical appearance indicative of its function in flexion with conjunct internal rotation, in which respect it is similar to the African apes. Despite its similar helical form, the medial cuneiform facet is shallower and the degree of external rotation of the facet relative to the distal facet is slightly lower giving the long axes of the proximal and distal facets a more parallel alignment. The head of the first metatarsal is also greatly reduced in size. This is particularly apparent on the medial half of the head. The medial plantar cornu of the head is markedly less well developed than the lateral from inferior view (Figure 3.6.17B). From this view it is also apparent that the head has a medially directed flexion relative to the base of the bone. Similarly, the head is flexed and rotated inferiorly relative to the base indicating that the bone is more curved in *Pongo* than it is in the African apes.

From *Homo* to *Gorilla*

The key difference between the *Homo* and *Gorilla* first metatarsals is the stouter appearance of the bone in *Homo*. The distance between the proximal and distal surfaces in *Gorilla* is relatively greater, as is the superoinferior distance between the superior and inferior borders of the proximal and distal facets. The proximal articular surface is roughly comparable in size between the two species, however the head of the first metatarsal is strikingly smaller in *Gorilla*. Thus, overall the first metatarsal of *Gorilla* is more gracile than that of *Homo*. The proximal articular surface is helical in appearance in *Gorilla*, unlike the flatter appearance in *Homo*. It is also rotated internally relative to the head of the bone while the long axes of the proximal and distal facets are close to parallel in *Homo* (Figure 3.6.18A). The head of the bone is flexed and rotated inferiorly in *Gorilla* relative to *Homo* indicating that the bone is more curved in *Gorilla*. The degree of flexion between the dorsal and plantar surfaces of the head is also greater in *Gorilla* (Figure 3.6.18B).

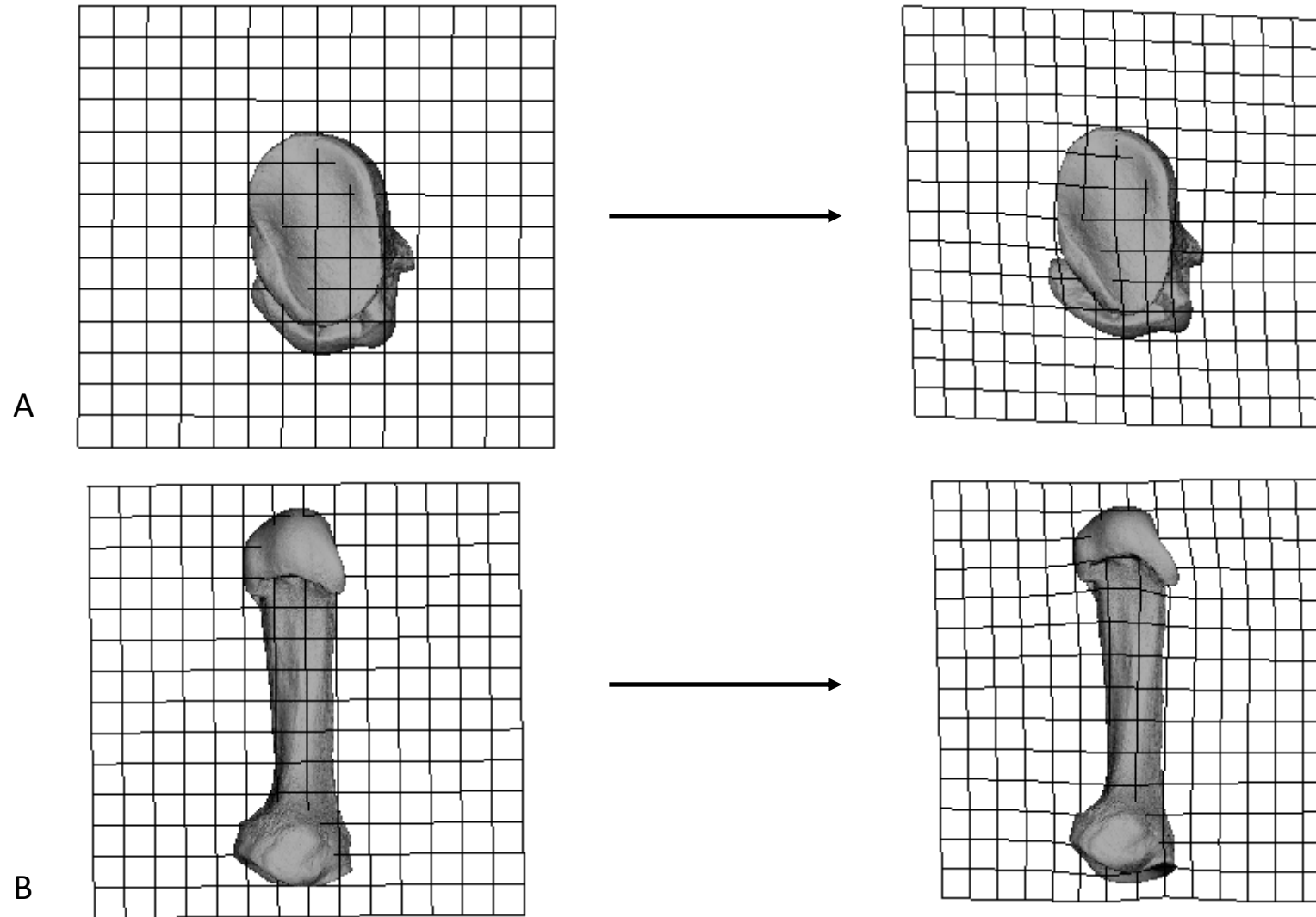


Figure 3.6.17. Demonstration of the warp from the *Pan* mean first metatarsal (left) to the *Pongo* mean (right). A) Proximal view. B) Inferior view

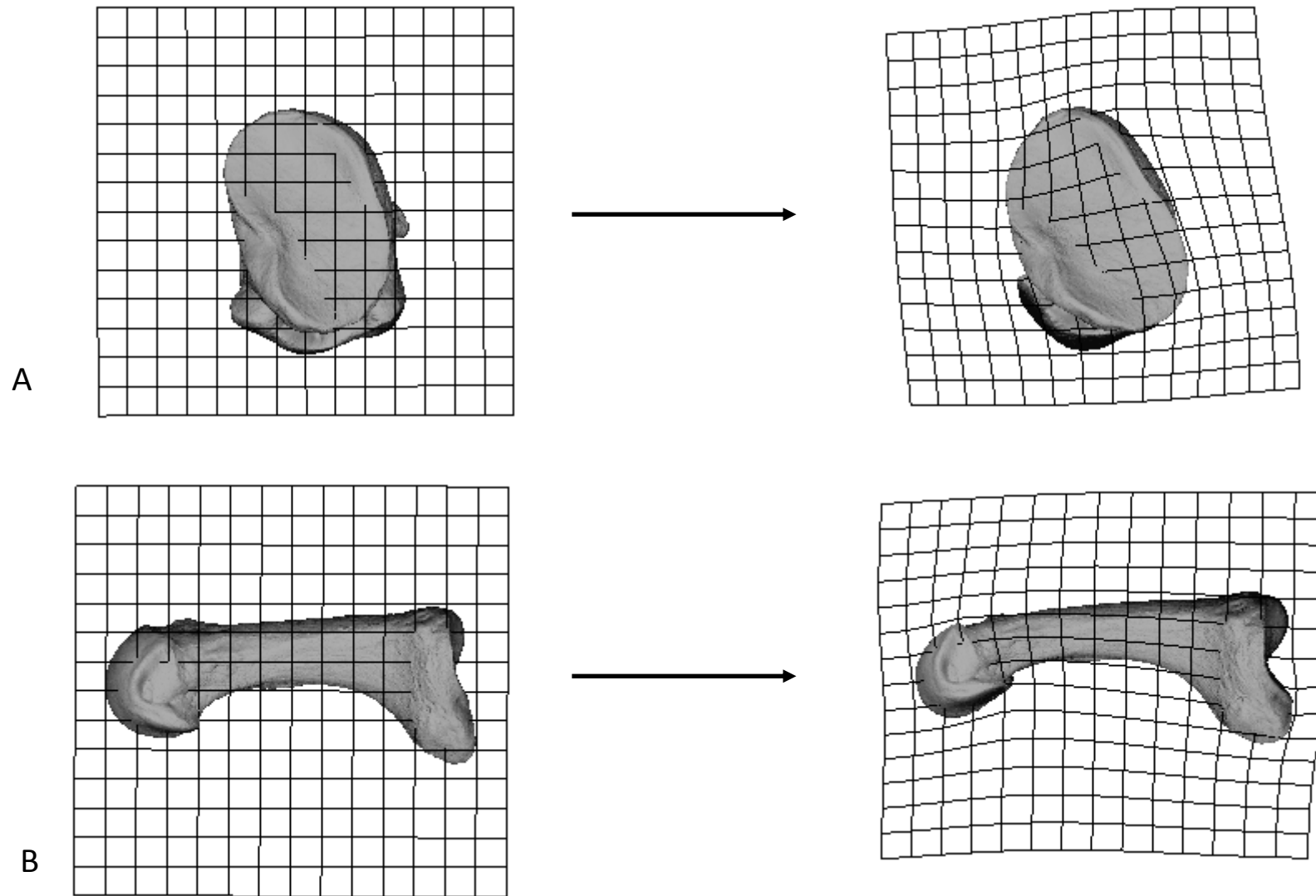


Figure 3.6.18. Demonstration of the warp from the *Homo* mean first metatarsal (left) to the *Gorilla* mean (right). A) Proximal view. B) Medial view

From *Pongo* to *Theropithecus*

The first metatarsal of *Theropithecus* is markedly smaller than *Pongo* in both its mediolateral and superoinferior dimensions. The proximodistal length of the bone is also smaller in *Theropithecus*, but to a much more modest degree. This gives the bone a highly gracile appearance in comparison to *Pongo*. The proximal facet is greatly reduced in size relative to the length of the bone and also lacks the helical form found in *Pongo*. The proximal facet in *Theropithecus* instead bears constriction on both the medial and lateral midpoints splitting the facet into superior and inferior halves and is flatter overall (Figure 3.6.19A). The head of the first metatarsal is also small in *Theropithecus* relative to the length of the bone. Additionally, the plantar surface of the head lacks any plantar cornua, distinguishing it from all ape species. The head of the first metatarsal is rotated and flexed toward the dorsal side of the bone (Figure 3.6.19B) indicating that the bone is straighter in *Theropithecus* than it is in *Pongo*. The superior border of the proximal facet is placed closer to the distal end of the bone giving the facet an anteriorly directed slope from inferior to superior. This feature contributes to the straighter appearance of the bone from medial and lateral view.

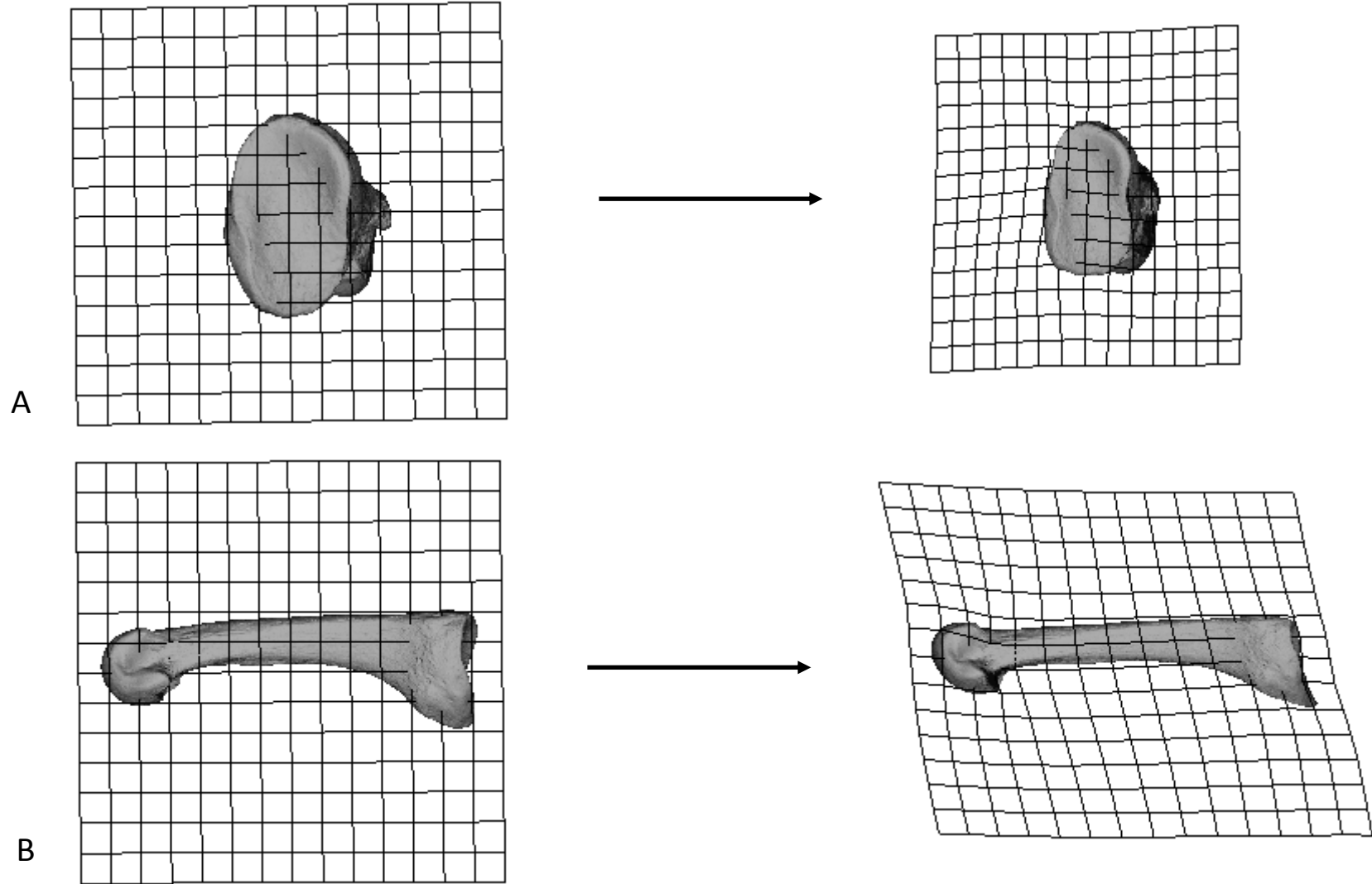


Figure 3.6.19. Demonstration of the warp from the *Pongo* mean first metatarsal (left) to the *Theropithecus* mean (right). A) Proximal view. B) Medial view

3.6.3.2. Proximal first metatarsal

From *Gorilla* to *Pongo*

The differences between *Pongo* and *Gorilla* for the proximal first metatarsal largely reflect the differences observed between *Pan* and *Pongo* when the complete bone was analysed. This gives some confidence to the findings for the first metatarsal given the fragmentary nature of the fossil material. The proximal first metatarsal of *Pongo* retains its general helical appearance in common with the African apes. The facet is moderately shallower in *Pongo*, but the difference is slight. The facet is noticeably smaller than it is in *Gorilla*. This is most obvious with respect to the inferior half of the facet and the inferolateral corner in particular (Figure 3.6.20). This corresponds well to differences found when the complete bone was analysed.

From *Gorilla* to *Pan*

The bones in these two species are largely similar, and no well-defined differences are apparent from this analysis. The proximal surface is helical in form in both species and there is little difference in depth of the facet surface, although it is marginally deeper in *Pan* this difference is negligible. The facet seems to be superoinferiorly shorter in *Pan* but mediolaterally wider. However, these differences are also small. In total, there is little to distinguish between the two species on the basis of proximal first metatarsal morphology alone.

From *Pongo* to *Oreopithecus*

Warping to *Oreopithecus* from *Pongo* indicates a difference which is similar to that between *Pongo* and *Gorilla*. The superior part of the facet is broad while the inferior half of the facet is greatly diminished, especially in its inferolateral corner. The facet retains its helical formation and is in fact moderately deeper in *Oreopithecus* than it is in *Pongo*. The mediolateral constriction of the inferior half of the facet is what most clearly aligns *Oreopithecus* with *Pongo*, however (Figure 3.6.21). Unfortunately, it is difficult to conclude very much from the base of the first metatarsal alone.

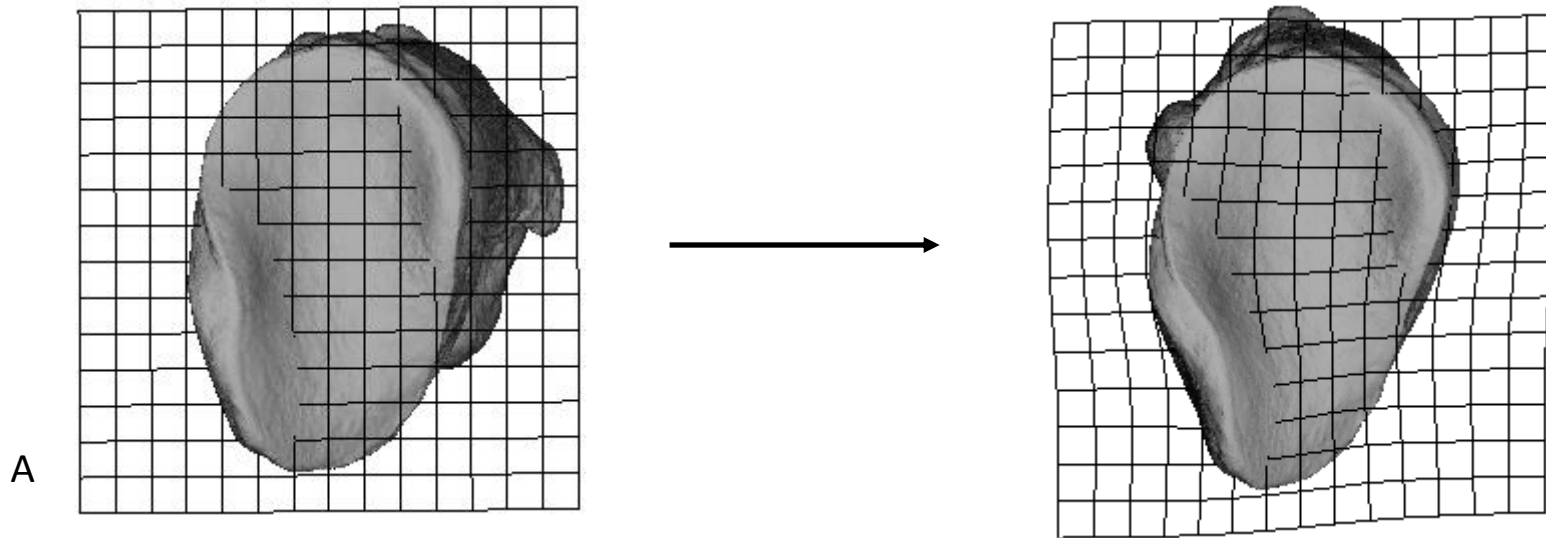


Figure 3.6.20. Demonstration of the warp from the *Gorilla* mean proximal first metatarsal (left) to the *Pongo* mean proximal first metatarsal (right).

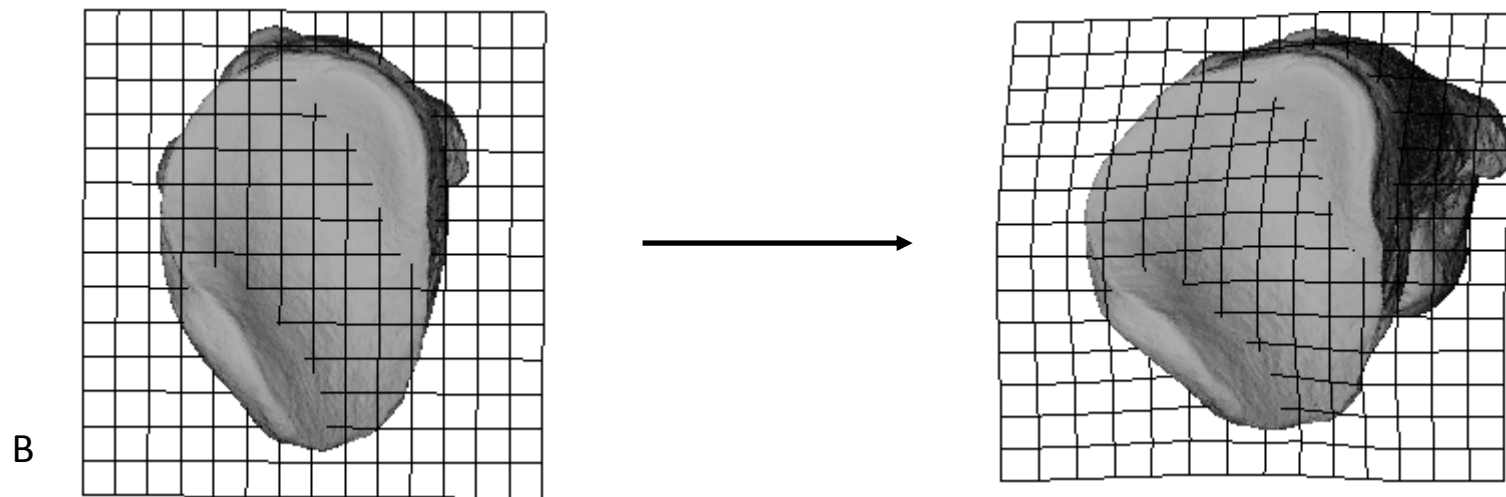


Figure 3.6.21. Demonstration of the warp from the *Pongo* mean proximal first metatarsal (left) to the *Oreopithecus* proximal first metatarsal (right).

3.6.3.3. Distal first metatarsal

From *Pan* to *Gorilla*

The warp provides differences which reflect those found using the complete first metatarsal, which adds some confidence to the findings presented. The distal first metatarsal of *Gorilla* is stouter than in *Pan*. Its mediolateral breadth is relatively greater while its proximodistal length is reduced, and this gives the head of the bone a less bulbous appearance. The angulation between the superior and inferior borders of the head is more obtuse in *Gorilla* compared to *Pan*. Additionally, the plantar cornua are better-developed in *Gorilla*, producing definitive medial and lateral cornua.

From *Pan* to *Homo*

The differences found between the two species mirror those found between *Pan* and *Gorilla* but are starker. The distal first metatarsal of *Homo* is stouter in appearance than in *Pan*. The mediolateral width of the head is increased while the proximodistal length of the head is shortened. The plantar cornua are better-developed in *Homo*, but the difference is not as pronounced as it is between *Pan* and *Gorilla*. The angulation between the superior and inferior borders of the head, from medial or lateral view, is much more obtuse in *Homo* (Figure 3.6.22) and this effect is markedly more pronounced than it is in the warp to *Gorilla*. The head of the *Homo* first metatarsal overall appears much more rounded than bulbous.

From *Pan* to *Oreopithecus*

Warping to *Oreopithecus* from the *Pan* mean distal first metatarsal shows that *Oreopithecus* has a strongly mediolaterally constricted dorsal border, while the plantar border retains a greater width (Figure 3.6.23). The plantar cornua are not well developed, but are present, to a degree similar to that in *Pan*. The curvature of the head of the first metatarsal is also comparable to that found in *Pan*. The differences between the two are few and slight, and it is not possible to extract many features of interest, such as length/width, curvature of the bone, etc. from isolated epiphyses.

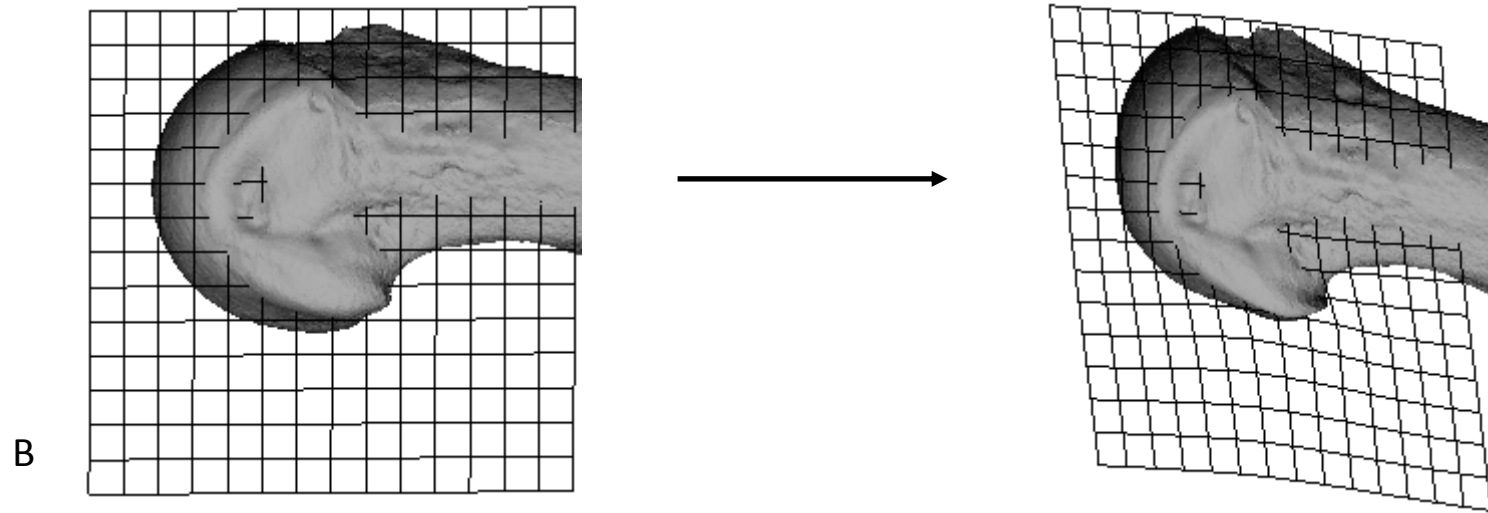


Figure 3.6.22. Lateral view of the warp from the *Pan* mean distal first metatarsal (left) to the *Homo* mean distal first metatarsal (right).

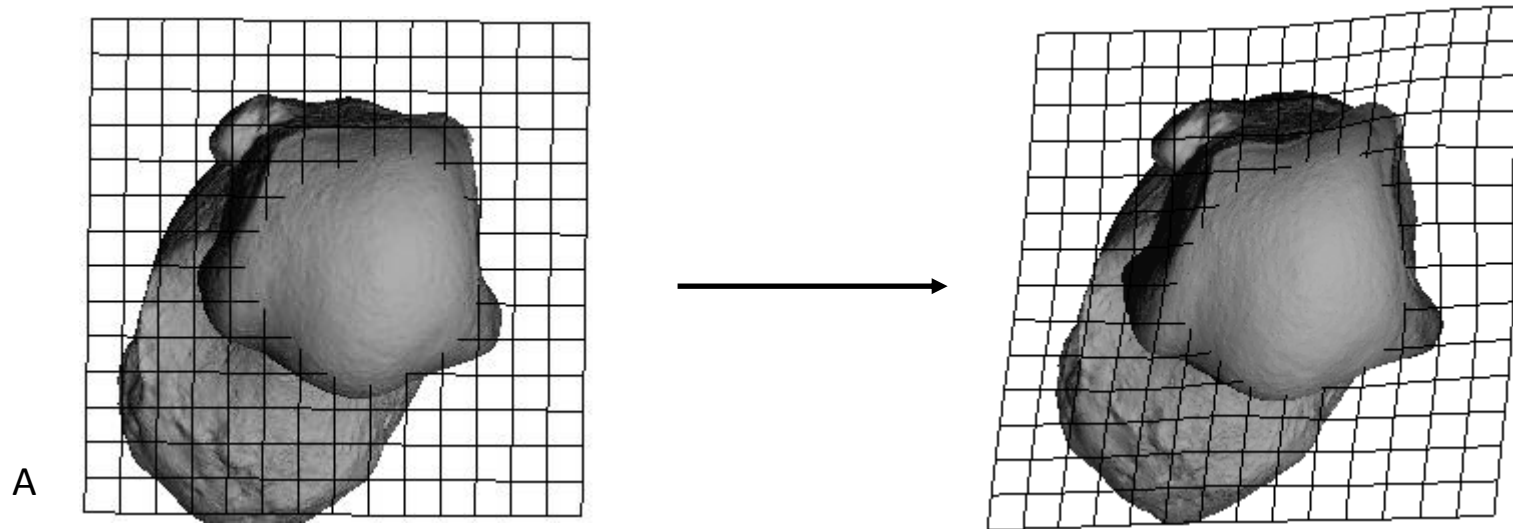


Figure 3.6.23. Distal view of the warp from the *Pan* mean distal first metatarsal (left) to the *Oreopithecus* distal first metatarsal (right).

3.7. Summary

The following hypotheses were tested for each of the pedal elements included in the study. Hypotheses 1-7 concern morphological relationships between extant species and fossils; Hypotheses 8-12 concern size relationships between extant species and fossils.

1. *Gorilla* and *Pan* are most similar in terms of ecology and behaviour and therefore will be more similar to each other in pedal anatomy than to any other species.
2. *Pongo* and the African apes are more similar to one another in terms of ecology and behaviour (though substantial differences clearly exist) and will therefore be more similar in pedal anatomy to each other than to either *Homo* or *Theropithecus*, which species, in the context of this study, are more “specialised” (*Homo* a committed biped and *Theropithecus* a pronograde, digitigrade, quadruped).
3. *Theropithecus* represents an outgroup as the only non-hominoid, digitigrade, quadruped and will therefore be the most different of all extant species included in the study.
4. *Oreopithecus* is markedly different in shape to *Theropithecus* and therefore the cercopithecoid hypothesis for *Oreopithecus* has justifiably been discarded.
5. *Oreopithecus* is most similar in shape to one of the African apes, reflecting its probable heritage from the Miocene hominoids of Europe. The details of the similarities and differences to African apes will permit an assessment of the likelihood of unique pedal function.
6. OH8 is most similar in shape to *Homo* reflecting its status as an obligate biped.
7. *Nacholapithecus* is most similar in shape to *Theropithecus* reflecting its pronograde, quadrupedal body shape and position as a stem hominoid.
8. *Gorilla/Homo* will be the largest among the extant species due to the large body size of *Gorilla* and the increased level of force transmission in *Homo*.
9. *Theropithecus* will be the smallest among the extant species due to its small body size.
10. *Oreopithecus* is comparable in size to *Pan*, lacking the increased robusticity of the pedal skeleton which would be expected in a habitually bipedal primate, but having a substantially more robust foot than *Theropithecus*.
11. OH8 is smaller than *Homo* reflecting its small body size and occurrence early in the emergence of obligate bipedalism.
12. *Nacholapithecus* is intermediate in size between *Theropithecus* and the smallest hominoid reflecting the increase in body size which is characteristic of the stem hominoids.

Hypothesis 1 was confirmed for each of the tarsals studied; *Pan* and *Gorilla* were found to be most similar to one another in shape. The features shared between the two include the wedge-shaped trochlea, medially flaring medial malleolar facet, divergence of the head from the body of the talus, expansion of the superior and medial aspects of the talar facet of the navicular, encroachment of the first metatarsal facet onto the medial side of the medial cuneiform, alignment of the navicular-medial cuneiform articulation predominantly along a mediolateral axis, and laterally directed navicular-lateral cuneiform articulation. Hypothesis 1 was rejected for the complete first metatarsal, confirmed for the proximal first metatarsal, and rejected for the distal first metatarsal. The features of the first metatarsal seemed to be generally shared, e.g. torsion of the bone bringing the axes of the head and base into an oblique alignment, helical and highly curved form of the medial cuneiform facet, inferior orientation of the head relative to the base indicating a longitudinal curvature to the bone. However, the clearest difference between the two relates to the increased robusticity of the bone in *Gorilla*. It is shorter, wider, and deeper than it is in *Pan*. The surface area of the head in particular is increased relative to the base in *Gorilla*.

Hypothesis 2 was rejected for all bones other than the navicular and first metatarsal indicating that differences in the morphology of the bones of the foot are not well-explained in terms of arboreal/terrestrial adaptations. The greater similarities between the African apes and *Homo/Theropithecus* regarding the talus and cuneiforms do not show a regular pattern (e.g. it is not due to a consistently closer relationship between *Gorilla* and *Homo*, or any other repeated similarity of that sort.) Therefore, it implies that the foot of *Pongo* bears some unique features linked to functional requirements that are not particularly similar to those experienced by the African apes. The unique features of the *Pongo* foot include: the parallel-sided trochlea with a strongly elevated lateral rim, the small, non-flaring medial malleolar facet, small head of the talus, highly laterally flexed lateral cuneiform facet of the navicular with a high curvature of the articular surface, perpendicular long axes of the proximal and distal facets of the medial cuneiform, extreme encroachment of the first metatarsal facet onto the medial side of the medial cuneiform, and small size of the first metatarsal.

Hypothesis 3 was confirmed for the navicular and medial cuneiform but not for any of the other bones included in the study. There was no consistent pattern to the evidence leading to the rejection of the hypothesis. It is unclear whether the closer similarity of some hominoids to *Theropithecus* is an

indication of close proximity of *Theropithecus* (possibly indicating a deep origin for these features that has persisted) or whether it is indicative simply of high levels of variation among the hominoids. The inclusion of a greater number of cercopithecoids would be necessary to resolve this issue. Some of the clear similarities between *Theropithecus* and African apes includes an elevated lateral trochlea rim, medially flaring medial malleolar facet (although this feature is morphologically different than it is in African apes, it is still present), T-shaped distal lateral cuneiform facet, and small and mediolaterally broad/dorsoplantarly short navicular facet of the lateral cuneiform. The navicular of *Theropithecus* was clearly distinct from any other group with a strong proximal projection of the medial border of the navicular facet. The medial cuneiform was long and narrow with a strong constriction of the medial and lateral borders of the distal facet at their midpoints. The Procrustes distances in general show that *Theropithecus* was consistently distant from other extant species, but this effect was not consistent with respect to all species and all bones and therefore hypothesis 3 had to be rejected for most of the bones.

Hypothesis 4 was accepted for all bones, there was no evidence whatsoever to support the contention that *Oreopithecus* was a cercopithecoid. Hypothesis 5 was accepted for all tarsals; *Oreopithecus* was most similar in form to one of the African apes. In its navicular, medial cuneiform, and distal first metatarsal, *Oreopithecus* was most similar in morphology to *Pan*. In talus, intermediate cuneiform, and lateral cuneiform morphology, *Oreopithecus* was most similar to *Gorilla*. In its proximal first metatarsal morphology *Oreopithecus* was most similar in form to *Pongo*. The results for the proximal and distal first metatarsal are tentative and provide no real information about the robusticity of the bone, which would have been useful. However, the remaining tarsal morphology clearly aligns *Oreopithecus* with the extant African apes. Features that *Oreopithecus* shares with the African apes include; the wedge-shaped trochlea, elevated lateral trochlear rim, expansion of the medial and superior aspects of the talar facet of the navicular, encroachment of the first metatarsal facet onto the medial side of the medial cuneiform, and posterior sloping of the superomedial corner of the distal intermediate cuneiform.

Hypothesis 6 was confirmed for all tarsals; OH8 was closest in form to *Homo*. The first metatarsal of OH8 was not included in the study as its morphology was not preserved well enough. The evidence seems to point clearly to a general similarity of OH8 and extant *Homo*, however, there were some notable differences including: the presence of a keel along the midline of the trochlea, some minor flexion of the lateral cuneiform facet on the distal navicular, relatively small navicular facet of the medial cuneiform compared to the distal facet, slight curvature of the first metatarsal facet of the

medial cuneiform, more T-shaped distal facets of the intermediate and lateral cuneiforms. Overall, however, the similarities between OH8 and *Homo* are clearly greater in number than the apparent differences.

Hypothesis 7 was rejected for the talus and accepted for the medial cuneiform, indicating that *Nacholapithecus* was not similar to *Theropithecus* in talar morphology but was similar to *Theropithecus* in its medial cuneiform morphology. However, the closest neighbour of *Nacholapithecus* was *Pan*, which was actually closer to *Theropithecus*, so the differences in shape between these taxa are close but confusing. Similarly, although *Theropithecus* was *Nacholapithecus*' closest neighbour in terms of medial cuneiform shape, the distance between the two was actually very high, which may indicate that the similarities between the two are not that striking among the sample presented. Nonetheless, *Nacholapithecus* exhibits a keel along the midline of the trochlea with an elevated lateral trochlea rim, a flaring medial malleolar facet which is expanded on its anterior half, a moderately divergent talar head, moderately sized and curved talar head, and a long and narrow medial cuneiform with a small navicular facet.

Of all the size hypotheses, those concerning the extant taxa were confirmed for all bones. *Homo* and *Gorilla* were consistently the largest while *Theropithecus* was consistently the smallest of the extant taxa. These results were expected given known features of these taxa concerning body size and locomotion. *Oreopithecus* was consistently found to be smaller than expected for all pedal elements considering its hominoid status. The close similarity in size between *Oreopithecus* and *Theropithecus* was an unusual result. OH8 was found to be similar in size to *Pan* for all pedal elements reflecting reconstructions of its size and taking into account its presumed mode of locomotion. Hypotheses concerning the size of *Nacholapithecus* were also confirmed. It was intermediate in size between *Theropithecus* and extant apes.

4. Discussion

4.1. Talus

4.1.1. Extant species

The results confirmed that the African apes were more similar in shape to each other with respect to talus morphology than either was to any other extant species, thus hypothesis 1 is accepted. However, the two species were significantly different in shape, despite the fact that the Procrustes difference between them was the smallest of any pairwise comparison for the talus. The similarities between *Pan* and *Gorilla* are indicative of adaptation which stresses dorsiflexion and inversion of the foot, confirming the findings of previous studies (Latimer *et al.* 1987; DeSilva 2009). The talus of the African apes has unequal heights of the medial and lateral trochlea rims. The lateral rim is elevated relative to the head, which would have the effect of bringing the sole of the foot to tilt medially, particularly in dorsiflexion (Lewis 1980; Latimer *et al.* 1987; Aiello and Dean 2002). This, coupled with the long, divergent medial rim of the trochlea (giving a greater area of contact for the anterior part of the distal tibia), indicates that the foot of *Pan* and *Gorilla* is habitually inverted (DeSilva 2008) and adapted to support body weight in this position.

The medial malleolar facet surface is not perpendicular to that of the trochlea which is a clear adaptation to support body weight in inversion. The inferior border of the anterior half of the facet is flexed away from the body of the talus about the proximodistal axis in the sagittal plane and the anterior border is flexed away from the body about the dorsoplantar axis in the same plane (Kanamoto *et al.* 2011; Parr *et al.* 2014). The effect of this is to create a hollow cup on the anterior half of the medial malleolar facet to receive the medial malleolus (Gebo 1992) (see Fig. 3.1.11 & 3.1.13). In inversion a significant portion of the medial malleolar facet will lie inferior to the medial malleolus and provide a greater platform for support (Aiello and Dean 2002) and this is indispensable for effective climbing in heavy hominoids. The medial malleolar facet is also greatly expanded on its anterior half offering a greater area of contact between tibia and talus in dorsiflexion as well as inversion (Humphry 1867; DeSilva and Papakyrikos 2011; Marchi 2015). This habitual inversion of the foot is married to habitual dorsiflexion; the mediolateral distance between the anterior limits of the trochlear rims is greater than the distance posteriorly, lending the trochlea a wedge-shaped appearance in superior view (Fig. 3.1.11A & 3.1.13A). This causes the ankle to be at its most secure (in its close-packed position) in dorsiflexion, during which the distal trochlea causes separation of the tibia and fibula, tautening the relevant ligaments of the ankle and bringing the ankle joint into a

stable configuration (Latimer *et al.* 1987). The African apes also possess a moderately long talar neck (Day and Wood 1968). The medial border of the head is a moderate distance from the anterior border of the medial malleolar facet. This distance is very short in *Pongo* and greatest in *Homo*. This can be explained as a way to reduce shear stress on the neck of the talus when the head is strongly deviated from the body of the talus by bringing the talonavicular articulation closer to the tibiotalar articulation, reducing the distance between the moments of these joints (Aiello and Dean 2002).

The differences observed between the African ape tali are best explained as a reflection of the greater terrestrial component in the locomotor repertoire of *Gorilla* (Dunn *et al.* 2014; Knigge *et al.* 2015). This fact may also be related to the greater body weight of the *Gorilla*. Both male and female *Gorilla* are considerably larger than their counterparts in *Pan* (McHenry 1992), and Harcourt-Smith (2002) found no evidence for shape differences between the sexes of extant apes. Therefore, the shape differences described here likely represent a real shape difference between species that is caused by a difference in overall size of *Gorilla*, and are not likely to reflect differences in the size of males relative to females. The lower lateral trochlea rim compared to other ape species (Fig. 3.1.11B) is due to the increased prevalence of force transmission in a vertical direction from the ground as a component of the locomotory repertoire and requires that the trochlea be oriented more parallel to the ground. However, at heel strike during terrestrial quadrupedal locomotion the foot of *Gorilla* is still inverted (Gebo 1992; Schmitt and Larson 1995). The outward flexion of the medial facet is much more pronounced in *Gorilla* and likely reflects the demands of huge body weight imposed on the ankle joint and the requirement of more extensive support for the tibia in an inverted posture (Aiello and Dean 2002; Kanamoto *et al.* 2011; Parr *et al.* 2014). However, the similarities of the tali of *Pan* and *Gorilla* are more numerous and apparent than the differences. This is unsurprising as the two occupy similar habitats and engage in comparable locomotor behaviours both terrestrially and arboreally. The fact that there are fewer differences than similarities between the African apes is also feasibly attributable to the vastly different sizes of the two species and the physical requirements this imposes on the skeletal anatomy of *Gorilla*. But the locomotory similarities between the two imposes greater selective pressure than the difference in size.

The results revealed that the non-human apes were not collectively closer to one another to the exclusion of *Homo* and *Theropithecus*, disconfirming hypothesis 2 and indicating that there is a good deal of variation among the apes compared to the supposedly relatively specialised species. This was apparent considering that *Pongo* was more distant from *Gorilla* than was *Homo*, and more distant from *Pan* than was *Theropithecus*. The extreme wedging of the trochlea is absent in *Pongo* (Fig.

3.1.13A), resembling *Homo* in this regard, however, the two do not share a similar overall morphology of the trochlea. The lateral rim of the trochlea of *Pongo* is higher than the medial and this is expressed more strongly than in any other ape species (Fig. 3.1.13B). This suggests that *Pongo* places a greater emphasis on inversion of the foot at the ankle than the African apes (Aiello and Dean 2002) and this is symptomatic of suspensory, or highly arboreal, behaviour during which the hands and feet are reaching between branches in the canopy (Thorpe and Crompton 2006).

The medial malleolar facet in *Pongo* is unlike the African ape condition in lacking the extreme flexion of this facet away from the body of the talus. The facet is also very different to other species in that it is narrow throughout its dorsoplantar dimension, lacking the expanded anterior half, therefore not forming a cup to support the medial malleolus. Instead, the surface of the facet is more or less perpendicular to the trochlea, similar to the morphology in *Homo*, and the facet is quite slender in appearance. This fact, when considered alongside the absence of wedging of the trochlea, indicates that the tibia moves directly over the trochlea into dorsiflexion and is not restricted by the flaring cup typical of the African apes (Szalay and Langdon 1986). However, given the more pronounced inversion suggested by the more elevated lateral trochlear rim, the medial malleolar facet could still perform a minor weight-bearing function in above-branch or terrestrial locomotion, or vertical climbing. A major difference between the locomotor repertoires of African apes and *Pongo* is the much greater incidence of suspension in *Pongo* (Hunt 1996). Suspension is a high risk behaviour, especially when feeding at terminal branches (Thorpe and Crompton 2005), and so it may be reasonable to suspect that this should be reflected in the skeleton of *Pongo*. In suspensory postures the talocrural joint would be under tension rather than compression (Langdon 1986), and thus the flaring of these facets would confer little benefit in this posture. The modest flare of the malleolar facets could be explained as a way to keep the malleoli close to the body of the talus and thus reduce the strain placed on ligaments of the ankle during tension. *Pongo* has been suggested to use suspensory postures in a third to a half of its positional behaviour (Hunt 1991), or as little as a fifth of its positional behaviour (Thorpe and Crompton 2006), while it is much lower in the other non-human apes (practically non-existent in adult *Gorilla* and *Pan*, although quite prevalent in juvenile *Pan* (Doran 1997)) This represents a key difference in behaviour between *Pongo* and the African apes which has clear consequences upon the ankle morphology of *Pongo*.

However, the divergence of the head from the body of the talus is present in both *Pongo* and the African apes, but the head of the talus is quite high in *Pongo* in comparison to other species, not being angled downwards, sitting at approximately the same height as the medial trochlear rim (Fig.

3.1.13B). The neck is longer than in African apes and the trochlear rim extends further distally reducing the distance between the tibiotalar articulation and the talonavicular articulation. The long neck of the talus would otherwise be subject to greater shear stress in weight-bearing in a variety of postures (Aiello and Dean 2002). The torsion of the neck is also low, most likely as a similar adaptation to reduce shear stress. This is coupled to a more pronounced curvature of the head suggesting that the level of mobility of the talonavicular joint is higher in *Pongo*, but the size of the head is small indicating that the talonavicular joint of *Pongo* is less well-adapted to withstand compressive forces. This is commensurate with the increased prevalence of suspension in *Pongo* and the need for a highly mobile ankle joint.

Hypothesis 3 was rejected as *Theropithecus* was not found to be consistently strongly different to all other species. This suggests that there is a moderate level of shared function between all extant species with respect to upper talus morphology, though the greatest similarity was found between *Theropithecus* and *Pan*. The lateral trochlear rim is elevated noticeably higher than the medial relative to the inferior surface and head (Fig. 3.1.15B). This feature is related to the fact that *Theropithecus* is a semiplantigrade quadrupedal primate (Gebo 1992) and assumes an inverted position at the ankle when walking in comparison to other cercopiths; squatting also forms a relatively larger component of its positional repertoire (Krentz 1993). Thus, inversion of the ankle is prevalent in *Theropithecus* as well as all non-human ape species, but for functionally different reasons. The medial malleolar facet lacks any significant flaring along most of its length but the anterior part is deviated medially and tilted anteriorly, this is considerably more exaggerated in *Theropithecus* than in African apes. Given the elevated heel during terrestrial walking, and the extreme flexion of all joints of the lower limb during squatting, the head of the talus is habitually directed inferiorly. Thus, the anterior part of the medial malleolar facet is brought close to a horizontal alignment, parallel to the ground, and can support the medial malleolus throughout the locomotor cycle and during static postures (Harrison 1989), during which the head of the talus is tilted inferiorly. Additionally, *Theropithecus* shuffles bipedally between feeding patches using highly flexed hips, knees and ankles (Wrangham 1980). Thus the anterior part of the articulation between tibia and talus is well-developed to accommodate this posture.

4.1.2. Fossil species

There was no strong similarity between *Oreopithecus* and *Theropithecus* confirming hypothesis 4: *Oreopithecus* does not resemble a cercopithecoïd. However, there was good reason to infer a strong similarity between *Oreopithecus* and the African apes, confirming hypothesis 5. The morphology of the talus in *Oreopithecus* most closely resembles that of *Gorilla*. The trochlear rims are subequal in height in *Oreopithecus* (Szalay and Langdon 1986), and although this feature can only be measured relative to the neck of the talus it is clearly apparent (*contra* Köhler and Moyà-Solà 1997; see Fig. 3.1.11). The medial trochlear rim is approximately at the level of the neck and head while the lateral rim is noticeably, elevated in comparison. This feature is not as pronounced as it is in either *Pongo* or *Theropithecus*. The elevated lateral rim suggests some degree of adaptation to inversion at the ankle (Latimer *et al.* 1987) in a manner comparable to *Gorilla*. The head of the talus lacks the inferior inflection typical of the *Homo* talus and is instead directed more distally, suggesting the absence of a human-like longitudinal arch and indicating that the foot of *Oreopithecus* may actually have been capable of midfoot flexion in a manner similar to that observed in African apes. However, it is worth noting that the OH8 talus was similarly found to be ape-like with respect to these aspects of the morphology in isolation, but other aspects of the pedal skeleton indicated that the foot was adapted to bipedalism. Thus, caution must be exercised in a similar manner for *Oreopithecus*; in the first place because an ape-like upper ankle morphology does not necessarily preclude habitual bipedalism (Stern and Susman 1983; Lovejoy *et al.* 2009a), and secondly because the inclusion of the remaining morphology of the foot could, in principle, distance *Oreopithecus* from the extant apes.

The trochlea of *Oreopithecus* is noticeably wider distally than it is proximally (Figure 3.1.11A) and the anterior third of the medial malleolar facet is flexed moderately medially, while the anterior border is flexed proximally away from the head and the inferior border is flexed outwards away from the body along a proximodistal axis as found in *Gorilla* (and also *Pan*). Consequently, the distal third of the medial malleolar facet forms a shallow cup to receive the medial malleolus (Langdon 1986). The morphology of the trochlea and medial malleolar facet suggest that the foot of *Oreopithecus* was, in principle, well-adapted to dorsiflexion and inversion at the ankle (DeSilva 2009). If this is indeed the case then *Oreopithecus* may have included a considerable amount of vertical climbing in its behavioural repertoire, or at the very least have been adapted to climb safely and efficiently. The head of the talus is moderate in size and curvature of its articular surface, and the neck is not excessively long. These features suggest that there was a reasonable degree of movement taking place between the talus and navicular, particularly in dorsiflexion and inversion. The length of the

neck of the talus probably therefore reflects a compromise morphology in which shear stress on the neck was avoided by not having an excessively long neck (Aiello and Dean 2002). From the available morphology it also appears that the head was distally directed indicating that the foot lacked a longitudinal arch (Szalay and Langdon 1986). These features suggest that *Oreopithecus* did not have an ankle joint suitable to habitual terrestrial bipedal locomotion. Furthermore, the finding that the talus of *Oreopithecus* was not significantly larger than that of *Theropithecus* is difficult to explain if *Oreopithecus* was habitually bipedal. It could imply that reconstructions placing the body size of *Oreopithecus* around 32kg (Jungers 1987) are over-estimates, or could alternatively imply a reduced importance of the hind limb in locomotion and a forelimb-dominated locomotory repertoire.

While OH8 was found to be most similar in shape to *Homo*, confirming hypothesis 6, it was also quite similar in shape to the African apes, particularly *Pan*, suggesting a mosaic morphology existed in the ankle. From superior view the trochlea lacks the pronounced wedging found in *Pan* but also lacks the straight and parallel trochlea rims observed in *Homo*. The medial malleolar facet is flexed away from the body of the talus medially about the proximodistal axis but this is not as pronounced as it is in *Pan* (Fig. 3.1.12). Similarly, the anterior border of the medial malleolar facet is flexed posteriorly away from the head about the dorsoplantar axis, but again not to the extent seen in *Pan*. The effect of this is that the medial malleolar facet does provide a slight cup to receive the anterior part of the medial malleolus in inversion and dorsiflexion (Parr *et al.* 2014) but this feature is not as well-developed as it is in the African apes, so it can be concluded that *Homo habilis* seems not to have been as well adapted to inversion and dorsiflexion as the African apes are, at least with respect to this single feature. However, *Homo habilis* is clearly different from *Homo sapiens* in lacking a flat, vertically aligned medial malleolar facet. Therefore, the anterior border of the medial malleolus will contact the anterior border of the medial malleolar facet in dorsiflexion indicating a weight-bearing function, unlike the unobstructed anterior portion of the *Homo* medial malleolar facet (Aiello and Dean 2002). Furthermore, the lateral trochlear rim is elevated higher than the medial relative to the height of the head, further pointing to an inverted set to the ankle and suggesting that the leg followed a more arced, ape-like path over the talus during bipedal progression (Harcourt-Smith 2002). Thus, overall the upper ankle morphology of OH8 suggests that it may have retained some capability to climb in a manner similar to the African apes, though probably to a lesser degree. And while the ankle was most similar in form to *Homo sapiens* the function was not markedly similar to extant *Homo* and suggests that the bipedalism of *Homo habilis* was different to that of modern humans.

The head of the talus of OH8 lies medial to the body rather than distally as it does in *Homo* giving the neck of the talus an ape-like angle (Fig. 3.1.12). Therefore OH8 seems to have had a more ape-like

medially and distally directed talar head, which would suggest some preference to transmitting force to the medial side of the foot (Aiello and Dean 2002). Superficially this would seem to suggest some degree of divergence between the first and lateral digits in OH8 unlike the distally directed head of *Homo* which would indicate strong adduction of the first digit. However, the head does seem to display a greater degree of torsion and inferior flexion than in the African apes, which could be indicative of the presence of a longitudinal arch in the foot of OH8. In all, the talus of OH8 is difficult to interpret but it seems that the ankle of OH8 retained some features conducive to climbing while also displaying a departure from this ape-like morphology towards a more modern human-like morphology and function. The size of the OH8 talus also mirrors these considerations. It retains a size similar to *Pan* and therefore lacks the human-like vast increase in size of the talus relative to body-size which comes with obligate bipedalism and therefore may suggest that OH8 was not an obligate biped and retained a significant level of other locomotory behaviour in its behavioural repertoire.

The talus of *Nacholapithecus* was found to be closest to the African apes suggesting that *Theropithecus* does not provide a good model for the talus of *Nacholapithecus*, nor of the talus possessed by the stem hominoids in general, rejecting hypothesis 7. The similarity of *Theropithecus* to *Pan*, then, may indicate that this is a general catarrhine cluster, but the inclusion of a greater number of catarrhine species would be necessary to resolve this. *Nacholapithecus* exhibits a wedge shaped trochlea which aligns it with the African apes and *Theropithecus* (Fig. 3.1.14 & 3.1.15). However, the pronounced widening of the facet anteriorly is not a consequence of the medial deviation of the anterior portion of the medial malleolar facet, as it is in *Theropithecus* (Krentz 1993). The result of this feature in *Theropithecus* is a fairly deep cup for the medial malleolus which faces quite prominently posteriorly and will prevent excessive anterior movement of the tibia on the talus (Strasser 1988), the cup formed in *Nacholapithecus* is shallow and implies that a greater range of movement was permitted between tibia and talus (Aiello and Dean 2002) and this suggests that a degree of hominoid-like climbing may have been practiced in this taxon. There is evidence that the foot had an inverted set at the ankle, or at least that it was adapted to positional behaviours which included inversion. The lateral trochlear rim is markedly more elevated than the medial rim, which will cause the sole of the foot to be oriented medially in anatomical position (Aiello and Dean 2002).

The head of the talus of *Nacholapithecus* is narrow in its dorsoplantar dimension and broad mediolaterally and not as highly curved as in apes. This suggests that *Nacholapithecus* had a relatively low degree of movement between talus and navicular. In *Theropithecus* this is explained as part of the functional suite of characters which imply a proximodistal orientation for loading

(Langdon 1986); increasing compressive forces and reducing bending moments across the tarsals (which also manifests as proximodistally lengthened tarsals). However the head of the talus in *Nacholapithecus* is larger and flatter than it is in *Theropithecus*. Therefore, *Nacholapithecus* represents an intermediate morphology between hominoids and cercopithecoids. There is some medial deviation of the head and neck, similar to non-human apes, but a lack of any inferior inclination of the neck and there is very little torsion of the head. These features also point towards a proximodistal alignment of the direction of force transmission through the foot, which would align *Nacholapithecus* more closely with *Theropithecus*.

4.2. Navicular

4.2.1. Extant species

Pan and *Gorilla* have highly similar naviculae confirming hypothesis 1, this provides evidence for their similar ecology and locomotory behaviour. The talar facet has approximately the same surface area as the combined surface area of the three cuneiform facets (fig. 3.2.12B). This fact suggests that force is transmitted through the navicular in a multidirectional fashion. The depth of the talar facet suggests that a moderate degree of movement is possible between the two bones, which supports the conclusion that force transmission in a variety of positions is important (Sarmiento and Marcus 2000). However, the expansion of the medial and superior portions of the facet (Fig. 3.2.12A) suggests that there is some preference for loading the navicular through its medial and superior aspects. The expansion of the medial side of the facet (and bone overall) can be viewed as a response to the mechanical requirements of loading the first metatarsal during climbing and weight support on the medial side of the midfoot. The relatively greater expansion of the superior border of the talar facet can be explained as the morphological adaptation required for support during midfoot dorsiflexion (DeSilva 2009). The constriction of the inferior border of the facet also indicates that dorsiflexion at the talonavicular joint is a key adaptation. This adaptation is vital in climbing for these large-bodied species, being able to grip branches while simultaneously propelling body weight upwards.

The key feature of the distal surface of the navicular is the extreme flexion between the plane of the lateral cuneiform facet and the planes of the medial and intermediate cuneiform facets (which are approximately congruent) (Langdon 1986). This feature is shared among all non-human apes and not found in either *Homo* or *Theropithecus*. It is a curious morphology since the distal articular surfaces

of the intermediate and lateral cuneiforms themselves lie in roughly the same plane. One possible explanation for the flexion of the facet for the lateral cuneiform away from the other two could be that it allows direct transmission of force from the ankle to the lateral digits when the foot is inverted, through the articulation between the lateral cuneiform and cuboid (Sarmiento and Marcus 2000). It also appears that the articulation with the talus is directed towards the planes of the medial and intermediate cuneiform. This fact is a consequence of the oblique orientation of the plane of the lateral cuneiform facet, shortening the proximodistal length of the lateral side of the bone. The orientation of the talar articulation additionally serves to favour force transmission to the medial side of the foot from the navicular and, similarly, to support force transmission from the medial side of the foot (especially the first digit) to the navicular (Harcourt-Smith 2002).

The medial side of the bone (roughly indicative of the medial tuberosity) has a pronounced inferior orientation in *Pan* (Fig 3.2.12A), as well as in *Gorilla* and *Homo*. This feature is here interpreted as increasing the lever advantage of tibialis posterior in a dorsiflexed position (Langdon 1986; Sarmiento and Marcus 2000), providing greater propulsive force to the foot, particularly during midfoot flexion. Additionally, the expansion of this area of the bone in the African apes may reflect its function in bearing weight during midfoot flexion or quadrupedal walking on large supports (Sarmiento 1994; DeSilva 2008). The rotation of the lateral and medial cuneiform facets away from one another brings their inferior borders closer together and distances their superior borders, forming the transverse arch of the foot (Sarmiento and Marcus 2000). The intermediate cuneiform facet is small and wedged inferiorly between the medial and lateral cuneiform facets in the African apes. The medial cuneiform facet is the largest by quite a margin so although the navicular seems to be adapted to multidirectional force transmission there is clear emphasis on transmission to and from the medial side of the foot. The superior side of the bone proximodistally narrower than the inferior side, a feature associated with the midfoot dorsiflexion discussed above. Emphasis for force transmission is placed on the superior aspect of the tarsal bones of the medial column of the foot (DeSilva 2010). The African apes present a picture of a midfoot which emphasises mobility and multidirectional force transmission with a preference to loading the foot on the medial side and an ability to function during dorsiflexion at the midfoot. This is expected given that climbing forms a significant aspect of the locomotory behaviour of these species.

Pongo and the African apes are more similar to one another than any are to either *Homo* or *Theropithecus*, confirming hypothesis 2 for the navicular. These similarities may be due to their similar habitat use and locomotion compared to the more specialised, and wholly terrestrial, species

of *Homo* and *Theropithecus*. However, despite these similarities there are clear differences between *Pongo* and the other non-human apes. The overall surface area of the proximal facet is not comparable to that of the combined surface area of the cuneiform facets (Fig. 3.2.15), unlike the African apes. This is due to a less prominent development of the medial portion of the facet. Consequently, the transmission of force from the talus directed medially is seemingly less emphasised in *Pongo*. This is related to the reduced size of the first digit and the weak grasping capability of *Pongo*. Instead, it uses the appendages in suspension more often and the first digit is not vital in this behaviour (Hunt 1996). The less well-developed medial portion of the proximal facet also has the consequence that the talar facet is oriented towards the intermediate cuneiform facet rather than facing more medially as in the African apes (Sarmiento and Marcus 2000), further emphasising the greater importance of the lateral digits in the foot of *Pongo*. Furthermore, the smaller medial portion of the facet in *Pongo* lacks the inferior inclination found in the African apes and *Homo*. Instead the medial portion is flexed towards the dorsal side of the bone. This feature may increase the lever advantage of tibialis posterior in an inverted and plantarflexed position, and this would be a valuable adaptation to aid in suspensory postures, during which inversion and plantarflexion of the foot of the foot is pronounced (Hunt 1996). However, it may also be symptomatic of the reduced robusticity of the navicular tuberosity and the relative increase in importance of the digital flexors in *Pongo* (Langdon 1986). The depth of the articulation with the talus is comparable to that of the African apes indicating a reasonable degree of mobility at this joint.

The medial cuneiform facet is greatly reduced in size in *Pongo*, relative to the African apes, in both its dorsoplantar and mediolateral axis relative to the other cuneiform facets, and relative to other species. This fact is concordant with the fact that the first digit of *Pongo* is greatly reduced in size giving it a reduced functional importance (Marchi 2005). The lateral cuneiform facet is the largest of the three facets and is rotated such that its lateral border lies more inferiorly, as well as being flexed laterally (Fig. 3.2.15B). This rotation of the lateral cuneiform facet away from the others produces a transverse arch as in other species when the dorsoplantar long axes of the medial and lateral cuneiforms are brought into opposition with each other, and this is more pronounced in *Pongo* than African apes (Oxnard and Lisowski 1980). The lateral flexion of the facet, as in apes, would seem to indicate laterally directed force transmission from the navicular through the lateral cuneiform. Furthermore, the facet has a strongly concave surface indicating high mobility in the midfoot of *Pongo* (Langdon 1986), particularly in rotation between the navicular and lateral cuneiform. The significance of this increased mobility to allow force to be transmitted to the lateral side of the foot in suspensory postures, which present a variety of different orientations and pronounced inversion, is of great importance for *Pongo*.

Unlike other species, *Pongo* does not exhibit a great deal of wedging of the intermediate cuneiform. While the inferior border of the intermediate cuneiform facet of the navicular is narrower mediolaterally than the superior border, the facet is close to rectangular in outline. This is due both to the diminished medial cuneiform facet and the pronounced rotation of the lateral cuneiform facet, the consequence is that the intermediate cuneiform and second digit bears an increased robusticity and significance in the foot of *Pongo*. *Pongo* shares the posterior sloping of the superior aspect of the distal surface with other apes. This would suggest some emphasis on dorsiflexion, however, this feature is not as pronounced in *Pongo*, particularly with respect to the diminished medial cuneiform facet. Thus, the adaptation to loading the foot in dorsiflexion is not as pronounced in *Pongo*.

In *Homo* the smaller facet for the head of the talus (Fig. 3.2.13A) is argued to reflect the less mobile foot of *Homo* and the more restricted directional component of force transmission from the talus distally. The flatter surface of the facet is also evidence of reduced mobility between the talus and navicular in *Homo* (Sarmiento and Marcus 2000). Further evidence for reduced mobility at the talonavicular joint and a limited directional component to force transmission can be adduced from the straight proximal and distal surfaces in superior or inferior view. The proximal and distal surfaces are parallel and flat lacking the pronounced curvature and the proximal projection of the medial border of the talar facet found in ape naviculae. The less well-developed medial side of the talar facet in *Homo* (Figure 4.42) suggests that weight-bearing on the medial side of the navicular is not as pronounced as it is in apes. Indeed, the navicular may be functioning to redirect the longitudinal axis of the first metatarsal laterally from the medially directed head of the talus (Sarrafian 1983), this realignment of the longitudinal axis of the foot produces a more directly proximal to distal force transfer.

Homo shares with *Theropithecus* a fairly flat superior border to the proximal facet lacking the strong expansion found in apes. This fact is unsurprising, as the human midfoot is more rigid than that of apes, and the ligamentous anatomy of the talus, navicular and cuneiforms prevent high levels of mobility during walking, there is little adaptive advantage to increasing the surface area of the superior part of the talar facet relative to the inferior part. The inferior border of the *Homo* proximal navicular is not constricted as it is in other apes. In *Homo* this border extends inferiorly to a sharp point roughly around its midpoint. This is the location for the strongest part of the insertion of the spring ligament (Sarrafian 1983; Gomberg 1985). Thus this plays a key role in maintaining the rigidity

of the human foot and supporting the head of the talus. The absence of this feature in apes further points towards the mobility of the foot in those species. The lack of development of the superior border of the talar facet in *Homo* and the pronounced development of the inferior border also suggest that force is habitually applied inferiorly from the talus to the navicular.

Distally, the *Homo* navicular is quite different from that of other apes. The planes of the cuneiform facets are all more or less concurrent, there is no apparent flexion between the lateral cuneiform facet and other two (Sarmiento and Marcus 2000). *Homo* is actually similar to *Theropithecus* in this respect (Fig. 3.2.13). However, *Homo* has a much flatter distal surface than *Theropithecus*. The flatter distal surface of the navicular in *Homo* reflects the low mobility between the navicular and the cuneiforms and the tight-packing of the tarsal skeleton (Oxnard and Lisowski 1980). This indicates that the human foot acts more like a single rigid unit than is the case in apes, which is the key difference in foot function between humans and apes and reflects the obligate bipedalism of *Homo*. In contrast to other apes in this study the medial cuneiform facet of the *Homo* navicular has a greater superoinferior dimension while it is narrower mediolaterally. In the apes the broader mediolateral dimension was interpreted as signalling a relatively greater component of mediolaterally directed force transmission from the first digit. In *Homo* this pattern is reversed and the emphasis on loading longitudinally through the foot, and the simultaneous restriction of first ray abduction, is forwarded here as the explanation for these differences in dimensions of these facets.

Coincident with the mediolateral narrowing of the medial cuneiform facet is a broadening of the intermediate cuneiform facet in *Homo*, which also has a clear inferior border unlike the African apes, although this is not as well-developed as it is in *Pongo*. The broadening gives a more equal surface area to the three cuneiform facets and is concordant with more direct proximal to distal force transmission in the human foot discussed above. In apes the curvature of the navicular and relatively larger articulations with the medial and lateral cuneiforms favour force transmission in a variety of different directions. The absence of the pronounced flexion of the lateral cuneiform facet in *Homo* also gives the facet a greater anteroposterior dimension on its lateral side and thus the overall robusticity of the bone is greater. Finally, the superior border is not as narrow in *Homo* as in ape species which is an indication that the foot is arched (Berillon 2003), and that the rigidity of the foot does not allow midfoot flexion to occur.

Hypothesis 3 was confirmed for the navicular; *Theropithecus* consistently had the greatest Procrustes distance from the other extant species. However, it bears similarities with all of the species studied here in certain respects but has a number of unique features of its own. The superior border of the talar facet lacks the expansion characteristic of the African apes (Sarmiento and Marcus 2000). The midpoint of the inferior border projects inferiorly in a manner similar to *Homo*. This feature anchors the fibres of the spring ligament in *Homo* (Sarrafian 1983), which prevent the head of the talus from sliding inferiorly along the navicular during the habitual inferior orientation of the talus during walking. The talar facet has a pronounced proximal projection of the medial border from superior view. However, the facet is quite flat along its lateral two thirds, which also lie opposite the distal surface of the bone indicating a proximal to distal alignment of the talus and navicular in contrast to pronounced the medial orientation found in apes. The medial side of the facet is thus acting to prevent medial dislocation or movement of the talar head across the navicular; when the heel is raised and the head of the talus is directed towards the ground there is particular need for stability at this joint (Langdon 1986).

Distally, the cuneiform facets all lie in approximately the same plane. *Theropithecus* is roughly similar to *Homo* in this regard and this further supports a proximal to distal alignment of the medial column of the foot in contrast to the multidirectional situation in the ape foot. The medial cuneiform facet is small in size, it is narrow superoinferiorly and not as extensive mediolaterally relative to the other cuneiform facets as it is in apes. This fact suggests that there is a reduced importance of the hallux in grasping and weight-bearing in *Theropithecus* (Gebo 1989). The intermediate cuneiform facet is unique in this study, it is the only example of one whose inferior border extends beyond that of the neighbouring two cuneiform facets (Fig. 3.2.13B), and by quite some margin. The facet is also highly constricted at its midpoint while the superior and inferior portions are relatively expanded. Additionally, its superior border has a posterior slope which is absent from the neighbouring facets. The exact implications of these features are unclear.

4.2.2. Fossil species

Oreopithecus is most unlike *Theropithecus* in navicular shape, confirming hypothesis 4, while it is most like *Pan*, confirming hypothesis 5 for the navicular. The inferior border of the proximal facet is relatively straight bearing moderate constriction (Figs. 3.2.14 & 3.2.15), lacking the human/*Theropithecus*-like beak at its midpoint. This evidence conforms with the distally directed

head of the talus to point to a foot which lacked a longitudinal arch and had substantial midfoot laxity (Szalay and Langdon 1986). The superior border of the navicular facet is expanded similar to *Pan* and the medial side of the facet is lengthened relative to the lateral making the overall shape of the facet *Pan*-like rather than the more symmetrical oval shape found in *Pongo*. This would seem to indicate that there is a relatively greater emphasis on loading the navicular through its superior and medial aspects (Sarmiento and Marcus 2000), i.e. in inverted and dorsiflexed postures such as those found in vertical climbing. However, the medial portion of the facet, and the navicular tuberosity, exhibit a superior inflection like that of *Pongo* and unlike that of the African apes. This could indicate that the navicular had a reduced or absent role in weight-bearing (Harcourt-Smith 2002) in *Oreopithecus*, or that it is adapted to increasing the lever advantage of tibialis posterior in inversion from a plantarflexed position, which would be valuable in suspensory behaviours (Madar *et al.* 2002). The medial side of the bone is also more gracile than it is in *Pan* and the size of the bone is similar to *Theropithecus* rather than the ape species. Therefore, the navicular tuberosity may have been ill-suited to load-bearing in an African ape-like manner.

The flexion of the lateral cuneiform facet away from the others is not as pronounced as it is in *Pongo* but is still clearly present, aligning *Oreopithecus* with the African apes. This feature, in conjunction with the morphology of the talar facet, indicates an ape-like range of motion between talus, navicular and cuneiforms (Sarmiento and Marcus 2000). The medial cuneiform facet has a narrow dorsoplantar dimension similar to that observed in *Pongo* but the orientation of the facet from inferomedial to superolateral and its curvature aligns *Oreopithecus* with the African apes. It indicates the presence of some mediolateral loading throughout a range of dorsiflexion at the joint (Sarmiento and Marcus 2000); importantly the facet surface is not flat in form (*contra* Szalay and Langdon 1986). The intermediate cuneiform facet is not rectangular as it is in *Pongo*, and the orientation of the cuneiform facets mirror that found in *Pan* indicating the presence of a transverse arch in *Oreopithecus*. The talar facet also aligns itself towards the medial cuneiform facet in superior view, as it does in *Pan*. This is due to the expansion of the medial part of the facet and flexion of the lateral cuneiform facet and this provides additional evidence for an emphasis on loading to the medial side of the bone in *Oreopithecus* along with the expansion of the medial side of the talar facet (Sarmiento and Marcus 2000). Taken together with the talus the navicular presents a view of *Oreopithecus* having a highly mobile ankle and midfoot. The morphological similarity with *Pan* suggests that vertical climbing was prevalent in the behavioural repertoire of *Oreopithecus*. However, the poorly developed navicular tuberosity and small size of the bones suggests that *Oreopithecus* may have been ill-adapted to walking bipedally.

The OH8 navicular is decidedly human-like and is statistically indistinguishable from *Homo*. OH8 shares with *Homo* a talar facet which is smaller in surface area than the combined surface area of the cuneiform facets. Furthermore, the talar facet is close to parallel with the distal surface (which is much flatter than it is in apes) signalling a more restricted proximal to distal weight-transfer from talus to navicular (Sarmiento and Marcus 2000). The OH8 navicular also lacks the strong expansion of the medial side of the navicular facet observed in the African apes further indicating that there is a reduced emphasis on loading through the medial side of the bone in OH8 compared to African apes (Harcourt-Smith 2002). OH8 has, like *Homo*, a projection of bone inferiorly midway along the inferior border of the facet. In *Homo* this feature is the attachment site for the spring ligament (Sarrafian 1983; Gomberg 1985) and is functionally important in securing the midfoot and preventing inferior movement of the talus on the navicular, and thus maintaining a high longitudinal arch. The surface of the talar facet is also not as strongly curved and concave as it is in apes, matching instead the flatter form found in *Homo* and indicating that there was a reduced capacity for movement at this joint. This is further evidence for a predominantly direct proximal to distal direction of force transmission through this joint.

The distal surface of the bone is, similarly, strikingly human-like. The cuneiform facets are rather flat and all lie almost in the same plane. The strong flexion of the lateral cuneiform facet away from the other two is absent. Consequently, the lateral side of the bone is quite broad proximodistally. It is still slightly narrower than the medial side, as it is in humans, but the proximodistal breadth of the bone is more uniform than it is in apes. This is evidence that further supports a more human-like proximal to distal weight transference through the tarsus (Langdon 1986), and a reduced mobility between the navicular and cuneiforms (Sarmiento and Marcus 2000). The superior side of the distal surface does not slope proximally as it does in the African apes, in which it is argued here to indicate adaptation to dorsiflexion at the midfoot. The cuneiform facets also resemble *Homo* in having a tightly curved alignment with respect to their orientations with a plantar concavity suggesting the presence of a well-formed transverse arch (Lewis 1980b). The mediolateral dimension of the medial cuneiform facet is greatly reduced giving the facet a stout appearance and a deep dorsoplantar dimension, as in *Homo*. This would therefore seem to suggest that there was a reduced mediolateral component of loading at the navicular-medial cuneiform articulation in favour of more regular dorsoplantar loading (Langdon 1986). The features of the OH8 navicular indicate that the foot likely had a longitudinal arch and concentrated the transmission of force longitudinally along the foot from proximal to distal. There is no evidence for midfoot flexion found in the navicular. Therefore, the navicular of OH8 points to a considerable degree of bipedal behaviour.

4.3. Medial cuneiform

4.3.1. Extant species

The results showed that, of the extant species, *Pan* and *Gorilla* were closest to one another in medial cuneiform shape and had the lowest Procrustes distance of any pairwise comparison between extant species. This is indicative of their ecological and locomotory similarities and confirmed hypothesis 1. However, there were notable differences in morphology between the two (see below). The African apes share an oblique alignment of the long axes of the proximal and distal facets. The long axis of the proximal facet is rotated externally such it runs from inferomedial to superolateral, while the distal facet maintains a more dorsoplantar alignment (Fig. 3.3.12 & 3.3.13). In comparison to *Homo* the facet has a greater mediolateral dimension in the African apes, while in comparison to *Pongo* the facet has a greater dorsoplantar dimension. This indicates that the joint between the medial cuneiform and navicular is adapted to greater mediolateral force transmission than in *Homo* and is adapted to greater dorsoplantar force transmission than *Pongo*. This morphology is consistent with a hallux which is in a stable position while grasping various diameter supports (Sarmiento 1994), and during dorsiflexion at the midfoot. The biconcave curvature of the navicular facet of the medial cuneiform demonstrates the ability of this joint to accommodate weight support in these various positions.

The facet for the first metatarsal also has a curvature to its surface in African apes. It is convex when viewed medially and helical in shape (Schultz 1930). The helix runs from superomedial to inferolateral creating a twist towards the midline of the foot. The medial half of the facet is situated on the medial side of the bone with the lateral half facing distally. The effect of this is to orient the first metatarsal articulation medially, away from the lateral digits (Berillon 1999; McHenry and Jones 2006). The inferolateral corner of the facet is also expanded providing a greater area of contact for the first metatarsal in flexion, thus, flexion at this joint necessarily runs towards the inferolateral corner of the facet drawing the first digit across the foot towards the lateral digits. This morphology facilitates grasping (Gebo 1985), which is essential for effective climbing in the African apes. However, the degree of encroachment of the distal facet onto the medial side of the bone (and, by extension, the degree of abduction of the hallux) is lower in *Gorilla*. This fact is attributed to the lower prevalence of climbing and increased terrestriality in *Gorilla*. The increased terrestriality of *Gorilla* and its large body size place different functional demands on the foot compared to *Pan*; the hallux is used to transfer force more directly from proximal to distal through the foot. This means that

adduction of the hallux is beneficial allowing the first digit to act in propulsion in concert with the lateral digits.

The medial cuneiform of *Gorilla* is also clearly stouter than that of any other non-human species. The mediolateral dimension of the bone is greater, and the proximodistal dimension shorter, than in either *Pongo* or *Theropithecus* (Fig. 3.3.13). In *Pongo* and *Theropithecus* the first metatarsal has practically no weight-bearing role and so the extreme length relative to width of the medial cuneiform is not maladaptive. The medial cuneiform of *Gorilla* is also stouter than that of *Pan* but the difference is less pronounced. This is because the hallux does perform a significant weight-bearing function in *Pan*. The medial cuneiform of *Gorilla* is adapted to withstand loading in many different directions and to facilitate strong grasping in a large ape, and therefore is a stouter bone (Tocheri *et al.* 2011).

The medial cuneiform of *Pongo* was not found to form a close morphological grouping with the African apes, disconfirming hypothesis 2. *Pan* was more similar in shape to *Homo* than it was to *Pongo*. *Pongo* was marginally more similar in shape to *Gorilla* than it was to *Pan*, but had quite a large Procrustes distance from both species, the reasons for these differences are discussed below. The navicular facet is strongly rotated so that its long axis lies almost directly perpendicular to the long axis of the distal facet giving a highly mediolateral set to the proximal facet (Fig.3.3.14A). This is a feature unique to *Pongo*. The consequence of this is that the articulation between the navicular and medial cuneiform has a very slender dorsoplantar dimension and the curvature in this dimension is not as pronounced as the curvature of the facet in its mediolateral dimension, which is also slight. This indicates that movement between these two bones is primarily in the mediolateral direction (Sarmiento and Marcus 2000). However, the overall curvature of the facet is not as great as that observed in *Gorilla*, and is in fact relatively flat indicating lower mobility at this joint in *Pongo* than *Gorilla*, despite the similarities in shape between the two. The navicular facet of the medial cuneiform of *Pongo* slopes anteriorly from inferior to superior which is apparent in medial or lateral view, which will give a dorsal tilt to the bone distally when articulated with the navicular. The distal surface of the bone is similarly tilted such that the facets remain parallel. This would have the effect of orienting the first metatarsal relatively dorsally, permitting the hallux to oppose the sides of the lateral digits during suspension and contributing to the overall transverse arch of the foot (Lewis 1980c).

The distal articular surface has a strong medial rotation accompanied with medial deviation of the distal facet relative to the proximal facet (McHenry and Jones 2006). As a result *Pongo* has the most strongly medially oriented facet for the first metatarsal of any species presented in this study (Fig. 3.3.14B). Consequently, the facet for the first metatarsal is further from that for the second than in any species. From this observation one can infer that *Pongo* possesses the most divergent first digit of all species represented. However, this divergence is not a feature related to grasping but instead caused by the greater importance of the lateral digits in *Pongo*. Thus, the divergence of the first ray is probably required to allow the lateral digits to function unhindered when suspended from a branch. The superior and inferior halves of the distal facet are expanded while the midpoint is constricted, this is similar to the *Gorilla* morphology and the convexity and helical nature of the facet will similarly cause internal rotation with flexion. The extreme rotation of the distal facet, coupled with the mediolaterally aligned navicular facet, makes the medial cuneiform of *Pongo* quite wide. The greater width of the bone is advanced to explain the superficial similarity with *Gorilla*. However, the medial cuneiform is long relative to its height and width in *Pongo* which would reduce its suitability to transmit force from and to the first metatarsal as shearing forces imposed on the medial cuneiform would be higher (Strasser 1988; Szalay and Dagosto 1988).

Theropithecus has a medial cuneiform that was markedly different in shape from all other extant species confirming hypothesis 3 concerning its greater functional and morphological difference to all extant apes. The navicular facet of the medial cuneiform of *Theropithecus* is considerably smaller relative to the overall size of the bone than it is in other species. The facet has an almost triangular outline because the inferior and lateral borders merge nearly into one continuous curved border between the medial and superior border (Fig. 3.3.15A). The small size of the facet and poorly developed inferior and lateral borders indicate that the first digit is not well-adapted to weight-bearing since the articulation between the medial cuneiform and navicular is not robust, nor is the articulation particularly mobile. This implies that the hallux is of reduced functionality in *Theropithecus* relative to the apes. The bone is mediolaterally quite narrow and extremely long proximodistally (Fig. 3.3.15B) which further supports its poor adaptation to weight-bearing, particularly along a mediolateral axis (Langdon 1986). The distal facet is also small in comparison to the overall size of the bone (Gebo 1986; 1989). It is quite long and lacks the pronounced encroachment onto the medial side of the bone observed in apes and has a distal convexity which will limit the ability of the first metatarsal to oppose the lateral digits, but not preclude it. This suggests that the first digit is ill-adapted to strong grasping (Strasser 1988). Furthermore, the distal facet is almost bisected with a distinct superior and inferior articular surface joined by a narrow strip of bone half way along the joint surface. The implications of these features point clearly to the

practical absence of weight-bearing in the hallux of *Theropithecus* and the vastly lower mobility of the first digit relative to the non-human apes.

Homo was found to be considerably more similar in shape to *Pan* than to any other extant species. This is an unusual result as the reduced divergence of the first digit in *Gorilla*, and its stouter medial cuneiform, seem to more closely align it with *Homo*. The navicular facet of *Homo* is much flatter than in the non-human apes, this illustrates the low level of mobility in the midfoot of *Homo* in comparison to the more mobile ape foot. The greater dimension of the facet is aligned on a superoinferior axis while it is narrow mediolaterally. This is consistent with a reduction of the mediolateral component to loading through the first digit and emphasis on movement and force transmission between the medial cuneiform and navicular along a superoinferior axis (Harcourt-Smith 2002), although the flatness of the articulation indicates that there is little movement between these bones.

The first metatarsal facet is directed distally, parallel to the navicular facet (Fig. 3.3.17). This morphology is unlike that in the non-human apes (McHenry and Jones 2006), in which species the distal end of the bone is rotated medially causing a substantial portion of the facet to lie on the medial side of the bone and thus contributing to the divergence of the first digit (Berillon 1999). *Homo* is similar to *Theropithecus* in the degree to which both species have a distally directed first metatarsal facet, however, the morphology of the facet is vastly different in these species. *Homo* has a well-developed facet surface which is expanded in both its superior and inferior portions. This implies that although there is little movement between the medial cuneiform and first metatarsal, the joint is subject to high loads. This inference is corroborated by the fact that the medial cuneiform is robust; it has a short proximodistal length and broad mediolateral width. It is most similar to *Gorilla* in this measure and quite different from the other apes. This further supports the conclusion that the bone is adapted to withstand significant loading. *Gorilla* bears a similar adaptation and this is here explained in similar terms. The proximodistal shortening of the bone in *Homo* is best explained as a response to the relatively unidirectional loading pattern applied to the human foot (Langdon 1986). Shortening of the bone increases its resistance to high bending moments applied longitudinally through the foot throughout the walking cycle.

The proximal and distal facets are parallel and vertically aligned in the coronal plane which can be seen in lateral view in *Homo* (Fig. 3.3.17B), unlike in any other species presented here. The

orientation of these facets in *Homo* could be related to the greater rigidity of the pedal skeleton imposing a more direct and unidirectional loading pattern (Harcourt-Smith 2002). In other species, the tilting of these facets may be to compensate for the changing positional relationships of the navicular and first metatarsal relative to each other given the greater mobility of the pedal skeleton in these species. The fact that the facets are tilted anteriorly will direct the first digit plantarly, priming it for grasping in both dorsiflexion and plantarflexion.

4.3.2. Fossil species

The findings for the medial cuneiform of *Oreopithecus* were particularly interesting. *Oreopithecus* bears the greatest similarity to *Pan* and the two are quite distinct from any other species. This fact simultaneously confirms hypothesis 4 relating to the non-cercopithecoid nature of *Oreopithecus*, and confirms hypothesis 5 relating to the hominoid status of *Oreopithecus*. The navicular facet is similar in outline, size, orientation, and curvature to *Pan* (Fig. 3.3.12A). The implication is that the articulation between medial cuneiform and navicular is capable of transmitting high levels of force while accommodating a reasonable degree of mobility. It is difficult to see why Szalay and Langdon (1986) deemed the articulation between navicular and medial cuneiform to be hinged rather than sellar, particularly as they proceeded to conclude that *Oreopithecus* had a *Pan*-like foot, but one which evolved entirely independently. The results here clearly indicate a reciprocally curved articulation between the two bones. Thus, *Oreopithecus* can be inferred to have had a similar range of motion at this joint principally to allow force transmission along a mediolateral axis throughout a range of dorsiflexion between the navicular and medial cuneiform (Sarmiento and Marcus 2000), indicative of the importance of climbing. The transmission of force along a mediolateral axis throughout a range of dorsiflexion is further supported by the orientation of the navicular facet relative to the distal facet, in which *Oreopithecus* clearly resembles *Pan*; the facet runs from inferomedial to superolateral emphasising the compromise between loading primarily through a mediolateral axis, but with a significant component of dorsoplantar loading.

Oreopithecus possessed a highly curved (Fig. 3.3.12B; 3.3.13B & 3.3.14B), helical distal facet which is indicative of the non-human apes in contrast to the flatter distal facet in *Homo* and *Theropithecus*. This suggests that *Oreopithecus* was well adapted to opposition of the first digit against the lateral digits or sole of the foot. *Oreopithecus* shares with the non-human apes an enlargement of the inferior half of the distal facet, particularly on its lateral side, which similarly suggests that there was

an emphasis on stabilising the first digit in flexion (Lewis 1972). The form of the joint between the medial cuneiform and first metatarsal would produce conjunct internal rotation in *Oreopithecus*. These facts indicate that the first digit complex of *Oreopithecus* functioned in a manner highly similar to *Pan*. i.e. that the hallux could grasp powerfully, indicating that slow, ape-like climbing probably comprised a large component of the locomotory repertoire of *Oreopithecus*. The orientation of the distal facet is ape-like. There is considerable encroachment of the distal facet onto the medial side of the bone (Figs. 3.3.12, 3.3.13, 3.3.14) that would naturally give the first metatarsal an abducted set (McHenry and Jones 2006), which would be amplified in extension owing to the helical shape of the facet (Lewis 1972). However, the facet is not as medially divergent as it is in *Pongo* nor as convergent as *Gorilla*. The fact that *Pan* is more similar in shape to *Oreopithecus* than it is to *Gorilla* suggests that the hallux of *Oreopithecus* functioned in a way highly similar to that of *Pan*.

The morphology of the OH8 medial cuneiform is most similar to *Homo* confirming hypothesis 6 and indicating that OH8 most likely represented an obligate biped. The greatest dimension of the navicular facet is aligned oblique to the dorsoplantar long axis of the first metatarsal facet but has a similar orientation to *Homo* (Fig. 3.3.17). This implies that the articulation between the navicular and medial cuneiform loaded primarily along a dorsoplantar axis with strain applied longitudinally across the foot (Langdon 1986). In *Homo* the loading in these bones occurs through and along the high longitudinal arch of the foot (Aiello and Dean 2002) and there is comparably very little mediolateral loading when contrasted with the morphology of the apes (Sarmiento and Marcus 2000). Thus, there is some evidence to suggest that the OH8 foot had a longitudinal arch allowing the foot to function as a rigid lever in a human-like manner. The shape of the navicular facet resembles that of *Homo* but is not as flat in OH8, although it also lacks the pronounced curved surface found in non-human apes. The navicular facet is also not as large relative to the overall size of the bone as it is in *Homo*. It is about half of the overall height of the bone whereas it is relatively much taller in *Homo*. This may indicate that the joint between the navicular and medial cuneiform was not subjected to such high/frequent loads as it is in *Homo*. This could be explained as a result of the smaller size of OH8, but a different locomotor repertoire (for example including a greater climbing component and reduced bipedal progression) could also account for this difference. However, the morphology clearly resembles *Homo* in form and probable function, thus, the smaller stature of OH8 is likely the principal factor explaining this difference.

The distal facet lies parallel to the proximal facet further supporting a proximal to distal direction of force transmission in the OH8 foot (McHenry and Jones 2006). However, the surface of the first

metatarsal facet is not as flat as it is in *Homo*. It is not as highly curved as it is in the non-human apes, but this feature may explain the moderate difference in shape of medial cuneiform between OH8 and *Homo*. The OH8 medial cuneiform is also relatively longer and narrower (Fig. 3.3.17) than the stout *Homo* medial cuneiform, this may also account for the moderate differences between OH8 and *Homo*. The slightly more gracile medial cuneiform of OH8 is probably related to its much lower body size (Jungers 1988) and therefore lower shear stress during bipedal progression. Furthermore, the distal facet is convex distally in lateral view, compared to the concave morphology found in *Homo*. This concavity is a feature which will serve to reduce the movement at this joint in conjunction with the overall flatness of the facet. The convexity and slight curvature of the OH8 first metatarsal facet align it towards non-human apes, and may indicate some degree of mobility at this joint (Oxnard and Lisowski 1980), although the clear flatness of the facet would suggest that this would be minimal. It is clear that, in all, the OH8 medial cuneiform is most like that of *Homo*. The alignment of the facets suggest a longitudinal direction for loading the first digit and the facets are much flatter than they are in other species presented here, revealing that the range of movement about the medial cuneiform is reduced and force was transmitted predominantly along a proximodistal axis in a manner similar to *Homo*.

The medial cuneiform of *Nacholapithecus* has no strong morphological affinities to any other species presented here as demonstrated by the large Procrustes distances between it and all other extant species. However, *Nacholapithecus* was found to be most similar to *Theropithecus*, offering some evidence to support hypothesis 7. From the principal components analysis it was clear that *Nacholapithecus* was intermediate between the extremes of *Theropithecus* and the African apes. This is an expected finding for a stem hominoid which still retained its cercopithecoid-like pronograde posture (Nakatsukasa *et al.* 1998), but had begun to diverge considerably in its morphology. *Nacholapithecus* lacks the large navicular facet found in the extant ape species. The facet is relatively small compared to the overall size of the bone indicating that there is comparatively little transmission of force occurring at this joint (Langdon 1986). The facet also lacks the teardrop shape typical of *Theropithecus* (Fig. 3.3.15) Instead the facet has the roughly rectangular outline shared by all the hominoids, and the exact implications of this are unclear but the general increase in size suggest some increase in force transmission, and therefore stability, at the navicular-medial cuneiform joint. The facet is also more curved in *Nacholapithecus* compared to *Theropithecus*, indicating that there was increased movement between the navicular and medial cuneiform compared to cercopithecoids (Szalay and Langdon 1986; Sarmiento and Marcus 2000).

The distal facet bears a moderate amount of medial encroachment onto the medial side of the bone which indicates a degree of abduction and grasping behaviour of the first digit (McHenry and Jones 2006), this feature is much more clearly expressed than it is in *Theropithecus*. However, the mediolateral width of the bone is reduced and the proximodistal length is increased, in which regard it resembles *theropithecus* rather than the apes. This would imply that the medial cuneiform is not well adapted to force transmission in a mediolateral direction in contrast to apes (Langdon 1986; Strasser 1988) and similar to *Theropithecus*. Although the distal facet does encroach onto the medial side of the bone this is not excessive or comparable to the extent seen in *Pan* (Fig. 3.3.16). Therefore, it is unlikely that *Nacholapithecus* possessed a hallux capable of an extant ape-like range of abduction and it probably lacked powerful grasping. The distal facet is reniform in shape (Ishida *et al* 2004) with some constriction at its midpoint. This is not as pronounced as in *Theropithecus*, in which species the morphology restricts movement to mediolateral flexion (Strasser 1988). However, the first digit of the foot of *Nacholapithecus* was clearly incapable of ape-like function but was more robust than the medial cuneiform of *Theropithecus* suggesting at least some increase in loading in the foot of *Nacholapithecus*. This increased weight bearing is probably also linked to a shift from semiplantigrady to plantigrady during the emergence of the hominoids which would result in persistent contact between the substrate and the hallux during locomotion.

4.4. Intermediate cuneiform

4.4.1. Extant species

The results revealed that *Pan* and *Gorilla* were most similar to one another in terms of intermediate cuneiform morphology, confirming hypothesis 1. In both *Pan* and *Gorilla* the bone has a considerably greater superoinferior dimension relative to the proximodistal dimension (Fig. 3.4.13 & 3.4.15). The low proximodistal breadth of the bone implies that it is not adapted to withstand compressive forces but does reduce the strain placed on the bone caused by high bending moments (Strasser 1988). This therefore seems like an adaptation for stability during grasping in the foot of the African apes. This is further supported by the curvature of the navicular facet surface in *Pan* and *Gorilla*. The proximally directed concavity, coupled with the long superoinferior dimension, indicate that the articulation between the navicular and intermediate cuneiform is capable of a considerable range of movement. In addition, the fact that the superior part of the articulation is considerably greater suggests that the joint may be preferentially loaded through its superior part during dorsiflexion of the midfoot (Langdon 1986). The narrowing of the navicular facet from superior to inferior wedges it between the larger medial and lateral cuneiforms inferiorly as the dorsoplantar axes of these bones are rotated in

opposition, bringing their inferior borders closer, and creating the transverse arch on the medial side of the foot (Lewis 1980b).

The expansion of the superior half of the second metatarsal facet relative to the inferior portion is consistent with the above evidence pointing to adaptation for dorsiflexion in the midfoot (DeSilva 2010). The joint appears to be stabilised during dorsiflexion at both the navicular-intermediate cuneiform, and intermediate cuneiform-second metatarsal articulations. The superomedial corner of the distal facet is angled posteriorly and receives a beak projecting from the superomedial corner of the proximal second metatarsal. This feature is consistent with grasping during mid-foot dorsiflexion, allowing the second metatarsal to translate dorsally across the intermediate cuneiform and simultaneously producing external rotation as it does so (Sarmiento 1994). The lateral side of the intermediate cuneiform is noticeably shorter than the medial side of the bone, in both *Pan* and *Pongo*. This feature compensates for the laterally-facing lateral cuneiform facet. By shortening the lateral side of the intermediate cuneiform the planes of the distal facets of the intermediate and lateral cuneiform are brought into closer alignment. This adaptation also has the consequence that the larger medial side of the bone could be interpreted as a response to loading from the medial side of the foot (Sarmiento and Marcus 2000) and, in fact, the feature serves both purposes well.

There are some clear differences in morphology of the intermediate cuneiform between *Pan* and *Gorilla*, the most illuminating of which concern the form of the navicular facet. In *Gorilla* the facet has a greater superoinferior dimension than the distal facet and has a greater curvature to its surface. The most obvious physiological difference between the two is the extreme body weight of *Gorilla*. It could be argued that a larger articular surface between the intermediate cuneiform and navicular is needed to support this massive body weight and that contact between these bones is required throughout a greater range of motion at the joint, explaining the greater curvature of the articulation. However, the slightly longer and more curved articulation between the intermediate cuneiform and navicular is unlikely to be of great individual significance in supporting the massive weight of *Gorilla*, but will certainly contribute.

It was found that *Pongo* and the African apes did not form a morphologically close grouping reflecting their shared arboreality and broadly comparable locomotor repertoires in contrast to the terrestrial and relatively “specialised” species of *Homo* and *Theropithecus*. Therefore, hypothesis 2 was rejected. The intermediate cuneiform of *Pongo* exhibits a much broader inferior border of the

proximal facet than any other species examined here (Fig. 3.4.17A). This matches the square outline of the facet found on the navicular. The stoutness of the articulation between the intermediate cuneiform and navicular, and the lower curvature of the articulation compared to the African apes, suggest that the joint is relatively more stable in *Pongo*. This may be a necessary alteration given the extreme deviation of the first metatarsal and the stability needed in a large, suspensory primate which relies more heavily on its lateral digits than its grasping first digit (Gebo 1989; Marchi 2005). The greater proximodistal length of the bone in *Pongo* is probably also related to the highly divergent hallux and its reduced functionality. The second digit takes on a greater share of the weight-bearing functions in a variety of postures and a stouter intermediate cuneiform would be beneficial in this respect. This supports the observed locomotor behaviour of *Pongo* in which grasping with the hallux is uncommon during suspension by hooking the lateral digits over branches (Thorpe and Crompton 2006). The extreme shortness of the lateral side of the bone functions similarly in *Pongo* as it does in African apes. It compensates for the fact that the lateral cuneiform facet of the navicular is flexed strongly laterally and permits the distal articular surfaces of the intermediate and lateral cuneiforms to lie roughly in the same plane.

Distally, the intermediate cuneiform of *Pongo* is unlike any of the other non-human apes. The medial side of the facet is well-developed (Fig. 3.4.17A), probably to compensate for the poorly developed and widely divergent hallux. This further supports the notion that the reduced functionality and importance of the hallux is mitigated against by an increased importance of the second digit. The distal facet has a posteriorly sloping superomedial corner. This recession receives a corresponding beak from the second metatarsal and will thus cause the second metatarsal to rotate in opposition to the first in dorsiflexion. This grants some mobility to the midfoot while grasping and is particularly valuable in arboreal settings, when reaching between branches (Thorpe and Crompton 2006). There is no inferior constriction of the medial half of the bone. Consequently, the medial half of the facet is quite extensive, and this is most probably also related to the extreme divergence of the first metatarsal and increased importance and stability of the second digit. The lateral border of the intermediate cuneiform and the medial border of the lateral cuneiform mirror each other in *Pongo* suggesting that there are extensive ligamentous attachments between these bones (Rose 1984), but also a considerable mobility. Thus, the reduced importance of the hallux is coincident with increased stability of and between the lateral digits and cuneiforms. The greater size of the superior half of the facet compared to the inferior half suggests that the joint is especially stable in dorsiflexion as in the African apes, this fact could be of great importance when reaching for a distant branch while suspending from another, combining mobility and stability.

The intermediate cuneiform of *Homo* was unlike that of the apes, it was most similar in form to *Theropithecus* of the extant species. The clearest difference is in the robusticity of the bone. In *Homo* the bone is proximodistally broader and mediolaterally wider (Fig. 3.4.18). This is because the *Homo* foot loads differently to that of the apes. There is little movement between the intermediate cuneiform and navicular, this is evidenced by the flat articulation between the two and the strong wedging of the intermediate cuneiform between the medial and lateral cuneiforms. Thus, there is relatively very little mediolaterally directed loading through the intermediate cuneiform. But because there is an emphasis on proximodistally directed force transmission, and very low bending moments due to the rigidity of the foot, the increased length of the intermediate cuneiform is a response to unidirectional and heavy loading such as that imposed by human-like bipedalism (Aiello and Dean 2002). Additionally, the long and narrow intermediate cuneiform in humans could compensate for the relative shortening of the phalanges, to reduce excessive shear on the metatarsals, or possibly to provide buttressing to the compressive forces generated during walking (Langdon 1986).

The facet for the second metatarsal is narrow mediolaterally throughout its dorsoplantar length unlike any of the non-human apes. The superior half of the facet is appreciably wider than the inferior half but this disparity is not as pronounced as it is in other non-human ape species. The superior expansion of the facet in the non-human apes is explained as a response to dorsiflexion at the midfoot and loading the joint dorsally. The recess of the superomedial corner of the bone also allows the second metatarsal to twist and oppose the first metatarsal in apes. This adaptation is absent in *Homo* due to the more rigid midfoot. The relatively constant width of the facet indicates that the second metatarsal is securely wedged between the medial and lateral cuneiforms (Saraffian 1983; Johnson *et al.* 2008), this is conducive to human bipedalism in which it is vital that the foot performs as a rigid lever. The distal facet is rotated anteriorly angling the second metatarsal inferiorly in *Homo*, evidencing the presence of a longitudinal arch in the foot. *Homo* is similar to *Theropithecus* with respect to the general dimensions of this facet but the morphology of the facet is different between these two species. The facet surface is flat in *Homo* and approximately parallel to the surface of the navicular facet, unlike the curved surface of *Theropithecus* and the strong midpoint constriction.

Homo is unique in displaying a mediolateral narrowing of the bone from proximal to distal in superior view. This feature is a symptom of the distal convergence of the cuneiforms in *Homo* as opposed to the pronounced divergence of these bones in other species (McHenry and Jones 2006), implying an axis for force transmission aligned roughly proximal to distal. In *Homo* the narrowing of the bone

distally serves to secure the base of the second metatarsal between the neighbouring cuneiforms (Johnson *et al.* 2008). Despite the narrowing of the bone distally, the medial and lateral sides of the bone are approximately equal in length, maintaining the parallelism of the proximal and distal facets. This further implies a direct proximal to distal axis of force transmission through the foot in *Homo* with a limited mediolateral component.

The close proximity of *Theropithecus* to *Homo* disconfirmed hypothesis 3 for the intermediate cuneiform; *Theropithecus* cannot be viewed as an outgroup. The similarity between the two species is difficult to explain but some similarities in function can be discerned between the two. There are, however, clear morphological differences between the two which also highlight their different postural behaviour. The navicular facet of *Theropithecus* has an excessive concavity (Fig. 3.4.18A), much greater than that observed in any other species, which would seem to suggest that the articulation between navicular and intermediate cuneiform is highly mobile in *Theropithecus*. However, *Theropithecus* shares with *Homo* a proximal facet which narrows from superior to inferior but differs in the pronounced rate of constriction. The appearance of the proximal facet in *Theropithecus* (and the morphology of the navicular) suggests that the bone is prevented from moving along a superoinferior axis because the medial and lateral cuneiforms project outwards into the constricted borders of the intermediate cuneiform. Thus, the cuneiforms and navicular of *Theropithecus* are stabilised (Strasser 1988). The bone is also long proximodistally and narrow mediolaterally indicating that force is likely transmitted through the bone in a unidirectional manner, which does not emphasise bending or grasping motions of the metatarsals. The metatarsals will be under compression in *Theropithecus* (Krentz 1996) as it is a digitigrade primate. Therefore, it resembles *Homo* in this respect and implies that a long proximodistal dimension to the intermediate cuneiform may in fact be an ancestral condition lost in the African apes.

4.4.2. Fossil species

Oreopithecus is most similar to the African apes by a considerable margin confirming hypothesis 4 and hypothesis 5. The proximal facet is triangular in outline and the inferior border narrows to a sharp point as it does in the African apes (Fig. 3.4.15), unlike the sub-rectangular shape of *Pongo*. The extreme narrowness of the inferior part of the facet suggests that the bone is poorly adapted to loading when plantarflexed on the navicular, while the broader superior border is better suited to loading in dorsiflexion (Langdon 1986). The narrow inferior portion of the bone also points to

wedging of the intermediate cuneiform between the medial and lateral cuneiforms which suggests the presence of a transverse arch in the foot of *Oreopithecus* (Sarmiento and Marcus 2000). However, the very poorly developed navicular facet of *Oreopithecus* suggests that it may not have been well-adapted to weight-bearing at all. The flatness of the facet relative to the African apes indicates a clearly lower mobility between navicular and intermediate cuneiform in *Oreopithecus*. This is difficult to square with the suggestion of Köhler and Moyà-Solà (1997) that the functional axis of the foot was between the second and first metatarsals (as opposed to the third) which would presumably entail a well-developed intermediate cuneiform to cope with the stress imposed by high levels of bipedal activity. Furthermore, the fact that the bone is considerably smaller than extant ape bones and similar in size to *Theropithecus* suggests that the foot was not as robust as one might expect of a habitual biped. The bone is short proximodistally compared to its dorsoplantar height and mediolateral width, which it shares with African apes; this is explained as an adaptation to reduce shearing stress on the bone when loading through a range of grasping behaviours in those species (Langdon 1986). However, the overall gracility of the bone in *Oreopithecus* and the poorly developed articulation with the navicular make this difficult to reconcile with the view that strong grasping was highly important to *Oreopithecus*.

The superior border of the distal facet is broader than the superior border of the proximal facet (Fig. 3.4.15B) indicating that the bone is wedged proximally between the medial and lateral cuneiforms, and there is a large dorsal articulation with the second metatarsal. *Oreopithecus* very closely resembles *Gorilla* in this respect. This suggests that there is very limited adaptation to force transmission in a proximal to distal axis, instead the emphasis may be on loading through the intermediate cuneiform in dorsiflexion. The distal facet is similar to that of *Gorilla*. The lateral border of the facet is approximately straight from superior to inferior. The superior border is noticeably broader mediolaterally than the inferior border and the superomedial corner of the facet is expanded. This indicates that the ligamentous attachments between the cuneiform bones were similar in form to African apes (Gomberg 1985), and therefore probably offered a similar degree of laxity which may indicate that the foot was poorly adapted to bipedal behaviour. However, bipedal walking above-branch (Thorpe *et al.* 2007) may offer a solution to this, but the gracility of the bones again makes this difficult to argue for. The posteriorly sloping superomedial recess is weakly expressed, but noticeably present. This could indicate a similar adaptation to cause external rotation of the second metatarsal in dorsiflexion to aid in opposing the first digit in this posture. The morphology of the intermediate cuneiform of *Oreopithecus* is mosaic in nature and seemingly contradictory. The morphology of the bone would perhaps be conducive to above-branch bipedalism

in which grasping branches was pivotal. However, the low mobility between navicular and intermediate cuneiform, as well as small size, make any degree of certainty difficult.

The OH8 intermediate cuneiform is indistinguishable in morphology from *Homo* confirming hypothesis 6, but in some features also resembles *Theropithecus*. The shorter and flatter navicular facet in OH8, in which it is similar to *Homo*, is evidence that there was a limited range of motion at the joint between the navicular and intermediate cuneiform. The facet is triangular in outline, most closely resembling the African apes and *Homo*, and unlike the more rectangular outline found in *Pongo*. This feature is linked to pronounced wedging of the bone inferiorly between the medial and lateral cuneiforms forming a transverse arch in the foot. The distal facet is mediolaterally narrow throughout its entire dorsoplantar length, resembling *Homo*. Similar to the *Homo* morphology, the superior border is appreciably broader than the inferior border but this is not as strongly expressed as it is in other species. This indicates a reduction in the importance of mediolateral weight-transfer and an emphasis on loading along a dorsoplantar axis. OH8 also lacks the recess on its superomedial corner found in the apes. These facts indicate that the articulation between the intermediate cuneiform and second metatarsal is not well-adapted for dorsiflexion, nor for loading in this position (Langdon 1986). Indeed, the morphology suggests that the articulation between cuneiform and metatarsal is rigid as it is in *Homo*. The constant mediolateral narrowness of the facet is a good indication that the second metatarsal was similarly wedged between the medial and lateral cuneiforms in a human-like manner (Aiello and Dean 2002). This is further evidenced by the noticeably shorter mediolateral width of the superior border of the distal facet compared to the superior border of the proximal facet. The OH8 intermediate cuneiform also shares with *Homo* a relatively greater proximodistal breadth compared to its dorsoplantar height. This feature is indicative of lengthening of the midfoot in response to loading along a proximodistal axis and also to compensate for the shortening of the metatarsals (Strasser 1988). The anterior tilt of the distal facet is shared with *Homo* and is indicative of a longitudinal arch in the foot, thus is a sound proxy for OH8 having exhibited obligate bipedal locomotory behaviour.

4.5. Lateral cuneiform

4.5.1. Extant species

Hypothesis 1 was once again confirmed for the lateral cuneiform when the results revealed the great similarity of this bone between the African apes. In both species the navicular facet has a moderate

level of curvature to its surface, which is lower than the degree of curvature of the navicular facet of the *Pongo* lateral cuneiform (Fig. 3.5.11B vs. 3.5.12B). This indicates that the African ape articulation between navicular and lateral cuneiform may not be as mobile as it is in *Pongo* (Langdon 1986). The implication of this is that the midfoot of the African apes is relatively more stable than that of *Pongo*. This reflects the greater need for stability when grasping branches during climbing in the African apes, compared to the greater need for mobility in *Pongo* (Hunt 1991; 1996; Thorpe & Crompton 2006). The medial border of the navicular facet lies closer to the distal side of the bone than does the lateral border of the facet. This morphology is commensurate with the oblique orientation of the lateral cuneiform facet of the navicular, which is directed laterally. By having a lateral cuneiform with a longer lateral than medial side (in conjunction with an intermediate cuneiform whose medial side is longer than the lateral) the planes of the distal facets of the lateral and intermediate cuneiforms are brought into alignment, which thus aligns the longitudinal axes of the second and third metatarsals. The laterally directed articulation between navicular and lateral cuneiform is interpreted here as an adaptation for (at least some) laterally directed force transmission from the navicular, through the lateral cuneiform and directly to the cuboid (Sarmiento and Marcus 2000). This feature is compatible with the need for support in a foot which is weight-bearing in an inverted and dorsiflexed position such as during vertical climbing (DeSilva 2009). This view is further evinced by the extensive articular facet for the cuboid (Rose 1984; Sarmiento 1987).

The distal facet of the lateral cuneiform is tilted anteriorly such that the dorsal border extends slightly further distally from the proximal surface than does the inferior border (Fig. 3.5.14B). The significance of this feature is difficult to explain. The effect of it would be to give the third metatarsal base a plantar orientation (Berillon 2003), this morphology is shared with both *Pongo* and *Homo* and is therefore curious given the highly different positional behaviours of these different species. This morphology in *Pongo* can be explained in the context of increased levels of suspension, and so regular use of the digits in a strongly plantarflexed posture, while in *Homo* it is a consequence of the high longitudinal arch and functions as an aid to bring the heads of the metatarsals into contact with the ground in walking. Since the African apes are well-adapted to neither suspension nor human-like bipedalism this morphology seems peculiar. It could perhaps be an adaptation to terrestrial quadrupedalism, a means to increase traction and grip in order to propel the body forwards. Or alternatively it could aid in grasping during vertical climbing by orienting the third metatarsal toward the hallux. The articular surface for the third metatarsal is large in size and the plane of the facet is parallel to the navicular facet in medial or lateral view, i.e. the navicular facet also has an anterior tilt (a fact distinguishing the apes from *Homo*). There is no feature present to receive a proximally projecting beak (Fig. 3.5.11B), unlike the morphology of the intermediate cuneiform, but there is

pronounced expansion of the superior half of the facet relative to the inferior half, especially on its medial side. This is in agreement with evidence already presented for weight-bearing on a dorsiflexed and inverted mid-foot (DeSilva 2009), which is the position habitually adopted during climbing in the African apes.

The African apes differ in the outline of the navicular facet. In *Pan* the facet is rectangular with an equal length to the medial and lateral borders of the facet (Fig. 3.5.14A). In contrast, the medial border of the navicular facet of *Gorilla* is considerably shorter than the lateral causing the inferior border to slope upwards from lateral to medial (Fig. 3.5.11A). The reasons for this difference in shape are difficult to ascertain. Indeed, the differences may be due to chance rather than having a functional explanation. However, one possible interpretation is that there is an emphasis on stabilising the lateral side of the articulation between the navicular and lateral cuneiform in *Gorilla*. Due to the large body size of *Gorilla* the level of force transmitted from the navicular to the cuboid through the lateral cuneiform will be higher and therefore this part of the articulation is more well-developed.

Pongo did not form a close morphological grouping with the African apes on the basis of the lateral cuneiform, refuting hypothesis 2. This suggests that the morphology of the bone is not more similar among the arboreal species included compared to the terrestrial species. Therefore, the morphology of the lateral cuneiform likely represents some key adaptations to specific positional behaviour. The navicular facet of the lateral cuneiform of *Pongo* bears the most highly curved surface of any species (Fig. 3.5.12). This indicates the highest level of mobility at the navicular – lateral cuneiform joint (Rose 1984). The greater mobility of the joint in *Pongo* is a result of the greater incidence of moving in a multidirectional manner through the canopy from a suspended posture (Gebo 1989; 1992). It may be necessary for *Pongo* to reach out from one branch to another in a number of directions. Therefore, having a midfoot which is mobile in this way, while permitting the lateral digits to continue grasping a supporting branch, is clearly of great benefit. (Although, Thorpe and Crompton (2006) found that suspension was not significantly more common in *Pongo*.) The medial side of the navicular facet also lies closer to the distal surface of the bone than does the lateral side of the facet. This functions as in the African apes, to correct the laterally directed articulation with the cuboid and bring the distal facets of the lateral and intermediate cuneiforms into alignment. This gives the lateral cuneiform a highly wedged appearance, the fact that the articulation between navicular and lateral cuneiform is directed more strongly laterally in *Pongo* suggests that the transfer of force to the cuboid is more pronounced. This is likely because of the extreme divergence of the hallux and the

increased importance of the lateral digits in *Pongo*, as well as the increased inversion of the foot of *Pongo*.

The facet for the third metatarsal of *Pongo* is vaguely similar in form to the African apes in that it is very roughly T-shaped. The inferior portion of the facet is more slender than it is in the other apes and in this respect *Pongo* resembles *Homo* and *Theropithecus*. The lateral side of the superior portion of the facet is similar in form to the African apes. It is rectangular in outline and well-developed, extending laterally beyond the inferior portion of the bone. The medial portion, however, is narrow and tapers to a fine point, which is unique to *Pongo*, and mirrors the morphology of the lateral side of the intermediate cuneiform. Additionally there is a recess in the superomedial corner (Fig. 3.5.12B), which is not as pronounced as it is on the intermediate cuneiform, but is clearly present, and this feature is likely linked to the increased inversion of the foot of *Pongo* due to the positionally diverse nature of being highly arboreal. Similarly to the recess found on the intermediate cuneiform the third metatarsal will oppose the hallux in dorsiflexion at the midfoot. The greater development of the lateral side of the distal facet in *Pongo* further supports the conclusion that the lateral cuneiform is loaded predominantly on the lateral side due to the increased importance of the lateral digits and extreme inversion of the foot.

Homo was markedly different in shape from all of the other extant species. The navicular facet of the lateral cuneiform is mediolaterally narrow and dorsoplantarily long (Fig. 3.5.13A), as is the case with the navicular facets of the other two cuneiforms. This is concordant with the convergence of the cuneiforms distally in *Homo* and indicates a reduction in the importance of mediolaterally directed force transmission and an emphasis on loading in a dorsoplantar direction along a proximodistal axis. The medial side of the navicular facet lies closer to the distal facet in *Homo* but this is not expressed as strongly as it is in other apes (among which *Pongo* exhibits the greatest asymmetry between the planes of the proximal and distal facets), therefore the proximal and distal facets are more parallel in humans. This further demonstrates the adaptation of *Homo* to a proximodistal axis of force transmission through the medial column of the foot (Saraffian 1983). And is indicative of the rigidity of the foot and its ability to function as a lever about the fulcrum of the heel. Furthermore, the oblique alignment of the planes of the proximal and distal facets may contribute to the convergence of the medial and lateral cuneiforms distally (Lewis 1980b) and account for the distal narrowing of the intermediate cuneiform. This is a key adaptation of the human foot resulting in a keystone effect of the intermediate cuneiform, increasing the rigidity of the human midfoot. From superior view this

feature is quite clear based on the convexity of the lateral side of the bone, in comparison to the straight border of African apes or concave border of *Pongo*.

The facet for the third metatarsal has a long dorsoplantar dimension and is fairly constant in width mediolaterally throughout its entire length. This adds further support to the reduced importance of mediolateral transfer and points towards an emphasis on dorsoplantar loading along a proximodistal axis. The distal lateral cuneiform in humans lacks the pronounced superior expansion of the facet observed in other species included in this study, but there is still a slight expansion of the lateral side. This suggests that there is a reduced emphasis on loading through the superior part of the articulation between the lateral cuneiform and third metatarsal in humans, which is to be expected in the foot of an animal that lacks the midfoot dorsiflexion found in the non-human apes; the joint mirrors the morphology of the intermediate cuneiform/second metatarsal joint. Additionally, the narrowness and height of the bone further suggests an emphasis on the reduction of importance of a mediolateral component of force transmission through the cuneiforms. On the contrary, an emphasis is placed on loading in a dorsoplantar direction (Langdon 1986). The great length of the lateral cuneiform is explained as compensation for the reduced length of the digits of the foot and to reduce the shear stress placed on the metatarsal through bending by assuming some of the force placed on the metatarsals and there by relieving stress.

The lateral cuneiform of *Theropithecus* was found to be most similar in shape to *Pan* and was not markedly different from the ape species. This suggests that the morphology of the lateral cuneiform does not reflect plantigrade/digitigrade adaptations and therefore hypothesis 3 was rejected. The navicular facet of the lateral cuneiform has an unusual shape (Fig. 3.5.14A), but one that is most similar to *Homo*. The lateral border is shortened while the medial border is lengthened relative to the superior and inferior borders (Langdon 1986), this indicates an extreme reduction in the importance of the laterally directed weight-transfer from navicular to cuboid (a feature shared with *Homo*). The curvature of the facet is moderate; not as flat as it is in *Homo* nor as curved as in *Pongo* (Langdon 1986). This suggests a moderate degree of movement is possible between the navicular and lateral cuneiform, but not a great deal. This is expected in a habitually heel elevated position. The foot of *Theropithecus* requires rigidity, and is adapted to withstand compression in a digitigrade posture. However, as pressure is applied towards the sole of the foot the tarsals and metatarsals are subjected to high bending moments. A small degree of mobility between the navicular and cuneiforms will help to alleviate this stress.

The proximal and distal facets are approximately parallel from superior view which further supports the emphasis of proximodistal force transmission through the foot of *Theropithecus*, especially as the functional axis of the foot lies along the third metatarsal (Strasser and Delson 1987). The articulation with the cuboid is very small suggesting that there is very little regular force transmission from medial to lateral from the lateral cuneiform (Strasser 1988), which is expected in a primate which moves its hindlimb primarily through the parasagittal plane and exhibits very little pronation and supination of the foot. The distal facet has an ape-like form roughly appearing to be T-shaped (Langdon 1986). However, the medial arm is not as well-developed in *Theropithecus* compared to the apes. The greater development of the superior portion of the distal facet is fitting considering the foot position of *Theropithecus* during walking and the dorsiflexed foot posture due to the raised heel.

4.5.2. Fossil species

Oreopithecus is most like *Gorilla* in its lateral cuneiform morphology, however, it is also similar to *Pongo* in some features and the Procrustes distance between *Oreopithecus* and other species means was large. Therefore, hypothesis 5 was accepted but with caution and due attention given to the fact that the similarities between *Oreopithecus* and *Gorilla* were not as strong as was the case for other bones in this study. The lateral border is long as it is in *Gorilla* (Fig. 3.5.11A), but the inferior border is strongly curved and runs superiorly to merge with the medial border as in *Pongo* (Fig. 3.5.12A), making the medial border noticeably shorter than the lateral. The surface of the facet is moderately curved, more so than in *Gorilla*, resembling *Pongo*, but not as extremely curved. Therefore it seems that *Oreopithecus* was adapted to a greater degree of mobility at this joint in comparison to *Gorilla*, which could in turn indicate an increased requirement for loading in a greater variety of directions/foot positions and perhaps a fairly large suspensory component to the positional repertoire (Rose 1984). It is also feasible that increased mobility of the midfoot could permit extended limb arboreal bipedalism of the sort observed in *Pongo* (Crompton *et al.* 2010). However, the fact that the tarsals of *Oreopithecus* are consistently smaller than those of *Pongo* are difficult to explain if bipedal behaviour formed a significant component of the locomotory behaviour of *Oreopithecus*. This is particularly true in light of the fact that the body weight of *Oreopithecus* was probably comparable to that of *Pongo* (Jungers 1988). The medial border of the facet is situated closer to the distal surface of the bone than the lateral border, a feature found in all of the apes to compensate for the lateral flexion of the lateral cuneiform facet on the navicular and which additionally will act to direct force from the navicular towards the cuboid and lateral foot (Langdon

1986; Rose 1994). The situation of the medial border of the facet distally more closely resembles *Pongo* and therefore suggests a relatively high level of weight transfer towards the lateral side of the foot and may indicate that the foot was highly inverted in *Oreopithecus*.

Oreopithecus is like both *Gorilla* and *Pongo* in having a narrow inferior portion of the distal facet relative to the superior border, forming a T shape, but this feature is more prominently expressed in *Pongo*. The greater size of the superior portion of the facet relative to the inferior portion suggests that *Oreopithecus* shares with both *Gorilla* and *Pongo* a preference to loading the bone in dorsiflexion. However, the superomedial corner of the facet is reduced in size and bears a posterior slope, displaying a *Pongo* like constriction. This provides further evidence to a preference on loading the lateral cuneiform on its lateral side to an extreme degree. The explanation for this could be that the foot of *Oreopithecus* was highly inverted, indicative of suspensory behaviour. The sloping of the superomedial corner also supports this view as it would allow the third metatarsal to oppose the hallux when reaching between branches in a suspensory posture. However, the incredibly small size of the bone makes interpreting these features difficult.

OH8 was found to be most similar in shape to *Homo*. However, the Procrustes distance was relatively large between the two and there are some notable differences. Therefore hypothesis 6 was accepted, but with caution. The navicular facet is significantly broader across its dorsoplantar dimension than its mediolateral dimension (Fig. 3.5.13A) suggesting that this is the axis through which it is best suited to loading (Langdon 1986), aligning it closely with *Homo* and clearly distinguishing it from the apes. The implication is that there is very little emphasis on the mediolateral movement of force which comes with a grasping hallux. (This feature is found in each of the cuneiform articulations with the navicular and indicates a relatively lesser importance of mediolaterally directed weight transference while dorsoplantar loading is emphasised). Furthermore, the navicular facet is flat in OH8 indicating that there was very little mobility at the navicular – lateral cuneiform joint, supporting the interpretation of the OH8 foot as possessing human-like rigidity. The bone also lacks the ape-like oblique orientation with the distal facet in OH8; the two facets are in approximately parallel alignment which further supports direct proximodistally directed weight transfer (Rose 1984).

The distal facet also resembles the *Homo* morphology. The pronounced ape-like expansion of the superior part of the facet is absent in OH8, although the lateral side of the superior border is slightly more expanded than the medial side, as it is in *Homo*. In contrast to the other species the OH8 facet

is mediolaterally narrow throughout its entire length. This morphology suggests a reduction in the importance of loading through the superior aspect of the articulation between the lateral cuneiform and third metatarsal. This suggests that the midfoot was not capable of midfoot dorsiflexion. Furthermore, the anterior tilt of the distal facet relative to the proximal facet is further evidence of a well-developed longitudinal arch in OH8. This evidence indicates that the foot is capable of functioning as a rigid lever during regular bipedal locomotion. The narrowness of the distal facet also suggests that the articulation is poorly adapted for mediolaterally directed loading, similar to the navicular facet. The bone is mediolaterally narrow throughout its length while being broad in its dorsoplantar dimension and proximodistally long which also resembles the *Homo* shape overall. This indicates that the lateral cuneiform of OH8 was well suited to loading in a dorsoplantar direction along a proximodistal axis, in which it again resembles the *Homo* condition and appears to be well-adapted for obligate bipedalism.

4.6. First metatarsal

4.6.1. Extant species

The results for the first metatarsal showed that the African apes were not more similar to each other than to any other species (Table 3.6.1), *Pan* was more similar to *Pongo*. This result disconfirms hypothesis 1 for the first metatarsal, an unusual finding in this study after hypothesis 1 was accepted for all the tarsals already examined. The difference between *Pan* and *Gorilla* seems to be primarily as a result of the more gracile bone in *Pan* (Fig. 3.6.16). The proximal facet of the first metatarsal is very small relative to the overall size of the bone in *Pan* compared to *Homo*, and moderately small compared to *Gorilla*, but larger compared to *Pongo* and *Theropithecus*. This indicates that, while there is significant weight-bearing taking place at this joint in *Pan*, it is not as pronounced as it is in *Homo* or *Gorilla*. The helical and concave proximal facet is clear evidence that the hallux has a grasping function in *Pan* (Schultz 1930), which utilises conjunct rotation as the hallux is flexed, internally rotating and adducting the first metatarsal towards the midline of the foot (Langdon 1986; Lovejoy *et al.* 2009a). The effect of this will be amplified distally along the bone as the dorsoplantar long axis of the head is internally rotated relative to that of the base of the metatarsal (Morton 1922). *Pan* expresses these features more strongly than *Gorilla*. This can be attributed to the lower body weight of *Pan*; *Gorilla* has presumably sacrificed an amount of mobility in favour of support of its great body weight (McHenry and Jones 2006).

The strong angulation between the superior and inferior portions of the head of the first metatarsal in *Pan* indicate a greater range of movement in flexion and extension of the first digit. Additionally, the rotation and placement of the head of the first metatarsal towards the plantar side of the bone in *Pan*, giving the first metatarsal a greater longitudinal curvature, indicates that the bone is more prone to flexion than it is in *Gorilla*. This is further evidence that the hallux and foot of *Pan* is better suited to performing in a grasping manner, which is related to the relatively greater prevalence of arboreality in *Pan*. The first metatarsal of *Pan* is also long relative to its width, having a more gracile overall appearance which is likely largely responsible for its greater similarity to *Pongo*, while *Gorilla* has a wider, stouter first metatarsal which is further evidence of the ability of *Pan* to better combine mobility and weight support, a vital feature in the context of a greater incidence of arboreal behaviour.

Despite the lower Procrustes distance between *Pan* and *Pongo* for the first metatarsal, *Pan* still had the lowest Procrustes distance from *Gorilla* of any species, while *Homo* had the greatest Procrustes distance from *Theropithecus* of any hominoid. The facet for the navicular is larger relative to overall bone size in *Gorilla* compared to *Pan* and much larger than in either *Pongo* or *Theropithecus*. This is apparent simply in the length of the facet but the shorter diaphysis exaggerates this feature; the reduced length of the first metatarsal therefore increases the relative size of the facet. The helical appearance of the proximal facet compliments the helical form of the first metatarsal facet on the medial cuneiform and clearly indicates grasping capability at this joint (Lovejoy *et al.* 2009a). The long axis of the head of the first metatarsal is rotated internally relative to the long axis of the proximal facet (Morton 1922), but this is not as strongly expressed in *Gorilla*. This feature brings the first digit into opposition with the lateral digits. The opposition created by the torsion between the base and head of the first metatarsal is increased by the internal rotation promoted alongside flexion at the joint between the medial cuneiform and first metatarsal. The decreased disparity between the orientations of the proximal and distal facets in *Gorilla* shows that there is a reduced importance in function of the hallux in a grasping. The closer alignment of the orientations of these facets and the more convergent hallux suggest that the hallux is transferring force longitudinally more frequently in *Gorilla*, linked to this species' greater terrestriality. Therefore, the hallux more frequently functions on a flat surface and acts to transfer force in the direction of travel.

Gorilla differs from the morphology of *Pan* in having a less acute angle of flexion between the superior and inferior portions of the head and more extensive development of the inferior portion. However, the degree of angulation of the head is greater than it is in *Homo*, in which species the

angulation of the head is more obtuse. This suggests that a greater range of flexion and extension possible at this joint is greater than it is in *Homo*, but lower than in *Pan*. This evidence further supports the use of the hallux more frequently on a flat surface and a reduced importance of grasping relative to *Pan*, as noted above. The larger size of the head of the first metatarsal shows clearly that the hallux bears a greater load than is the case in *Pan*. Overall, *Gorilla* possesses a stouter first metatarsal which closer approximates the human condition in being shorter and broader than other species (Riesenfeld 1975), this is most likely due to the extreme body weight of *Gorilla* (McHenry and Jones 2006) and not to a general similarity in locomotory behaviour.

Pongo bears a strong resemblance to *Pan* in its first metatarsal morphology (Fig. 3.6.17). However, the proximal facet is more slender than it is in *Pan* relative to overall bone size and is very narrow in its mediolateral dimension in comparison to dorsoplantar height (Tuttle and Rogers 1966). This indicates that the joint is subjected to lower levels of force transmission than is the case in *Pan*, a result which is expected given that the hallux is highly divergent in *Pongo*. The medial cuneiform facet is also helical in form matching the morphology of the medial cuneiform (Lewis 1972; Latimer and Lovejoy 1990). This indicates that, although the medial cuneiform – first metatarsal joint transmits lower levels of force in *Pongo* than in other apes, it is capable to a degree of movement comparable to that observed in *Pan*, but seems to lack the level of stability of the hallux in *Pan*. Of all the apes *Pongo* has the highest torsion of the first metatarsal (Drapeau and Harnon 2013) which is evidence of the greater divergence of the first metatarsal in *Pongo*. This pronounced torsion could be linked to the greater arboreality of *Pongo* and the need to oppose the hallux to the lateral digits in a wider range of orientations and thickness of supports, compared to other species. It has been suggested that the *Pongo* hallux grasps against the sole of the foot rather than against the second digit (Drapeau and Harnon 2013). This would mean that *Pongo* has a less accurate grasp than that of the African apes, but grasping against the sole of the foot may increase the power of its grasp despite its relatively more gracile and highly diverged hallux.

The head of the first metatarsal of *Pongo* is the most diminished in size of any ape species relative to overall bone size (Tuttle and Rogers 1966), although it is not excessively smaller than *Pan*. In this feature *Pongo* shares a similarity with *Theropithecus*. The implication is that there is a low level of force transmission at the joint. The dorsolateral portion of the articular surface of the head is poorly developed in *Pongo*. From dorsal view this gives the appearance that the head is flexed medially away from the shaft of the bone. This feature orients the articulation between metatarsal and proximal phalanx more medially, aiding in opposition. Similarly to *Pan* the dorsal and plantar aspects

of the head are acutely angulated suggesting a high range of movement with the proximal phalanx, particularly in flexion, which could compensate for the high divergence of the hallux by increasing the mobility of the distal segments. The bone is short and extremely gracile compared to other apes (Jashashvili *et al.* 2015), bearing a similarity to *Theropithecus* in this respect and likely demonstrating the reduced importance and function of the hallux in a weight-bearing capacity in *Pongo*.

The long axes of the base and head of the first metatarsal in *Homo* are close to parallel in contrast to the ape condition, in which they are closer to perpendicular, resulting in a high degree of torsion along the shaft of the bone. This has been well documented (e.g. Morton 1922; Aiello and Dean 2002; Zipfel *et al.* 2009; Drapeau and Harnon 2013) and is indicative of the adducted, non-opposable hallux of *Homo* compared to the divergent, opposable hallux of the apes. Furthermore, this alignment of the long axes lies along the dorsoplantar axis and adds more support to the dorsoplantar direction of force transmission in the human foot. The surface area of the medial cuneiform facet is vastly increased relative to the overall size of the bone in *Homo* pointing to the greater habitual stress placed on this articulation than is the case in other species (Aiello and Dean 2002; McHenry and Jones 2006). The flatness of the facet demonstrates that there is very little movement at the joint, supporting the evidence from the cuneiforms, which indicates that the midfoot is stable and rigid in *Homo*. This aids in transferring force effectively through the foot.

The bone is extremely stout in *Homo*; it is much shorter from its proximal to distal end and has a greater cross sectional area of the diaphysis and the head and base are much more robust also (Fig. 3.6.18), which shows that the human first metatarsal is well adapted to weight-bearing in contrast to other species presented here (Marchi 2005). The reduction in length of the diaphysis reduces its exposure to bending moments and increases its resistance to the high loading to which it is subjected. The surface area of the distal articular surface is massively expanded in comparison to other species. This is due to the lack of opposability of the hallux and its key importance in the toe-off phase of the walking cycle. At this moment the head of the first metatarsal is propelling the entire body weight forward, its increased robusticity is a response to this. The angulation of the superior and inferior aspects of the head is not as acute in humans and is predominantly directed dorsally. Thus the range of motion distal to the first metatarsal is reduced in *Homo* while the capacity for weight-bearing is massively increased. The low mobility of the joint is concentrated in extension of the first digit, which is the position of the first metatarsal –proximal phalanx articulation at toe-off.

The first metatarsal of *Theropithecus* was found to be relatively similar to that of *Pongo* and *Pan*, disconfirming hypothesis 3 and suggesting that the morphology of the cercopithecoid was not excessively different to that of the hominoids and that other factors played an important role, such as the extreme specialisation of *Homo* and extreme body weight of *Gorilla*. *Theropithecus* possesses a proximal facet which is moderately deep but lacks the well-developed helical form of the ape first metatarsal (Lewis 1972). This morphology suggests that *Theropithecus* is adapted for mobility at this joint but lacks the specialised conjunct flexion and internal rotation of the ape foot. However, the tilt of the medial cuneiform on the navicular, and lack of medial encroachment of the distal facet of the medial cuneiform onto the medial side of the bone, means that simple flexion and adduction of the hallux will produce a grasp, not as powerfully adapted as it is in the apes, but the feature is still present (Strasser 1988).

The first metatarsal is long and narrow in *Theropithecus*, a feature which also suggests that the hallux is not well suited to powerful grasping nor weight-bearing. The long axes of the proximal and distal facets are close to parallel giving the bone a low level of torsion; another feature which provides evidence for the relatively poorly developed grasp of *Theropithecus* (Drapeau and Harmon 2013). Furthermore, the surface area of the head of the first metatarsal is greatly diminished relative to the overall size of the bone, further evidence for the comparably low importance of the first metatarsal, and its inability to bear considerably high forces, relative to other species assessed here. However, the high radius of curvature of the head from superior to inferior from medial and lateral view suggests that *Theropithecus* possess a range of motion at the metatarsophalangeal joint similar to that found in apes, unlike in *Homo*.

4.6.2. Fossil species

The fact that there was no complete first metatarsal available for *Oreopithecus* makes it difficult to draw informative conclusions about the morphological relationships and function of the first metatarsal. However, comparison of the proximal and distal ends of the bones with extant species allows some tentative inferences to be made. The base of the first metatarsal was found to be most similar in morphology to *Pongo*. It bears the non-human ape-like helical surface, which, taken together with the morphology of the distal medial cuneiform, suggests that the hallux of *Oreopithecus* was well-adapted for grasping. The facet is relatively wider mediolaterally than it is in *Pongo* which could indicate a greater ability to transmit force through the joint than *Pan*. However,

the centroid size of the base of the first metatarsal of *Oreopithecus* is low. This suggests that, for an ape of similar body size (Jungers 1988) the hallux of *Oreopithecus* would have been less well-suited to withstanding high levels of force compared to that of *Pongo*. The head of the metatarsal is most like *Pan* and indicates that the first digit was capable of a good range of motion about the first metatarsal. The greater development of the plantar portion of the facet also further suggests that emphasis may have been similarly placed on flexion in *Oreopithecus*.

Given the morphology and function of the hallux of *Pongo*, then, it seems unlikely that the hallux of *Oreopithecus* could have played a significant weight-bearing role, but was seemingly capable of some degree of ape-like grasping nonetheless. One possible explanation for these observations could be that *Oreopithecus* was predominantly a brachiator. This is a view which has not received much attention since the earliest discovery of *Oreopithecus* (Delson 1986), but could neatly account for the gracility of the foot of *Oreopithecus*. However, the morphology of the trunk and forelimb do not seem to support this conclusion (Harrison 1986). Comparison of the pedal bones with those of extant brachiators may provide an interesting insight into the function of the foot, and the behavioural affinities, of *Oreopithecus*. It may have utilised a unique repertoire of locomotor behaviours not seen in any ape.

5. Conclusions and future research

The results of this study have revealed numerous interesting morphological traits and interspecific trends for the medial column of the pedal skeleton in a number of primates. The differences and similarities in shape were interpreted in light of the known positional behaviour for each extant species in order to construct a framework from which to estimate the function of the medial column of the foot in a number of fossil specimens. It was found that the African apes were consistently very similar, and in some cases indistinguishable from one another. In cases where differences were apparent between the two groups this was attributed to the greater body size and/or increased terrestriality of *Gorilla*.

It was found that the medial column of the foot of *Pan* is well-adapted to loading in dorsiflexion and inversion, features which are predominantly associated with vertical climbing (DeSilva 2009). Furthermore, the powerful grasping hallux is well suited to the grasping postures necessary in vertical climbing. The mobility of the midfoot was found predominantly to facilitate dorsiflexion in this region from evidence such as the narrower navicular on its dorsal side. However, there are indications of adaptations relevant to mediolateral movements and force transfer such as the highly laterally flexed 3rd naviculocuneiform articulation (Rose 1994). The overall anatomy of *Pan* is one which facilitates a powerful grasp during midfoot dorsiflexion. This allows a firm grip of the substrate while the heel generates propulsive force to climb (Gebo 1996; Isler 2006). The interpretation of the pedal anatomy of *Pan* in the context of vertical climbing adaptations does not preclude or ignore its varied locomotor repertoire. Instead, it takes into account the fact that climbing is a dangerous activity and being well-adapted to it is selectively advantageous (Pontzer and Wrangham 2004; Hanna *et al.* 2008; DeSilva 2009).

Gorilla was found to largely resemble *Pan* in its adaptations for dorsiflexion and inversion. The conclusions reached for the relevance of these features therefore were similar. Since climbing is a high risk behaviour it is selectively advantageous to be skeletally well-adapted to it even if it does not form a major proportion of the locomotor repertoire (Gebo 1996). There are observable differences between the African apes, however, in the analysis of some bones. For example, the more equal heights of the trochlear rims of the talus, and the increased robusticity and reduced torsion of the hallux in *Gorilla*. These features are likely to be correlated to the greater terrestriality of *Gorilla* and its larger size than *Pan* (Doran 1997; Harcourt-Smith 2002). The mobility between joints was found to

be marginally lower, judged by their degree of curvature, and this too is linked to increased terrestriality/decreased arboreality. Given that *Gorilla* is using its foot in a more predictable way, more of the time, the need to load the foot in a variety of postures is lessened, although still present. As a corollary of this, greater stress is placed on the joints of the foot and therefore increased robusticity is required to meet the demands placed on the bones and joints.

It was found that the medial column of the foot of *Pongo* was the most highly adapted to mobility, both at the ankle and the midfoot. The talus lacks the wedging found in African apes permitting a greater range of dorsiflexion and plantarflexion at the ankle (Szalay and Langdon 1986). *Pongo* also exhibited the greatest disparity between the height of its trochlea rims suggesting that it has the most highly inverted foot position (Aiello and Dean 2002). However, *Pongo* did not display the African ape-like flaring of the malleolar facets which are interpreted as providing support to the malleoli during compressive behaviours which occur in inversion (Marchi 2015). This is interpreted in a manner similar to that for vertical climbing in African apes. Even though compressive behaviours do form a significant part of the locomotor behaviour of *Pongo* (Thorpe and Crompton 2006) they do not represent the highest risk behaviour. Suspension is a relatively much more dangerous behaviour and the unusual adaptations of the foot are presented in view of that fact. The midfoot is highly mobile with a focus on the lateral toes of the medial column, and reduced importance of the hallux. These adaptations permit the hooking of the lateral digits over the branches (Hunt *et al.* 1991) and the foot to move into inversion and dorsiflexion from this position. The upper ankle joint is also presented as an adaptation conducive to this behaviour. The medial malleolar facet is small, indicating that it is not well-adapted to compression, and the low level of flaring of the malleolar facet compared to African apes is interpreted as reducing the distance ligaments have to travel. The ligamentous anatomy of the ankle will be of greater importance under tension (such as during suspension) than the skeletal morphology.

The foot of *Homo* presented no unusual features and presented the morphology expected of a well-understood bipedal primate. The articulation with the tibia is perpendicular and in a neutral position between dorsiflexion and plantarflexion. The ability to invert at the upper ankle joint is limited, indicated by the absence of flaring of the medial malleolar facet which limits ankle movements to avoid injury (Sarrafian 1983). There is a general pattern of aligning the articulations of the medial column directly distally which also indicates that movement, and the direction of force transmission, is quite restricted in *Homo* compared to other apes. As well as aligning the articulations distally the bones of the midfoot are also lengthened to increase their ability to withstand compressive forces at

toe-off and to reduce the effects of a shortened metatarsus (Aiello and Dean 2002). Finally, the articulations in the medial column of the *Homo* foot indicate that the mobility between the bones is greatly reduced, which is expected of a rigid, bipedal foot.

Theropithecus provided some interesting insights and a novel comparison in this type of study. It was found that *Theropithecus* possessed many unique traits, but also that there were numerous traits shared with the extant apes and some with *Homo*. The upper ankle joint is similar in form to that of African apes. The medially sloping trochlea and medial divergence of the anterior part of the medial malleolar facet are expressed to a similar degree in *Theropithecus*, although the salient differences, such as the greater angulation between the anterior and posterior halves of the medial malleolar facet, are noted in the discussion. This indicates that *Theropithecus* is well-adapted to inversion of the foot at the upper ankle joint. *Theropithecus* habitually exhibits inverted foot postures (Krentz 1993) and this provides some evidence that upper ankle inversion is an ancestral condition for Hominoidea (Lewis 1980a; Gebo 1996).

The general lengthening of the navicular, particularly on its lateral side, is shared with *Homo*, excluding the non-human ape species. Of particular note is the distally oriented lateral cuneiform facet which is shared only by *Homo* and *Theropithecus* and represents adaptation to reduced midfoot mobility and restriction of the direction of movement and force transmission in the foot. This may provide some additional support to the notion that the human foot evolved from a cercopithecoid-like morphology rather than an ape-like one (Lovejoy *et al.* 2009a). However, this could also have been independently evolved in both lineages, but if a proximodistally broad navicular with distally directed lateral cuneiform facet were, in fact, the ancestral condition for Hominoidea then it would present a difficult dilemma. The presence of this morphology would entail that either the highly flexed lateral cuneiform facet was independently arrived at in extant ape lineages, or the morphology arose in a common ancestor and was lost again in the *Homo* lineage. Therefore, the principal of parsimony would make it most likely that the common ancestor of extant hominoids possessed a laterally facing 3rd naviculocuneiform joint which was subsequently lost in the *Homo* lineage. Comparison with more fossil and extant material is needed to resolve these questions.

Other adaptations in the foot of *Theropithecus* are unique such as the long slender medial cuneiform indicating that the joint is maladapted to loading. The constriction of the intermediate cuneiform between the medial and lateral cuneiforms is also unique and is interpreted as an adaptation to

severely reduce the amount of movement possible at the midfoot. Each of the cuneiforms, as well as the navicular, are lengthened proximodistally as a response to the compressive forces generated through the foot during heel-elevated terrestrial locomotion (Strasser 1988; Patel 2010) and the well-developed cup for the medial malleolus indicates that *Theropithecus* frequently engages in highly flexed postures at the ankle (Krentz 1993).

Oreopithecus was found to be most similar to the African apes throughout the pedal skeleton examined in this study, though some similarities between *Oreopithecus* and *Pongo* were also observed. There was no evidence to suggest that *Oreopithecus* shared any cercopithecoid traits of the medial column. Where similarities between *Oreopithecus* and *Theropithecus* were present it was always in a context in which *Theropithecus* grouped closely with the ape species. Thus, this study found no support from the pedal skeleton that *Oreopithecus* was a cercopithecoid (Szalay and Delson 1979). The talus has a higher lateral trochlear rim (Szalay and Langdon 1986; *contra* Köhler and Moyà-Solà 1997) indicating an inverted set to the ankle. And the similar height of the head and medial rim indicates that there was no inferior inclination of the neck of the talus and thus that the foot was flat longitudinally. Köhler and Moyà-Solà (1997) contended that the lateral digits were permanently laterally abducted. No metrical data are provided to corroborate this claim, nor are any references which had previously claimed it to be the case. No evidence to support this was found in the present study. The talonavicular joint is largely African ape-like in form, stressing loading through the dorsal and medial aspects, and similarly medially deviated from the body of the talus. In their reconstruction the navicular is placed in an awkward orientation relative to the talus. Sarmiento and Marcus (2000) also claim that divergence between the digits was uniquely high in *Oreopithecus* based on evidence of the angle of the lateral cuneiform facet compared to the other facets of the navicular. No such evidence could be found here, rather the navicular of *Oreopithecus* is intermediate between African apes and *Pongo* with respect to the angulation of the lateral cuneiform facet.

In all, the reconstruction of the *Oreopithecus* foot by Köhler and Moyà-Solà (1997) is unconvincing (Begun 2007). There is no evidence that the hallux is uniquely widely divergent, as they posit. The orientation of the 1st naviculocuneiform facet, the morphology of the medial cuneiform and the orientation of the 1st metatarsal facet place *Oreopithecus* closest in form to African apes (Szalay and Langdon 1986), and possibly *Pan* specifically. The implication of which is that grasping ability of the hallux of *Oreopithecus* was similar to that of African apes and that the hallux would not have functioned well during prolonged bipedal support. There is also no evidence for the contention that

the lateral digits are widely divergent. In their reconstruction of the foot Köhler and Moyà-Solà (1997; figure 3) display the laterally directed lateral digits. With regards to the medial column of the foot they seem to represent the lateral cuneiform as having approximately equal lengths to its medial and lateral side. This study, however, found that the lateral cuneiform of *Oreopithecus* is ape like, and very similar to *Pongo* in the highly curved surface with a clear distal placement of the medial border relative to the lateral. This feature will act to oppose the lateral flexion of the lateral cuneiform facet. Furthermore, as mentioned above, their placement of the navicular in relation to the talus is highly unusual.

Finally, there is no reason to conclude that the hallux was oriented in such an abducted position from the medial cuneiform. The degree of hallux divergence is comparable to *Pan*. From this it is not possible to hypothesise a high incidence of bipedalism in *Oreopithecus*. Therefore, bipedalism to the extent that it is practiced in *Pan* may be the most likely interpretation of the pedal anatomy of *Oreopithecus*. The possibility of arboreal bipedalism (Crompton *et al.* 2010) may account for the grasping foot of *Oreopithecus* in view of certain other features of the postcranium (such as dorsal wedging of the bodies of lumbar vertebrae) which have been argued to suggest bipedalism (Köhler and Moyà-Solà 1997; Rook *et al.* 1999). However, these reconstructions have been called into question (Russo and Shapiro 2013). Furthermore, the fact that the pedal bones of *Oreopithecus* were consistently found to be much smaller than expected for its body size is difficult to account for in a bipedal framework, arboreal or otherwise. It is clear that *Oreopithecus* retained some degree of prehensility of its hallux, but this need not preclude the possibility that it incorporated a substantial amount of bipedal behaviour into its locomotor repertoire (e.g. Lovejoy *et al.* 2009a). It is, however, unlikely that *Oreopithecus* exhibited an unusually high amount of bipedal behaviour. Its general hominoid body plan makes it a reasonable assumption that at least some small amount of the positional behaviour of *Oreopithecus* constituted bipedalism, as is known for all extant apes (Hunt *et al.* 1991; Hunt 1994; Crompton *et al.* 2008). Furthermore, the small size of the foot in *Oreopithecus* may indicate that it was adapted to a forelimb dominated locomotor repertoire. Brachiation has previously been posited as a possible locomotor mode for *Oreopithecus* (Delson 1986).

The findings of this study are in general agreement with the findings of some other studies which assessed the OH8, *Homo habilis* foot (Archibald *et al.* 1972; Harcourt-Smith 2002; Proctor 2008). The OH8 foot is most similar to *Homo* with respect to every bone analysed, however, there were some clear differences, most notably of the talus. The higher lateral trochlear rim would seem to preclude human-like direct movement of the leg over the foot (Harcourt-Smith 2002) instead forcing the leg to

follow an arcuate path as it passes over the leg (Aiello and Dean 2002). Since it is known that apes are perfectly capable of walking in this manner (Elftman and Manter 1935a) it does not imply that the OH8 foot was unsuitable for habitual, or even obligate, bipedalism. The finding does, however, suggest that the individual to which the foot belonged walked in a manner not like that of modern humans, and probably unlike bipedal walking in extant apes. However, all other bones were most similar to *Homo* and reflected adaptation to obligate bipedalism. The naviculocuneiform joints are all oriented distally (as a consequence of the broadening of the lateral side of the navicular) despite the medially divergent talar head. This indicates a proximal to distal alignment of force transmission through the foot, and the tightly curved arch formed by the cuneiform facets is evidence for a relatively high transverse arch. The first metatarsal clearly lacks an ape-like degree of abduction, however there is some medial encroachment of the facet onto the medial side of the medial cuneiform. The evidence of all tarsal elements distal to the talus in this study indicates that the OH8 foot was adapted to withstand loading through compression and along a dorsoplantar axis. The fact that the findings of this study corroborate those reported in one other similar study (Harcourt-Smith 2002) offers some support that the methods used were accurate and the conclusions reached have been well-founded.

Nacholapithecus provided some rather confusing results. It was found that there was a general likeness of the talus morphology of *Nacholapithecus* with that of *Theropithecus* and *Pan*. This included a medially sloping trochlea surface, medial protrusion of the anterior part of the medial malleolar facet, medial divergence of the head and reasonably high curvature of the head. *Theropithecus* was separated from other ape species in features relating to the degree of angulation of the medial malleolar protrusion mentioned above, the fact that this part of the medial malleolus formed a very deep cup, and the fact that the proximal part of the medial malleolar facet is more perpendicular to the trochlea. It is notable that *Nacholapithecus* was found not to resemble *Theropithecus* in these regards. This is a surprising result because from visual inspection the tali of *Nacholapithecus* and *Theropithecus* seem very similar in each of the features which separate *Theropithecus* from the apes. These findings were also apparent from the analysis of the partial talus. The result is very difficult to interpret. There are no features which are obviously shared between *Nacholapithecus* and the apes which exclude *Theropithecus*, nor are there any features of *Theropithecus* which are obviously absent in *Nacholapithecus*. More careful and detailed study of the talus, involving a greater number of catarrhine genera and isolating parts of the talar morphology would be needed to resolve the issue. Alternatively, this confusing result could also indicate that the method used is inappropriate or that there was some error involved during data collection for *Nacholapithecus*.

The medial cuneiform of *Nacholapithecus* represented a unique morphology among the groups presented in this study. The small navicular facet indicates that the bone was not well-suited to bearing large loads. However, the shape of the joint is reminiscent of that of hominoids and unlike the tear-drop shape of *Theropithecus*. Additionally, the facet was flat indicating very low mobility at the joint in *Nacholapithecus*, unlike *Gorilla* (Harcourt-Smith 2002). The similar shape of the joint to hominoids may be used to infer that the joint loaded in a similar way to hominoids, but that the joint was not loaded as frequently, or to such an extent, as the extant hominoids. The distal surface of the bone is unique in form, also. There is some medial encroachment of the distal facet onto the medial surface of the bone, though this is not as excessive as that observed for the non-human apes. The reniform facet also resembles that of non-human apes. However, the extreme length and height of the bone compared to its width makes it poorly adapted to ape-like mediolateral loading of the bone (Langdon 1986). Thus, there are some features of the *Nacholapithecus* pedal skeleton which align it with modern hominoids which indicates that some degree of hominoid-like grasping function and ankle mobility was present in the pedal skeleton of stem hominoids 15Mya (Ishida *et al.* 2004). However, there remain several primitive characters, such as the extreme narrowness of the medial cuneiform which point to a generalised quadrupedal adaptation.

There are a number of key areas of interest which require further study to investigate some questions raised in this thesis. The first is whether or not the similarity of *Homo* and *Theropithecus* with respect to the lateral side of the navicular represents a convergent feature or if it is ancestral for Hominoidea. Given the proposals of Lovejoy *et al.* (2009a) it would provide further support to their hypothesis that the last common ancestor of humans and apes had a cercopithecoid-like foot, were it found to be true. Unfortunately, only a very small fragment of the navicular of *Ardipithecus* was recovered which would not allow an evaluation of this feature. Second, the inclusion of more Miocene hominoid pedal remains and comparisons of them in the context of a wider range of primate species would permit a better understanding of the pedal morphology present in the stem hominoids. Features of the forelimb of *Nacholapithecus* have been argued to indicate a move to a greater incorporation of vertical climbing in the behavioural repertoire (Nakatsukasa *et al.* 2003b). There are some features presented here which may indicate the development of a more ape-like grasping foot, but comparison with more Miocene apes and more extant primate taxa is needed to provide clarity. Third, more complete studies of the foot and leg of *Oreopithecus* are needed, particularly comparisons to known brachiators, throughout the postcranial skeleton. More accurate reconstructions of the articulations of the foot are needed to better understand its function and

more metrical analyses and comparisons of the bones of the *Oreopithecus* foot are required, particularly as they relate to the orientation of the digits and functional axis of the foot. It is remarkable that *Oreopithecus* is one of the best known Miocene hominoids and that its pedal skeleton is represented by most of the bones (though some are incomplete) and yet there is a surprising lack of research into this potentially very interesting and unusual ape.

6. References

Adams, D. C., Rohlf, F. J. & Slice, D. E. 2004. Geometric morphometrics: ten years of progress following the 'revolution'. *Italian Journal of Zoology*. 71: 5-16

Adamczyk, P. G., Collins, S. H. & Kuo, A. D. 2006. The advantages of a rolling foot in human walking. *Journal of Experimental Biology*. 209: 3953-3963

Aerts, P., Van Damme, R., Van Elsacker, L. & Duchene, V. 2000. Spatio-Temporal Gait Characteristics of the Hind-Limb Cycles During Voluntary Bipedal and Quadrupedal Walking in Bonobos (*Pan paniscus*). *American Journal of Physical Anthropology*. 111: 503-517

Agustí, J. & Anton, M. 2002. *Mammoths, Sabretooths, and Hominids*. Columbia University Press. New York

Agustí, J., Cabrera, L. & Garcés, M. 2001. Chronology and zoogeography of the Miocene hominoid record in Europe. In De Bonis, L., Koufos, G. D. & Andrews, P. (eds) *Hominoid Evolution and Climatic Change in Europe. Volume 2: Phylogeny of the Neogene Hominoid Primates of Eurasia*. Cambridge University Press. Cambridge, UK.

Agustí, J., Cabrera, L., Garcés, M. & Parés, J. M. 1997. The Vallesian mammal succession in the Vallès-Penedès basin (northeast Spain): Paleomagnetic calibration and correlation with global events. *Palaeogeography, Palaeoclimatology, Palaeoecology*. 133: 149-180

Aiello, L. & Dean, C. 2002. *An Introduction to Human Evolutionary Anatomy*. Elsevier Academic Press. London.

Alba, D. M., Almécija, S. & Moyà-Solà, S. 2010. Locomotor inferences in *Pierolapithecus* and *Hispanopithecus*: Reply to Deane and Begun (2008). *Journal of Human Evolution*. 59: 143-149

Almécija, S., Tallman, M., Alba, D. M., Pina, M., Moyà-solà, S. & Jungers, W. L. 2013. The femur of *Orrorin tugenensis* exhibits morphometric affinities with both Miocene apes and later hominins. *Nature Communications*. 4: 2888-3000

Almécija, S., Shrewsbury, M., Rook, L. & Moyà-Solà, S. 2014. The Morphology of *Oreopithecus bambolii* Pollical Distal Phalanx. *American Journal of Physical Anthropology*. 153: 582-597

Andrews, P. 1992. Evolution and environment in the Hominoidea. *Nature*. 360: 641-646.

Andrews, P. & Martin, L. 1987. Cladistic relationships of extant and fossil hominoids. *Journal of Human Evolution*. 16: 101-118

Ankel-Simons, F. 2000. *Primate Anatomy: An Introduction*. 2nd Edition. Academic Press. London.

Archibald, J. D., Lovejoy, C. O. & Heiple, K. G. 1972. Implications of relative robusticity in the Olduvai metatarsus. *American Journal of Physical Anthropology*. 37: 93-96

Asfaw, B., White, T., Lovejoy, O., Latimer, B., Simpson, S. & Suwa, G. 1999. *Australopithecus garhi*: A New Species of Early Hominid from Ethiopia. *Science*. 284: 629-6

Azzarolli, A., Boccaletti, M., Delson, E., Moratti, G. & Torre, D. 1986. Chronological and Paleogeographical Background to the Study of *Oreopithecus bambolii*. *Journal of Human Evolution*. 15: 533-540

Baab, K. L., McNulty, K. P. & Rohlf, F. J. 2012. The Shape of Human Evolution: A Geometric Morphometrics Perspective. *Evolutionary Anthropology*. 21: 151-165

Bartoníček, J. 2003. Anatomy of the tibiofibular syndesmosis and its clinical relevance. *Surgical and Radiologic Anatomy*. 25: 379-386.

Bates, K. T., Collins, D., Savage, R., McClymont, J., Webster, E., Pataky, T. C., D'Aout, K., Sellers, W. I., Bennett, M. R. & Crompton, R. H. 2013. The evolution of compliance in the human lateral mid-foot. *Proceedings of the Royal Society B*. 280: 1818

Begun, D. R. 1992a. *Dryopithecus crusafonti* sp. nov., a new Miocene Hominid Species from Can Ponsic (Northeastern Spain). *American Journal of Physical Anthropology*. 87: 291-310

Begun, D. R. 1992b. Phyletic Diversity and Locomotion in Primitive European Hominids. *American Journal of Physical Anthropology*. 87: 311-340

Begun, D. R. 2000. Middle Miocene Hominoid Origins. *Science*. 287: 2375

Begun, D. R. 2002. European hominoids. In Hartwig, W. C. (ed) *The Primate Fossil Record*. Cambridge University Press. Cambridge.

Begun, D. R. 2005. *Sivapithecus* is east and *Dryopithecus* is west, and never the twain shall meet. *Anthropological Science*. 113: 53-64.

Begun, D. R. 2007. Fossil Record of Miocene Hominoids. In Henke, W. & Tattersall, I. (eds) *Handbook of Paleoanthropology (Volume 2): Primate Evolution and Human Origins*. Springer-Verlag. New York.

Begun, D. R. & Kivell, T. L. Knuckle-walking in *Sivapithecus*? The combined effects of homology and homoplasy with possible implications for pongine dispersals. *Journal of Human Evolution*. 60: 158-170

Begun, D. R., Nargolwalla, M. C. & Kordos, L. 2012. European Miocene Hominids and the Origin of the African Ape and Human Clade. *Evolutionary Anthropology*. 21: 10-23

Begun, D. R., Teaford, M. F. & Walker, A. 1994. Comparative and functional anatomy of *Proconsul* phalanges from the Kaswanga Primate Site, Rusinga Island, Kenya. *Journal of Human Evolution*. 26: 89-165

Berge, C. 1994. How did the australopithecines walk? A biomechanical study of the hip and thigh of *Australopithecus afarensis*. *Journal of Human Evolution*. 26: 259-273

Berger, L. R., de Ruiter, D. J., Churchill, S. E., Schmid, P., Carlson, K. J., Dirks, P. H. G. M. & Kibii, J. M. 2010. *Australopithecus sediba*: A New Species of *Homo*-Like Australopithecine from South Africa. *Science*. 328: 195-204

Berillon, G. 1999. Geometric pattern of the hominoid hallux tarsometatarsal complex. Quantifying the degree of hallux abduction in early hominids. *Comptes Rendus de l'Academie des Sciences*. 328: 627-633

Berillon, G. 2003. Assessing the Longitudinal Structure of the Early Hominid Foot: A Two-dimensional Architecture Analysis. *Human Evolution*. 18: 113-122

Bjarnason, A., Chamberlain, A. T. & Lockwood, C. A. 2011. A methodological investigation of hominoid craniodental morphology and phylogenetics. *Journal of Human Evolution*. 60: 47-57

Bland, M. J. 1995. Multiple significance tests: the Bonferroni method. *The British Medical Journal*. 310: 170.

Bleuze, M. 2012. Proximal femoral diaphyseal cross-sectional geometry in *Orrorin tugenensis*. *HOMO*. 63: 153-166

Bojsen-Møller, F. 1979. Calcaneocuboid joint and stability of the longitudinal arch of the foot at high and low gear push off. *Journal of Anatomy*. 129: 165-176

Bojsen-Møller, F. & Flagstad, K. E. 1976. Plantar aponeurosis and internal architecture of the ball of the foot. *Journal of Anatomy*. 121: 599-611

Bookstein, F. L. 1986. Size and shape spaces for landmark data in two dimensions. *Statistical Science*. 1 (2): 181-222.

Bookstein, F. L. 1989. Principal Warps: Thin-Plate Splines and the Decomposition of Deformations. *IEEE Transactions on Pattern Analysis and Machine Intelligence*. 2: 567-585

Bookstein, F. L. 1991. *Morphometric Tools for Landmark Data: Geometry and Biology*. Cambridge University Press. Cambridge.

Bookstein, F. L. 1996. Landmark methods for forms without landmarks: morphometrics of group differences in outline shape. *Medical Image Analysis*. 1: 225-243

Boschetto, H. B., Brown, F. H. & McDougall, I. 1992. Stratigraphy of the Lothidok Range, northern Kenya, and K/Ar ages of its Miocene primates. *Journal of Human Evolution*. 22: 47-71

Brooks, H. S. J. 1887. On the short muscles of the pollex and hallux of the anthropoid apes, with special reference to the opponens hallucis. *Journal of Anatomy and Physiology*. 22: 78-95.

Bruce, G. 2003. The Barbican Centre, York. Report on an Archaeological Evaluation. OSA Report No: OSA03EV08. *On Site Archaeology Ltd*.

Bruce, G. & McIntyre, L. 2009. Mass graves at All Saints Church, Fishergate, York. *York Historian*. 26: 79-84.

Brunet, M., Guy, F., Pilbeam, D., Mackaye, H. T., Likius, A., Ahounta, D., Beauvilain, A., Blondel, C., Bocherens, H., Boisserie, J. R., De Bonis, L., Coppens, Y., Dejax, J., Denys, C., Doringier, P., Eisenmann, V., Fanone, G., Fronty, P., Geraads, D., Lehmann, T., Lihoreau, F., Louchart, A., Mahamat, A., Merceron, G., Mouchelin, G., Otero, O., Campomanes, P. P., Ponce de Leon, M., Rage, J. C., Sapanet, M., Schuster, M., Sudre, J., Tassy, P., Valentin, X., Vignaud, P., Viriot, L., Zazzo, A. & Zollikofer, C. 2002. A new hominid from the Upper Miocene of Chad, Central Africa. *Nature*. 418: 145-151

Brunet, M., Guy, F., Pilbeam, D., Lieberman, D. E., Likius, A., Mackaye, H. T., Ponce de León, M. S., Zollikofer, C. P. E. & Vignaud, P. 2005. New material of the earliest hominid from the Upper Miocene of Chad. *Nature*. 434: 752-755

Cameron, D. W. 1997. A revised systematic scheme for the Eurasian Miocene fossil Hominidae. *Journal of Human Evolution*. 33: 449-477

Caravaggi, P., Pataky, T., Günther, M., Savage, R. & Crompton, R. 2010. Dynamics of longitudinal arch support in relation to walking speed: contribution of the plantar aponeurosis. *Journal of Anatomy*. 217: 254-261

Casanovas-Vilar, I., van Dam, J. A., Moyà-Solà, S. & Rook, L. 2011. Late Miocene insular mice from the Tusco-Sardinian palaeobioprovince provide new insights on the palaeoecology of the *Oreopithecus* faunas. *Journal of Human Evolution*. 61: 42-49

Cela-Conde, C. J. 1998. The problem of hominoid systematics, and some suggestions for solving it. *South African Journal of Science*. 94: 255-262

Chen, H., Cheng, Y., Liu, D., Zhang, X., Zhang, J., Que, C., Wang, G. & Fang, G. 2010. Color structured light system of chest wall motion measurement for respiratory volume evaluation. *Journal of Biomedical Optics*. 15 (2): Article number 026013.

Chatterjee, H. J. 2009. Evolutionary Relationships Among the Gibbons: A Biogeographic Perspective. In Lappan, S. & Whittaker, D. J. (eds) *The Gibbons*. Springer

Chatterjee, H. J., Ho, S. Y. W., Barnes, I. & Groves, C. 2009. Estimating the phylogeny and divergence times of primates using a supermatrix approach. *BMC Evolutionary Biology*. 9: 259

Clarke, R. J. & Tobias, P. V. 1995. Sterkfontein Member 2 Foot Bones of the Oldest South African Hominid. *Science*. 269: 521-524

Colville, M. R., Marder, R. A., Boyle, J. J. & Zarins, B. 1990. Strain measurements in lateral ankle ligaments. *The American Journal of Sports Medicine*. 18: 196-200

Conroy, G. C. 1990. *Primate Evolution*. W. W. Norton and Company Ltd. London.

Conroy, G. C. & Ponzer, H. 2012. *Reconstructing Human Origins: 3rd Edition*. W. W. Norton & Company. London.

Coppens, Y. 1994. East Side Story: The Origin of Humankind. *Scientific American*. 270: 88-95

Crompton, R. H., Vereecke, E. E. & Thorpe, S. K. S. 2008. Locomotion and posture from the common hominoid ancestor to fully modern hominins, with special reference to the last common panin/hominin ancestor. *Journal of Anatomy*. 212: 501-543

Crompton, R. H., Sellers, W. I. & Thorpe, S. K. S. 2010. Arboreality, terrestriality and bipedalism. *Philosophical Transactions of the Royal Society B*. 365: 3301-3314

Crompton, R. H., Pataky, T. C., Savage, R., D'Août, K., Bennett, M. R., Day, M. H., Bates, K., Morse, S. & Sellers, W. I. 2011. Human-like external function of the foot, and fully upright gait, confirmed in the 3.66 million year old Laetoli hominin footprints by topographic statistics, experimental footprint formation and computer simulation. *Journal of the Royal Society Interface*. doi: 10.1098/rsif.2011.0258

Day, M. H. & Wood, B. A. 1968. Functional Affinities of the Olduvai Hominid 8 Talus. *Man*. 3: 440-455

Deane, A. S. & Begun, D. R. 2008. Broken fingers: retesting locomotor hypotheses for fossil hominoids using fragmentary proximal phalanges and high-resolution polynomial curve fitting (HR-PCF). *Journal of Human Evolution*. 55: 691-701

DeSilva, J. M. 2008. *Vertical climbing adaptations in the anthropoid ankle and midfoot: implications for locomotion in the Miocene catarrhines and Plio-Pleistocene hominins*. PhD Thesis. University of Michigan.

DeSilva, J. M. 2009. Functional morphology of the ankle and the likelihood of climbing in early hominins. *Proceedings of the National Academy of Sciences*. 106: 6567-6572

DeSilva, J. M. 2010. Revisiting the "Midtarsal Break". *American Journal of Physical Anthropology*. 141: 245-258

DeSilva, J. M. & Papakyrikos, A. 2011. A Case of Valgus Ankle in an Early Pleistocene Hominin. *International Journal of Osteoarchaeology*. 21: 732-742

DeSilva, J. M., Proctor, D. J. & Zipfel, B. 2012. A complete second metatarsal (StW 89) from Sterkfontein Member 4, South Africa. *Journal of Human Evolution*. 63: 487-496

DeSilva, J. M. & Gill, S. V. 2013. A midtarsal (midfoot) break in the human foot. *American Journal of Physical Anthropology*. 38: 495-499

de Terra, H. 1956. New Approach to the Problem of Man's Origin. *Science*. 124: 1282-1285

Doran, D. M. 1996. Comparative positional behavior of the African apes. In, McGrew, W. C., Marchant, L. F. & Nishida, T. *Great Ape Societies*. Cambridge University Press.

Doran, D. M. 1997. Ontogeny of locomotion in mountain gorillas and chimpanzees. *Journal of Human Evolution*. 32 : 323-344

Drapeau, M. S. M. 2008. Articular morphology of the proximal ulna in extant and fossil hominoids and hominins. *Journal of Human Evolution*. 55: 86-102

Drapeau, M. S. M. & Harmon, E. H. 2013. Metatarsal torsion in monkeys, apes, humans and australopiths. *Journal of Human Evolution*. 2013. 64: 93-108

Dryden, I. L. & Mardia, K. V. 1998. *Statistical Shape Analysis*. John Wiley & Sons Ltd. Chicester.

- Dunn, R. H., Tocheri, M. W., Orr, C. M. & Jungers, W. L. 2014. Ecological Divergence and Talar Morphology in Gorillas. *American Journal of Physical Anthropology*. 153: 526-541
- Dunsworth, H. & Walker, A. 2002. Early Genus *Homo*. In Hartwig, W. C. 2002. *The Primate Fossil Record*. University Press. Cambridge.
- Eftman, H. & Manter, J. 1935a. Chimpanzee and human feet in bipedal walking. *American Journal of Physical Anthropology*. 20: 69-79
- Eftman, H. & Manter, J. 1935b. The Evolution of the Human Foot, with Especial Reference to the Joints. *Journal of Anatomy*. 70: 56-67.
- Elton, S. 2002. A Reappraisal of the Locomotion and Habitat Preference of *Theropithecus oswaldi*. *Folia Primatologica*. 73: 252-280
- Erdemir, A., Hamel, A. J., Fauth, A. R., Piazza, S. J. & Sharkey, N. A. 2004. Dynamic Loading of the Plantar Aponeurosis in Walking. *The Journal of Bone and Joint Surgery*. 86: 546-552
- Ersoy, A., Kelley, J., Andrews, P. & Alpagut, B. 2008. Hominoid phalanges from the middle Miocene site of Paşalar, Turkey. *Journal of Human Evolution*. 54: 518-529
- Filler, A. G. 2007. Emergence and optimization of upright posture among hominiform hominoids and the evolutionary pathophysiology of back pain. *Neurosurgery Focus*. 23: E4, 1-6.
- Finarelli, J. A. & Clyde, W. C. 2004. Reassessing hominoid phylogeny: evaluating congruence in the morphological and temporal data. *Paleobiology*. 30: 614-651.

Fleagle, J. G. 1999. *Primate Adaptation and Evolution*. 2nd Edition. Academic Press. New York.

Fleagle, J. G., Simons, E. L. & Conroy, G. C. 1975. Ape Limb Bone from the Oligocene of Egypt. *Science*. 189: 135-137

Foley, R. A. 1993. Comparative evolutionary biology of *Theropithecus* and the Hominidae. In Jablonski, N. G. (ed) *Theropithecus: The rise and fall of a primate genus*. Cambridge University Press.

Frankel, V. H. & Nordin, M. 1989. Biomechanics of the Ankle. In Nordin, M. & Frankel, V. H. (eds) *Basic Biomechanics of the Musculoskeletal System*. Williams & Wilkins. Media, Pennsylvania.

Galik, K., Senut, B., Pickford, M., Gommery, D., Treil, J., Kuperavage, A. J. & Eckhardt, R. B. 2004. External and Internal Morphology of the BAR 1002'00 *Orrorin tugenensis* Femur. *Science*. 305: 1450-1453

Gebo, D. L. 1985. The Nature of the Primate Grasping Foot. *American Journal of Physical Anthropology*. 67: 269-277

Gebo, D. L. 1986. Anthropoid Origins – the Foot Evidence. *Journal of Human Evolution*. 15: 421-430

Gebo, D. L. 1989. Locomotor and phylogenetic considerations in anthropoid evolution. *Journal of Human Evolution*. 18: 201-233

Gebo, D. L. 1992. Plantigrady and Foot Adaptations in African Apes: Implications for Hominid Origins. *American Journal of Physical Anthropology*. 89: 29-58.

Gebo, D. L. 1993a. Functional Morphology of the Foot in Primates. In Gebo, D. L. (ed) *Postcranial Adaptation in Nonhuman Primates*. Northern Illinois University Press. Illinois

Gebo, D. L. 1993b. Reply to Dr. Meldrum. *American Journal of Physical Anthropology*. 91: 382-385.

Gebo, D. L. 1996. Climbing, Brachiation, and Terrestrial Quadrupedalism: Historical Precursors of hominid Bipedalism. *American Journal of Physical Anthropology*. 101: 55-92

Gebo, D. L., MacLatchy, L., Kityo, R., Deino, A., Kingston, J. & Pilbeam, D. 1997. A Hominoid Genus from the Early Miocene of Uganda. *Science*. 276: 401-404

Gebo, D. L. & Schwartz, G. L. 2006. Foot Bones From Omo: Implications for Hominid Evolution. *American Journal of Physical Anthropology*. 129: 499-511

Geissman, T. 1995. Gibbon systematics and species identification. *International Zoo News*. 42: 467-501

Gentili, S., Mottura, A. & Rook, L. 1998. The Italian primate fossil record: recent finds and their geological context. *Geobios*. 5: 675-686

Glinkowski, W., Sitnik, R., Witkowski, M., Kocon, H., Bolewicki, P. & Goreci, A. 2009. Method of pectus excavatum measurement based on structured light technique. *Journal of Biomedical Optics*. 14 (4): Article number 044041.

Godinot, M. 2015. Fossil Record of the Primates from the Paleocene to the Oligocene. In Hanke, W. & Tattersall, I. (eds) *Handbook of Paleoanthropology 2nd Edition*. Springer. London.

Gomberg, D. N. 1985. Functional Differences of the Three Ligaments of the Transverse Tarsal Joint in Hominoids. *Journal of Human Evolution*. 14: 553-562

Goodman, M., Bailey, W. J., Hayasaka, K., Stanhope, M. J., Slightom, J. & Czelusniak, J. 1994. Molecular evidence on primate phylogeny from DNA sequences. *American Journal of Physical Anthropology*. 94: 3-24

Gosling, J. A., Harris, P. F., Humpherson, J. R., Whitmore, I. & Willan, P. L. T. 2008. *Human Anatomy: Colour Atlas and Textbook*. 5th Edition. Elsevier Limited. Philadelphia.

Gower, J. C. 1975. Generalized Procrustes analysis. *Psychometrika*. 40: 33-51

Green, D. J. & Alemseged, Z. 2012. *Australopithecus afarensis* Scapular Ontogeny, Function, and the Role of Climbing in Human Evolution. *Science*. 338: 514-517

Greiner, T. M. & Ball, K. A. 2014. Kinematics of Primate Midfoot Flexibility. *American Journal of Physical Anthropology*. 155: 610-620

Groves, C. 2001. *Primate Taxonomy*. Smithsonian Institution Press. London.

Gunz, P. & Mitteroecker, M. 2013. Semilandmarks: a method for quantifying curves and surfaces. *Hystix, the Italian Journal of Mammalogy*. 24(1): 103-109

Haeusler, M. 2003. New Insights Into the Locomotion of *Australopithecus africanus* Based on the Pelvis. *Evolutionary Anthropology*. 11: 53-57

Haeusler, M. & McHenry, H. M. 2004. Body proportions of *Homo habilis* reviewed. *Journal of Human Evolution*. 46: 433-465

Haile-Selassie, Y. 2001. Late Miocene hominids from the Middle Awash, Ethiopia. *Nature*. 412: 178-181

Haile-Selassie, Y. 2010. Phylogeny of early *Australopithecus*: new fossil evidence from the Woranso-Mille (central Afar, Ethiopia). *Philosophical Transactions of the Royal Society B*. 365: 3323-3331

Hall, S. J. 1999. *Basic Biomechanics*. 3rd Edition. WCB/McGraw-Hill. London.

Hammer, Ø., Harper, D.A.T., and Ryan, P. D. 2001. PAST: Paleontological Statistics Software Package for Education and Data Analysis. *Palaeontologia Electronica* 4(1): 9pp.

Hanna, J. B., Schmitt, D. & Griffin, T. M. 2008. The energetic cost of climbing in primates. *Science*. 320: 898

Harcourt-Smith, W. 2002. *Form and Function in the Hominoid Tarsal Skeleton*. PhD Thesis. University College London

Harcourt-Smith, W. E. H. & Aiello, L. C. 2004. Fossils, feet and the evolution of human bipedal locomotion. *Journal of Anatomy*. 204: 403-416

Harcourt-Smith, W. E. H., Tallman, M., Frost, S. R., Wiley, D. F., Rohlf, F. J. & Delson, E. 2008. Analysis of Selected Hominoid Joint Surfaces Using Laser Scanning and Geometric Morphometrics: A Preliminary Report. In Sargis, E. J. & Dagosto, M. (eds) *Mammalian Evolutionary Morphology: A Tribute to Frederick S. Szalay*. Springer. New York.

Harrison, T. 1986. A reassessment of the Phylogenetic Relationships of *Oreopithecus bambolii* Gervais. *Journal of Human Evolution*. 15:541-583

Harrison, T. 1987. The phylogenetic relationships of the early catarrhine primates: a review of the current evidence. *Journal of Human Evolution*. 16: 41-80

Harrison, T. 1989. New postcranial remains of *Victoriapithecus* from the middle Miocene of Kenya. *Journal of Human Evolution*. 18: 3-54

Harrison, T. 1992. A Reassessment of the Taxonomic and Phylogenetic Affinities of the Fossil Catarrhines from Fort Ternan, Kenya. *Primates*. 33: 501-522.

Harrison, T. 1998. Evidence for a tail in *Proconsul heseloni*. *American Journal of Physical Anthropology*. 105. Supplement 26: 93

Harrison, T. 2002. Late Oligocene to middle Miocene catarrhines from Afro-Arabia. In Hartwig, W. C. (ed) *The Primate Fossil Record*. Cambridge University Press. Cambridge.

Heizmann, E. P. J. & Begun, D. R. 2001. The oldest Eurasian hominoid. *Journal of Human Evolution*. 41: 463-481.

Hepburn, D. 1892. The comparative anatomy of the muscles and nerves of the superior and inferior extremities of the anthropoid apes. *Journal of Anatomy and Physiology*. 26: 323-356

Hermans, J. J., Beumer, A., de Jong, T. A. W. & Kleinrensink, G-J. 2010. Anatomy of the distal tibiofibular syndesmosis in adults: a pictorial essay with a multimodality approach. *Journal of Anatomy*. 217: 633-645.

Hesterberg, T., Monaghan, S., Moore, D. S., Clipson, A. & Epstein, R. 2003. Bootstrap Methods and Permutation Tests. In Moore, D. S., McCabe, G. P., Duckworth, W. M. & Alwan, L. C. *The Practice of Business Statistics: Using Data for Decisions*. W. H. Freeman. New York.

Hollis, J. M., Blasier, D. L. & Flahiff, C. M. 1995. Simulated Lateral Ankle Ligamentous Injury: Change in Ankle Stability. *The American Journal of Sports Medicine*. 23: 672-677

Humphry, F. R. S. 1867. On some points in the anatomy of the chimpanzee. *Journal of Anatomy and Physiology*. 1: 254-268.

Hunt, K. D. 1991. Positional Behaviour in the Hominoidea. *International Journal of Primatology*. 12: 95-118

Hunt, K. D. 1994. The evolution of human bipedality: ecology and functional morphology. *Journal of Human Evolution*. 26: 183-202

Ishida, H., Kunimatsu, Y., Nakatsukasa, M. & Nakano, Y. 1999. New Hominoid Genus from the Middle Miocene of Nachola, Kenya. *Anthropological Science*. 107: 189-191

Ishida, H. & Pickford, M. 1997. A new Late Miocene hominoid from Kenya: *Samburupithecus kiptalami* gen et sp. nov. *Comptes Rendus de l'Académie des Sciences*. 325: 823-829

Ishida, H., Kunimatsu, Y., Takano, T., Nakano, Y. & Nakatsukasa, M. 2004. *Nacholapithecus* skeleton from the Middle Miocene of Kenya. *Journal of Human Evolution*. 46: 69-103

Isidro, A. & Gonzalez-Casanova, J. C. 2002. A glimpse into the evolution of the hallucial tarso-metatarsal joint. *Foot and Ankle Surgery*. 8: 169-174

Isman, R. E. & Inman, V. T. 1969. Anthropometric studies of the human foot and ankle. *Bulletin of Prosthetics Research*. 11: 97-129

Isler, K. 2006. 3D-Kinematics of Vertical Climbing in Hominoids. *American Journal of Physical Anthropology*. 126: 66-81

Jashashvili, T., Dowdeswell, M. R., Lebrun, R. & Carlson, K. J. 2015. Cortical Structure of Hallucal Metatarsals and Locomotor Adaptations in Hominoids. *PLoS ONE*. DOI:10.1371/journal.pone.0117905

Johnson, A., Hill, K., Ward, J. & Ficke, J. 2008. Anatomy of the Lisfranc Ligament. *Foot and Ankle Specialist*. 1: 19-23

Jolly, C. J. 2001. A Proper Study for Mankind: Analogies From the Papionin Monkeys and Their Implications for Human Evolution. *Yearbook of Physical Anthropology*. 44: 177-204

Jungers, W. L. 1987. Body size and morphometric affinities of the appendicular skeleton in *Oreopithecus bambolii* (IGF 11778). *Journal of Human Evolution*. 16: 445-456

Kanamoto, S., Ogiwara, N. & Nakatsukasa, M. 2011. Three-dimensional orientations of talar articular surfaces in humans and great apes. *Primates*. 52: 61-68

Keith, A. 1923a. Man's posture: its evolution and disorders. I: Theories concerning the evolution of man's posture. *British Medical Journal*. 1: 451-454.

Keith, A. 1923b. Man's posture: its evolution and disorders. VI: The evolution of the human foot. *British Medical Journal*. 1: 669-672

Kelley, J. 2002. The hominoid radiation in Asia. In Hartwig, W. C. (ed) *The Primate Fossil Record*. Cambridge University Press. Cambridge.

Kendall, D. G. 1977. The Diffusion of Shape. *Advances in Applied Probability*. 9: 428-430

Kendall, D. G. 1989. A Survey of the Statistical Theory of Shape. *Statistical Science*. 4: 87-120

Kidd, R. S., O'Higgins, P. & Oxnard, C. E. 1996. The OH8 foot: a reappraisal of the functional morphology of the hindfoot utilizing multivariate analysis. *Journal of Human Evolution*. 31: 269-291

Kim, H. 2013. Statistical notes for clinical researchers: assessing normal distribution (2) using skewness and kurtosis. *Restorative Dentistry and Endodontics*. 38: 52-54

Kimbel, W. H. 2015. The Species and Diversity of Australopiths. In Henke, W. & Tattershall, I. *Handbook of Palaeoanthropology*. 2nd Edition. Springer. London.

Kimbel, W. H. & Delezene, L. K. 2009. "Lucy" Redux: A Review of Research on *Australopithecus afarensis*. *Yearbook of Physical Anthropology*. 52: 2-48.

Klenerman, L. & Wood, B. 2006. *The Human Foot: A Companion to Clinical Studies*. Springer-Verlag. London

Klingenberg, C. P. 2011. MorphoJ: an integrated software package for geometric morphometrics. *Molecular Ecology Resources* 11: 353-357

Klingenberg, C. P. & Monteiro, L. R. 2005. Distances and Directions in Multidimensional Shape Spaces: Implications for Morphometric Applications. *Systematic Biology*. 54(4): 678-688.

Knigge, R. P., Tocheri, M. W., Orr, C. M. & McNulty, K. P. 2015. Three-Dimensional Geometric Morphometric Analysis of Talar Morphology in Extant Gorilla Taxa from Highland and Lowland Habitats. *The Anatomical Record*. 298: 277-290

Köhler, M. & Moyà-Solà, S. 1997. Ape-like or hominid-like? The positional behaviour of *Oreopithecus bambolii* reconsidered. *Proceedings of the National Academy of Sciences*. 94: 11747-11750

Kommean, P. K., Smith, K. E. & Vannier, M. W. 1996. Design of a 3-D surface scanner for lower limb prosthetics: A technical note. *Journal of Rehabilitation Research and Development*. 33: 267-278

Kordos, L. & Begun, D. R. 2001. A new cranium of *Dryopithecus* from Rudabánya, Hungary. *Journal of Human Evolution*. 41: 689-700

Koufos, G. D. & de Bonis, L. 2005. The Late Miocene hominoid *Ouranopithecus* and *Graecopithecus*. Implications about their relationships and taxonomy. *Annales de Paléontologie*. 91: 227-240

Knussman, R. 1967. Das proximale Ende der Ulna von *Oreopithecus bambolii* und seine Aussage über dessen systematische Stellung. *Zeitschrift für Morphologie und Anthropologie*. 59: 57-76

Kramer, A. 1986. Hominid-Pongid Distinctiveness in the Miocene-Pliocene Fossil Record: The Logotham Mandible. *American Journal of Physical Anthropology*. 70: 457-473

Krentz, H. B. 1993. Postcranial anatomy of extant and extinct *Theropithecus*. In Jablonski, N. G. (ed) *Theropithecus: The rise and fall of a primate genus*. Cambridge University Press. Cambridge.

Langon, J. H. 1986. *Functional Morphology of the Miocene Hominoid Foot*. Karger. London.

Latimer, B., Ohman, J. C. & Lovejoy, C. O. 1987. Talocrural Joint in the African Hominoids: Implications for *Australopithecus afarensis*. *American Journal of Physical Anthropology*. 74: 155-175.

Latimer, B. & Lovejoy, C. O. 1990. Hallucal Tarsometatarsal Joint in *Australopithecus afarensis*. *American Journal of Physical Anthropology*. 82: 125-133

Leakey, M. D. & Hay, R. L. 1979. Pliocene footprints in the Laetoli beds at Laetoli, northern Tanzania. *Nature*. 278:317-323

Leakey, M. G., Feibel, C. S., McDougall, I., Ward, C. & Walker, A. 1998. New specimens and confirmation of an early age for *Australopithecus anamensis*. *Nature*. 393: 62-66

Leakey, M. G., Ungar, P. S. & Walker, A. 1995. A new genus of large primate from the Late Oligocene of Lothidok, Turkana District, Kenya. *Journal of Human Evolution*. 28: 519-531

Leakey, R. E. F. & Leakey, M. G. 1986. A New Miocene Hominoid from Kenya. *Nature*. 324: 143-146.

Leakey, R. E. F., Leakey, M. G. & Walker, A. C. 1988. Morphology of *Afropithecus turkanensis* From Kenya. *American Journal of Physical Anthropology*. 76: 289-307.

Leardini, A., Stagni, R. & O'Connor, J. J. 2001. Mobility of the subtalar joint in the intact ankle complex. *Journal of Biomechanics*. 34: 805-809

Lewin, R. 2005. *Human Evolution: an illustrated introduction*. 5th Edition. Blackwell Publishing Ltd. Oxford

- Lewis, O. J. 1972. The Evolution of the Hallucial Tarsometatarsal Joint in the Anthroidea. *American Journal of Physical Anthropology*. 37: 13-34
- Lewis, O. J. 1980a. The joints of the evolving foot. Part I. The ankle joint. *Journal of Anatomy*. 130: 527-543.
- Lewis, O. J. 1980b. The joints of the evolving foot. Part II. The intrinsic joints. *Journal of Anatomy*. 130: 833-857
- Livingstone, F. B. 1962. Reconstructing Man's Pliocene Pongid Ancestor. *American Anthropologist*. 64: 301-305
- Lovejoy, C. O. 2009. Reexamining Human Origins in Light of *Ardipithecus ramidus*. *Science*. 326: 74
- Lockwood, C. A. & Tobias, P. V. 1999. A large male hominin cranium from Sterkfontein, South Africa, and the status of *Australopithecus africanus*. *Journal of Human Evolution*. 36: 637-685
- Lovejoy, C. O., Latimer, B., Suwa, G., Asfaw, B. & White, T. D. 2009a. Combining Prehension and Propulsion: The Foot of *Ardipithecus ramidus*. *Science*. 326: 72
- Lovejoy, C. O., Suwa, G., Spurlock, L., Asfaw, B. & White, T. D. 2009b. The Pelvis and Femur of *Ardipithecus ramidus*: The Emergence of Upright Walking. *Science*. 326: 71
- Lovejoy, C. O., Simpson, S. W., White, T. D., Asfaw, B. & Suwa, G. 2009c. Careful climbing in the Miocene: The Forelimbs of *Ardipithecus ramidus* and Humans are Primitive. *Science*. 326: 70

Lovejoy, C. O. & McCollum, M. A. 2010. Spinopelvic pathways to bipedality: why no hominids ever relied on a bent-hip-bent-knee gait. *Philosophical Transactions of the Royal Society B*. 365: 3289-3299.

MacLatchy, L. 2004. The Oldest Ape. *Evolutionary Anthropology*. 13: 90-103

MacLatchy, L., Gebo, D., Kityo, R. & Pilbeam, D. 2000. Postcranial functional morphology of *Morotopithecus bishopi*, with implications for the evolution of modern ape locomotion. *Journal of Human Evolution*. 39: 159-183

Madar, S. I., Rose, M. D., Kelley, J., MacLatchy, L. & Pilbeam, D. 2002. New *Sivapithecus* postcranial specimens from the Siwaliks of Pakistan. *Journal of Human Evolution*. 42: 705-752

Marchi, D. 2005. The cross-sectional geometry of the hand and foot bones of the Hominoidea and its relationship to locomotor behaviour. *Journal of Human Evolution*. 49: 743-761

Marchi, D. 2015. Using the morphology of the hominoid distal fibula to interpret arboreality in *Australopithecus afarensis*. *Journal of Human Evolution*. 85: 136-148

Marzke, M. W., Longhill, J. M. & Rasmussen, S. A. 1988. Gluteus Maximus Muscle Function and the Origin of Hominid Bipedality. *American Journal of Physical Anthropology*. 77: 519-528

Marzke, M. W. & Shrewsbury, M. M. 2006. The *Oreopithecus* thumb: Pitfalls in reconstructing muscle and ligament attachments from fossil bones. *Journal of Human Evolution*. 51: 213-215

Matson, S. D., Rook, L., Oms, O. & Fox, D. L. 2012. Carbon isotopic record of terrestrial ecosystems spanning the Late Miocene extinction of *Oreopithecus bambolii*, Baccinello Basin (Tuscany, Italy). *Journal of Human Evolution*. 63: 127-139

McCrossin, M. L. & Benefit, B. R. 1993. Recently recovered *Kenyapithecus* mandible and its implications for great ape and human origins. *Proceedings of the National Academy of Sciences*. 90: 1962-1966.

McHenry, H. M. 1992. Body size and proportions in early hominids. *American Journal of Physical Anthropology*. 87: 407-431.

McHenry, H. M. 2002. Introduction to the fossil record of human ancestry. In Hartwig, W. C. (ed) *The Primate Fossil Record*. Cambridge University Press. Cambridge.

McHenry, H. M. & Jones, A. L. 2006. Hallucial convergence in early hominids. *Journal of Human Evolution*. 50: 534-539

McMinn, R. M. H., Hutchings, R. T. & Logan, B. M. 1996. *Colour Atlas of Foot and Ankle Anatomy*. 2nd Edition. Times Mirror International Publishers Limited. London

McPherron, S., Gernat, T. & Hublin, J. 2009. Structured light scanning for high-resolution documentation of *in situ* archaeological finds. *Journal of Archaeological Science*. 36: 19-24.

Meldrum, D. J. 1993. On Plantigrady and Quadrupedalism. *American Journal of Physical Anthropology*. 91: 379-385

Meldrum, D. J. 2004. Midfoot Flexibility, Fossil Footprints and Sasquatch steps: New Perspectives on the Evolution of Bipedalism. *Journal of Scientific Exploration*. 18: 65-79

Merceron, G., Kaiser, T. M., Kostopoulos, D. S. & Schulz, E. 2010. Ruminant diets and the Miocene extinction of European great apes. *Proceedings of the Royal Society B*. 277: 3105-3112.

Millán, M. S., Kaliontzopoulou, A., Rissech, C. & Turbón, D. 2015. A geometric morphometric analysis of acetabular shape of the primate hip joint in relation to locomotor behaviour. *Journal of Human Evolution*. 83: 15-27

Morton, D. J. 1922. Evolution of the Human Foot. *American Journal of Physical Anthropology*. 5: 305-336

Motley, T., Clements, J. R., Moxley, K., Carpenter, B. & Garrett, A. 2010. Evaluation of the Deltoid Complex in Supination External Rotation Ankle Fractures. *The Foot and Ankle Online Journal*. 3: 1

Moyà-Solà, S. & Köhler, M. 1996. A *Dryopithecus* Skeleton and the Origins of Great Ape Locomotion. *Nature*. 379: 156-159

Moyà-Solà, S., Köhler, M. & Rook, L. 1999. Evidence of hominid-like precision grip capability in the hand of the Miocene ape *Oreopithecus*. *Proceedings of the National Academy of Sciences*. 96: 313-317

Moyà-Solà, S., Köhler, M. & Rook, L. 2005. The *Oreopithecus* thumb: a strange case in hominoid evolution. *Journal of Human Evolution*. 49: 395-404

Moyà-Solà, S., Köhler, M., Alba, D. M., Casanovas-Vilar, I. & Galindo, J. 2004. *Pierolapithecus catalunicus*, a New Middle Miocene Great Ape from Spain. *Science*. 316: 1339-1334

Moyà-Solà, S., Köhler, M., Alba, D. M., Casanovas-Vilar, I., Galindo, J., Robles, J. M., Cabrera, L., Garcés, M., Alméija, S. & Beamud, E. 2009. First Partial Face and Upper Dentition of the Middle Miocene Hominoid *Dryopithecus fontani* from Abocador de Can Mata (Vallè-Penedès Basin, Catalonia, NE Spain): Taxonomic and Phylogenetic Implications. *American Journal of Physical Anthropology*. 139: 126-145

Nagano, A., Umberger, B. R., Marzke, M. W. & Gerritsen, K. G. M. 2005. Neuromusculoskeletal Computer Modelling and Simulation of Upright, Straight-Legged, Bipedal Locomotion of *Australopithecus afarensis* (A.L. 288-1). *American Journal of Physical Anthropology*. 126: 2-13

Nakatsukasa, M. 2008. Comparative study of Moroto vertebral specimens. *Journal of Human Evolution*. 55: 581-588

Nakatsukasa, M., Ward, C. V., Walker, A., Teaford, M. F., Kunimatsu, Y. & Oghihara, N. 2004. Tail loss in *Proconsul heseloni*. *American Journal of Physical Anthropology*. 46: 777-784

Nakatsukasa, M., Kunimatsu, Y., Nakano, Y., Takano, T. & Ishida, H. 2003. Comparative and functional anatomy of phalanges in *Nacholapithecus kerioi*, a Middle Miocene hominoid from northern Kenya. *Primates*. 44: 371-412

Nakatsukasa, M., Tsujikawa, H., Shimizu, D., Takano, T., Kunimatsu, Y., Nakano, Y. & Ishida, H. 2003a. Definitive evidence for tail loss in *Nacholapithecus*, an East African Miocene hominoid. *Journal of Human Evolution*. 45: 179-86.

Nakatsukasa, M., Yamanaka, A., Kunimatsu, Y., Shimizu, D. & Ishida, H. 1998. A newly discovered *Kenyapithecus* skeleton and its implications for the evolution of positional behaviour in Miocene East African hominoids. *Journal of Human Evolution*. 34: 657-664

Nakatsukasa, M., Pickford, M., Egi, N. & Senut, B. 2007. Femur length, body mass, and stature estimates of *Orrorin tugenensis*, a 6 Ma hominid from Kenya. *Primates*. 48: 171-178

Napier, J. 1993. The Antiquity of Human Walking. In Ciochon, R. L. & Fleagle, J. G. (eds) *The Human Evolution Source Book*. Prentice Hall. New Jersey.

Niven, L., Steele, T. E., Finke, H., Gernat, T. & Hublin, J. 2009. Virtual skeletons: using a structured light scanner to create a 3D faunal comparative collection. *Journal of Archaeological Science*. 36: 2018-2023.

Nordstokke, D. W., Zumbo, B. D., Cairns, S. L. & Saklofske, D. H. 2011. The operating characteristics of the nonparametric Levene test for equal variances with assessment and evaluation data. *Practical assessment, Research & Evaluation*. 16:1-8

Nowak, M. G., Carlson, K. J. & Patel, B. A. 2010. Apparent Density of the Primate Calcaneo-Cuboid Joint and Its Association with Locomotor Mode, Foot Posture, and the "Midtarsal Break". *American Journal of Physical Anthropology*. 142: 180-193

Nystrom, P. & Ashmore, P. 2008. *The Life of Primates*. Pearson Prentice Hall. New Jersey.

O'Higgins, P. 2000. The study of morphological variation in the hominid fossil record: biology, landmarks and geometry. *Journal of Anatomy*. 197: 103-120.

O'Higgins, P., Chadfield, P. & Jones, N. 2001. Facial growth and the ontogeny of morphological variation within and between the primates *Cebus apella* and *Cercocebus torquatus*. *Journal of the Zoological Society of London*. 254: 337-357

Ohman, J. C., Lovejoy, C. O. & White, T. D. Questions About *Orrorin* Femur. *Science*. 307: 845

Oxnard, C. E. 1984. *The Order of Man: A Biomathematical anatomy of the primates*. Yale University Press. London.

Oxnard, C. E. & Lisowski, F. P. 1980. Functional Articulation of Some Hominoid Foot Bones: Implications for the Olduvai (Hominid 8) Foot. *American Journal of Physical Anthropology*. 52: 107-117

Oxnard, C. & O'Higgins, P. 2009. Biology clearly needs morphometrics. Does morphometrics need biology? *Biological Theory*. 4(1): 84-97.

Palastanga, N., Field, D. & Soames, R. 1994. *Anatomy and Human Movement: Structure and Function*. 2nd Edition. Butterworth-Heinemann Ltd. Oxford.

Pankovich, A. M. & Shivaram, M. S. 1979a. Anatomical basis of variability in injuries of the medial malleolus and the deltoid ligament:1. Anatomical Studies *Acta Orthopaedica Scandinavica*. 50: 217-223

Pankovich, A. M. & Shivaram, M. S. 1979b. Anatomical basis of variability in injuries of the medial malleolus and the deltoid ligament:2. Clinical Studies *Acta Orthopaedica Scandinavica*. 50: 225-236

Park, S. C. & Chang, M. 2009. Reverse engineering with a structured light system. *Computers and Industrial Engineering*. 57: 1377-1384.

Parr, W. C. H., Soligo, C., Smaers, J., Chatterjee, H. J., Ruto, A., Cornish, L. & Wroe, S. 2014. Three-dimensional shape variation of talar surface morphology in hominoid primates. *Journal of Anatomy*. 225: 42-59.

Pavlidis, G., Koutsoudis, A., Arnaoutoglou, F., Tsioukas, V. & Chamzas, C. 2007. Methods for 3D digitization of cultural heritage. *Journal of Cultural Heritage*. 8: 93-98.

- Patel, B. A. 2010. The Interplay Between Speed, Kinetics and Hand Postures During Primate Terrestrial Locomotion. *American Journal of Physical Anthropology*. 141: 223-234
- Patel, B. A. & Grossman, A. 2006. Dental metric comparisons of *Morotopithecus* and *Afropithecus*: Implications for the validity of the genus *Morotopithecus*. *Journal of Human Evolution*. 51: 506-512
- Perez, S. I., Bernal, V. & Gonzalez, P. N. 2006. Differences between sliding semi-landmark methods in geometric morphometrics, with an application to human craniofacial and dental variation. *Journal of Anatomy*. 208: 769-784
- Perry, G. H. & Dominy, N. J. 2009. Evolution of the human pygmy phenotype. *Trends in Ecology and Evolution*. 24: 218-225
- Pickford, M. 2006. Paleoenvironments, Paleoecology, Adaptations, and the Origins of Bipedalism in Hominidae. In Ishida, H., Tuttle, R., Pickford, M., Ogiwara, N. & Nakatsukasa, M. (eds) *Human Origins and Environmental Backgrounds*. Springer. USA.
- Pickford, M., Senut, B., Gommery, D. & Treil, J. 2002. Bipedalism in *Orrorin tugenensis* revealed by its femora. *Comptes Rendus de l'Académie des Sciences*. 191-203
- Pickford, M., Senut, B., Gommery, D. & Musiime, E. 2009. Distinctiveness of *Ugandapithecus* from *Proconsul*. *Estudios Geológicos*. 65: 183-241.
- Pilbeam, D. R. 1982. New Hominoid Skull Material from the Miocene of Pakistan. *Nature*. 295: 232-234.

Pontzer, H. & Wrangham, R. W. 2004. Climbing and the daily energetic cost of locomotion in wild chimpanzees: implications for hominoid locomotor evolution. *Journal of Human Evolution*. 46: 317-335

Posdamer, J. L. & Altschuler, M. D. 1982. Surface measurement by space-encoded projected beam systems. *Computer Graphics and Image Processing*. 18: 1-17.

Postan, D., Carabelli, G. S. Poitevin, L. A. 2011. Spring Ligament and Sustentaculum Tali Anatomical Variations: Anatomical Research Oriented to Acquired Flat Foot Study. *The Foot and Ankle Online Journal*. 4: 1

Proctor, D. J. 2010a. *Three-dimensional morphometrics of the proximal metatarsal articular surfaces of Gorilla, Pan, Hylobates, and shod and unshod humans*. PhD Thesis. University of Iowa.

Proctor, D. J. 2010b. Brief Communication: Shape Analysis of the MT 1 Proximal Articular Surface in Fossil Hominins and Shod and Unshod *Homo*. *American Journal of Physical Anthropology*. 143: 631-637

Proctor, D. J., Broadfield, D. & Proctor, K. 2008. Quantitative Three-Dimensional Shape Analysis of the Proximal Hallucial Metatarsal Articular Surface in *Homo, Pan, Gorilla* and *Hylobates*. *American Journal of Physical Anthropology*. 135: 216-224

Raaum, R. L. 2015. Molecular Evidence on Primate Origins and Evolution. In Henke, W. & Tattersall, I. (eds) *Handbook of Paleoanthropology*. 2nd Edition. Springer. London.

Radinsky, L. 1973. *Aegyptopithecus* Endocasts: Oldest Record of a Pongid Brain. *American Journal of Physical Anthropology*. 39: 239-248

Raichlen, D. R., Gordon, A. D., Harcourt-Smith, W. E. H., Foster, A. D. & Haas, W. R. Jr. 2010. Laetoli Footprints Preserve Earliest Direct Evidence of Human-Like Bipedal Biomechanics. *PlosOne*. 5(3): e9769.

Rak, Y., Ginzberg, A. & Geffen, E. 2007. Gorilla-like anatomy on *Australopithecus afarensis* mandible suggests *Au. Afarensis* link to robust australopiths. *Proceedings of the National Academy of Sciences*. 104: 6568-6572

Rasmussen, D. T. 2002. Early Catarrhines of the African Eocene and Oligocene. In Hartwig, W. C. (ed) *The Primate Fossil Record*. Cambridge University Press. Cambridge.

Rasmussen, O. 1985. Stability of the Ankle Joint: Analysis of the Function and Traumatology of the Ankle Ligaments. *Acta Orthopaedica Scandinavica*. 56(S211): 1-75

Raza, S. M., Barry, J. C., Pilbeam, D., Rose, M. D., Shah, S. M. I. & Ward, S. 1983. New Hominoid Primates from the Middle Miocene Chinji Formation, Potwar Plateau, Pakistan. *Nature*. 306: 52-54

Remis, M. 1995. Effects of Body Size and Social Context on the Arboreal Activities of Lowland Gorillas in the Central African Republic. *American Journal of Physical Anthropology*. 97: 413-433

Reno, P. L., DeGusta, D., Serrat, M. A., Meindl, R. S., White, T. D., Eckhardt, R. B., Kuperavage, A. J., Galik, K. & Lovejoy, C. O. 2005. Plio-Pleistocene Hominid Limb Proportions. *Current Anthropology*. 46: 575-588

Renström, P. A. F. H. & Lynch, S. A. 1998. Ankle ligament injuries. *Revista Brasileira de Medicina do Esporte*. 4: 71-80

Richmond, B. G. & Jungers, W. L. 2008. *Orrorin tugenensis* Femoral Morphology and the Evolution of Hominin Bipedalism. *Science*. 319: 1662-1664

Richmond, B. G. & Strait, D. S. 2000. Evidence that humans evolved from a knuckle-walking ancestor. *Nature*. 404: 382-385.

Richmond, B. G., Begun, D. R. & Strait, D. S. 2001. Origin of Human Bipedalism: The Knuckle-Walking Hypothesis Revisited. *Yearbook of Physical Anthropology*. 44: 70-105

Riesenfeld, A. 1975. Volumetric Determination of Metatarsal Robusticity in a Few Living Primates and in the Foot of *Oreopithecus*. *Primates*. 16: 9-15

Rocchini, C., Cignoni, P., Montani, C., Pingi, P. & Scopigno, R. 2001. A low cost 3D scanner based on structured light. *Eurographics*. 20 (3): 1-10.

Rohlf, F. J. & Slice, D. E. 1990. Extensions of the procrustes method for the optimal superimposition of landmarks. *Systematic Zoology*. 39: 40-59

Rook, L., Harrison, T. & Engesser, B. 1996. The taxonomic status and biochronological implications of new finds of *Oreopithecus* from Baccinello (Tuscany, Italy). *Journal of Human Evolution*. 30: 3-27.

Rook, L., Bondioli, L., Köhler, M., Moyà-Solà, S. & Macchiarelli, R. 1999. *Oreopithecus* was a bipedal ape after all: Evidence from the iliac cancellous architecture. *Proceedings of the National Academy of Sciences*. 96: 8795-8799

Rook, L., Oms, O., Benvenuti, M. G. & Papini, M. 2011. Magnetostratigraphy of the Late Miocene Baccinello-Cinigiano basin (Tuscany, Italy) and the age of *Oreopithecus bambolii* faunal assemblages. *Palaeogeography, Palaeoclimatology, Palaeoecology*. 305: 286-294

Rose, M. D. 1984. Hominoid Postcranial Specimens from the Middle Miocene Chinji Formation, Pakistan. *Journal of Human Evolution*. 13: 503-516

Rose, M. D. 1988. Another look at the anthropoid elbow. *Journal of Human Evolution*. 17: 193-224

Rose, M. D. 1991. The Process of Bipedalization in Hominins. In Coppens, Y. & Senut, B. (eds) *Origine(s) De la Bipédie Chez les Homininés*. Paris. CNRS

Rose, M. D. 1993. Locomotor Anatomy of Miocene Hominoids. In Gebo, D. L. (ed) *Postcranial Adaptation in Nonhuman Primates*. Northern Illinois University Press.

Rose, M. D., Nakano, Y. & Ishida, H. 1996. *Kenyapithecus* postcranial specimens from Nachola, Kenya. *African Study Monographs*. Supplement 24: 3-56.

Rosenberger, A. L. & Delson, E. 1985. The dentition of *Oreopithecus bambolii*: systematic and paleobiological implications. *American Journal of Physical Anthropology*. 66: 222-223

Rossie, J. B. & MacLatchy, L. 2013. Dentognathic remains of an *Afropithecus* individual from Kalodirr, Kenya. *Journal of Human Evolution*. 65: 199-208

Ruff, C. B. 2002. Long Bone Articular and Diaphyseal Structure in Old World Monkeys and Apes. I: Locomotor Effects. *American Journal of Physical Anthropology*. 119: 305-342

Ruff, C. B. 2009. Relative limb strength and locomotion in *Homo habilis*. *American Journal of Physical Anthropology*. 138: 90-100.

Rule, J., Yao, L. & Seeger, L. L. 1993. Spring Ligament of the Ankle: Normal MR Anatomy. *American Journal of Roentgenology*. 161: 1241-1244

Russo, G. A. & Shapiro, L. J. 2013. Reevaluation of the lumbosacral region of *Oreopithecus bambolii*. *Journal of human Evolution*. 65: 253-265

Ruvolo, M., Pan, D., Zehr, S., Goldberg, T., Disotell, T. R. & von Dornum, M. 1994. Gene trees and hominoid phylogeny. *Proceedings of the National Academy of Sciences*. 91: 8900-8904

Sammarco, G. J. 1989. Biomechanics of the foot. In Nordin, M. & Frankel, V. H. (eds) *Basic Biomechanics of the Musculoskeletal System*. Williams & Wilkins. Media, Pennsylvania.

Sarmiento, E. E. 1987. The Phylogenetic Position of *Oreopithecus* and Its Significance in the Origin of the Hominoidea. *American Museum Novitates*. 2881.

Sarmiento, E. E. 1994. Terrestrial Traits in the Hands and Feet of Gorillas. *American Museum Novitates*. 3091: 1-56

Sarmiento, E. E. 2010. Comment on the Paleobiology and Classification of *Ardipithecus ramidus*. *Science*. 328: 1105

Sarmiento, E. E. & Marcus, L. F. 2000. The Os Navicular of Humans, Great Apes, OH8, Hadar and *Oreopithecus*: Function, Phylogeny, and Multivariate Analyses. *American Museum Novitates*. 3288

Sarmiento, E. E. & Meldrum, D. J. 2011. Behavioural and phylogenetic implications of a narrow allometric study of *Ardipithecus ramidus*. *HOMO – Journal of Comparative Human Biology*. 62: 75-108

Sarrafian, S. K. 1983. *Anatomy of the Foot and Ankle: Descriptive: Topographic: Functional*. J. B. Lippincott Company. Philadelphia.

Sato, K. & Inokuchi, S. 1984. Three-Dimensional Surface Measurement by Space Encoding Range Imaging. *Journal of Robotic Systems*. 2 (1): 27-39.

Sawada, Y., Pickford, M., Senut, B., Itaya, T., Hyodo, M., Miura, T., Kashine, C., Chujo, T. & Fujii, H. 2002. The age of *Orrorin tugenensis*, an early hominid from the Tugen Hills, Kenya. *Comptes Rendus Palevol*. 1: 293-303

Schmitt, D. & Larson, S. G. 1995. Heel Contact as a Function of Substrate Type and Speed in Primates. *American Journal of Physical Anthropology*. 96: 39-50

Schrager, C. G. & Voloch, C. M. 2013. The precision of the hominid timescale estimated by relaxed clock methods. *Journal of Evolutionary Biology*. 26:746-755

Schultz, A. H. 1930. The skeleton of the trunk and limbs of higher primates. *Human Biology*. 2: 303-438

Senut, B., Pickford, M., Gommery, D., Mein, P., Cheboi, K. & Coppens, Y. 2001. First hominid from the Miocene (Lukeino Formation, Kenya). *Comptes Rendus de l'Académie des Sciences*. 332: 137-144

Shetty, N. & Bendall, S. 2011. Understanding the gait cycle, as it relates to the foot. *Orthopaedics and Trauma*. 25: 236-240

Shoshani, J., Groves, P., Simons, E. L. & Gunnell, G. F. 1996. Primate Phylogeny: Morphological vs Molecular results. *Molecular Phylogenetics and Evolution*. 5: 102-154

Simons, E. L. 1993. New endocasts of *Aegyptopithecus*: oldest well-preserved record of the brain in anthropoidea. *American Journal of Science*. 239-A: 383-390

Slice, D. E. 2005. Modern Morphometrics. In Slice, D. E. (ed) *Modern Morphometrics in Physical Anthropology*. Kluwer Academic. New York.

Slice, D. E. 2007. Geometric Morphometrics. *Annual Review of Anthropology*. 36: 261-281.

Spoor, C. F., Sondaar, P. Y. & Hussain, S. T. 1991. A new hominoid hamate and first metacarpal from the Late Miocene Nagri Formation of Pakistan. *Journal of Human Evolution*. 21: 413-424

Springer, M. S., Meredith, R. W., Gatesy, J., Emerling, C. A., Park, J., Rabosky, D. L., Stadler, T., Steiner, C., Ryder, O. A., Janečka, J. E., Fisher, C. A. & Murphy, W. J. 2012. Macroevolutionary Dynamics and Historical Biogeography of Primate Diversification Inferred from a Species Supermatrix. *PLOS ONE*. 7: e49521

Stanford, C. B. 2006. Arboreal Bipedalism in Wild Chimpanzees: Implications for the Evolution of Hominid Posture and Locomotion. *American Journal of Physical Anthropology*. 129: 225-231.

Stern Jr., J. T. 2000. Climbing to the Top: A Personal Memoir of *Australopithecus afarensis*. *Evolutionary Anthropology*. 9: 113-133

Stern Jr., J. T. & Susman, R. L. 1983. The Locomotor Anatomy of *Australopithecus afarensis*. *American Journal of Physical Anthropology*. 60: 279-317

Strait, D. S. & Grine, F. E. 2004. Inferring hominoid and early hominid phylogeny using craniodental characters: the role of fossil taxa. *Journal of Human Evolution*. 47: 399-452

Strasser, E. 1988. Pedal evidence for the origin and diversification of cercopithecoid clades. *Journal of Human Evolution*. 17: 225-245

Strasser, E. 1992. Hindlimb Proportions, Allometry, and Biomechanics in the Old World Monkeys (Primates, Cercopithecidae). *American Journal of Physical Anthropology*. 87: 187-213

Strasser, E. & Delson, E. 1987. Cladistic analysis of cercopithecoid relationships. *Journal of Human Evolution*. 16: 81-99

Straus, W. L. 1957. *Oreopithecus bambolii*. *Science*. 126:345-346

Susman, R. L. 2004. *Oreopithecus bambolii*: an unlikely case of hominidlike grip capability in a Miocene ape. *Journal of Human Evolution*. 46: 105-117

Susman, R. L. 2005. *Oreopithecus*: still apelike after all these years. *Journal of Human Evolution*. 49: 405-411

Sutton, J. B. 1883. On some points in the anatomy of the chimpanzee (*Anthropithecus troglodytes*). *Journal of Anatomy and Physiology*. 18: 66-85.

Suwa, G., Asfaw, B., Kono, R. T., Kubo, D., Lovejoy, C. O. & White, T. D. 2009. The *Ardipithecus ramidus* skull and Its Implications for Hominid Origins. *Science*. 326: 68

Szalay, F. S. 1975. Haplorhine relationships and the status of the Anthropoidea. In Tuttle, R. H. (ed) *Primate Functional Morphology and Evolution*. Mouton. The Hague.

Szalay, F. S. & Delson, E. 1979. *Evolutionary History of the Primates*. New York Academic Press. New York.

Szalay, F. S. & Langdon, J. H. 1986. The Foot of *Oreopithecus*: an Evolutionary Assessment. *Journal of Human Evolution*. 15: 585-621

Szalay, F. S. & Dagosto, M. 1988. Evolution of hallucial grasping in the primates. *Journal of Human Evolution*. 17: 1-33

Thorpe, S. K. S. & Crompton, R. H. 2006. Orangutan Positional Behaviour and the Nature of Arboreal Locomotion in Hominoidea. *American Journal of Physical Anthropology*. 131: 384-401

Thorpe, S. K. S., Holder, R. L. & Crompton, R. H. 2007. Origin of Human Bipedalism as an Adaptation for Locomotion on Flexible Branches. *Science*. 316: 1328-1331

Tocheri, M. W., Solhan, C. R., Orr, C. M., Femiani, J., Frohlich, B., Groves, C. P., Harcourt-Smith, W. E., Richmond, B. G. & Shoelson, B. 2011. Ecological Divergence and medial cuneiform morphology in gorillas. *Journal of Human Evolution* 60: 171-184

Tryfonidis, M., Jackson, W., Mansour, R., Cooke, P. H., Teh, J., Ostlere, S. & Sharp, R. J. 2008. Acquired adult flat foot due to isolated plantar calcaneonavicular (spring) ligament insufficiency with a normal tibialis posterior tendon. *Foot and Ankle Surgery*. 14: 89-95

Tuttle, R. H. 1969. Knuckle-Walking and the Problem of Human Origins. *Science* 166:953-961

Tuttle, R. H. 2006. Are Human Beings Apes, or are Apes People Too? In Ishida, H., Tuttle, R., Pickford, M., Ogiwara, N. & Nakatsukasa, M. (eds) *Human Origins and Environmental Backgrounds*. Springer. USA.

Tuttle, R. H. & Rogers, C. M. 1966. Genetic and Selective Factors in Reduction of the Hallux in *Pongo pygmaeus*. *American Journal of Physical Anthropology*. 24: 191-198

Venkataraman, V. V., Kraft, T. S. & Dominy, N. J. 2013. Tree climbing and human evolution. *Proceedings of the National Academy of Sciences*. 110: 1237-1242

Vereecke, E. E., D'Août, K., DeClercq, D., Van Elsacker, L. & Aerts, P. 2003. Dynamic Plantar Pressure Distribution During Terrestrial Locomotion of Bonobos (*Pan paniscus*). *American Journal of Physical Anthropology*. 120: 373-383

Vignaud, P., Douring, P., Mackaye, H. T., Likius, A., Blondel, C., Boisserie, J., de Bonis, L., Eisenmann, V., Etienne, M., Geraads, D., Guy, F., Lehman, T., Lihoreau, F., Lopez-Martinez, N., Mourer-Chauviré, C., Otero, O., Rage, J., Scuster, M., Viriot, L., Zazzo, A. & Brunet, M. 2002. Geology and palaeontology of the Upper Miocene Toros-Menalla hominid locality, Chad. *Nature*. 418: 152-155

Walker, A., Leakey, R. E., Harris, J. M. & Brown, F. H. 1986. 2.5-Myr *Australopithecus boisei* from west of Lake Turkana, Kenya. *Nature*. 327: 517-522

Wall-Scheffler, C. M., Geiger, K. & Steudel-Numbers, K. L. 2007. Infant Carrying: The Role of Increased Locomotory Costs in Tool Development. *American Journal of Physical Anthropology*. 133: 841-846.

Wang, W. J. & Crompton, R. H. 2004. Analysis of the human and ape foot during bipedal standing with implications for the evolution of the foot. *Journal of Biomechanics*. 37: 1831-1836

Ward, C. V. 2002. Interpreting the Posture and Locomotion of *Australopithecus afarensis*: Where do we stand? *Yearbook of Physical Anthropology*. 45: 185-215

Ward, C., Leakey, M. & Walker, A. 1999. The New Hominid Species *Australopithecus anamensis*. *Evolutionary Anthropology*. 7: 197-205

Ward, C. V., Walker, A. & Teaford, M. F. 1991. *Proconsul* did not have a tail. *Journal of Human Evolution*. 21: 215-220

Ward, C. V., Walker, A. & Teaford, M. F. 1999. Still no evidence for a tail in *Proconsul heseloni*. *American Journal of Physical Anthropology*. 108: Supplement 28. 273

Ward, C. V., Walker, A., Teaford, M. F. & Odhiambo, I. 1993. Partial Skeleton of *Proconsul nyanzae* From Mfangano Island, Kenya. *American Journal of Physical Anthropology*. 90: 77-111

Ward, C. V., Leakey, M. G. & Walker, A. 2001. Morphology of *Australopithecus anamensis* from Kanapoi and Allia Bay, Kenya. *Journal of Human Evolution*. 41: 255-368

Ward, C. V., Kimbel, W. H. & Johanson, D. C. 2011. Complete Fourth Metatarsal and Arches in the Foot of *Australopithecus afarensis*. *Science*. 331: 750-753

Ward, S., Brown, B., Hill, A., Kelley, J. & Downs, W. 1999. *Equatorius*: A New Hominoid Species from the Middle Miocene of Kenya. *Science*. 285: 1382-1386.

Ward, S. & Duren, D. L. 2002. Middle and late Miocene African hominoids. In Hartwig, W. C. (ed) *The Primate Fossil Record*. Cambridge University Press. Cambridge.

Wheeler, P. E. 1992. The influence of the loss of functional body hair on the water budgets of early hominids. *Journal of Human Evolution*. 23: 379-388

White, T. D. 2002. Earliest hominids. In Hartwig, W. C. (ed) *The Primate Fossil Record*. Cambridge University Press. Cambridge.

White, T. D., Suwa, G. & Asfaw, B. 1994. *Australopithecus ramidus*, a new species of early hominid from Aramis, Ethiopia. *Nature*. 371: 306-312

White, T. D. & Folkens, P. A. 2005. *The Human Bone Manual*. Elsevier Academic Press. London.

White, T. D., Ambrose, S. H., Suwa, G., Su, D. F., DeGusta, D., Bernor, R. L., Boissarie, J-R., Brunet, M., Delson, E., Frost, S., Garcia, N., Giaourtsakis, I. X., Haile-Selassie, Y., Howell, F. C., Lehmann, T., Likius, A., Pehlevan, C., Saegusa, H., Semprebon, G., Teaford, M. & Vrba, E. 2009. Macrovertebrate Paleontology and the Pliocene Habitat of *Ardipithecus ramidus*. *Science*. 326: 87-93

Whittle, M. W. 2007. *Gait Analysis: An Introduction*. Butterworth Heinemann. Philadelphia.

WoldeGabriel, G., Ambrose, S. H., Barboni, D., Bonnefille, R., Bremond, L., Currie, B., DeGusta, D., Hart, W. K., Murray, A. M., Renne, P. R., Jolly-Saad, M. C., Stewart, K. M. & White, T. D. 2009. The Geological, Isotopic, Botanical, Invertebrate and Lower Vertebrate Surroundings of *Ardipithecus ramidus*. *Science*. 326: 65

Wolpoff, M. H., Senut, B., Pickford, M. & Hawks, J. 2002. *Sahelanthropus* or '*Sahelpithecus*'? *Nature*. 419: 581-582

Wood, B. & Richmond, B. G. 2000. Human evolution: taxonomy and paleobiology. *Journal of Anatomy*. 196: 19-60.

Wrangham, R. W. 1980. Bipedal Locomotion as a Feeding Adaptation in Gelada Baboons, and its Implications for Hominid Evolution. *Journal of Human Evolution*. 9: 329-331

Wunderlich, R. E., Walker, A. & Jungers, W. L. 1999. Rethinking the Positional Repertoire of *Oreopithecus*. *American Journal of Physical Anthropology*. 108: 528

Young, N. M. 2003. A reassessment of living hominoid postcranial variability: implications for ape evolution. *Journal of Human Evolution*. 45: 441-464

Young, N. M. & MacLatchy, L. 2004. The phylogenetic position of *Morotopithecus*. *Journal of Human Evolution*. 46: 163-184

Zalmout, I. S., William J. Sanders, W. J., MacLatchy, L. M., Gunnell, G. F., Al-Mufarreh, Y. A., Ali, M. A., Nasser, A. H., Al-Masari, A. M., Al-Sobhi, S. A., Nadhra, A. O., Matari, A. H., Wilson, J. A. & Gingerich, P. D. 2010. New Oligocene primate from Saudi Arabia and the divergence of apes and Old World monkeys. *Science*. 466: 360-364

Zelditch, M. L., Swiderski, D. L., Sheets, H. D. & Fink, W. L. 2004. *Geometric Morphometrics for Biologists: A Primer*. Elsevier Academic Press. London.

Zexiao, X., Jianguo, W. & Quimei, Z. 2005. Complete 3D measurement in reverse engineering using a multi-probe system. *International Journal of Machine Tools and Manufacture*. 45: 1474-1486.

Zipfel, B. DeSilva, J. M. & Kidd, R. S. 2009. Earliest Complete Hominin Fifth Metatarsal – Implications for the Evolution of the Lateral Column of the Foot. *American Journal of Physical Anthropology*. 140: 532-545

Zipfel, B., DeSilva, J. M., Kidd, R. S., Carlson, K. J. & Churchill, S. E. 2011. The Foot and Ankle of *Australopithecus sediba*. *Science*. 333: 1417-1420

Zollikofer, C. P. E., Ponce de León, M. S., Lieberman, D. E., Guy, F., Pilbeam, D., Likius, A., Mackaye, H. T., Vignaud, P. & Brunet, M. 2005. Virtual cranial reconstruction of *Sahelanthropus tchadensis*. *Nature*. 434: 755-759